

Nuffield Department of Clinical Neurosciences

Structural, Quantitative and Functional MRI for the Study of Demyelinating Diseases of the Spinal Cord

A thesis submitted for the degree of Doctor of Philosophy (DPhil) in Clinical Neurosciences

Dr Romina Mariano

The Queen's College, University of Oxford

Michaelmas Term, 2020

Supervisors

Prof Jacqueline Palace

Prof Yazhuo Kong

Acknowledgements

First and foremost, I would like to thank my supervisors Prof Jacqueline Palace and Prof Yazhuo Kong for this opportunity and for their excellent guidance, mentorship and assistance in the production of this work.

This project would not have been possible without the generous financial support of the Rhodes Trust, the Oppenheimer Memorial Trust and the Goodger and Schorstein Scholarship; as well as the Multiple Sclerosis Society, United Kingdom.

The personal support I received from Rhodes House, and its community, was invaluable. In this respect I would especially like to thank Mary Eaton and Warden Elizabeth Kiss.

I thank all the participants that so willingly gave of their time to contribute to this research and all the staff at the Oxford Centre for Functional Imaging of the Brain (FMRIB). In particular, to Michael Sanders, Jon Campbell and David Parker. I am grateful for the support of all the staff in the Neuromyelitis Optica Service and Multiple Sclerosis Clinical Trials team, in particular Maria Isabel Leite, Ana Cavey, Rosie Everett and Joy Hodder.

Thank you to my colleagues who provided unrelenting support throughout this process: Silvia Messina, Adriana Roca-Fernandez, Ruth Geraldes, Pedro Cruz, and Maciej Jurynczyk.

Finally, to my husband, Byron for his unwavering love and support and tireless proofreading. To my big and wonderful Italian-South African family, especially my parents Gianni and Manuela, Lizzy, my second mother, and my siblings Francesco, Gianpaolo and Erin, who supported and encouraged my move to a new country in pursuit of this endeavour. Despite the pandemic having kept us apart for more than a year now, they have been a pillar of strength through this most challenging time.

Abstract

Structural, Quantitative and Functional MRI for the Study of Demyelinating Diseases of the Spinal Cord

Dr Romina Mariano, The Queen's College

Myelin-oligodendrocyte glycoprotein associated disease (MOGAD) is a recently described inflammatory demyelinating disorder of the central nervous system. It has been shown to be distinct from both aquaporin-4 (AQP4) antibody (Ab) neuromyelitis optica spectrum disorder (NMOSD) and multiple sclerosis (MS). Spinal cord involvement is a hallmark feature of all three diseases and a central cause of disability, and so, is an important phenotype to study. This thesis consists of a retrospective clinical study and then a cross-sectional research MRI study that compares structural, quantitative and resting-state functional MRI scans across MOGAD, AQP4-NMOSD, MS and healthy volunteers (HV).

The principal clinical research findings are:

- MOGAD myelitis presents more frequently with short cord lesions, multiple cord lesions, conus lesions and involvement of either the brain or optic nerves at the time of the acute attack; these MRI lesions are likely to resolve at follow-up.
- MOGAD myelitis results in significant sphincter dysfunction, despite good motor recovery. Conus lesions are associated the need for long term catheter dysfunction and the presence of a brainstem lesion during the acute attack may predict higher long term disability.

The principal research MRI findings are:

- AQP4-NMOSD myelitis shows the most severe, localised damage in areas of the cord involved during the acute episode. In MS, metrics show significant differences compared to HV but the relationship with lesion location is not as pronounced. In MOGAD, metrics are comparable to HV after recovery from myelitis but localised grey matter atrophy is noted in the affected area of the cord.
- Patients with relapsing MOGAD show significantly more thoracic cord atrophy than monophasic MOGAD, even where the relapse occurred outside of the spinal cord. This may indicate that relapsing MOGAD denotes a more severe phenotype.
- Non-conventional MRI metrics show clinical relevance: cervical cord cross-sectional area associates with disability outcomes and spinothalamic fractional anisotropy with pain scores, independent of disease type.
- Distinct and robust functional networks exist in the spinal cord without a particular task. Damage in the spinal cord may lead to either a compensatory increase or a decrease in connectivity related to atrophy and cord lesions.

The publications from this work, which form part of this thesis, have added to the growing body of research into the study of MOGAD. Additionally, advanced spinal cord imaging techniques were used, which add novelty to the research and its conclusions.

Publications related to this thesis

The use of the content of the publications related directly to this thesis is fully referenced in all the relevant chapters. I confirm all the written content, figures and tables used in this thesis from these publications was produced by me and presented here with the permission of all co-authors.

Papers

Mariano R, Messina S, Roca-Fernandez A, Leite MI, Kong Y, Palace JA. Quantitative spinal cord MRI in MOG-antibody disease, neuromyelitis optica and multiple sclerosis. Brain. 2020 Nov 18:awaa347. doi: 10.1093/brain/awaa347.

Mariano R, Messina S, Kumar K, Kuker W, Leite MI, Palace J. Comparison of Clinical Outcomes of Transverse Myelitis Among Adults With Myelin Oligodendrocyte Glycoprotein Antibody vs Aquaporin-4 Antibody Disease. JAMA Netw Open. 2019 Oct 2;2(10).

Mariano R, Flanagan EP, Weinshenker BG, et al. A practical approach to the diagnosis of spinal cord lesions. Practical Neurology 2018;18:187-200.

Abstracts

Mariano R, Messina S, Roca-Fernandez A, et al. Spinal cord involvement in MOGAD, AQP4-Ab NMOSD and MS. Association of British Neurologists Annual Meeting 2020. J Neurol Neurosurg Psychiatry 2021 (in press).

Mariano R, Messina S, Roca-Fernandez A, et al. Multimodal cervical cord MRI in MOGAD, AQP4-Ab NMOSD and MS. P1369. International Society for Magnetic Resonance in Medicine (ISMRM) Virtual Conference and Exhibition 2020 (E-Library: https://www.ismrm.org/e-library/)

Mariano R, Messina S, Roca-Fernandez A, et al. Cervical cord atrophy in AQP4-Ab NMOSD, MOG-Ab disease and MS. P1093. European Committee for treatment and research in Multiple Sclerosis (ECTRIMS), Berlin 2019. Multiple Sclerosis Journal 2018;25(2) doi.org/10.1177/1352458518798582

Mariano R, Kumar K, dos Passos G, et al. Clinical and MRI features of onset myelitis in MOG-antibody disease. P341. European Committee for treatment and research in Multiple Sclerosis (ECTRIMS), Berlin 2018. Multiple Sclerosis Journal 2018; 24(2) doi.org/10.1177/1352458518798582

Publications indirectly related to this thesis

Messina S*, Mariano R*, Geraldes R, et al. The influence of smoking on the pattern of disability and relapse risk in AQP4-postitive neuromyelitis optica spectrum disorder, MOG-Ab disease and multiple sclerosis. Mult Scler Relat Disord. 2021 (in press).

Messina S, Mariano R, Roca-Fernandez A, Cavey A, Jurynczyk M, Leite MI, et al. Contrasting the brain imaging features of MOG-Antibody disease, with AQP4-Antibody NMOSD and Multiple Sclerosis. medRxiv 2020: 2020.09.22.20198978.

O'Connell K, Hamilton-Shield A, Woodhall M, Messina S, Mariano R, Waters P, et al. Prevalence and incidence of neuromyelitis optica spectrum disorder, aquaporin-4 antibody-positive NMOSD and MOG antibody-positive disease in Oxfordshire, UK. J Neurol Neurosurg Psychiatry 2020; 91: 1126–1128.

Asseyer S, Hamblin J, Messina S, Mariano R, Siebert N, Everett R, Küker W, Bellmann-Strobl J, Ruprecht K, Jarius S, Leite MI, U Brandt A, Paul F, Palace J. Prodromal headache in MOG-antibody positive optic neuritis. Mult Scler Relat Disord. 2020 May;40:101965. doi: 10.1016/j.msard.2020.101965. Epub 2020 Jan 25. PMID: 32062443.

Papp D, Smith A, Mariano R, et al. High-resolution quantitative maps of magnetisation transfer, R1 and R2* of the cervical cord in clinically feasible acquisition time using vendor-provided sequences. International Society for Magnetic Resonance in Medicine (ISMRM) Virtual Conference and Exhibition 2019 (E-Library: https://www.ismrm.org/e-library/)

Summary table of contents

Chapter 1: Introduction and background - 15 -

Chapter 2: Thesis aims and structure - 62 -

Chapter 3: Clinical Features of Myelitis in MOGAD and AQP4-NMOSD - 65 -

Chapter 4: Non-conventional MRI study methods, cohort and assessments - 102 -

Chapter 5: Structural Spinal Cord MRI in MOGAD, AQP4-NMOSD and MS - 116 -

Chapter 6: Quantitative Spinal Cord MRI in MOGAD, AQP4-NMOSD and MS - 140 -

Chapter 7: The Clinical Relevance of Structural and Quantitative MRI metrics - 159 -

Chapter 8: Functional MRI in the Spinal Cord of MOGAD, AQP4-NMOSD and MS - 180 -

Chapter 9: Discussion - 214 -

Bibliography - 228 -

Detailed table of contents

1. CHAPTER 1: INTRODUCTION AND BACKGROUND ..... - 15 -

1.1 MOTIVATION FOR THIS THESIS AND TERMINOLOGY ..... - 15 -

1.2 HISTORICAL CONTEXT ..... - 17 -

1.3 THE CURRENT UNDERSTANDING OF MOGAD ..... - 18 -

1.3.1 Substrates and antibodies ..... - 19 -

1.3.2 Pathology ..... - 21 -

1.3.3 Epidemiology ..... - 23 -

1.3.3.1 Incidence and prevalence ..... - 23 -

1.3.3.2 Demographics ..... - 24 -

1.3.4 Clinical presentation ..... - 25 -

1.3.4.1 Spinal cord presentation ..... - 25 -

1.3.4.2 Other clinical presentations ..... - 31 -

1.3.5 Disease course and outcomes ..... - 31 -

1.3.6 MRI features ..... - 34 -

1.3.6.1 Spinal cord imaging ..... - 34 -

Spinal cord clinical imaging recommendations ..... - 34 -

1.3.6.2 Brain imaging ..... - 39 -

1.3.7 Other relevant investigations for spinal cord presentation ..... - 43 -

1.3.8 Diagnosis and diagnostic challenges ..... - 44 -

1.3.9 Treatment ..... - 46 -

1.3.10 Summary ..... - 48 -

1.4 SPINAL CORD MRI ..... - 50 -

1.4.1 Challenges in cord MRI ..... - 50 -

1.4.2 Quantification of structural imaging ..... - 53 -

1.4.3 Advanced imaging techniques and their use in neuroinflammatory conditions ..... - 54 -

1.4.3.1 DTI ..... - 56 -

1.4.3.2 MTR ..... - 56 -

1.4.3.3 fMRI ..... - 57 -

1.4.4 Summary ..... *- 59 -*

2. CHAPTER 2: THESIS AIMS AND STRUCTURE ..... - 63 -

2.1 THESIS OBJECTIVES AND AIMS ..... - 63 -

2.2 STRUCTURE OF THE THESIS ..... - 64 -

2.3 STATISTICAL APPROACH ..... - 65 -

3. CHAPTER 3: CLINICAL FEATURES OF MYELITIS IN MOGAD AND AQP4-NMOSD ..... - 66 -

3.1 INTRODUCTION AND BACKGROUND ..... - 66 -

3.2 OBJECTIVES AND AIMS ..... - 67 -

3.3 HYPOTHESIS ..... - 68 -

3.4 METHODS ..... - 68 -

3.4.1 Ethics ..... *- 68 -*

3.4.2 MOG and AQP4 antibody testing ..... *- 68 -*

3.4.3 Cohort ..... *- 69 -*

3.4.4 MRI review ..... *- 70 -*

3.4.5 Statistical analysis ..... *- 71 -*

3.4.6 Definitions of terms used within this chapter ..... *- 72 -*

3.5 RESULTS ..... - 73 -

3.5.1 Demographic data ..... *- 73 -*

3.5.2 Clinical presentation ..... *- 75 -*

3.5.3 Acute spinal cord MRI features ..... *- 76 -*

3.5.4 Acute intracranial imaging ..... *- 78 -*

3.5.4.1 Brain imaging ..... - 78 -

3.5.4.2 Brainstem imaging ..... - 78 -

3.5.5 Features of cerebrospinal fluid analysis ..... *- 80 -*

3.5.6 Relapses ..... *- 80 -*

3.5.7 Disability ..... *- 86 -*

3.5.7.1 Recovery from onset myelitis attacks with no relapse for at least one year ..... - 86 -

3.5.7.2 Total cohort analysis of factors associated with disability after first myelitis ..... - 88 -
3.5.7.3 Total cohort analysis of disability throughout disease course ..... - 90 -
3.5.7.4 Total cohort analysis of long-term sphincter dysfunction ..... - 91 -
3.5.8 Follow-up clinical MRI scans ..... - 93 -
3.6 DISCUSSION ..... - 94 -
3.7 LIMITATIONS ..... - 101 -
3.8 CONCLUSION ..... - 101 -
4. CHAPTER 4: NON-CONVENTIONAL MRI STUDY METHODS, COHORT AND ASSESSMENTS ..... - 103 -
4.1 INTRODUCTION ..... - 103 -
4.2 STUDY DESIGN ..... - 103 -
4.2.1 Ethics ..... - 103 -
4.2.2 Study visit ..... - 104 -
4.2.3 Power considerations ..... - 104 -
4.2.4 Participant recruitment ..... - 105 -
4.2.5 Inclusion criteria ..... - 105 -
4.2.6 Exclusion criteria ..... - 106 -
4.2.7 Statistics ..... - 107 -
4.2.8 Data protection ..... - 107 -
4.3 STUDY COHORT DEMOGRAPHICS AND CLINICAL DATA ..... - 107 -
4.4 CLINICAL DATA AND COHORT STUDY VISIT ASSESSMENTS ..... - 109 -
4.4.1 Clinical data collection ..... - 109 -
4.4.1.1 Severity and treatment of the acute attacks ..... - 110 -
4.4.2 Motor disability ..... - 111 -
4.4.3 Bladder dysfunction ..... - 111 -
4.4.4 Pain scoring ..... - 112 -
4.4.5 Fatigue scoring ..... - 113 -
4.5 MRI HARDWARE AND IMAGING MODALITIES ..... - 113 -
4.5.1 Imaging hardware ..... - 113 -

4.5.2 Imaging sequences ... *- 114 -*

4.5.3 Rationale for sequence and software selection ... *- 115 -*

4.6 LIMITATIONS ... - 116 -

5. CHAPTER 5: STRUCTURAL SPINAL CORD MRI IN MOGAD, AQP4-NMOSD AND MS ... 118

5.1 INTRODUCTION AND BACKGROUND ... 118

5.2 OBJECTIVES AND AIMS ... 120

5.3 HYPOTHESES ... 120

5.4 METHODS ... 121

5.4.1 Subjects ... *121*

5.4.2 MRI Acquisition ... *122*

5.4.3 MRI analysis ... *122*

5.4.3.1 Cervical cord cross-sectional area ... 122

5.4.3.2 Cervical cord grey matter ... 123

5.4.3.3 Cervical cord lesions ... 124

5.4.3.4 Thoracic cord cross-sectional area ... 124

5.4.4 Statistical analysis ... *125*

5.5 RESULTS ... 127

5.5.1 Cervical cord lesions ... *128*

5.5.2 Cervical cord CSA ... *129*

5.5.3 Thoracic cord CSA ... *130*

5.5.4 Cervical cord grey matter CSA ... *132*

5.5.5 Cumulative cord involvement ... *133*

5.5.6 Monophasic versus relapsing disease in MOGAD ... *134*

5.6 DISCUSSION ... 136

5.7 LIMITATIONS ... 141

5.8 CONCLUSION ... 141

6. CHAPTER 6: QUANTITATIVE SPINAL CORD MRI IN MOGAD, AQP4-NMOSD AND MS ... 142

6.1 INTRODUCTION AND BACKGROUND ... 142

6.2 OBJECTIVE AND AIMS 144
6.3 HYPOTHESES 144
6.4 METHODS 145
6.4.1 Subjects *145*
6.4.2 MRI acquisition *146*
6.4.3 MRI analysis *146*
6.4.3.1 Cervical Cord DTI 146
6.4.3.2 Cervical Cord MTR 147
6.4.4 Statistical analysis *148*
6.5 RESULTS 149
6.5.1 Cervical cord DTI *150*
6.5.2 Cervical cord MTR *153*
6.5.3 Cumulative cord involvement *155*
6.5.4 Monophasic versus relapsing MOGAD *156*
6.6 DISCUSSION 156
6.7 LIMITATIONS 159
6.8 CONCLUSION 160
7. CHAPTER 7: THE CLINICAL RELEVANCE OF STRUCTURAL AND QUANTITATIVE MRI METRICS 161
7.1 INTRODUCTION AND BACKGROUND 161
7.2 OBJECTIVES AND AIMS 163
7.3 HYPOTHESES 163
7.4 METHODS 164
7.4.1 Subjects and clinical assessments *164*
7.4.2 MRI: acquisition and analysis *164*
7.4.3 Statistics *167*
7.4.3.1 Clinical outcome models 167
7.4.3.2 Discriminatory model 168
7.5 RESULTS 168

7.5.1 Disability ... *168*

7.5.2 Sphincter dysfunction ... *170*

7.5.3 Pain ... *171*

7.5.4 Fatigue ... *173*

7.5.5 Discriminatory model ... *173*

7.6 DISCUSSION ... 177

7.7 LIMITATIONS ... 181

7.8 CONCLUSION ... 182

8. CHAPTER 8: FUNCTIONAL MRI IN THE SPINAL CORD OF MOGAD, AQP4-NMOSD AND MS ... 183

8.1 INTRODUCTION AND BACKGROUND ... 183

8.2 OBJECTIVES AND AIMS ... 185

8.3 HYPOTHESES ... 186

8.4 METHODS ... 186

8.4.1 Subjects ... *186*

8.4.2 Assessment of lesions ... *188*

8.4.3 MRI pre-processing ... *188*

8.4.4 MRI analysis ... *189*

8.4.5 Statistical analysis ... *191*

8.5 RESULTS ... 192

8.5.1 Healthy volunteer cohort analysis ... *192*

8.5.1.1 Connectivity pairs ... 192

8.5.1.2 Cervical vertebral levels ... 193

8.5.1.3 Individual subjects ... 194

8.5.1.4 Age and sex ... 195

8.5.1.5 Cross-sectional area ... 197

8.5.1.6 Exploratory analysis of quantitative MRI metrics in the healthy volunteers ... 198

8.5.2 MOGAD, AQP4-NMOSD and MS cohort analysis ... *199*

8.5.2.1 Connectivity pairs ... 199

8.5.2.2 Cervical vertebral levels ... 201

8.5.2.3 Individual subjects 202
8.5.2.4 Cross-sectional area 203
8.5.2.5 Exploratory analysis of quantitative MRI metrics 204
8.5.3 Four-group comparison of MOGAD, AQP4-NMOSD, MS and HV 205
8.5.4 Effect of lesions 207
8.5.5 Clinical outcomes 208
8.6 DISCUSSION 209
8.7 LIMITATIONS 215
8.8 CONCLUSION 216
9. CHAPTER 9: DISCUSSION 217
9.1 INTRODUCTION 217
9.2 SUMMARY OF KEY FINDINGS 217
9.2.1 Overall research objectives (as described in Chapter 2) 217
9.2.2 Key findings 218
9.2.2.1 Clinical presentation of myelitis in MOGAD 218
9.2.2.2 Acute MRI findings 218
9.2.2.3 Long-term outcomes and follow-up imaging 219
9.2.2.4 Structural and quantitative MRI findings 219
9.2.2.5 Resting-state functional MRI 221
9.3 INTERPRETATION AND APPLICATION OF FINDINGS AND SUGGESTIONS FOR FUTURE WORK 223
9.3.1 A focus on MOGAD 223
9.3.1.1 The establishment of criteria for early and accurate diagnosis (i.e., what should prompt testing for MOG-antibody) 225
9.3.1.2 A better understanding of the underlying disease mechanisms and pathogenesis. 226
9.3.1.3 Predictors of outcomes such as relapse-risk and disability 227
9.3.2 A focus on spinal cord MRI 228
9.3.2.1 Clinical MRI 229
9.3.2.2 Non-conventional MRI 229
10. BIBLIOGRAPHY 232

1. Chapter 1: Introduction and background

1.1 Motivation for this thesis and terminology

Myelin-oligodendrocyte glycoprotein associated disease (MOGAD) is a recently described inflammatory demyelinating disorder of the central nervous system. Ongoing research into this condition shows it to be distinct from both aquaporin-4 (AQP4) antibody (Ab) neuromyelitis optica spectrum disorder (NMOSD) and multiple sclerosis (MS), although there is phenotypic overlap and much of the research into MOGAD is conducted in reference to these two more well-established conditions.

The spinal cord is often less well studied, particularly as imaging the cord presents unique challenges. However, spinal cord involvement is a hallmark feature of all three diseases and a central cause of disability, and so, is an important phenotype to study. A focus on spinal cord involvement also enables the study of these conditions in an eloquent area of the central nervous system, which is less affected by additional confounders such as non-specific lesions.

Over the period of time in which the research presented in this thesis was conducted our knowledge and understanding of MOGAD has grown exponentially. Much of what is described in this introductory chapter was not known when this work began. The publications from this study, which form part of this thesis, have added to the growing body of research into the study of spinal cord involvement in MOGAD, as it compares to AQP4-NMOSD and MS. Additionally, advanced spinal cord imaging techniques were used which add novelty to the research and its conclusions.

This chapter sets the context for the work presented in this thesis. It begins by reviewing our current understanding of MOGAD, as it compares to NMOSD and MS, with a focus on the features of spinal cord involvement in adult populations. It then describes the use of advanced MRI techniques used in spinal cord imaging. Existing literature, where these techniques have been applied to these conditions, is outlined and the clinical application is highlighted.

Throughout this thesis the term AQP4-NMOSD will be used to specify NMOSD with positive AQP4-Ab, as opposed to the antibody-negative cases; MOGAD will be used to describe patients with inflammatory demyelination and positive MOG-Ab; and in the case of MS, this will refer to relapsing-remitting MS, unless otherwise specified. In all tables and figures the conditions (and in later chapters healthy volunteers (HV)) will be represented consistently by the following colours and shapes:

■ MOGAD = blue/square

● AQP4-NMOSD = green/circle

▲ MS = red/triangle

◆ HV = orange/diamond

The only exception is in Chapter 8, where colours will be used to differentiate individual participants in the figures as it is of interest to track the individual across the dataset. This is clearly noted in the relevant figures.

1.2 Historical context

MS, as we know it today, was first described in 1866 when Jean-Martin Charcot and Edme Vulpian gave a report on the clinical features and autopsy findings of "*la sclerose en plaque disseminee*" to the Societe Medicale des Hopitaux (Murray, 2005), although the first report is thought to have been as early as 1824 as it appears in "*Maladies de la moelle epiniere*" by Charles Prosper Ollivier d'Angers (Murray, 2005).

Neuromyelitis optica was first described in 1894 by Eugene Devic and Fernand Gault who reported a case of optic neuritis and myelitis (neuro-myelite optique) (Devic, 1894). In this report they discuss its relationship with MS due to noted similarities in the pathological process and clinical picture. Until recently neuromyelitis optica was thought to be a variant of MS (Jarius and Wildemann, 2013). The discovery of antibodies to AQP4 in 2004 provided a biomarker that served to establish it as an entity distinct from MS (Lennon *et al.*, 2004, 2005). This also allowed for the establishment of a wider phenotype of disease attributable to AQP4-Abs.

The role of MOG and antibodies to MOG have been explored for decades. In particular, immunisation using MOG inducing experimental autoimmune encephalitis (EAE) has been established as an important model of MS (Gold *et al.*, 2006; Constantinescu *et al.*, 2011). Early studies of serum MOG-Ab suggested it may be present more commonly in MS than in HV or other neurological diseases (Karni *et al.*, 1999; Lindert *et al.*, 1999; Reindl *et al.*, 1999). However, there was a lack of consistency, and a large number of controls and patients with non-MS disorders that were also noted to be positive. It was the emergence of conformation-dependent assay for the detection of MOG-Ab by O'Conner et al. that

revealed, for the first time, the indication that in humans (first in children and later in adults) that these antibodies represent a distinct phenotype of central nervous system demyelination (O'Connor *et al.*, 2007). Finally, it was the establishment of a cell-based assay to full-length MOG and restriction to immunoglobulin-1 antibodies that provided an assay with improved specificity for a new clinical entity of non-MS demyelination (Waters *et al.*, 2015).

Initially, the testing and description of patients with positive MOG-Abs was largely limited to patients diagnosed with NMOSD but who were negative for AQP4-Ab (Kitley *et al.*, 2012*b*, 2013, 2014; Sato *et al.*, 2014). The idea that MOG-Ab should be grouped as a subset of NMOSD remained a controversial topic until recently, over the last two years, when it became clear that the presence of MOG-Ab represents a condition that is not limited to the definition of antibody-negative NMOSD. In more recent literature the term MOGAD was established as an acronym to denote this distinct disease.

From the above it is clear that these are three distinct conditions, but they are inextricably linked by their history and the phenotypic overlap. Therefore, in order to answer the many questions that still remain regarding in MOGAD it is important to study it alongside its two most important differentials.

1.3 The current understanding of MOGAD

This sub-chapter provides an overview of the current literature on MOGAD in comparison to AQP4-NMOSD and MS, with a focus on spinal cord involvement in adult populations relevant to the research conducted in this study.

1.3.1 Substrates and antibodies

MOG is a myelin protein that constitutes approximately 0.05% of total myelin proteins (Johns and Bernard, 1999), which are required for creation and function of myelin (Slavin *et al.*, 1997; Ramanathan *et al.*, 2016). The exact function of MOG is still unknown. Its expression begins later than that of other myelin proteins and it is, therefore, a late marker of oligodendrocyte maturation and thought to potentially play a role in the control and maintenance of myelination (Slavin *et al.*, 1997; Johns and Bernard, 1999). It is expressed on the outermost surface of the myelin sheath and the oligodendrocyte plasma membrane which facilitates its accessibility for autoantibodies (see Figure 1.1) (Reindl *et al.*, 2013). Interestingly, in a range of developmental animal models (mouse, rat, guinea pig and bovine) MOG displayed a caudo-rostral gradient of expression, appearing in the spinal cord before the brain (Slavin *et al.*, 1997). In rat models MOG expression exists in oligodendrocytes of both the white and grey matter of the spinal cord (Kang *et al.*, 2013).

Although MOG-Ab is a marker for MOGAD, the exact pathogenic role of these antibodies is also not yet well established. As described above, there has been an evolution in the development of MOG-Ab tests over the last few years and it is of the utmost important that the appropriate testing is done to avoid misdiagnosis. Live cell-based assays with specific secondary antibodies have proven to be the most specific, as described above (Waters *et al.*, 2015). All patients diagnosed with MOGAD for the purposes of this thesis were confirmed positive based on the methodology described by Waters et al.

In NMOSD, the discovery of the causative antibody, AQP4-Ab, defined this condition as a primary astrocytopathy causing secondary demyelination (Fujihara *et al.*, 2012; Lucchinetti

et al., 2014). This discovery facilitated the clinical, pathological and radiological distinction of NMOSD from MS. It is present in up to 70% of patients with NMOSD and plays a crucial role in diagnosis (Wingerchuk *et al.*, 2015). Cell-based assays have been shown to be the most sensitive and specific (Waters *et al.*, 2008; Wingerchuk *et al.*, 2014).

AQP4 (see Figure 1.1) is found in astrocytes of the white and grey matter along the whole spinal cord, strongly present in astrocytic end-feet encircling capillaries and building up the glia limitans as well as in the astrocyte processes enveloping myelinated neuronal fibres in the white matter. In the grey matter of the spinal cord AQP4 demonstrates a distinctive laminar pattern (Oklinski *et al.*, 2016).

However, it must be noted that in both AQP4-NMOSD and MOGAD, understanding the features of the conditions that increase the pre-test probability, prior to antibody testing, is essential to avoid false-positives (Jarius *et al.*, 2011, 2018). Therefore, studying the spinal cord features suggestive of MOGAD during an acute attack is important. Timing is also essential, as levels may fluctuate throughout the course of the disease and in response to treatment; in both cases antibodies appear to be increased at the time of the acute attack (Jurynczyk *et al.*, 2017*b*; Cobo-Calvo *et al.*, 2018). Thus, patients should preferably have serology sent for analysis before (or early in) the acute treatment because serum concentration of antibodies may decrease with immunotherapy and outside of an acute relapse (Mariano *et al.*, 2018). Antibodies in AQP4-NMOSD rarely become negative, unless low-positive to begin with, and in MOGAD, 8-25% of patients have been shown to have negative results on follow-up testing (Jurynczyk *et al.*, 2017*b*; Cobo-Calvo *et al.*, 2018).

Unlike AQP4-NMOSD and MOGAD, a specific autoantigen for MS has not been identified and so it does not meet the full definition of an autoimmune disease (Lemus *et al.*, 2018). Environmental, genetic and lifestyle factors have been implicated in MS; these include previous Ebstein-Barr virus infection, low vitamin D levels, adolescent obesity and gut microbiota (Ramagopalan and Sadovnick, 2011).

Figure 1.1 *A schematic representation of a neuron with the targets for AQP4-Ab (green), the AQP4 antigen on the astrocyte end-feet, and MOG-Ab (blue), the MOG myelin protein expressed on the outermost myelin sheath.*

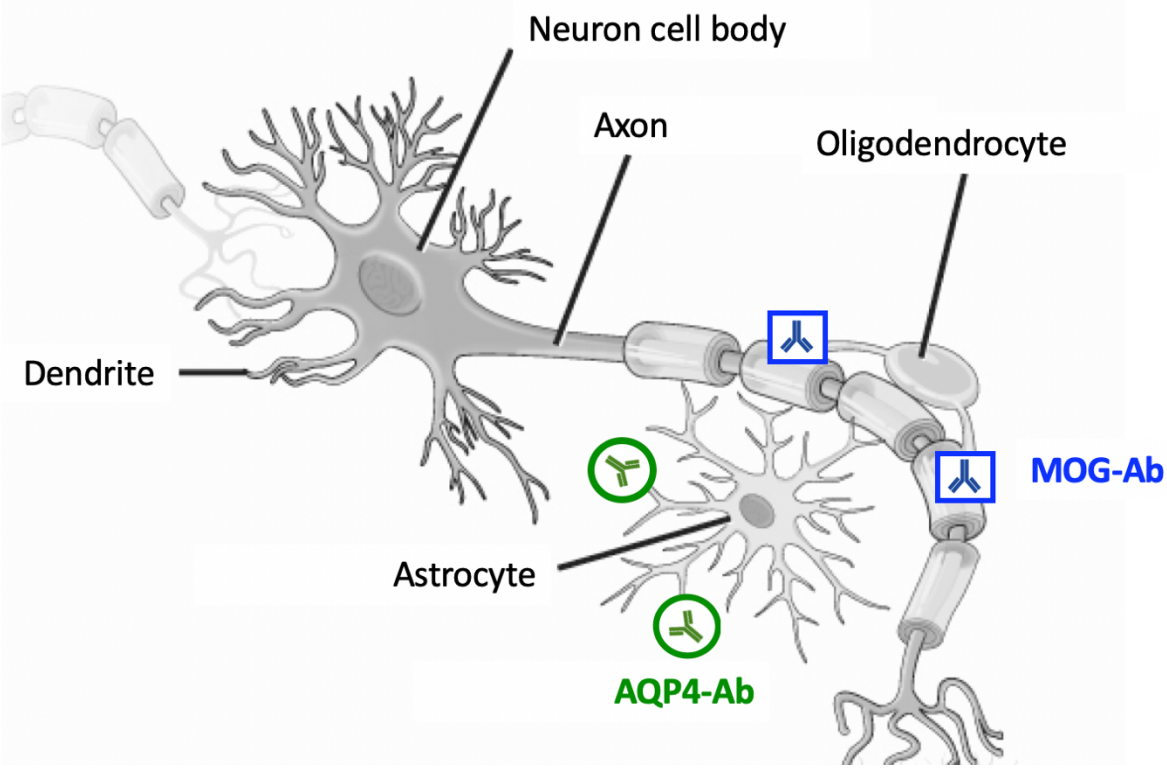


Image adapted from http://cnx.org/contents/GFy_h8cu@10.53:rZudN6XP@2/Introduction under licence CNX OpenStax, CC BY 4.0 <https://creativecommons.org/licenses/by/4.0>, via Wikimedia Commons

1.3.2 Pathology

Pathological distinction exists between all three conditions. The pathology of MS has been studied extensively, with the hallmark feature being the presence of focal demyelinated

plaques with varying degrees of inflammation, gliosis and neurodegeneration (Kuhlmann *et al.*, 2008). Active MS lesions show significant heterogeneity, and, on this basis, four different pathological patterns have been categorised (Lucchinetti *et al.*, 2000). Pattern 2 lesions are characterised by active demyelination, complement deposition and inflammation (Lucchinetti *et al.*, 2000). This is of interest as acute brain lesions in MOGAD have been described as similar to Pattern 2 MS lesions, with demyelination and activated complement. However, more recent studies have shown that MOGAD lesions are dominated by CD4+ T-cells and granulocytes, and not CD8+ T-cells and CD20+ B-cell infiltrates seen in MS (Höftberger *et al.*, 2020). AQP4-NMOSD has distinct pathology which can broadly be categorised by primary loss of AQP4 immunoreactivity on astrocytes, astrocyte loss, activation of complement and infiltration with inflammatory cells including lymphocytes and plasma cells (Misu *et al.*, 2007; Lucchinetti *et al.*, 2014; Popescu *et al.*, 2015).

Studies specific to pathology of spinal cord lesions in MOGAD have not yet been reported. In MS, post-mortem studies have described lesions and demyelination involving both the white and grey matter, with more demyelination noted in the grey matter upon direct comparison, neuronal loss and reduction in neuronal size (Gilmore *et al.*, 2009*b*, *a*). Atrophy was noted to not always be related to the presence of local lesions (Evangelou *et al.*, 2005). In AQP4-NMOSD the white matter and grey matter are both frequently and extensively involved. Histopathology shows perivascular lesions, white matter lesions, damage of grey matter astrocytes, holocord lesions and destruction with marked atrophy (Hayashida *et al.*, 2017). The myelin damage in AQP4-NMOSD is associated with less selective tissue destruction and necrotic changes (Lucchinetti *et al.*, 2014).

1.3.3 Epidemiology

1.3.3.1 Incidence and prevalence

As MOGAD is only recently described and assays are not yet widely available, the exact frequency of this condition is largely unknown. Additionally, studies are often conducted in tertiary referral centres and this may lead to selection bias. Moreover, the first studies of MOGAD were in the context of Ab-negative NMOSD criteria so other phenotypes would not have been considered (Kitley *et al.*, 2014; Sato *et al.*, 2014; Höftberger *et al.*, 2015).

A few recent studies have provided insight into the incidence and prevalence of this condition. In Catalonia, Spain, Sepulveda et al. described a prevalence of 0.12/100 000 and incidence of 0.09/million person-years (Sepúlveda *et al.*, 2018). In Denmark, Papp et al. described a prevalence of 0.18/100 000 and incidence of 0.13/million person-years (Papp *et al.*, 2018). A recent Dutch nationwide study reported an incidence of 1.6/million person-years (with a higher incidence of 1.3/million person-years in children) (de Mol *et al.*, 2020). However, perhaps most interestingly, a study in Oxford, United Kingdom, directly comparing the incidence and prevalence of MOGAD to AQP4-NMOSD found that MOGAD was nearly twice as common in the predominately white population: prevalence of 2.0/100 000 versus 1.2/100 000 and incidence of 3.4/million person-years versus 2.0/million person-years (O'Connell *et al.*, 2020).

The prevalence and incidence of NMOSD vary from 0.7-1.87/100 000 and 0.3-7.3/million person-years (Hor *et al.*, 2020), and this appears to be driven by ethnic differences.

While still considered a rare disease, MS is more common than both NMOSD and MOGAD, particularly with increasing distance from equatorial geographies (Alonso and Hernan, 2008). The United Kingdom prevalence is 120/100 000 but ranges from as low as 2.8/100 000 in Sub-Saharan Africa to 177/100 000 in high-income North America (Wallin *et al.*, 2019).

Unlike in MS (Rodríguez Cruz *et al.*, 2016), no seasonal variation has been noted in either NMOSD or MOGAD (Dos Passos *et al.*, 2020).

1.3.3.2 Demographics

While a female preponderance is described in both AQP4-NMOSD (9:1) (Hor *et al.*, 2020) and MS (2-4:1) (Compston and Coles, 2008), three large national studies of MOGAD, from the United Kingdom, France and Sri Lanka, have described 49-57% of patients as being female; therefore, sex ratios are considered to be roughly 1:1. The mean age of onset is 26-36 years. Ethnicity appears to mirror the local population. In the United Kingdom, patients were noted to be 85.7% white (local population 87.1% white); in France, 92.9% of patients with MOGAD were white (local population 87.1% white); and in Sri Lanka, 85.0% of MOGAD patients were Sinhalese (local population 75.0% Sinhalese) (Jurynczyk *et al.*, 2017*b*; Cobo-Calvo *et al.*, 2018; Senanayake *et al.*, 2018).

The mean age of onset in AQP4-NMOSD is 30-40 years and is more common in Afro-Caribbean populations (Hor *et al.*, 2020). MS typically occurs between 20-30 years and is more common in white populations (Compston and Coles, 2008).

1.3.4 Clinical presentation

Clinical presentations across all three conditions are dependent on the lesion location at the onset, with clinical manifestations of spinal cord involvement being a hallmark feature in all three conditions. In particular, MOGAD often clinically and radiologically resembles AQP4-NMOSD (Mader *et al.*, 2011, Kitley *et al.*, 2014; dos Passos *et al.*, 2018) and spinal cord involvement often occurs at the onset of the disease in both conditions, making it an important presentation to recognise and on which the diagnosis would be made.

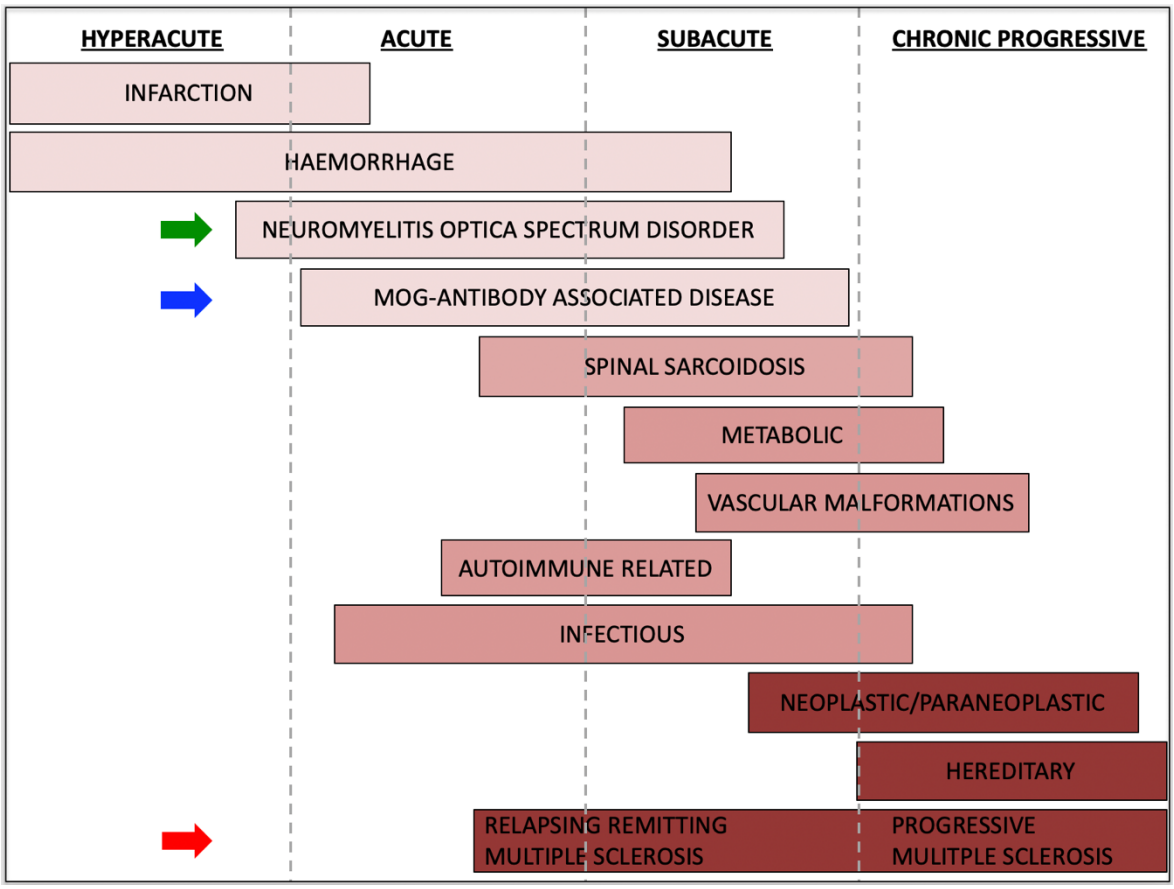
1.3.4.1 Spinal cord presentation

In MOGAD spinal cord disease has been reported in roughly 27-30% of presentations and the frequency of this presentation is age-related, more commonly occurring in adult patients (Jurynczyk *et al.*, 2017*b*; Cobo-Calvo *et al.*, 2018). In AQP4-NMOSD spinal cord disease occurs in 40% of patients (Pandit *et al.*, 2015). Up to 83% of patients with MS have spinal cord involvement (Muccilli *et al.*, 2018), although cord lesions in up to 31.2% of patients may be asymptomatic (Granella *et al.*, 2017).

Symptoms of spinal cord involvement tend to be acute or subacute (onset of days to weeks) as shown in Figure 1.2 alongside other important differentials of spinal cord disease (Mariano *et al.*, 2018). In adults, inflammatory myelitis is the most common cause of an acute or subacute spinal cord presentation (Mariano *et al.*, 2018). Very rarely AQP4-NMOSD has been reported to present hyper-acutely and can risk being misdiagnosed as a vascular event (Suchdev *et al.*, 2017). Differentiating these conditions from other conditions that cause spinal cord disease is aided by differences in imaging findings and other investigations, which are shown in Table 1.1. Both Figure 1.2 and Table 1.1 were

adapted from Mariano et al. 2018. At the time of publication, patients with MOGAD were included in the NMOSD category and so both the figure and table have been edited to show that MOGAD is now a separate and distinct entity. This, again, underscores the rapid evolution of this disease over the duration of this study.

Figure 1.2 Onset timeline. *The acute onset timeline of spinal cord involvement of MOGAD (blue arrow), AQP4-NMOSD (green arrow) and MS (red arrow) in the context of other differentials of acute spinal cord disease. Figure adapted from* (Mariano *et al.*, 2018).



Patients with spinal cord disease typically present with either motor impairment or sensory impairment of the upper and lower extremities, with or without sphincter dysfunction. Both the EDMUS (Confavreux *et al.*, 1992) or EDSS (Kurtzke, 1983) are well recognised methods of capturing severity of disability, having been validated in patients with MS (Cohen *et al.*, 2012). Although these have not been specifically validated with those with

AQP4-NMOSD or MOGAD, they are widely used in clinical practice. While both capture neurological manifestations that localise to the spinal cord, they are predominantly measures of motor function and, as a result, other important outcomes, such as sphincter dysfunction, pain and fatigue, may be overlooked. Although the bowel-bladder Functional System Score of the EDSS score captures self-reported bladder, bowel and sexual dysfunction (Kurtzke, 1983), specialised testing is required for quantitative assessment (Panicker *et al.*, 2015). Despite this, they still provided a standardised manner in which to capture disability acutely which can then be compared to the same scoring methodology at recovery. However, pain and fatigue are both important symptoms to consider as they both occur in MOGAD and AQP4-NMOSD and have been shown to be associated with spinal cord presentations (Kanamori *et al.*, 2011; Kong *et al.*, 2016, Tackley *et al.*, 2016*b*; Masuda *et al.*, 2020).

Both MOGAD and AQP4-NMOSD commonly have severe presentations of spinal cord involvement with significant disability at nadir (Jurynczyk *et al.*, 2017*b*; Cobo-Calvo *et al.*, 2018). In MS severe presentations are considered to be far less frequent and patients may present with sensory symptoms that occur in the absence of objective neurological signs on examination even when seen during relapse (Palace, 2001).

Table 1.1 Differentials in the diagnosis of spinal cord lesions. *Characteristics of the differential diagnoses of spinal cord lesions. *CSF may show variable pleocytosis or mildly raised protein, not specific, may be dependent on sample timing. Table adapted from* (Mariano *et al.*, 2018).

Differential	MRI Sagittal	MRI Axial	CSF	Other	Confirmatory
NMOSD	Typically long (>3 vertebral segments). T1 hypointense and T2 hyperintense.	Central grey matter involvement; bright spotty lesion on T2.	* Oligoclonal bands uncommon (10%); IgG index rarely raised (8%)	Optic neuritis; brainstem symptoms	Aquaporin-4 antibody testing
MOGAD	Typically long (>3 vertebral segments). Conus involvement. Growing evidence for short lesions and multiple lesions.	Central cord involvement.	* Oligoclonal bands uncommon (12-13%)		MOG antibody testing
MS	Short lesions, often <1 vertebral segment and consistently <3.	Postero-lateral lesions (<half the axial area).	* Oligoclonal bands 85-95% MS and 70% clinically isolated syndrome	Abnormal visual evoked potentials (30%)	Diagnostic criteria
Atypical MS (long standing or primary progressive)	Long diffuse or confluent lesions may occur.	Diffuse cord involvement may be a feature found in primary progressive MS.	* Oligoclonal bands >95% MS and 70% clinically isolated syndrome	Abnormal visual evoked potentials (>50%)	Diagnostic criteria
Paraneoplastic	Usually long (>3 vertebral segments). However, MRI may be normal.	Central grey matter/tract-specific; symmetrical.	*	Diagnosis of malignancy	Antineuronal antibody testing

Differential		MRI Sagittal	MRI Axial	CSF	Other	Confirmatory
Sarcoid		Variable length but more often long (>3 vertebral segments). Variable enhancement; minimal cord enlargement; enhancing nodules.	Variable: dorsal cord subpial GAD enhancement may help differentiate from NMOSD.	* Oligoclonal bands uncommon; CSF ACE (not sensitive)	Lung/eyes/skin involvement	Biopsy
Vascular	**Infarction**	Typically long (>3 vertebral segments). Do not enhance with contrast; 'pencil-like' lesion.	Tract specific: most commonly anterior and often involvement of anterior horn cells leads to snake/owl eye appearance; associated vertebral body infarct 4-35%.	Normal (may be abnormal with underlying spinal disease)	Onset typically sudden; pain at level of lesion (59-70%)	MRI and clinical findings
	Malformation	Commonly long (>3 vertebral segments). Conus involved in >80% of cases; dilated perimedullary vessels enhance on T1 and seen as flow voids on T2.	Oedema seen as centromedullary T2 hyperintensity; vessels (flow voids) on dorsum.	* Oligoclonal bands (27%)	Typically patients fluctuate with exercise	Spinal angiogram
	Haemorrhage	Long or short lesions may occur. MRI changes vary with time due to ageing of blood.	Intra/extra-medullary mass; low central signal with border of increased signal.	* Xanthrochromia possible	Commonly associated with underlying vascular malformation	MRI

Differential		MRI Sagittal	MRI Axial	CSF	Other	Confirmatory
Metabolic		Typically long (>3 vertebral segments). Contrast enhancement is rare.	Symmetric T2 hyperintensity dorsal tracts.	*	Variable cytopenias; typically anaemia	B12/copper levels/genetic testing
Infective	**Viral**	Usually long (>3 vertebral segments), but length may be variable.	Predominantly central grey matter.	*	Prodromal illness	Difficult to confirm
	Tuberculosis	More commonly short (<3 vertebral segments).	White matter nodules or target lesions.	Marked pleocytosis and raised protein	Constitutional symptoms; lung/lymph nodes	Polymerase chain reaction
	Parasitic	More commonly short (<3 vertebral segments).	Eccentric nodular pattern.	*	Systemic features of infection	Antibody testing
Neoplastic	**Astrocytoma**	Variable length. Heterogenous or no enhancement; irregular margins.	Eccentric location; may be exophytic and appear extramedullary.	* Cytology may be more useful than in cerebral malignancy	Neurofibromatosis I	Biopsy
	Ependymoma	Variable length. Rostral and caudal cysts; homogenous enhancement (75%); clear borders.	Variable but more commonly central than other malignancies.	* Cytology may be more useful than in cerebral malignancy		Biopsy
	Metastatic	Short lesions most common.	Eccentric location.	* Cytology may be more useful than in cerebral malignancy		MRI and biopsy (primary or spinal cord)

1.3.4.2 Other clinical presentations

In MOGAD, patients most commonly present with optic neuritis and this is often bilateral. Other presentations include acute disseminating encephalomyelitis (ADEM), which is most common in children, brainstem attacks and, more recently, cortical disease and seizures have also been described (Ogawa *et al.*, 2017) as well as reports of acute flaccid myelitis (Dubey *et al.*, 2019). Patients may also present with a combination of features and some may fulfil the criteria for antibody-negative NMOSD (Hamid *et al.*, 2017). The NMOSD diagnostic criteria is discussed in more detail below and are shown in Table 1.3.

Similarly, in AQP4-NMOSD, in addition to spinal cord involvement, patients often present with optic neuritis, area postrema syndrome (the archetypal presentation, of severe and protracted vomiting with or without hiccoughs) (Wingerchuk *et al.*, 2015), and, less commonly, encephalopathy may occur with large lesions in the brain parenchyma, inappropriate ADH secretion may be caused by lesions in the hypothalamus (Pu *et al.*, 2015), and daytime somnolence, memory disturbance and behavioural changes have been reported with lesions in the brainstem and hypothalamus (Viegas *et al.*, 2009). Of note, area postrema syndromes, subsequently followed by a spinal cord presentation, may risk a misdiagnosis of a post-infective cause of myelitis. The length and severity of the vomiting, which persist for weeks without other gastrointestinal manifestations, are suggestive of AQP4-NMOSD (Mariano *et al.*, 2018).

1.3.5 Disease course and outcomes

Comparative studies between MOGAD and AQP4-NMOSD show that, despite similar onset severity, MOGAD appears to be overall milder, with better recovery and fewer relapses

(Kitley *et al.*, 2013, 2014; Sato *et al.*, 2014). Motor disability at follow-up is less frequent but bladder, bowel and erectile dysfunction is common with spinal cord involvement and long-term visual impairment can occur after optic neuritis (Jurynczyk *et al.*, 2017*b*; Juryńczyk *et al.*, 2019).

Disability in MOGAD is relapse-related and appears to be driven by the degree of recovery from the onset attack and may also be related to the overall number of attacks (Jurynczyk *et al.*, 2017*b*). However, there is heterogeneity in terms of the clinical course described by recent studies. This heterogeneity may be due to age-related differences. MOGAD was first described in a paediatric population and so many studies are either of children alone or include both adults and children. Young children have been shown to have faster and better recovery than older children and adults (Cobo-Calvo *et al.*, 2018). Another reason for the heterogeneity may be that a bias exists in current studies as many monophasic MOGAD patients would not present acutely and so remain undiagnosed; studies that have included predominantly relapsing cohorts have shown poorer outcomes (Jarius *et al.*, 2016*b*, *a*). Finally, it may be that the heterogeneity is a feature of the condition and so understanding what drives these differences would be essential.

Predictors of relapse and disability are largely unknown, although there has been some suggestion that patients who become seronegative may be less likely to relapse in future (Jurynczyk *et al.*, 2017*b*; Cobo-Calvo *et al.*, 2018). Relapses have been reported in 34-46% of patients in cohort studies (Jurynczyk *et al.*, 2017*b*; Cobo-Calvo *et al.*, 2018; Senanayake *et al.*, 2018). The dominant relapse phenotype is optic neuritis (Jurynczyk *et al.*, 2017*b*).

In AQP4-NMOSD, the presence of AQP4-Ab itself is a predictor of relapse (Weinshenker *et al.*, 2006). Patients typically relapse if left untreated, with each relapse carrying the risk of increased disability (Tackley *et al.*, 2016*a*). Relapse rates have been noted to be higher in Afro-Caribbean ethnicity, in children and in those with a shorter disease duration. Relapse rates are lower in treated patients, and disability outcomes are better in treated patients (Tackley *et al.*, 2016*a*). Relapses can be severe and disabling but a gradual progression of the disease is exceedingly rare (Wingerchuk *et al.*, 2007).

In MS, after the initial attack (defined as clinically isolated syndrome), around 85% of patients have a disease course characterised by a recurrence of attacks, which is known as the relapsing-remitting phase. In this phase the majority of the disability is related to relapses, with an average relapse frequency of 1.1 per year (Patzold and Pocklington, 1982). Most patients will then enter a progressive phase where disability accumulates independently of relapses, known as secondary progressive MS. Age is one of the strongest predictors of entry into the secondary progressive phase (Vukusic and Confavreux, 2003). For the purposes of the research presented in this thesis, recruited patients were limited to those with relapsing-remitting MS, as this phase most closely resembles the relapsing course of the antibody-mediated conditions and evidence of disability accumulation outside of relapse would strongly suggest against either MOGAD or AQP4-NMOSD.

In addition to the above, a specific study on the clinical presentation and outcomes in MOGAD myelitis, as it compares to AQP4-NMOSD, has been described in Mariano et al. 2019 (Mariano *et al.*, 2019). This study forms the content of Chapter 3. Another study specific to myelitis in MOGAD will be discussed alongside the findings of this study presented in Chapter 3 (Dubey *et al.*, 2019).

1.3.6 MRI features

MRI is an essential tool in the diagnosis and management of neuroinflammatory conditions and features significantly in both the diagnostic criteria for NMOSD (Table 1.3) and MS (Table 1.4). Additionally, MRI aides in excluding other differential diagnoses (Table 1.1). MRI lesions in the spinal cord are also exceptionally useful for differential diagnosis as they do not occur in most common neurological conditions, such as migraine and cerebrovascular disorders, which are often associated with non-specific multifocal white matter lesions in the brain which may be difficult to interpret (Geraldes *et al.*, 2018).

Spinal cord MRI recommendations will be considered, together with the typical features of spinal cord involvement in the three conditions, after which the brain MRI features will be discussed. All the MRI images shown below as examples are shown with permission for the use of clinical images under the Oxford MS and NMOSD Tissue Bank (REC reference number: 16/SC/0224).

1.3.6.1 Spinal cord imaging

Spinal cord clinical imaging recommendations

Spinal cord MRI provides for a means of direct evaluation of the cord and of intrinsic focal lesions, such as those present in MOGAD, AQP4-NMOSD and MS. The overall diagnostic and prognostic value of routine spinal cord MRI in patients with spinal cord disease has not been well established.

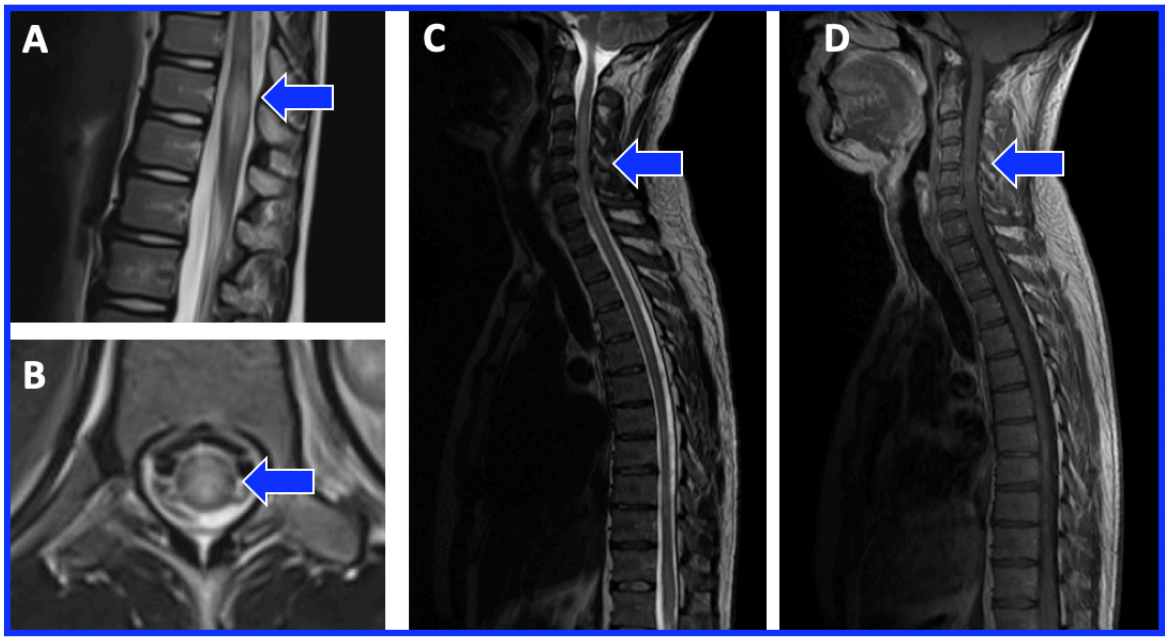
Recommendations for the assessment of focal spinal cord lesions are to include a combination of at least two sagittal sequences, either two T2-weighted sequences

(standard T2, proton density weighted, short tau inversion recovery, phase-sensitive inversion recovery) or the combination of a T2-weighted sequence combined with a T1-weighted image (Filippi *et al.*, 2019). Lesions should also ideally be confirmed on axial imaging (Weier *et al.*, 2012), as it can assist in determining the significance of equivocal abnormalities seen on sagittal imaging (Weier *et al.*, 2012).

Spinal cord MRI features

Initial studies of MOGAD in adults were predominantly in patients with antibody-negative NMOSD and this may have led to a selection bias for the description of the typical longitudinally extensive transverse myelitis (LETM) seen in AQP4-NMOSD. When larger cohorts of MOGAD were studied, although LETM remains common, some important differences were noted. Patients with MOGAD more frequently have short cord lesions on MRI, particularly with older age at presentation (Jurynczyk *et al.*, 2017*b*). Lesions tend to involve the lower thoracic cord more commonly and, in particular, lesions in the conus were noted to be a prominent feature (Kitley *et al.*, 2014; Sato *et al.*, 2014). This prompted specific research into the acute MRI findings in MOGAD and this study forms the content of Chapter 3. Two other recent studies that describe important imaging features in MOGAD myelitis are discussed alongside the work in Chapter 3 (Dubey *et al.*, 2019; Ciron *et al.*, 2020). Figure 1.3 shows examples of spinal cord MRI features in MOGAD; additional images are shown in Chapter 3. Asymptomatic lesions have not been described in MOGAD myelitis but recently cases of symptomatic myelitis with no abnormalities detected in MRI have been reported (Pérez *et al.*, 2019; Sechi *et al.*, 2020). This will be discussed further in Chapter 6.

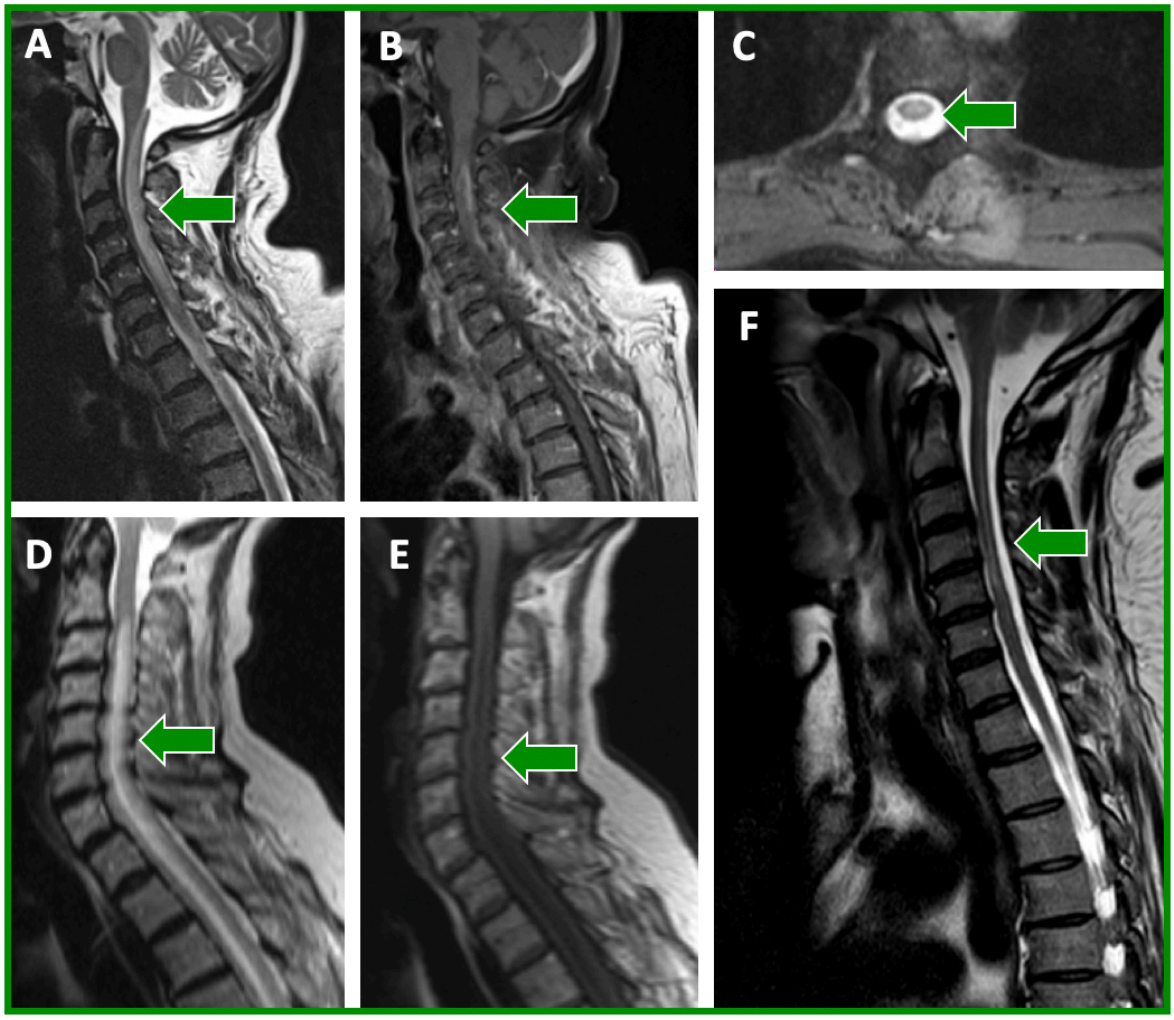
Figure 1.3 Spinal cord MRI in MOGAD. *Examples indicated by blue arrows of T2-weighted imaging showing (A) a conus lesion, (B) central cord involvement and (C) a long lesion (>3 vertebral segments) in the cervical cord; with (D) the corresponding T1-weighted image showing gadolinium enhancement.*



The most common cord lesion in AQP4-NMOSD is that of LETM, which denotes a lesion of ≥3 vertebral segments on sagittal imaging (Tackley *et al.*, 2014; Kim *et al.*, 2015). Lesions are hyperintense on T2-weighted imaging and hypointense on T1-weighted imaging (Kim *et al.*, 2015), unlike in MS, for which acute T1 hypointensity is rare (Valsasina *et al.*, 2018). Lesions in AQP4-NMOSD are reported to be more frequent in the cervical and upper thoracic cord (Cassinotto *et al.*, 2009; Asgari *et al.*, 2013). On axial imaging lesions are commonly central, with preferential involvement of the grey matter (Cassinotto *et al.*, 2009). Cervical cord lesions may extend into the medulla and, when this is associated with the typical symptoms of area postrema syndrome described above, this is considered to be highly suggestive of NMOSD (Dubey *et al.*, 2017). Gadolinium enhancement is common, most often patchy and irregular, and ring-enhancing lesions develop in about one-third of patients; this may distinguish AQP4-NMOSD from other causes of LETM but does not

distinguish it from MS (Zalewski *et al.*, 2017). 'Bright spotty lesions' (persistent areas of marked T2 hyperintensity within lesions) are characteristic of NMOSD (Hyun *et al.*, 2015). Although LETM is included in the diagnostic criteria for NMOSD, up to 14% may present with lesions shorter than three vertebral segments at the time of their initial myelitis presentation (Flanagan *et al.*, 2015*a*). Asymptomatic lesions have been reported in patients with AQP4-NMOSD, but are uncommon and are suspected to occur in <5% of cases (Collongues *et al.*, 2011, Flanagan *et al.*, 2015*b*). These lesions were found on imaging done as part of a work-up for acute presentations involving other areas of the central nervous system (optic nerve or brainstem) and do not appear to represent silent lesions outside of an acute relapse, which is typical of MS. The significance of these silent lesions in terms of predicting future attacks or disability is unknown. Follow-up imaging is heterogenous with lesions evolving into shorter lesions and with atrophy noted, particularly as a consequence of recurrent myelitis (Kim *et al.*, 2015). Figure 1.4 shows examples of spinal cord MRI features in AQP4-NMOSD.

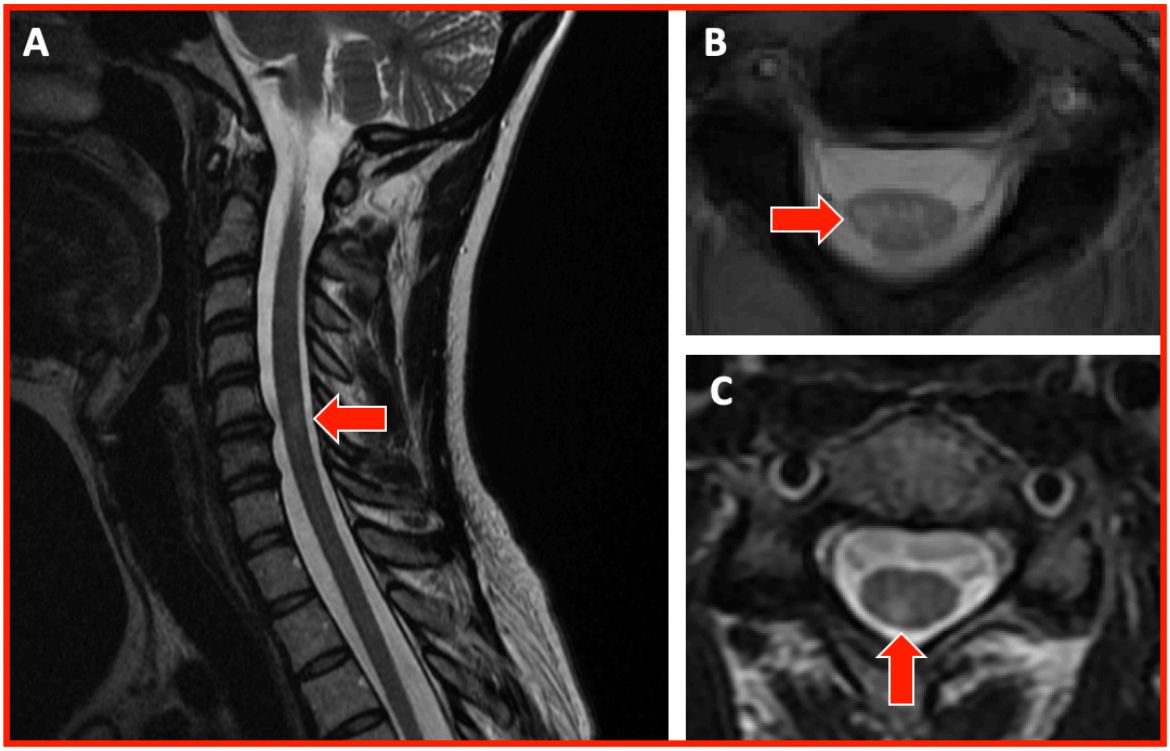
Figure 1.4 Spinal cord MRI in AQP4-NMOSD. *Examples indicated by green arrows showing (A) a long lesion (>3 vertebral segments) on T2-weighted imaging with the corresponding T1-weighted, gadolinium enhancement shown in (B); (C) central cord involvement; (D) another example of an acute long lesion with corresponding T1 hypo-intensity shown in (E); and finally, (F) a chronic lesion with atrophy.*



In MS, spinal cord lesions are typically short (defined as <3 vertebral segments) and usually less than one segment (Ciccarelli *et al.*, 2019). The lesions are partial and asymmetrical on axial views and are typically wedge-shaped. They may occur along the entire spinal cord but most frequently involve the cervical cord (Bot *et al.*, 2004; Eden *et al.*, 2019). Only a few of these cord lesions enhance with gadolinium (Rovira and De Stefano, 2016). Lesions are most commonly posterior or lateral but can also involve the grey matter (Ciccarelli *et al.*, 2019). Occasionally in MS, most typically in progressive subtypes, the presence of

diffuse cord involvement may mimic an LETM and lead to diagnostic uncertainty (Bergers *et al.*, 2002; Asnafi *et al.*, 2020). However, careful assessment of high-resolution axial images usually demonstrates discrete lesions which have coalesced and lead to the artefactual appearance of an LETM (Asnafi *et al.*, 2020). Asymptomatic lesions are also typical in MS and may occur in up to 83% of patients with early relapsing remitting MS (Bot *et al.*, 2004). Figure 1.5 shows examples of spinal cord MRI features in MS.

Figure 1.5 Spinal cord MRI in MS. *Examples indicated by red arrows of (A) a short (<3 vertebral segments) lesion on T2-weighted sagittal imaging and typical (B) lateral and (C) posterior asymmetrical lesions on axial T2-weighted imaging.*



1.3.6.2 Brain imaging

Brain MRI features are also important, even when the onset presentation can be localised clinically to the spinal cord. A summary of the brain MRI features in each condition is reflected in Table 1.2 and example images in Figures 1.6 – 1.8.

Table 1.2 Brain MRI. *Summary of the brain MRI findings in MOGAD, AQP4-NMOSD and MS.*

Brain MRI features	**MOGAD**	**AQP4-NMOSD**	**MS**
Normal/ abnormal	Abnormal in approximately 45% of patients at onset (Cobo-Calvo *et al.*, 2018; Ramanathan *et al.*, 2018)	Abnormal in 50-85% (Kim *et al.*, 2015), most commonly non-specific lesions (Matthews *et al.*, 2013)	Abnormal in 95% (Yetkin *et al.*, 1991)
Typical lesions in the brain	• Poorly demarcated "fluffy" lesions, infratentorial, brainstem or cerebellar peduncles, often adjacent to the 4th ventricle (Jurynczyk *et al.*, 2017*a*) • Thalamus and pons/bilateral or unilateral cortical involvement(Cobo-Calvo *et al.*, 2018) • Asymptomatic brain lesions in 20-50% (Baumann *et al.*, 2015; Salama *et al.*, 2019)	• Typical lesions occur in areas of high AQP4 expression (area postrema, brainstem, hypothalamus, periependymal tissue bordering the lateral, third and fourth ventricles and the Sylvian aqueduct • (Tackley *et al.*, 2014; Kim *et al.*, 2015) • Non-specific lesions are usually asymptomatic, while typical lesions are usually symptomatic. (Kim *et al.*, 2015)	• U or S shaped juxtacortical lesions • Cortical lesions • Periventricular lesions including the classic ovoid periventricular lesion or 'Dawson finger' • (Geraldes *et al.*, 2018; Filippi *et al.*, 2019)
Typical lesions in the optic nerves	Anterior involvement, often bilateral.	Long posterior optic nerve lesions often involving the chiasm (Kim *et al.*, 2015).	Unilateral short lesions (Filippi *et al.*, 2019).

Figure 1.6 Brain MRI in MOGAD. *Examples indicated by blue arrows of (A) bilateral cerebellar peduncle lesions, (B) cortical involvement, (C) fluffy large and bilateral lesions in pons and cerebellar peduncles, adjacent to fourth ventricle, (D) fluffy parenchymal lesions, (E) anterior optic nerve involvement and (F) bilateral fluffy lesions in the thalami.*

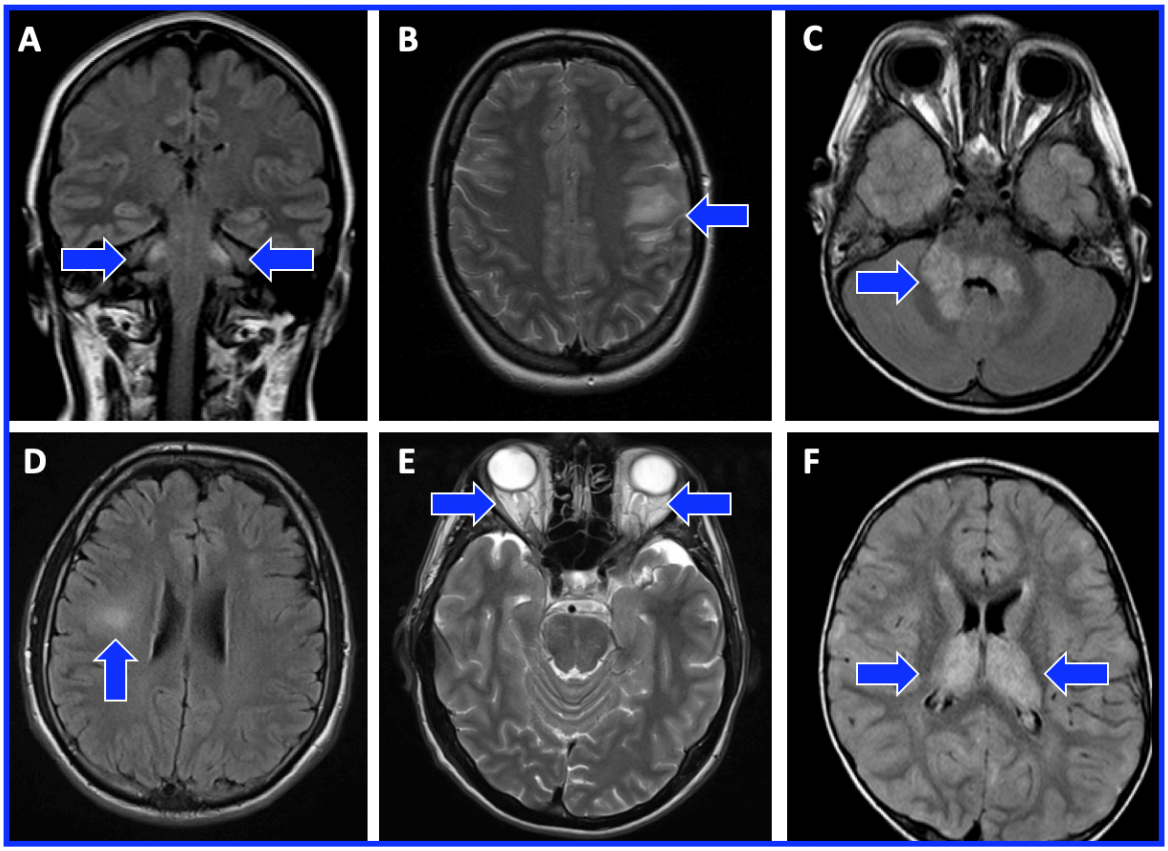


Figure 1.7 Brain MRI in AQP4-NMOSD. *Examples in indicated by green arrows of (A) a lesion in the dorsal medulla, (B) bilateral diencephalic hyperintensities, (C) lesions adjacent to the third ventricle, (D) a long optic nerve lesion with chiasm involvement, and (E) a coronal view of chiasm hyperintensity.*

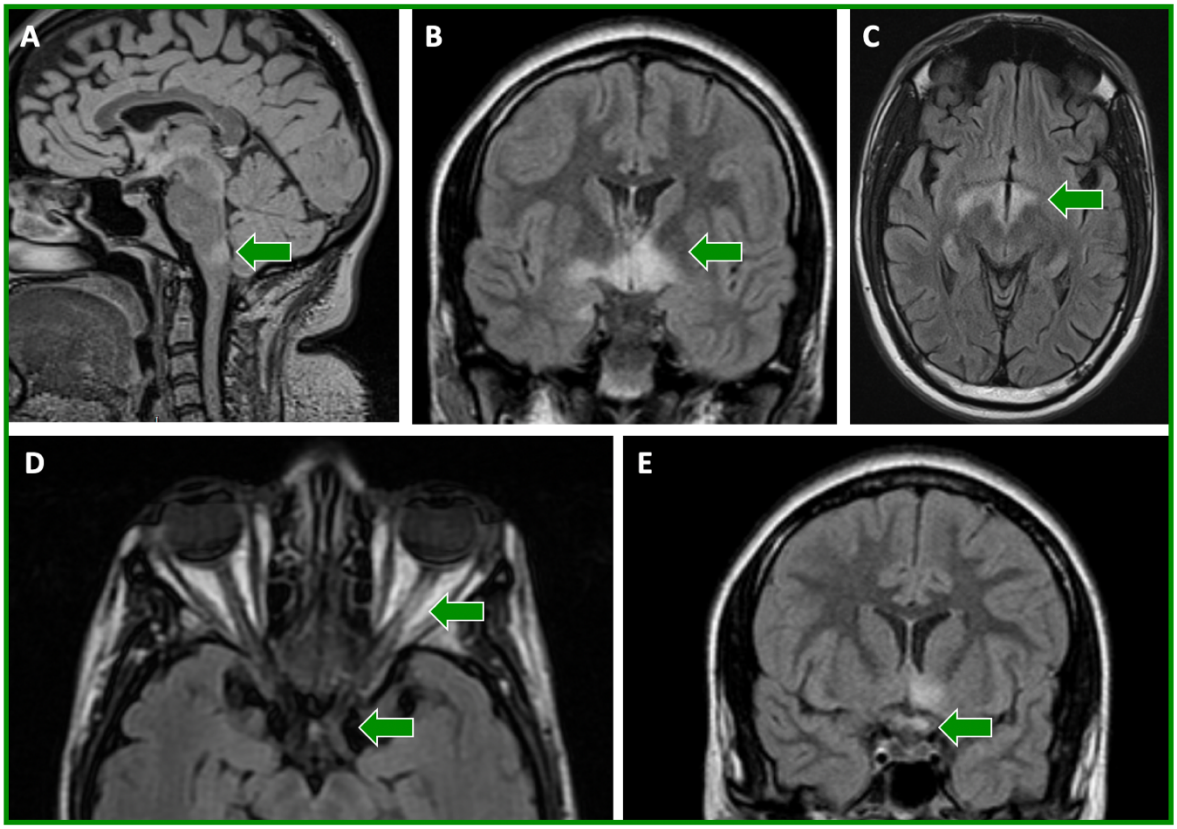
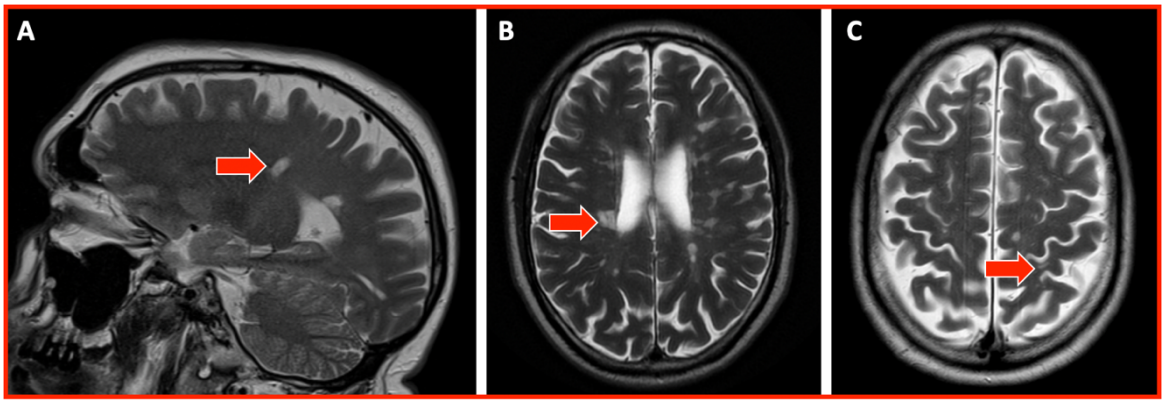


Figure 1.8 Brain MRI in MS. *Examples indicated by red arrows showing (A) A 'Dawson finger', visible as an ovoid, hyperintense, periventricular lesions perpendicular to the body of the lateral ventricle, (B) a periventricular lesion and (C) a juxtacortical lesion.*



1.3.7 Other relevant investigations for spinal cord presentation

Both cerebrospinal fluid (CSF) examination and somatosensory evoked potentials are useful investigations in the assessment of spinal cord disease. In particular, CSF oligoclonal bands are much more common in MS, positive in 85-95% of clinically definite MS and in 70-92% of patients with clinically isolated syndrome (Brändle *et al.*, 2016). In contrast, they are present in 10-20% of patients with AQP4-NMOSD (Wingerchuk *et al.*, 2015) and approximately 12-13% of patients with MOGAD (Jurynczyk *et al.*, 2017*b*; Jarius *et al.*, 2020). In the individual patient the presence of oligoclonal bands may be of limited diagnostic value if considered in isolation, and so should be considered in the context of other investigations. The presence of oligoclonal bands was recently updated to evidence dissemination in time as part of the 2017 McDonald criteria for MS (see Table 1.4) (Thompson *et al.*, 2018).

The slow conduction and loss of amplitude that may be noted on somatosensory evoked potentials are not pathologically specific (Leocani *et al.*, 2006). In AQP4-NMOSD, reduced or absent responses are more common than decreased latency and asymptomatic changes are uncommon (Ohnari *et al.*, 2016). The degree of abnormality in testing usually mirrors the severity of the attack (Tsao *et al.*, 2014). In MS, asymptomatic changes may occur, and multimodal evoked potentials correlate with EDSS and may predict disease progression over three years (Schlaeger *et al.*, 2014*b*). In MOGAD, normalisation of somatosensory evoked potentials after recovery from myelitis has been described (Kitley *et al.*, 2014). This may be a relevant finding and is discussed further in Chapter 6.

1.3.8 Diagnosis and diagnostic challenges

Both AQP4-NMOSD and MS have established criteria that have recently been updated, shown in Table 1.3 and Table 1.4 respectively (Wingerchuk *et al.*, 2015; Thompson *et al.*, 2018). Table 1.3 includes the more stringent criteria for antibody negative NMOSD (Wingerchuk *et al.*, 2015). No current diagnostic criteria exist for MOGAD.

As described above, initial testing for MOG-Ab in adults was conducted predominantly in antibody-negative NMOSD. Subsequent studies have considered this relationship from two perspectives: first, they have shown that up to 50% of patients diagnosed with antibody negative NMOSD were in fact MOG-Ab positive (Hamid *et al.*, 2018); secondly, they have looked at cohorts of MOGAD patients, finding that 5-20% of patients fulfil the antibody negative NMOSD criteria acutely and 19-32% do so at follow-up, with the higher percentages occurring in those that are relapsing (Jarius *et al.*, 2016*a*, Jurynczyk *et al.*, 2017*b*; Cobo-Calvo *et al.*, 2018; Ramanathan *et al.*, 2018). However, the increasing spectrum of clinical presentations associated with MOG-Ab means that if only these diagnostic criteria are applied many patients will likely be missed, as many possible MOGAD presentations, or combinations thereof, would not fulfil this diagnosis criteria (Juryńczyk *et al.*, 2019). The use of the antibody-negative NMOSD criteria would, in fact, exclude a patient with isolated cord involvement from being tested for MOG-Ab (Juryńczyk *et al.*, 2019). Additionally, the short lesions being increasingly described in MOGAD (detailed in Chapter 3), would be considered a 'red flag' (Wingerchuk *et al.*, 2015), further evidencing the need for the study of clinical features of myelitis in MOGAD that would motivate for MOG-Ab testing in the absence of other features of NMOSD.

Table 1.3 2015 NMOSD diagnostic criteria. *Extracted from (Wingerchuk et al., 2015)*

Diagnostic criteria for NMOSD with AQP4-Abs	1. At least one core clinical characteristic 2. Positive test for AQP4-Ab using best available detection method (cell-based assay strongly recommended) 3. Exclusion of alternative diagnoses
Diagnostic criteria for NMOSD without AQP4-Abs or NMOSD with unknown AQP4-Ab status	1. At least two core clinical characteristics occurring as a result of one or more clinical attacks and meeting all of the following requirements: a. At least one core clinical characteristic must be optic neuritis, acute myelitis with LETM, or area postrema syndrome b. Dissemination in space (two or more different core clinical characteristics) c. Fulfilment of additional MRI requirements, as applicable 2. Negative tests for AQP4-Ab using best available detection method, or testing unavailable 3. Exclusion of alternative diagnoses
Core clinical characteristics	1. Optic neuritis 2. Acute myelitis 3. Area postrema syndrome 4. Acute brainstem syndrome 5. Symptomatic narcolepsy or acute diencephalic clinical syndrome with NMOSD-typical diencephalic MRI lesions 6. Symptomatic cerebral syndrome with NMOSD-typical brain lesions
Additional MRI requirements for NMOSD without AQP4-Abs and NMOSD with unknown AQP4-Abs status	1. Acute optic neuritis: requires brain MRI showing (a) normal findings or only nonspecific white matter lesions, OR (b) optic nerve MRI with T2-hyperintense lesion or T1-weighted gadolinium enhancing lesion extending over half the optic nerve length or involving optic chiasm 2. Acute myelitis: requires associated intramedullary MRI lesion extending over >3 contiguous segments (LETM) OR >3 contiguous segments of focal spinal cord atrophy in patients with history compatible with acute myelitis 3. Area postrema syndrome: requires associated dorsal medulla/area postrema lesions 4. Acute brainstem syndrome: requires associated periependymal brainstem lesions

Table 1.4 2017 McDonald criteria for the diagnosis of multiple sclerosis. *Extracted from* (Thompson *et al.*, 2018)

Diagnostic criteria		
	Number of lesions with objective clinical evidence	**Additional data needed for a diagnosis of MS**
≥2 clinical attacks	≥2	None
≥2 clinical attacks	1 (as well as clear-cut historical evidence of a previous attack involving a lesion in a distinct anatomical location)	None
≥2 clinical attacks	1	Dissemination in space demonstrated by an additional clinical attack implicating a different CNS site or by MRI
1 clinical attack	≥2	Dissemination in time demonstrated by an additional clinical attack or by MRI **OR** demonstration of CSF-specific oligoclonal bands
1 clinical attack	1	Dissemination in space demonstrated by an additional clinical attack implicating a different CNS site or by MRI **AND** Dissemination in time demonstrated by an additional clinical attack or by MRI **OR** demonstration of CSF-specific oligoclonal bands
MRI criteria for dissemination in space and time		
Space	Dissemination in space can be demonstrated by one or more T2-hyperintense lesions that are characteristic of multiple sclerosis in two or more of four areas of the CNS: periventricular, cortical or juxtacortical, and infratentorial brain regions, and the spinal cord	
Time	Dissemination in time can be demonstrated by the simultaneous presence of gadolinium-enhancing and non-enhancing lesions at any time or by a new T2-hyperintense or gadolinium-enhancing lesion on follow-up MRI, with reference to a baseline scan, irrespective of the timing of the baseline MRI	

1.3.9 Treatment

A detailed description of all treatment options for each condition is outside of the scope of this thesis; however, points relevant to this study are addressed below.

Early and correct diagnosis is imperative to allow the implementation of the correct treatment. In MS, mild relapses may not be treated; but, in the antibody-mediated conditions, relapses must be treated early and aggressively with intravenous steroids and possible escalation to plasma exchange or intravenous immunoglobulin depending on the treatment response. Long-term treatment also differs between the conditions. In AQP4-NMOSD, treatments such as azathioprine or methotrexate can be implemented to prevent relapses (Wingerchuk *et al.*, 2015). However, more recently, clinical trials have provided evidence for the use of monoclonal antibodies for the treatment of NMOSD. Rituximab (an anti-CD20 monoclonal antibody) has been shown to be effective in NMOSD through case series and systematic reviews as well as in a recent multi-centre, randomised, double-blind, place-controlled trial (Tahara *et al.* 2020). Additionally, three recent phase III clinical trials have shown the efficacy of Satralizumab (an anti-IL-6 receptor monoclonal antibody) (Traboulsee *et al*., 2020), Inebilizumab (an anti-CD19, B-cell depleting monoclonal antibody) (Cree *et al*., 2019) and Eculizumab (an anti-complement C5 monoclonal antibody) (Palace*, et al*. 2021) in NMOSD. All three drugs were shown to reduce relapse risk and this effect was most significant in patients with AQP4-Ab, as opposed to antibody-negative cases. These newly-approved drugs offer promising options for patients with AQP4-NMOSD. However, these clinical trials did not include patients with MOGAD and no MOGAD-specific clinical trials have been conducted. Consequently, much remains unclear. Additionally, unlike in AQP4-NMOSD, patients may remain monophasic and so treatment algorithms include factors such as the severity of the onset attack, persistence of positive antibodies and the occurrence of relapses (Juryńczyk *et al.*, 2019). Predictors of relapse in MOGAD would therefore be exceptionally useful when deciding on treatment protocols.

Chapters 3, 5 and 6 investigate the differences between monophasic and relapsing MOGAD and assess for possible predictors in the context of MOGAD myelitis.

Finally, it is important to note that Beta-interferon and Natalizumab, commonly used disease modifying therapies in MS, have been reported to worsen NMOSD (Palace *et al.*, 2010; Barnett *et al.*, 2011; Min *et al.*, 2011). MS treatments have also been shown to either be ineffective or to worsen outcomes in MOGAD (Cobo-calvo *et al.*, 2019; Zhou *et al.*, 2019).

1.3.10 Summary

This chapter has set out the recent advancements in our knowledge of MOGAD. It is a newly described condition that has only recently been defined as a distinct entity. Some key considerations still need to be made. These are categorised as follows:

- The establishment of specific diagnostic criteria for MOGAD.
- A better understanding of the underlying disease mechanisms.
- A need for predictors of outcomes such as relapse and disability.

Spinal cord involvement is a hallmark feature of MOGAD and is an important cause of disability. This thesis seeks to contribute to the above considerations from the perspective of spinal cord involvement in MOGAD, by studying the acute and long-term imaging features as well as clinical outcomes of MOGAD myelitis. A non-conventional MRI study, using the techniques outlined in Chapter 1.4, studies the effect of spinal cord disease in

MOGAD as compared to AQP4-NMOSD, MS and a group of HV. The value of this approach is that the features of MOGAD will be highlighted in specific contrast to its most common differentials (being AQP4-NMOSD and MS). Throughout the thesis aspects of the role of the antibodies, the pathology described, and our greater knowledge of the disease course in AQP4-NMOSD and MS will inform the interpretation of the non-conventional MRI findings in order to elucidate the effect of MOGAD on the different tissue types in the spinal cord. The overall contribution of this thesis to these three considerations is detailed in Chapter 9.

1.4 Spinal cord MRI

The following section is a focused review of the challenges that need to be overcome when using spinal cord MRI and of the advanced spinal cord MRI techniques that have been applied to the conditions of interest, highlighting their clinical application.

1.4.1 Challenges in cord MRI

Spinal cord MRI is notoriously challenging due to the limited accessibility of the spinal cord (Cohen-Adad and Wheeler-Kingshott, 2014; Stroman *et al.*, 2014; Martin *et al.*, 2015). The challenges faced when imaging the spinal cord are common to all MRI applications, but are exacerbated by the difficult imaging environment, physiological motion and small cross-sectional dimensions of the spinal cord (Stroman *et al.*, 2014).

Challenges have not only been identified in the acquisition of spinal cord images, related to the difficult imaging environment, hardware and software limitations, but also in analysis pipelines after acquisition. It has also been highlighted that the difficulties faced in spinal cord MRI mean that only a few labs in the world are actively developing and using advanced spinal cord imaging techniques and this lack of critical mass of researchers further hinders its advancement (Stroman *et al.*, 2014; Wheeler-Kingshott *et al.*, 2014).

Some of the primary challenges described are:

- Low signal-to-noise ratio (the average signal intensity over the standard deviation of the surrounding noise within the image), indicating poorer image quality (Cohen-Adad and Wheeler-Kingshott, 2014).

- Artifacts generated by susceptibility differences at tissue interfaces (bone, tissue, air), resulting in image distortion due to this field inhomogeneity (Cohen-Adad and Wheeler-Kingshott, 2014; Stroman *et al.*, 2014).

- Motion artifacts: spinal cord MRI is particularly sensitive to any participant movement but in addition to physiological processes such as swallowing, pulsations in nearby blood vessels and in the CSF as well as that related to the cardiac and respiratory systems (Cohen-Adad and Wheeler-Kingshott, 2014; Stroman *et al.*, 2014).

- Lack of normative data and consensus or standardised protocols for acquisition and analysis across centres (Martin *et al.*, 2015).

- Manual methods of analysis leading to inconsistent results (Moccia *et al.*, 2019).

Although some of these challenges are inherent in the anatomy of the spinal cord, many advances have been made in order to address or correct for these, both in the acquisition, pre-processing and analysis of these images.

Examples of these solutions both in acquisition and analysis are:

Acquisition

- Accounting for field inhomogeneity:
    - Shimming is a method of using currents directed through specialised coils to 'correct' the magnetic field, making it more homogenous (Cohen-Adad and Wheeler-Kingshott, 2014; Stroman *et al.*, 2014).

    - Transverse or axial acquisition.
    - The use of a reduced field of view to lessen the impact of susceptibility differences (Wheeler-Kingshott *et al.*, 2002).
- Accounting for the small size of the cord:
    - Acquisition of high in plane resolution, for example, 1x1mm and relatively thin slices of 1-2mm (Stroman *et al.*, 2014).
    - The use of spatial saturation pulses designed to suppress signal from tissues (particularly moving tissues) outside the area of interest to reduce or eliminate movement (Cohen-Adad and Wheeler-Kingshott, 2014).
- Physiological motion:
    - Cardiac gating can be implemented and reduces cardiorespiratory related movement by synchronising acquisition to the cardiac or respiratory cycle (Cohen-Adad and Wheeler-Kingshott, 2014; Stroman *et al.*, 2014). Although this will increase acquisition time and so this trade-off needs to be considered.
    - Choosing the appropriate phase-encoding direction such that artifacts do not spread across the image (Stroman *et al.*, 2014).
- Subject-specific factors:
    - Subject set-up should include cushions and padding to limit cervical lordosis.

Analysis

- Techniques have been developed to correct for some of the above concerns after acquisition, for example, motion correction tools and, in the case of functional MRI,

recording physiological parameters during scanning allows for this data to be used to correct for physiological noise during analysis (Eippert *et al.*, 2017*a*).

- Analysis software has been developed that allows for segmentation of the spinal cord to be semi-automated or fully-automated (Gros *et al.*, 2019) and to identify tracts within the cord, while accounting for partial volume effects (Lévy *et al.*, 2015). Both tools mentioned are available within Spinal Cord Toolbox (SCT) (De Leener *et al.*, 2017), which was used in this study and is further described in Chapters 4 to 8 .

1.4.2 Quantification of structural imaging

Spinal cord atrophy results from different underlying pathological processes, such as demyelination, axonal loss and gliosis (Schmierer *et al.*, 2018). An increasing number of studies in MS have focused on spinal cord atrophy as a measure of disability (Rocca *et al.*, 2011, 2019, Kearney *et al.*, 2015) and as a potential outcome for clinical trials in progressive MS (Cawley *et al.*, 2018; Prados and Barkhof, 2018).

Several studies have looked at atrophy in patients with NMOSD and a single study at cervical cord atrophy in MOGAD (a summary of which is contained in Table 1.5 and Table 1.6, which can be found at the end of Chapter 1). Spinal cord atrophy is an important finding in clinical imaging in AQP4-NMOSD (Kim *et al.*, 2015; Wingerchuk *et al.*, 2015). The ability to quantify this tissue loss has the potential to be used a marker of disability in this condition (Schneider *et al.*, 2015, Chien *et al.*, 2018*b*). Additionally, the location of the atrophy has been shown to be important in that AQP4-NMOSD and MS have been described as having different patterns of atrophy when the brain and cord are compared,

with MS having more brain atrophy relative to the cord and the opposite occurring in AQP4-NMOSD (Liu *et al.*, 2015). Most studies have focused on cervical cord measurements, in particular the upper cervical cord, but thoracic cord atrophy has also been shown to be more relevant in AQP4-NMOSD than in MS (Nakamura *et al.*, 2020). The usefulness of this should be considered particularly in the antibody-mediated conditions where thoracic cord involvement is more common.

Finally, segmenting and measuring grey matter atrophy has also shown clinical relevance in MS (Schlaeger *et al.*, 2014*a*). Recent advancements in analysis techniques have made the segmentation and measurement of the grey matter more feasible (Prados *et al.*, 2016).

1.4.3 Advanced imaging techniques and their use in neuroinflammatory conditions

Recent technical improvements in MRI acquisition and analysis have made the use of advanced spinal cord MRI more feasible. Advanced imaging techniques consist of different acquisition protocols that each seek to measure underlying biological processes and microstructural abnormalities that may reflect neurodegeneration (Wheeler-Kingshott *et al.*, 2014). The most promising techniques to study the spinal cord in NMOSD and MS are considered to be magnetisation transfer imaging (MTR), diffusion tensor imaging (DTI), myelin water imaging (MWI), and magnetic resonance spectroscopy (MRS) (Ciccarelli *et al.*, 2019), DTI being the most mature (Martin *et al.*, 2015). These methods study neuroaxonal integrity (DTI), myelin content (MTR and MWI), and metabolic changes (MRS). Additionally, more recent studies have also considered the potential of functional connectivity in the spinal cord with functional MRI (fMRI) (Martin *et al.*, 2015).

At present, these non-conventional MRI techniques are largely restricted to research studies. Translation into the clinical setting requires more research into the clinical applicability of these measures for use in clinical trials or clinical practice and standardisation of acquisition protocols for use in specific diseases; its translation will likely be initially restricted to centres with experience in the use of these techniques (Martin *et al.*, 2015; Moccia *et al.*, 2019).

The use of advanced spinal cord MRI techniques specific to neuroinflammatory conditions in the spinal cord is largely limited to studies of MS (Kearney *et al.*, 2015; Moccia *et al.*, 2019). A few studies have assessed their applicability in NMOSD (a summary of which is contained in Table 1.6, which can be found at the end of Chapter 1) and no studies have thus far used these to study the spinal cord in MOGAD.

A large systematic review of the clinical applicability of advance spinal cord imaging was published in 2016 (Martin *et al.*, 2015) and showed mixed results depending on the type of acquisition, analysis methodology and bias related to factors such as manual drawing of regions of interest and lack of good clinical data. However, group level differences and clinical correlations still provided some interesting results. These factors were taken into consideration in the design of the study presented in this thesis. Specific inclusion criteria, high quality clinical data and semi-automated or fully-automated analysis techniques were implemented, as is shown in Chapters 4 to 8. Additionally, the quantitative methods selected were those that showed the best evidence overall, namely, DTI and MTR (Martin *et al.*, 2015), together with the addition of resting state fMRI, which provides a novel approach. These techniques are described in more detail below.

1.4.3.1 DTI

DTI is a method based on interpretation of water molecule movement within the central nervous system. The architecture of axons, and their myelin, facilitates water movement along their main direction and, by applying diffusion gradients, different measures can be calculated that are potential markers for axonal integrity and myelination: fraction anisotropy (FA), radial diffusivity (RD), mean diffusivity (MD), and apparent diffusion coefficient (ADC) (Cohen-Adad and Wheeler-Kingshott, 2014). The most robust evidence exists for the use of FA as a clinical measure in neurological disorders (Martin *et al.*, 2015).

DTI provides quantitative measures of microstructural abnormalities which have been shown to be abnormal in the spinal cord in both AQP4-NMOSD and MS, when compared with HV (Valsasina *et al.*, 2007; Qian *et al.*, 2011; Pessôa *et al.*, 2012; Naismith *et al.*, 2013). They have also been shown to be worse in NMOSD when compared to MS due to the more severe and destructive damage caused by lesions in NMOSD (Klawiter *et al.*, 2012).

Additionally, FA measured in the spinal cord has shown associations with clinical outcomes in both AQP4-NMOSD and MS, and tract-specific measures have shown relevance in their associations with outcomes relevant to the particular tract in AQP4-NMOSD, for example, FA within the dorsal column showing an association with measures of vibration perception (Naismith *et al.*, 2013).

1.4.3.2 MTR

MTR is a quantitative technique measuring the magnetisation exchange between freely mobile protons and those associated with macromolecules, such as myelin, providing an indirect estimate of myelin content, in addition to neuroaxonal integrity and water content

(Cohen-Adad and Wheeler-Kingshott, 2014). This has been most studied in the spinal cord of patients with MS wherein it has been shown to demonstrate abnormalities in both lesions and the normal appearing white matter, and is associated with disability, independent of lesion load; this shows it is clinically relevant beyond conventional imaging (Rovaris *et al.*, 2004; Charil *et al.*, 2006, Oh *et al.*, 2013*a*, *b*).

A study comparing cervical cord MTR between MS and NMOSD reflected no difference between the two conditions in the spinal cord, when all patients with NMOSD had lesions present. In the brain the normal-appearing tissue was affected in MS but not in NMOSD (Filippi *et al.*, 1999).

1.4.3.3 fMRI

fMRI is a neuroimaging technique based on the blood oxygenation level dependent (BOLD) contrast, first utilised in 1990 (Ogawa *et al.*, 1990). It is a non-invasive imaging method designed to represent neuronal activity (Cohen-Adad and Wheeler-Kingshott, 2014; Stroman *et al.*, 2014). The principle is based on the metabolic demand for oxygen: the increased blood flow to areas of metabolic demand leads to a relative decrease in deoxyhaemoglobin in the venous compartments. The paramagnetic properties of deoxyhaemoglobin lead to local variations of the magnetic field within the scanner (Cohen-Adad and Wheeler-Kingshott, 2014; Stroman *et al.*, 2014). These changes in T2 relaxation led to detectable signal changes that act as a surrogate marker for functionality. There are two general concepts in this field of functional neuroimaging: localisation and functional connectivity (Bijsterbosch *et al.*, 2017).

Localisation is achieved by well-designed task-based experiments that seek to localize functionally specialised parts of the brain that activate in response to particular tasks. Functional connectivity measures the similarity of the BOLD signal in different regions, in particular the temporal correlation between spontaneous fluctuations (Bijsterbosch *et al.*, 2017). This forms the basis of resting state fMRI (RS-fMRI). These slow fluctuations partition the resting brain into temporally synchronised networks, so-called resting state networks (RSNs). As functional connectivity may exist between areas that are not structurally connected (Honey *et al.*, 2009), studying functional connectivity may offer additional insight into pathological states.

fMRI was first applied to spinal cord using a motor task (Yoshizawa *et al.*, 1996). Several studies have since looked at the applicability of task-based fMRI in the spinal cord of people with MS in response to tactile or proprioceptive stimulation of the hand or wrist (Agosta *et al.*, 2008; Valsasina *et al.*, 2010; Rocca *et al.*, 2012). RS-fMRI in the spinal cord is a more recent and novel development (as recent as 2010) when the potential for this technique to show evidence of networks in the spinal cord in the absence of a stimulus was first shown (Wei *et al.*, 2010). This novel technique has been largely tested in HVs as proof of concept (Barry *et al.*, 2014; Kong *et al.*, 2014) with a focus on reproducibility (Barry *et al.*, 2016) and showing the results to be robust through different analysis pipelines and at different scanner strengths (Eippert *et al.*, 2017*b*; Barry *et al.*, 2018). Few studies have assessed disease-related alterations in human spinal cord activity using RS-fMRI. Martucci et al. demonstrated differences in the amplitude of low-frequency fluctuations in patients with fibromyalgia as compared to HVs and an association between this and the degree of fatigue experienced (Martucci *et al.*, 2019). Conrad et al. assessed functional networks in

the spinal cord of patients with MS at 7T and found localised changes related to lesions (Conrad *et al.*, 2018). This is discussed further in Chapter 8.

1.4.4 Summary

Many recent advancements have allowed for more detailed study of the spinal cord using MRI. The study designed for this thesis draws from the current literature and recommendations, considering the challenges and limitations. A multimodal spinal cord MRI protocol (described in Chapter 4) was set in order to study the spinal cord in MOGAD using techniques that have shown evidence of clinical relevance in AQP4-NMOSD and MS. It also contributes to the literature in AQP4-NMOSD where a limited number of studies have been done in the spinal cord using advanced MRI techniques (Table 1.6 below).

Table 1.5 A summary of the MRI studies of cord atrophy in MOGAD.

Mechanism	MRI Technique	Measurement	Anatomical area of interest	Field strength	Number of patients	Findings compared to healthy controls	Clinical correlates	Reference
Cord Atrophy	3D-T1	MUCCA	C2-C3	3T	15	←→	• Disability • Timed 25ft walk speed • 9-hole peg test	(Chien *et al.*, 2018*b*)

Table 1.6 A summary of non-conventional MRI studies in AQP4-NMOSD.

Mechanism	MRI Technique	Measurement	Anatomical area of interest	Field strength	Number of patients	Findings compared to healthy controls	Clinical correlates	Reference
Cord Atrophy	3D T1	Cervical cord and upper thoracic cord volume	C1-T3	1.5T and 3T	52	↓	Disability	(Cacciaguerra *et al.*, 2020)
	T2-weighted	Cervical and thoracic cord area	C2-C3 C3-C4 T8-T9 T9-T10	1.5T and 3T	42	↓	Disability	(Nakamura *et al.*, 2020)
	3D T1	Upper cervical cord volume	C2-C3	3T	38	↓	• Disability	(Chien *et al.*, 2018*b*)

Mechanism	MRI Technique	Measurement	Anatomical area of interest	Field strength	Number of patients	Findings compared to healthy controls	Clinical correlates	Reference
							• Timed 25ft walk speed • 9-hole peg test	
	3D T1	Upper cervical cord area	C2-C3	3T	35	↓	Disability	(Liu *et al.*, 2015)
	3D T1	Upper cervical cord area	C2-C3	1.5T	18	↓	Disability	(Schneider *et al.*, 2015)
	3D T1	Upper cervical cord area	C2-C3	3T	18	←→	Not assessed	(Matthews *et al.*, 2015)
Neuroaxonal integrity	DTI	FA, MD, RD	C1-C6	3T	10	↓ FA ↑ MD/RD	Disability	(Qian *et al.*, 2011)
		FA, AD, RD, MD	C2-C7	1.5T	8	↓ FA/AD ↑ MD/RD	Disability	(Pessôa *et al.*, 2012)
		FA, MD, RD	C1-C6	3T	11	Not compared	Disability Vibration sense	(Naismith *et al.*, 2013)
		FA, MD	C2-C6	1.5T	11	↓ FA ↑ MD	Disability	(Rivero *et al.*, 2014)
		FA, RD, MD, AD	C1-C6	3T	10	↓ FA/AD ↑ MD/RD	Disability	(Klawiter *et al.*, 2012)
Myelin loss	MT-weighted	MTR	Upper cervical cord	1.5 T	8	↓	Not assessed	(Filippi *et al.*, 1999)

Mechanism	MRI Technique	Measurement	Anatomical area of interest	Field strength	Number of patients	Findings compared to healthy controls	Clinical correlates	Reference
	MT-CSF	White matter:grey matter ratio	Upper cervical cord	3T	18	←→ to normal appearing matter	Not assessed	(Matthews *et al.*, 2015)
	Myelin water imaging	Myelin water fraction	C1-C7	3T	15	↓	None	(Combes *et al.*, 2017)
Astrocyte damage	Magnetic resonance spectroscopy	Myoinositol	C1-C3	3T	5	↓	Not assessed	(Ciccarelli *et al.*, 2013)

2. Chapter 2: Thesis aims and structure

This thesis was designed to study spinal cord involvement in patients with myelin oligodendrocyte glycoprotein associated disease (MOGAD), compared to those with aquaporin-4 positive neuromyelitis optica spectrum disease (AQP4-NMOSD), multiple sclerosis (MS) and healthy volunteers (HV).

2.1 Thesis objectives and aims

The overall objectives and aims of this study are as follows:

- To study the clinical course and radiological findings of myelitis in patients with MOGAD and compare them to patients with AQP4-NMOSD.

- To study the features of myelitis in MOGAD using structural and quantitative MRI measures, and compare them to patients with AQP4-NMOSD, MS and HV, in order to better understand the underlying disease mechanisms.

- To investigate differences in resting-state functional connectivity in patients with MOGAD, AQP4-NMOSD and MS, and compare them to HV.

- To determine the clinical applicability of the structural, quantitative and functional MRI measures as they relate to disability, relapse-risk, pain and fatigue.

These broad objectives are detailed further in each chapter and presented together with the hypotheses driving each part of the study.

2.2 Structure of the thesis

In order to address the objectives and aims listed above, two studies were undertaken:

- A retrospective clinical study, and
- A cross-sectional research MRI study.

This was done in order to, first, study and compare the acute clinical and imaging findings in MOGAD and AQP4-NMOSD and to, secondly, compare the clinical outcomes, follow-up imaging and disease course in an adult clinical population. This is presented in Chapter 3. The study design, methodology and results are all contained in Chapter 3.

The MRI study (Chapters 4 to 8) was designed to assess the effect of spinal cord involvement in MOGAD and AQP4-NMOSD and compare them to patients with relapsing-remitting MS and a cohort of HVs. This study was designed as a robust assessment of different components spinal cord (cervical cord, thoracic cord, grey matter and white matter). Each chapter covers this as follows:

- Chapter 4 describes the MRI study design, cohorts, assessments and MRI protocol.
- Chapter 5 studies and compares cervical cord (whole cord and cervical cord grey matter) and thoracic cord cross-sectional area.
- Chapter 6 studies and compares quantitative measures of demyelination and white matter integrity.

- Chapter 7 assesses the utility of the measures captured in Chapters 6 and 7 in relation to clinical outcomes and their ability to discriminate the conditions of interest.

- Chapter 8 explores the novel technique of spinal cord resting-state functional MRI and its utility in the study of neuroinflammatory conditions.

Finally, Chapter 9 highlights the key findings of this research, interprets them in light of their clinical applicability and discusses hypotheses derived from these findings that will drive future work.

2.3 Statistical approach

In each chapter, a detailed description of the statistics is provided. *p* values are provided, to three decimal places, for all analyses within the text and tables. For the purposes of figures, * denotes a *p* value of <0.05 and ** a *p* value of <0.01. In cases where the *p* value is between 0.05 and 0.1, the trend will be noted.

Statistical tests were parametric unless the Shapiro-Wilk normality test was violated, in which cases the non-parametric alternative was used. Models were selected provided the data met the necessary assumptions for testing.

3. Chapter 3: Clinical features of myelitis in MOGAD and AQP4-NMOSD

3.1 Introduction and background

Neuromyelitis optica spectrum disorder (NMOSD) and myelin oligodendrocyte glycoprotein associated disease (MOGAD) have been shown to be clinically and radiologically similar (Reindl *et al.*, 2013). However, recent cohort studies have begun to describe clinical presentations and MRI features that may be characteristic of MOGAD that require further investigation (Jurynczyk *et al.*, 2017*b*; Cobo-Calvo *et al.*, 2018; Senanayake *et al.*, 2018). Aquaporin-4 (AQP4) antibodies (Ab) are a highly specific pathological marker of NMOSD and associate with a chronic relapsing condition with high morbidity and mortality (Jarius and Wildemann, 2010), whereas growing evidence suggests that MOGAD is milder (Kitley *et al.*, 2014, Jurynczyk *et al.*, 2017*b*). Involvement of the spinal cord is a hallmark feature in each condition and disability appears to be attack-related.

Understanding the course of spinal cord involvement in these conditions, particularly in MOGAD which is a recently described entity, has important treatment and prognostic implications. Clinical suspicion is needed in order to test for antibodies appropriately (to ensure patients are not mislabelled as idiopathic but also to prevent unnecessarily testing those unlikely to have the condition, which increases the risk of false positives (Jarius *et al.*, 2018)). Therefore, clinical and investigative findings that are suggestive of MOGAD are important.

Our understanding of the spectrum of presentations in MOGAD is continuously evolving (dos Passos *et al.*, 2018). The work in this chapter has contributed to this growing field by studying the clinical features of myelitis associated with MOGAD in a cohort of patients from the United Kingdom. The work presented below is adapted from the publication: *Mariano R, Messina S, Kumar K, Kuker W, Leite MI, Palace J. Comparison of Clinical Outcomes of Transverse Myelitis Among Adults With Myelin Oligodendrocyte Glycoprotein Antibody vs Aquaporin-4 Antibody Disease. JAMA Netw Open. 2019 Oct 2;2(10).*

At the time of publication this was the second paper published on the clinical features of myelitis in these conditions and represented the largest adult cohort. Two additional patients with MOGAD have been added to the work presented below.

In this retrospective study the demographics, presentation, clinical and paraclinical features and outcomes in adult patients with spinal cord involvement who have tested positive for serum MOG-Ab or AQP4-Ab are described and compared. Clinical and imaging features are assessed for their association with poorer outcomes or increased relapse risk.

3.2 Objectives and aims

The objectives and aims of this chapter are as follows:

- To compare the clinical and radiological findings of the first myelitis in patients with MOGAD and compare them to patients with AQP4-Ab positive NMOSD.

- To describe the course of the disease in each condition: relapses (phenotype and frequency) and disability outcomes.

- To assess for factors associated with worse outcomes and relapse risk after the first attack of myelitis and at long-term follow-up.

3.3 Hypothesis

Three hypotheses were developed for this chapter, as follows

- Overlap will exist in both the clinical and imaging features of myelitis in MOGAD and AQP4-NMOSD. However, differences will be noted that, when present, will assist in identifying patients with MOGAD.

- Better recovery and less severe outcomes will be present in MOGAD myelitis.

- The difference in underlying pathogenesis will mean that clinical outcomes will be associated with different predictors in each condition.

3.4 Methods

3.4.1 Ethics

This study falls within the remit of the Oxford MS and NMOSD Tissue Bank (Ref: 16/SC/0224). All enrolled participants had signed consent for their clinical, imaging and laboratory information to be used for research and publication.

3.4.2 MOG and AQP4 antibody testing

Testing for the presence of AQP4-Ab and MOG-Ab was performed in the Autoimmune Neurology laboratory in Oxford, using cell-based assays as described in Chapter 1 (Wingerchuk *et al.*, 2014; Waters *et al.*, 2015). All MOG-Ab positive patients were negative

for AQP4-Ab; similarly, all AQP4-Ab positive patients were negative for MOG-Ab. As false positives are recognised to occur more commonly with MOG-Ab testing, all results were reviewed by the laboratory team and all cases were reviewed by the specialist team in Oxford. No borderline cases were included.

3.4.3 Cohort

All patients seen in the National Health Services (NHS) NMOSD Service at the John Radcliffe Hospital located in Oxford, United Kingdom, are entered into a Microsoft Access database to facilitate patient care. Each patient is offered the opportunity to consent for their clinical data to be used for research. Where consent is given, their clinical data is added to the NMOSD Database.

The database was screened for adult patients with either MOG-Ab or AQP4-Ab with at least one episode of myelitis during the course of their disease. Data collection took place from April 2018 to January 2019. Two further patients with MOGAD who fulfilled inclusion criteria were added to this database in April 2020. This screening process yielded an initial group of 155 patients.

From these 155 patients, 38 were excluded (five with confounding neurological co-morbidities, 13 who had not signed consent and 20 for whom no acute imaging and/or clinical details from the acute attack could be found). The final group of 117 patients reflected cohorts of 48 adult patients with MOGAD and 69 adult patients with AQP4-NMOSD. All of these patients had imaging done within four weeks of the acute attack.

The following data was collected:

- Demographic features (age-at-onset of their disease, gender, ethnicity), date of onset of the disease and date of last follow up which are used to calculate disease duration,

- Features of the onset myelitis (signs and symptoms), expanded disability status score (EDSS) at nadir, time to acute treatment and type of acute treatment,

- MRI features during acute attack; long-term disability outcomes (motor and sphincter dysfunction),

- Relapse history; long-term treatment; and features of any follow-up imaging done outside of acute relapse.

3.4.4 MRI review

The Oxford NMOSD Service receives referrals from the entire Southern United Kingdom. Unless patients are local to the Oxford City area, in which case they would be seen acutely at the John Radcliffe Hospital, the MRI scans are performed at their local healthcare facility and reviewed by the Oxford NMOSD Service upon referral. All scans were performed on either 1.5 or 3T scanners and included sagittal cervical and thoracic T1 (slice thickness 3-4mm; TE 6.8-12.2ms; TR 469-540) and T2 spinal cord imaging (slice thickness 3-4mm; TE 100-116ms; TR 3000-4840ms). Not all participants were given contrast. Where axial images were acquired, these were either T2 or T2* weighted images in the affected area (slice thickness 4-5mm).

All acute scans and any available follow-up imaging were reviewed together with the MRI reports by the Oxford NMOSD Service clinical team. These scans were also reviewed in a weekly imaging multi-disciplinary meeting with the Oxford University Hospitals Trust inflammatory neuro-radiologist in any case where the initial report was inconclusive or if the clinical presentation and scan findings were incongruent. This is particularly relevant in the spinal cord as imaging is notoriously difficult and interpretation can be subjective, especially in areas such as the conus.

3.4.5 Statistical analysis

Statistical analysis was performed using SPSS v26 and RStudio v.1.1.447. Mann-Whitney U-tests were used when comparing continuous variables. Fisher's exact test was used when comparing frequencies. The Kaplan-Meier method was used for estimating relapse risk and disability outcomes. There were no deaths in either cohort and the time factor used in the Kaplan-Meier analysis was from disease onset to the date of last follow-up. Nearest neighbour propensity score matching was used to create comparable groups for the Kaplan Meier analysis comparing MOGAD and AQP4-NMOSD. Cox regression was not used in this instance as the variables violated the Schoenfeld test. Binomial logistic and multivariate regression models were used to identify factors associated with relapse and disability. Variable selection for each regression model was based on *a priori* clinical hypotheses as recommended for clinical studies with small samples sizes (Heinze and Dunkler, 2017) and the covariates used in each model are explained alongside the results below.

Although age was used as a continuous variable in the regression analyses, for the purposes of the Kaplan-Meier analysis in the AQP4-NMOSD cohort age was binarised according to the median cut off of 50 years (i.e. two groups: <50 and ≥50).

3.4.6 Definitions of terms used within this chapter

The following terms are used within the text of this chapter:

- *First myelitis*: this denotes the first episode of myelitis experienced by a patient during the course of their disease.

- *Onset myelitis*: this indicates that the first episode of myelitis in the patient was also the first presentation of the condition

- *EDSS*: This Expanded Disability Status score (Kurtzke, 1983) ranges from 0 to 10 and is based on measures of impairment in the following systems: motor, cerebellar, brainstem, sensory, bladder and bowel function, visual function and cerebral. Scores from 1 to 4.5 indicate no walking impairment, a score of 5 indicates restricted walking distance, a score of 6 (often used as an outcome measure of substantial disability) indicates a walking aid is required and increasing numbers beyond 6 indicated the need for bilateral assistance when walking, use of a wheelchair or being confined to bed. A score of 10 indicates death.

- *Recovery EDSS*: the EDSS score after the first episode of myelitis and prior to any further relapses.

- *EDSS at last follow-up*: the EDSS score documented at the patient's last clinical encounter (in patients with multiple relapses this score may represent an accumulation of disability).

3.5 Results

3.5.1 Demographic data

Forty-eight (48) patients with MOGAD and 69 patients with AQP4-NMOSD were included. The demographics of each cohort are shown in Table 3.1. Differences were noted in age, sex and ethnicity. Disease duration was longer in those with AQP4-NMOSD. In both conditions it was more common for the myelitis to occur at the onset of the disease (33/48 [68.8%] in MOGAD and 54/69 [78.2%] in AQP4-NMOSD).

Table 3.1. Demographics and features of first myelitis. *p values shown are based on group comparisons and significant values are highlighted in bold. Adapted from (Mariano* et al*., 2019).*

Cohort Description	**MOGAD**	**AQP4-NMOSD**	***p* value**
Total number	48	69	
Sex M:F	22:26	12:57	**0.001**
Mean age at disease onset +/- std	35 +/- 12.1	48 +/- 14.9	**<0.00**
Ethnicity (%)			
White	41 (85.4)	40 (57.9)	**0.002**
East Asian	3 (6.3)	6 (8.7)	0.735
South Asian	1 (2)	4 (5.8)	0.647
Afro-Caribbean	0 (0)	16 (23.2)	**<0.001**
Mixed	3 (6.3)	3 (4.4)	0.688
Median disease duration in months (range)	27.7 (3.5-399.0)	81.9 (3.9-287.3)	**0.003**
First myelitis at disease onset (%)	33 (68.8)	54 (78.2)	0.285

Cohort Description	MOGAD	AQP4-NMOSD	*p* value
Concurrent symptoms present with myelitis (%)			
Optic neuritis	12 (25)	2 (2.9)	**<0.001**
Brainstem manifestations	6 (12.5)	8 (11.6)	1.000
Brain manifestations	4 (8.3)	1 (1.5)	0.157
Myelitis symptoms at onset (%)			
Sensory only	9 (18.8)	6 (8.7)	0.159
Pain	6 (12.5)	20 (28.9)	**0.043**
Sphincter involvement	36 (75)	39 (56.5)	0.051
Mean EDSS at nadir +/- std	5.8 +/- 2.1	6.5 +/- 2.0	0.071
Median EDSS at nadir (range)	5.5 (1-9)	7 (3-9.5)	
Median EDSS at recovery (range)	2 (0-8)	3 (1-8)	
Mean EDSS at last follow up +/- std	2 +/- 1.6	4.1 +/- 2.5	**<0.001**
Median EDSS at last follow up (range)	2 (0-8)	4 (1-8)	
EDSS 6 (%)	3 (6.3)	30 (43.5)	**<0.001**
Long-term sphincter dysfunction (%)	29 (60.4)	33 (47.8)	0.193
Long-term catheter usage (%)	9 (18.8)	16 (23.2)	0.650
Relapses			
Relapsing after myelitis (%)	17 (35.4)	36 (52.2)	0.090
Average time to relapse in months +/- std	31 +/- 33.6	32 +/- 32.8	0.872
Type of relapse (%)	*n = 17*	*n = 36*	
Optic neuritis	9 (52.9)	3 (8.3)	**<0.001**
Myelitis	2 (11.8)	25 (69.4)	**<0.001**
Optic neuritis & myelitis simultaneous	3 (17.7)	7 (19.4)	1.000
Brainstem manifestations	2 (11.8)	1 (2.8)	0.238
Brain manifestations	1 (5.8)	0 (0)	0.320

3.5.2 Clinical presentation

The frequency of motor and sensory symptoms at nadir did not significantly differ. The frequency of sphincter involvement in the acute setting was greater in MOGAD, very nearly reaching significance (36/48 [75.0%] vs 39/69 [56.5%], p=0.051). Neuropathic pain at presentation was less common in MOGAD than in AQP4-NMOSD (6/48 [12.5%] vs 20/69 [28.9%], p=0.043). This most commonly presented as back pain, often preceding the other symptoms.

The EDSS at nadir was not significantly different between groups. Patients with MOGAD presented more commonly with optic neuritis (ON) together with the first attack of myelitis (12/48 [25.0%] versus 2/69 [2.9%], $p = < 0.01$). There was no significant difference in the number of patients presenting with brain or brainstem manifestations at the time of the myelitis. In those with MOGAD brain manifestations constituted an acute disseminated encephalomyelitis (ADEM)-like presentation in four white adult patients. This presentation did not occur in any of the adult AQP4-NMOSD cohort.

Symptomatic brainstem lesions were roughly equal in each group (6/11 in MOG; 8/11 in AQP4-NMOSD); but, asymptomatic brainstem lesions did occur in both cohorts. In patients with MOGAD bulbar symptoms predominated with no reports of vomiting or hiccups. Four of these patients presented with brainstem features in the context of an ADEM-like presentation. The predominant features of brainstem involvement in AQP4-NMOSD were nausea, vomiting and hiccups. Other symptoms experienced were vertigo and dysphagia; and two patients required ventilatory support (high cervical lesion contiguous will medullary lesion).

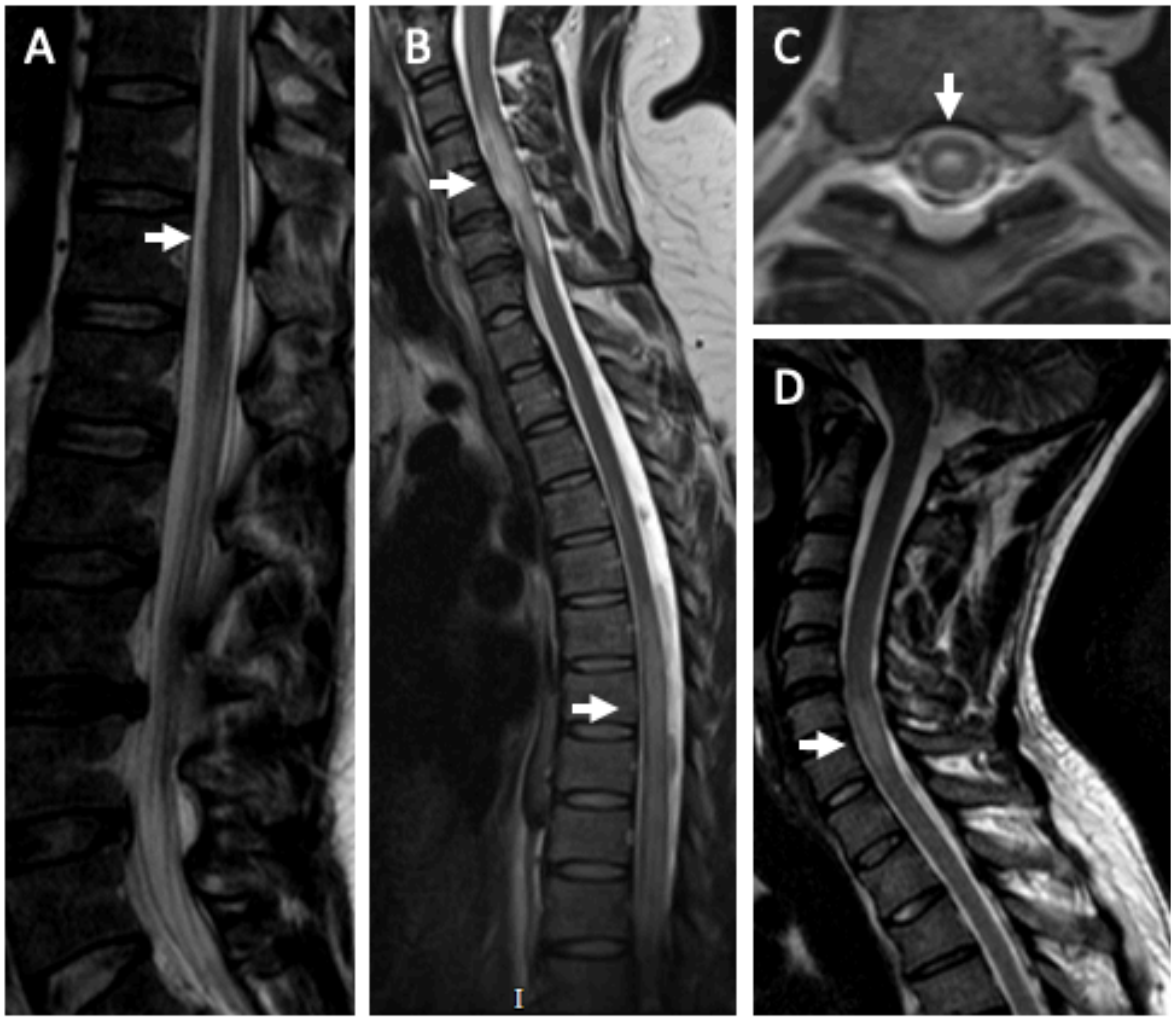
A minority of patients in either cohort were on therapeutic-dose background immunosuppressive therapy at the time of their first myelitis. Myelitis attacks were more commonly the onset presentation and in other cases it was often an isolated ON that preceded the myelitis. Antibody testing was often only done at the time of the spinal cord presentation and, as such, the diagnosis could not be made earlier.

3.5.3 Acute spinal cord MRI features

MRI features are summarised in Table 3.2 and examples of cord lesions are shown in Figure 3.1. Short lesions (<3 vertebral levels), with no additional long lesion, occurred in 12/48 [25.0%] of those with MOGAD and 8/69 [11.6%] of those with AQP4-NMOSD. The presence of short lesions was particularly prevalent in patients with MOGAD whose first myelitis attack occurred as a relapse and not at onset: 8/15 [53.3%] of these patients had only short lesions compared to those whose myelitis attack occurred at the onset of the disease where 4/33 [12.1%] had short lesions only. This pattern did not occur in the AQP4-NMOSD cohort where the distribution of short lesions was 7/54 [12.9%] at onset and 1/15 [6.7%] at relapse. 12/48 [25.0%] of patients with MOGAD presented with longitudinally extensive transverse myelitis (LETM), denoting a lesion of ≥3 vertebral levels, and additional short lesions, whereas this occurred in only 2/69 [2.9%] of those with AQP4-NMOSD. The remaining 24/48 [50.0%] of patients with MOGAD and 59/69 [85.5%] of patients with AQP4-NMOSD all presented with only long lesions. The mean total lesion length did not differ between the two groups and in both cohorts, this correlated with EDSS at nadir (Pearson's correlation: MOGAD r = 0.46, p = 0.003; AQP4-NMOSD r = 0.37, p = 0.003).

Those with MOGAD were more likely to have multiple lesions (20/48 [41.7%] versus 7/69 [10.1%]; p = < 0.01) and involvement of the conus (19/48 [39.6%] versus 8/69 [11.6%]; p = < 0.01). Eighteen (18) patients with MOGAD and 24 patients with AQP4-NMOSD had axial scans available. There were no significant differences in the axial location (central lesions most common in both groups: 13/18 [72.2%] in patients with MOGAD and 17/24 [70.8%] in patients with AQP4-NMOSD) or in the frequency of gadolinium enhancement within the four-week window that the acute scan period was considered (19/26 [73.1%] in patients with MOGAD and 38/48 [79.2%] in patients with AQP4-NMOSD).

Figure 3.1. Cord MRI features in MOGAD. *White arrows showing (A) conus lesion, (B) multiple lesions, (C) central location on axial imaging, and (D) short cervical lesion.*



3.5.4 Acute intracranial imaging

3.5.4.1 Brain imaging

White matter lesions on the brain MRI were more common in MOGAD than in AQP4-NMOSD (25/47 [53.2%] versus 14/62 [22.6%], p = <0.01). Of those with MOGAD and brain lesions (excluding brainstem lesions) 4/25 had ADEM-like (large, "fluffy") lesions that were symptomatic. The remaining patients were all asymptomatic with 3/25 [12.0%] having non-specific white matter lesions, 2/25 [8.0%] with lesions considered to be MS-like (juxta-cortical or periventricular) and the remaining 16/25 [64.0%] involving the deep grey matter, cerebellar peduncle, cerebral white matter.

In patients with AQP4-NMOSD it was more common to find brain lesions (excluding brainstem lesions) in the older patients making it difficult to differentiate those from age-related vascular changes in some cases. All lesions were asymptomatic in this cohort. Lesions in the brain constituted mainly 'non-specific' white matter lesions (10/14), one with cerebellar lesions, two with callosal lesions, and one with MS-like lesions (periventricular white matter lesions).

3.5.4.2 Brainstem imaging

The presence of associated brainstem lesions was not significantly different between groups. However, where an associated brainstem lesion occurred at the time of the myelitis it was more commonly contiguous with the cord lesion in AQP4-NMOSD (8/11 [72.7%]) versus MOGAD (3/11 [27.3%]).

Of the eleven patients with MOGAD and brainstem lesions, four had an ADEM-like presentation at onset, including lesions in the brain and brainstem, two had lower brainstem involvement contiguous with an upper cervical cord lesion, one had a lesion in the medulla that did not extend into the cord, one had a midbrain lesion and three had lesions in the pons.

Table 3.2. Features of acute cord and brain MRI. *p values shown are based on group comparisons and significant values are highlighted in bold. Adapted from (Mariano* et al*., 2019).*

MRI Features	**MOGAD**	**AQP4-NMOSD**	***p* value**
Sagittal cord MRI (%)	*n = 48*	*n = 69*	
Short lesion(s) only	12 (25)	8 (11.6)	0.080
Long lesion(s) only	24 (50)	59 (85.5)	**<0.001**
Long + short lesions	12 (25)	2 (2.9)	**<0.001**
Mean total lesion length +/-std	6.6 +/- 5.4	7.7 +/- 5.2	0.270
Single lesion	28 (58.3)	62 (89.9)	**<0.001**
Multiple lesions	20 (41.7)	7 (10.1)	**<0.001**
Conus involvement	19 (39.6)	8 (11.6)	**0.001**
Contrast enhancement	19/26 (73.1)	38/48 (79.2)	0.574
Axial cord MRI (%)	*n = 18*	*n = 24*	
Central	13 (72.2)	17 (70.8)	1.000
Lateral	3 (16.7)	3 (12.5)	1.000
Posterior	0 (0)	0 (0)	
Anterior	2 (11.1)	4 (16.7)	0.685
MRI brain (%)	*n = 47*	*n = 62*	
Brain lesion	25 (53.2)	14 (22.6)	**0.001**
Brainstem lesion	11 (23.4)	11 (17.7)	0.481

3.5.5 Features of cerebrospinal fluid analysis

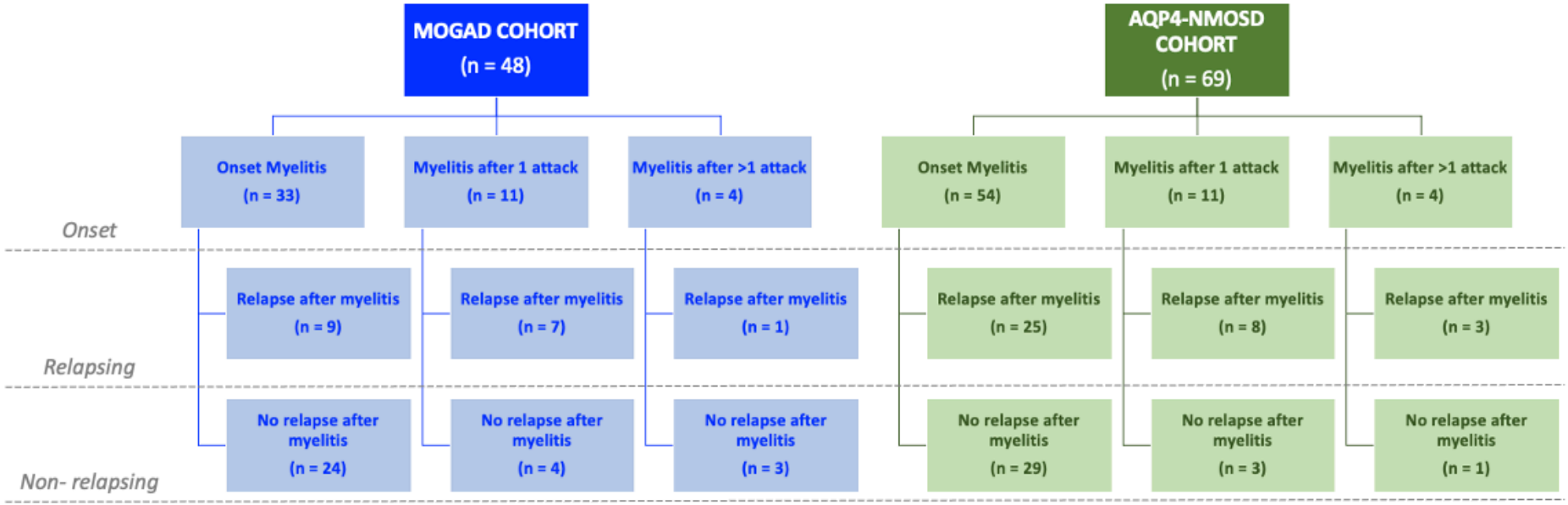
Of the samples available (25 MOGAD and 37 AQP4-NMOSD) there was no significant difference in cerebrospinal fluid (CSF) findings between the two groups. Cell counts were often raised (10-220 per µL in MOGAD; 14-162 per µL in AQP4-NMOSD). Protein was also commonly raised (55-190g/dL in MOGAD; 50-159g/dL in AQP4-NMOSD). Oligoclonal bands were positive in five patients with MOGAD [20.0%] and six with AQP4-NMOSD [16.2%].

3.5.6 Relapses

The number and type of relapses are described in the first instance without correcting for disease duration; this is accounted for in the regression models thereafter. The disease duration was significantly longer in the AQP4-NMOSD cohort. Additionally, this study was not based on an incident cohort. As an inclusion criterion for this study was an episode of cord involvement, whether at onset or relapse, the percentage of relapsing patients may be higher than that documented in epidemiological studies. Figure 3.2. shows a graphical representation of the disease course in each cohort. In the MOGAD cohort 15 myelitis attacks occurred as the first relapse after a previous non-myelitis attack (most commonly ON); eight of these patients went on to have a further relapse. Of the 33 patients with myelitis at onset, nine went on to relapse. Therefore, a total of 17 MOGAD patients had relapses after their first myelitis attack. In the AQP4-NMOSD cohort 15 myelitis attacks occurred as the first relapse after a previous non-myelitis attack (most commonly ON or area postrema); 11 of these patients went on to have a further relapse. Of the 54 patients with myelitis at onset, 25 had relapses. A total of 36 AQP4-NMOSD patients had relapses after their first attack of myelitis. Although it did not reach statistical significance in either

group, a higher percentage of those that had their first attack of myelitis as a relapse went on to have a further relapse after their myelitis, when compared to those with myelitis at onset (8/15 [53.3%] versus 9/33 [27.3%] in MOGAD and 11/15 [73.3%] versus 25/54 [46.3%] in AQP4-NMOSD).

Figure 3.2. Relapses. *The timing of the onset myelitis attack and subsequent relapses in MOGAD (blue) and AQP4-NMOSD (green) are shown in a graphical form.*



In those that had relapses, the median number was two (range = 1-6) in the MOGAD cohort and three (range = 1-8) in the AQP4-NMOSD cohort. After an attack of myelitis, those with MOGAD were more likely to have an ON relapse (9/17 [52.9%]) and those with AQP4-NMOSD were more likely to have another attack of myelitis (25/36 [69.4%]). This was significantly different when comparing the two groups (p = <0.01).

To better understand the predictors of having a relapse after an attack of myelitis a binary logistic regression model was built for each condition. Variables were selected based on *a priori* clinical hypotheses. The MOGAD model included: age, sex, disease duration, immunosuppressive treatment (binary variable), history of relapse prior to myelitis attack (binary variable) and the presence of ON at the time of the attack. The AQP4-NMOSD model included: age, sex, ethnicity, disease duration, immunosuppressive treatment (binary variable), history of relapse prior to myelitis attack (binary variable) and the presence of ON at the time of the attack. Ethnicity was added to the AQP4-NMOSD model as it is known to impact clinical outcomes (Kitley *et al.*, 2012*a*, Tackley *et al.*, 2016*a*; Palace *et al.*, 2019) but not to the MOGAD model as approximately 80% of patients of the MOGAD cohort were white. The ON phenotype has been shown to be associated with an increased risk of relapse in MOGAD and so this was included in this model (Jurynczyk *et al.*, 2017*b*). The treatment binary variable was included as '1' for those that went on to have long term immunosuppression after their myelitis attack and '0' for those that had not. In the case of MOGAD this was defined as at least six months of oral prednisolone and in the AQP4-NMOSD cohort this was defined as the inclusion of an immunosuppressive medication in addition to oral prednisolone.

In the MOGAD cohort only disease duration showed an association with relapse. The results are shown in Table 3.3.

Table 3.3. Logistic regression model: relapse in MOGAD. *Dependent variable = relapse after myelitis (yes/no).*

Parameter	Beta	Std. Error	Wald's X^2	*df*	*p* value	Odds Ratio	95% CI
Age	-0.013	0.038	0.113	1	0.737	0.987	0.917-1.063
Sex (female)	-0.802	0.789	1.033	1	0.309	0.096	0.096-2.105
Disease duration	**0.022**	**0.009**	**6.719**	**1**	**0.010 ***	**1.005**	**1.005-1.040**
Treatment (yes)	-0.719	0.832	0.748	1	0.387	0.402	0.402-10.482
Attack prior to myelitis (yes)	-0.806	0.862	0.875	1	0.350	0.082	0.082-2.419
Concurrent ON (yes)	0.082	0.896	0.008	1	0.927	0.188	0.188-6.283

Nagelkerke R^2 = 0.416; overall percentage prediction = 81.3%

In the AQP4-NMOSD cohort a longer disease duration and older age showed a significant association with increased risk for relapse, with a trend for Afro-Caribbean ethnicity to also pose an increased risk. The treatment variable was removed from the AQP4-NMOSD analysis, as the final solution for this variable could not be calculated. This is likely due to the fact that nearly all patients received treatment after their first myelitis (57/69 [82.6%]). The results are shown in Table 3.4.

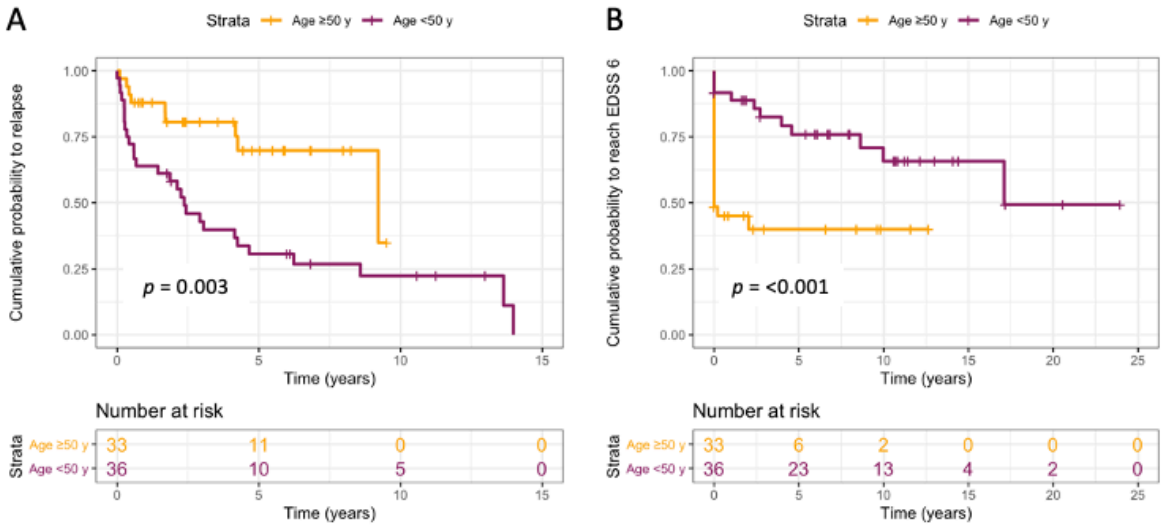
Table 3.4. Logistic regression model: relapse in AQP4-NMOSD. *Dependent variable = relapse after myelitis (yes/no).*

Parameter	Beta	Std. Error	Wald's X^2	*df*	*p* value	Odds Ratio	95% CI
Age	**-0.086**	**0.029**	**9.115**	**1**	**0.003 ****	**0.917**	**0.867-0.970**
Sex (female)	-0.423	0.959	0.194	1	0.659	0.655	0.100-4.295
Ethnicity (Afro-Caribbean)	1.518	0.829	3.353	1	0.067	4.561	0.899-23.148
Disease duration	**0.024**	**0.010**	**5.490**	**1**	**0.019 ***	**1.025**	**1.004-1.046**
Attack prior to myelitis (Yes)	0.985	1.057	0.868	1	0.352	2.678	0.337-21.266

Nagelkerke R^2 = 0.401; Prediction percentage = 83.3

To further explore the relationship with age and relapses in AQP4-NMOSD, a Kaplan-Meier analysis with a log-rank calculation was performed using the whole cohort data throughout the course of their disease (i.e., from onset to last follow-up). Using the median cut-off of 49 years of age, those in the younger group (n = 36) were more likely to relapse than those in the older group (n = 33) (log-rank: *p* = 0.003) (Figure 3.3.A).

Figure 3.3. Kaplan-Meier analysis. *Patients with AQP4-NMOSD stratified by age: ≥50 years in yellow and <50 years in magenta. (A) time to relapse and (B) time to EDSS 6. Figure adapted from (Mariano* et al.*, 2019).*



3.5.7 Disability

3.5.7.1 Recovery from onset myelitis attacks with no relapse for at least one year

To begin with, a sub-analysis was conducted to compare patients with MOGAD to those with AQP4-NMOSD with onset myelitis and who were relapse-free for at least one year. This was done to account for the impact of disability that may have been present from non-myelitis onset attacks and disability that may have been accumulated from relapses after the first myelitis. This is particularly important as those with AQP4-NMOSD were more likely to have recurrent attacks of myelitis. Although a minority of patients may experience further recovery from an attack of myelitis after one year, most recovery occurs within three to six months.

The groups consisted of 30 patients with MOGAD (mean age = 37.0 +/- 12.36; M:F = 16:14) and 44 patients with AQP4-NMOSD (mean age = 52.6 +/- 14.8; M:F = 7:37). Recovery EDSS in those with MOGAD (median: 1.5; range: 0-8) was better than in AQP4-NMOSD (median: 4; range: 1-8) ($p = <0.01$). Despite the better overall recovery EDSS in MOGAD and improvement of motor function, persistent bladder dysfunction (urgency, hesitancy, incontinence, frequent urinary tract infections) occurred slightly more frequently than in AQP4-NMOSD (18/30 [60.0%] MOGAD vs 21/44 [47.7%] AQP4-NMOSD). The number of patients requiring intermittent or in-situ catheterisation was roughly equal (6/30 [20.0%] MOGAD vs 11/44 [25.0%] AQP4-NMOSD). Persistent bowel symptoms (constipation, incontinence) occurred in 11/30 [36.7%] patients with MOGAD and 18/44 [40.9%] patients with AQP4-NMOSD. Erectile dysfunction more commonly occurred in males with MOGAD (6/16 [37.5%] in MOGAD vs 1/7 [14.3%] with AQP4-NMOSD). Acute treatment within

approximately 14 days of symptom onset was similar between the two groups and was received by 26/30 [86.7%] MOGAD patients and 40/44 [90.9%] AQP4-NMOSD patients. Acute treatment was not statistically analysed. Slightly more patients with AQP4-NMOSD received plasma exchange but, overall, the acute treatment was similar in both groups.

In the MOGAD cohort, patients received treatment as follows:

- 18 intravenous methylprednisolone,
- 5 intravenous methylprednisolone and plasma exchange,
- 1 intravenous methylprednisolone and intravenous immunoglobulin,
- 1 intravenous methylprednisolone, plasma exchange and intravenous immunoglobulin, and
- 1 high dose oral prednisolone.

In the AQP4-NMOSD cohort patients received treatment as follows:

- 24 intravenous methylprednisolone,
- 13 intravenous methylprednisolone and plasma exchange,
- 1 intravenous methylprednisolone and intravenous immunoglobulin, and
- 1 intravenous methylprednisolone, plasma exchange and intravenous immunoglobulin.

3.5.7.2 Total cohort analysis of factors associated with disability after first myelitis

A regression model was built for each condition to assess for factors that may predict poorer outcomes from the first myelitis.

In those with MOGAD, the presence of a brainstem lesion at the time of the myelitis was associated with more disability (Table 3.5).

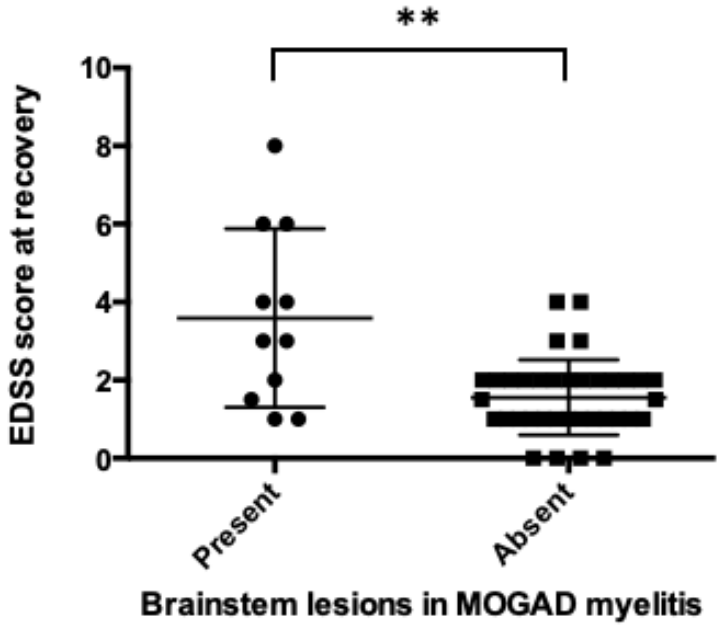
Table 3.5. Regression model: disability in MOGAD. *Dependent variable = recovery EDSS.*

	Beta	**Std. Error**	***p* value**	**Tolerance**	**VIF**
Age	0.001	0.018	0.991	0.882	1.134
Sex	-0.432	0.435	0.326	0.824	1.214
Disease duration	-0.110	0.003	0.422	0.835	1.198
Brain lesion on MRI	-0.029	0.455	0.842	0.751	1.331
Brainstem lesion on MRI	**0.491**	**0.550**	**0.002 ****	**0.714**	**1.400**
EDSS at nadir	0.109	0.109	0.052	0.747	1.339

Adjusted R^2 = 0.30; p = 0.002

The recovery EDSS scores of MOGAD patients with brainstem lesions were then compared directly to those without. The result of this supports the above finding. The median recovery EDSS in those with brainstem lesions on MRI at the time of their first attack of myelitis was significantly higher than in those with brainstem lesions (3.0 versus 1.5; *p* = 0.003) (Figure 3.4).

Figure 3.4. Mean recovery EDSS in patients with MOGAD. *EDSS scores stratified by the presence of a brainstem lesion at the time of the myelitis. Mean and standard deviation depicted. ** = p <0.01. Figure adapted from (Mariano et al., 2019).*



In AQP4-NMOSD, the severity of the onset attack and the age at onset were the strongest predictors of disability (Table 3.6). The presence of a brain lesion at onset just reached significance but as most patients had non-specific lesions and given that these lesions are also more common with increasing age, the clinical importance of this is not certain.

Table 3.6. Regression model: disability in AQP4-NMOSD. *Dependent variable = recovery EDSS.*

	Beta	**Std. Error**	***p* value**	**Tolerance**	**VIF**
Age	**0.305**	**0.015**	**0.002 ** **	**0.702**	**1.424**
Sex (female)	0.004	0.494	0.958	0.978	1.022
Disease duration	-0.033	0.003	0.696	0.873	1.145
Brain lesion on MRI	**0.165**	**0.467**	**0.049 ***	**0.920**	**1.086**
Brainstem lesion on MRI	0.115	0.529	0.197	0.799	1.252
EDSS at nadir	**0.597**	**0.117**	**0.000 ** **	**0.698**	**1.433**

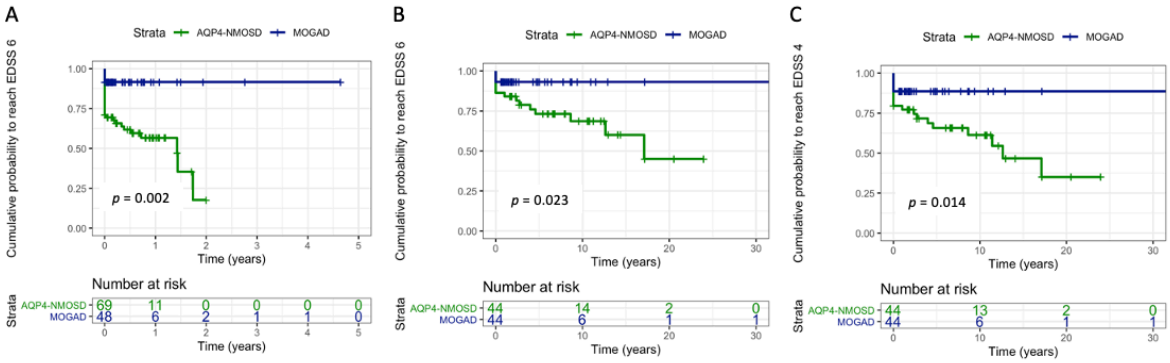
Adjusted R^2 = 0.65; p = <0.01

To further explore the effect of age in AQP4-NMOSD on disability the same subgroups used in the relapse analysis were entered into a Kaplan-Meier analysis with log rank calculation. The younger group (<50), although more likely to relapse was less likely to reach EDSS 6 over the course of their disease than the older group (≥50) (log-rank: p = <0.01, Figure 3.3.B). What is also clearly visible in this figure is the sharp initial drop in the older cohort denoting disability from onset myelitis.

3.5.7.3 Total cohort analysis of disability throughout disease course

The outcomes of both groups were then considered over the entire disease course in both cohorts. A Kaplan-Meier analysis with log-rank calculation was conducted to analyse the time to EDSS 6 in both cohorts. Those with AQP4-NMOSD were overall more likely to reach this endpoint (log rank: p = <0.001) (Figure 3.5.A). To account for the age and sex differences between the two cohorts, the same analysis was then conducted on propensity score matched groups using the nearest neighbour method. These cohorts consisted of 44 patients with MOGAD and 44 patients with AQP4-NMOSD. The mean age (35.69 +/- 12.01 versus 40.29 +/- 11.25, p = 0.668) and sex ratios (M:F = 18:26 versus 12:32 , p = 0.261) were no longer statistically significant. The AQP4-NMOSD cohort was still more likely to reach EDSS 6 (log rank: p = 0.023) (Figure 3.5.B). Finally, this analysis was conducted using EDSS 4 as the outcome. This score denotes severe disability but no assistance required to mobilise. Once again those with AQP4-NMOSD were more likely to reach this outcome (log-rank: p = 0.014) (Figure 3.5.C). These figures also show graphically that disability in MOGAD is predominantly acquired from the onset myelitis attack.

Figure 3.5. Kaplan-Meier Analysis. *Patients with AQP4-NMOSD (green) and MOGAD (blue). (A) time to EDSS 6 in the Total Cohort, (B) time to EDSS 6 in Propensity Score Matched Groups, and (C) time to EDSS 4 in Propensity Score Matched Groups. Figure adapted from (Mariano* et al.*, 2019).*

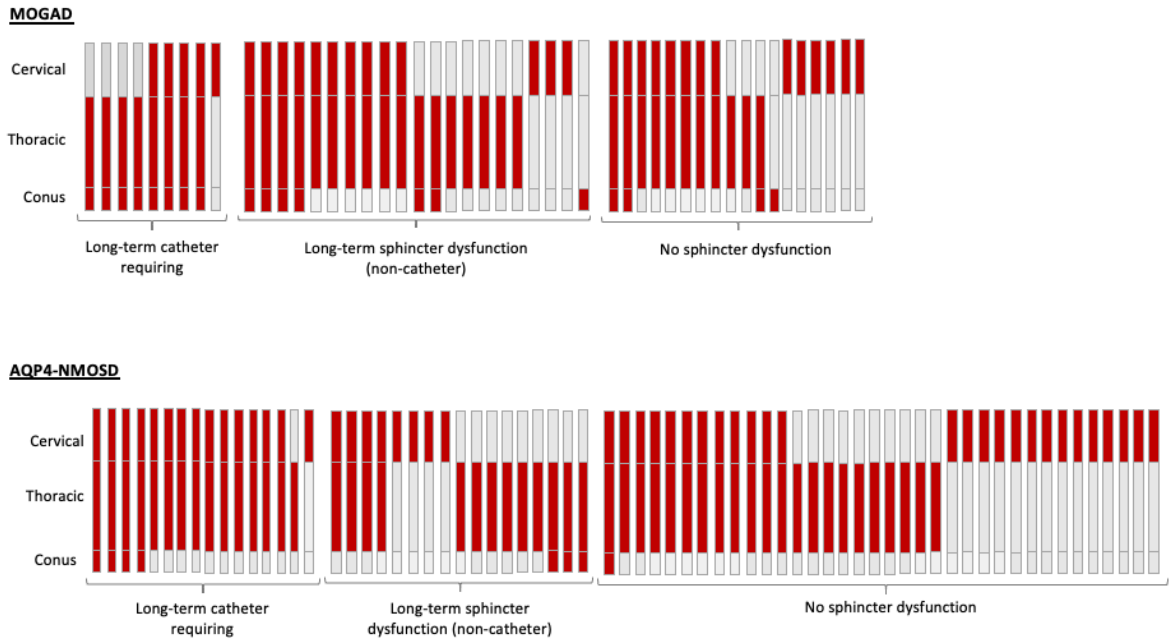


3.5.7.4 Total cohort analysis of long-term sphincter dysfunction

Sphincter dysfunction existed as a spectrum in both conditions from mild to severe. There was no significant difference in the frequency of residual long-term sphincter dysfunction between groups (29/48 [60.4%] in MOGAD versus 33/69 [47.8%] in AQP4-NMOSD) as well as no significant difference between long-term catheter requirements (9/48 [18.8%] in MOGAD versus 16/69 [23.2%] in AQP4-NMOSD). However, at last follow-up, those with MOGAD experienced this similar frequency of persistent sphincter dysfunction despite good recovery of mobility; whereas in AQP4-NMOSD those with sphincter dysfunction had these symptoms in the context of poorer mobility. Of the 16 patients in the AQP4-NMOSD cohort that required long term intermittent or in situ catheterisation, all were unable to mobilise independently, as denoted by an EDSS of >=6 (median = 7; range = 6-8). Of the nine patients in the MOGAD cohort, one required a single walking aid (EDSS = 6) and one required the use of a wheelchair (EDSS = 8); in the remaining patients, the sphincter dysfunction was the only disability outcome met (median = 4; range = 3-8).

The MOGAD cohort was then investigated more closely for a feasible explanation for the predominant of sphincter dysfunction. As shown in Table 3.2, conus lesions were significantly more common in MOGAD and so the presence of conus lesions was investigated further. Figure 3.6 shows the sagittal location of lesions in a graphical representation of each individual spinal cord.

Figure 3.6. Sagittal location of lesions and sphincter dysfunction at last follow-up in MOGAD and AQP4-NMOSD. *Areas affected by lesions shown in red and unaffected areas shown in grey. Figure adapted from (Mariano* et al*., 2019).*



The proportion of conus lesions present in MOGAD patients requiring long term catheterisation was significantly higher than in those who were not catheter-requiring (8/9 [88.8%] versus 4/16 [25.0%], p = 0.002). A logistic regression model was then built to further explore this relationship. The presence of a conus lesion significantly associated with the need for long-term catheterisation in MOGAD as shown in Table 3.7.

***Table 3.7. Logistic regression model: catheter requirement in MOGAD**. Dependent variable = catheter requirement (yes/no).*

Parameter	Beta	Std. Error	Wald's X^2	*df*	*p* value	Odds Ratio	95% CI
Age	0.002	0.044	0.002	1	0.960	1.002	0.919-1.093
Sex (female)	-1.053	1.123	0.880	1	0.348	0.349	0.039-3.152
Disease duration	-0.011	0.011	0.951	1	0.329	0.989	0.967-1.011
EDSS at nadir	0.258	0.248	1.082	1	0.298	1.294	0.796-2.103
Conus lesion (present)	**3.009**	**1.280**	**5.530**	**1**	**0.019 ***	**20.264**	**1.650-248.801**

Nagelkerke R^2= 0.385; Prediction percentage correct = 83.3%

In addition, at long term follow up the frequency of erectile dysfunction in males with MOGAD continued to be greater than in AQP4-NMOSD, although not quite statistically significant, a trend was noted (10/22 [45.5%] versus 1/12 [8.3%], *p* = 0.053); and persistent bowel symptoms were roughly equal in both cohorts (17/48 [35.4%] and 26/69 [37.7%]).

3.5.8 Follow-up clinical MRI scans

Twenty-six (26) patients with MOGAD and 41 patients with AQP4-NMOSD had follow-up MRI scans conducted at least six months outside of an acute relapse. These scans were done as a baseline investigation and not due to new symptoms or other clinical indication. Resolution of MRI abnormalities occurred in 16/26 [61.5%] of patients with MOGAD and 7/41 [17.1%] in AQP4-NMOSD (p = <0.001). In the AQP4-NMOSD cohort most patients had residual hyperintensity on T2 and atrophic changes. Resolution of MRI findings tended to occur in those with lower recovery EDSS scores, however, this did not reach significance in either cohort. No new MRI changes in areas not affected during a previous acute attack were noted in the follow-up scans of either cohort.

3.6 Discussion

In this chapter the largest single-centre cohort of adult patients with MOGAD myelitis is described and compared to adult patients with AQP4-NMOSD myelitis. The first objective was to study the clinical features of the first attack of myelitis in these conditions, in particular to describe myelitis in MOGAD.

The differences in the demographics between the two cohorts are in keeping with existing literature on these conditions. Increased age and a higher proportion of female and non-white patients is more common in AQP4-NMOSD (Pandit *et al.*, 2015). In MOGAD, patients are younger, the sex ratio is roughly equal and the ethnic split mirrors the local population, in this case predominantly white-British, as has been shown in recent epidemiological studies (Jurynczyk *et al.*, 2017*b*; Cobo-Calvo *et al.*, 2018; Senanayake *et al.*, 2018).

In both conditions, myelitis is more likely to occur at the onset attack. Previous studies in AQP4-NMOSD have shown that up to 47% of those with AQP4-NMOSD myelitis have disease limited to the spinal cord (either monophasic or recurrent attacks of myelitis) (Kitley *et al.*, 2013). The results of this chapter are in keeping with this trend in that 29/69 [42%] of patients had isolated cord involvement. Isolated cord disease occurred in only 5/48 [10%] patients with MOGAD. Those with MOGAD were more likely to have involvement of other sites at the time of the acute attack and to have non-myelitis relapses.

The acute signs and symptoms were largely similar, with severe presentations being common in both cohorts. More patients with MOGAD tended to have acute sphincter involvement (nearly reaching significance) and significantly more patients with AQP4-

NMOSD reported pain during the acute attack. Pain as a consequence of AQP4-NMOSD has been described, predominantly as a chronic neuropathic pain phenotype (Kong *et al.*, 2016, Tackley *et al.*, 2016*b*; Asseyer *et al.*, 2020). In addition to central damage that may cause pain in different aetiologies of spinal cord disease, some specific mechanism related to the loss of astrocytes and their role in regulation of neurotransmitters related to pain have been suggested, which may, in part, explain this outcome (Asseyer *et al.*, 2020).

As shown in Chapter 1, MRI findings are an essential part of diagnostic algorithms for neuroinflammatory conditions. Both the diagnostic criteria for NMOSD (Wingerchuk *et al.*, 2015) and the diagnostic criteria for multiple sclerosis (Thompson *et al.*, 2018) include MRI criteria. As we move toward specific diagnostic criteria for MOGAD, the findings that differentiate it from other neuroinflammatory conditions will be of the utmost importance. Spinal cord imaging will play an important role in this differentiation. Although the features of MOGAD and AQP4-NMOSD often overlap, there are some interesting differences that would warrant further study and would support testing for MOG-Ab. Patients with MOGAD were more likely to have multiple cord lesions, short cord lesions and involvement of the conus. The presence of short cord lesions is particularly relevant in patients with MOGAD whose first attack of myelitis occurred as a relapse where approximately half presented with short cord lesions only, which risks them being misdiagnosed as having multiple sclerosis. The importance of this is most well described in paediatric populations where those with MOGAD have been misdiagnosed with multiple sclerosis in the past (Hacohen *et al.*, 2017). Axial imaging of the spinal cord is therefore crucial in these cases, as is brain imaging. Brain lesions occurred in more than half of the patients with MOGAD at the time of their myelitis, with most being asymptomatic. Additionally, ADEM-like brain lesions

were present in those with MOGAD but not in any of this adult cohort of AQP4-NMOSD, where lesions were most commonly reported as non-specific white matter lesions. Therefore, in addition to concomitant ON, the presence of ADEM-like brain lesions occurring at the time of the myelitis would support testing for MOG-Ab.

The clinical and imaging findings from this United Kingdom-based cohort also support the findings from a study by Dubey et al. describing the features of myelitis in MOGAD in a cohort of patients from the Mayo Clinic (in the United States of America) (Dubey *et al.*, 2019). In this study the frequency of multiple cord lesions, short cord lesions, involvement of the conus and ADEM-like presentations in MOGAD were also described. Additional findings from this study included a presentation of acute flaccid myelitis in MOGAD, a presentation which was not included in this research but would be of interest for future studies. Features of spinal cord MRI described by Dubey et al. also included less frequent gadolinium enhancement in MOGAD than in AQP4-NMOSD, which was not found to be the case in the United Kingdom cohort. However, as described, in this United Kingdom cohort not all patients received contrast in the acute setting and MRI scans were conducted across different centres. Finally, the 'H-sign' was described by Dubey et al. which is T2 hyperintensity highly restricted to the grey matter in axial views of standard T2 imaging (Dubey *et al.*, 2019). Future work will also include a review of the MRI scans of the United Kingdom cohort, by a blinded rater, to assess for the presence of this sign. Finally, short cord lesions at the time of the first myelitis onset have also been recently described in 38.4% of a French cohort of MOGAD myelitis (Ciron *et al.*, 2020).

After considering the clinical presentation and imaging findings, the next objective was to study clinical outcomes: relapse and disability. AQP4-NMOSD has been shown to be a

relapsing disease and so all patients are initiated on treatment to prevent relapses after diagnosis (Kimbrough *et al.*, 2012; Jarius *et al.*, 2014). However, in MOGAD relapsing disease has been reported in 34-46% of patients (Jurynczyk *et al.*, 2017*b*; Cobo-Calvo *et al.*, 2018; Senanayake *et al.*, 2018). Being able to predict which patients go on to relapse would be very important when considering long-term treatment. The only factor significantly associated with relapses in MOGAD was disease duration. This was not an incident cohort and so many patients may only have been diagnosed at the time of a relapse and so this finding is not unexpected. No other clinical findings reached significance but there are still some interesting observations. The presenting phenotype appears to be an important factor in both conditions. In AQP4-NMOSD patients often have relapses involving the same site (Palace *et al.*, 2019). In this cohort 25/36 [69.4%] of the patients with AQP4-NMOSD went on to have recurrent attacks of myelitis. In MOGAD, ON appears to be a predominant phenotype. Patients with ON have been reported to be more likely to relapse and relapses are also more commonly ON (Jurynczyk *et al.*, 2017*b*). Patients with MOGAD in this cohort were more likely to have concomitant ON at the time of their myelitis attack and relapses were most commonly attacks of ON. This data indicates that patients with MOGAD may fulfil the 2015 NMOSD diagnostic criteria as has been shown in previous studies (Hamid *et al.*, 2017). If a patient presents with a clinical picture of antibody negative NMOSD, it would be prudent to test for MOG-Ab. However, the differences found in spinal cord MRI characteristics, as well as the less frequent occurrence of other NMOSD-specific findings (such as the typical nausea and vomiting associated with brainstem lesions) motivates for the development of a unique set of diagnostic criteria for MOGAD.

In the AQP4-NMOSD cohort, age was an important factor in the risk of relapse, supporting findings in a previous study (Tackley *et al.*, 2016*a*). This may be due to a longer disease duration in those diagnosed at a younger age, may indicate more active disease, or may suggest that compliance to immunotherapy is worse in younger patients. This finding should be studied further as disability is known to be relapse related.

While all results should be considered in light of age and sex differences, AQP4-NMOSD does appear to confer a worse overall disability, whether considering the outcomes after the first attack of myelitis or the disability at last follow-up. Propensity score matching was used to analyse more closely matched subgroups and this finding remained the same.

In the MOGAD cohort, involvement of the brainstem at the time of the myelitis (whether symptomatic or asymptomatic) associated with a poorer outcome. The mean EDSS at recovery in those with brainstem lesions was significantly higher than in those without (3.0 versus 1.5). A recent study of non-conventional brain MRI in these conditions has also shown that a lower brainstem volume, downstream of an acute attack, associated with worse disability outcomes in MOGAD (Messina *et al.*, 2020); and, brainstem involvement was found to be associated with a more aggressive general disease course in one of the first descriptions of MOGAD (Jarius *et al.*, 2016*a*), although this was focused on symptomatic brainstem involvement.

In patients with AQP4-NMOSD, age-at-onset had the strongest association with the long-term disability outcome of reaching EDSS 6. Older patients were less likely to relapse but accumulated their disability from the onset attack. In fact, disability from the onset attack

appears to be important in both conditions and so this motivates for aggressive acute treatment in order to recover as much function as possible.

While sphincter dysfunction is not limited to those with MOGAD, the proportion of those with long-term sphincter dysfunction is not proportional to the recovery of mobility, when compared to AQP4-NMOSD. Therefore, as an outcome measure, the EDSS score does not fully address the outcomes in MOGAD, as sphincter dysfunction remains of substantial concern and significantly impacts quality of life (Fumincelli *et al.*, 2017). The predilection for MOGAD to involve the conus has been consistently reported (Kitley *et al.*, 2014, Jurynczyk *et al.*, 2017*b*, Ciccarelli *et al.*, 2019; Dubey *et al.*, 2019). Conus involvement in this study was 39.6% and, although prior reports have varied from 4-75%, more recent studies are in keeping with these findings (Dubey *et al.*, 2019). The frequent involvement of the conus may be specific to the underlying pathogenesis of MOGAD. Dubey et al. made the interesting observation that lesions in the conus are present in experimental autoimmune encephalomyelitis models immunised with MOG peptide (Bannerman *et al.*, 2005; Dubey *et al.*, 2019). Additionally, as described in Chapter 1, it is interesting to note that in developmental animal models MOG displayed a caudo-rostral gradient of expression (Slavin *et al.*, 1997).

It is also shown that involvement of the conus is an important contributor to the requirement for long-term catheterisation. This finding should be interpreted with caution due to the small sample size and wide confidence interval but is a clinically plausible association and should be investigated further in a larger cohort. However, there were many patients with long-term sphincter dysfunction (non-catheter requiring) that did not have conus lesions, so lesion location does not fully explain all the long-term sphincter

symptoms in MOGAD. A recent study by Li et al., which studied the urodynamic and neurophysiological features of patients with persistent sphincter dysfunction in MOGAD also found that patients that had conus lesions required catheterisation for a significantly longer duration than those without conus lesions; but, that predominant urodynamic findings suggest ongoing lower urinary tract dysfunction results from supraconal injury (Li *et al.*, 2020). Understanding the mechanism of injury that leads to sphincter dysfunction, but recovery of motor dysfunction would be important in the evolution of our knowledge about MOGAD. Persistent sphincter dysfunction with good recovery of mobility should prompt clinicians to test for MOGAD. In AQP4-NMOSD the hypothesis is that the disease is generally more destructive and so leads to the combination of motor disability together with sphincter dysfunction.

Follow-up brain MRI, outside of a relapse, has shown resolution of lesions in MOGAD (Juryńczyk *et al.*, 2017) and an early description of four cases of myelitis in MOGAD also described normal cord MRIs at follow-up (Kitley *et al.*, 2014). The findings in this study of follow-up spinal cord MRI scans are in keeping with this. Sixty-one-and-a-half percent (61.5%) of available follow-up scans showed resolution of MRI lesions at least six months after the acute attack. This occurred in only 17.1% of patients with AQP4-NMOSD. Studies using non-conventional MRI methods to study the integrity of the normal appearing cord after an attack of myelitis would be needed to establish if this recovery is full. The pathological basis for these differences in clinical and MRI features should also be further explored. This resolution of imaging findings in MOGAD is also important when differentiating it from multiple sclerosis. Additionally, silent lesions occur at the time of the acute attack in MOGAD as shown in this work and previous literature (Baumann *et al.*,

2015, Jarius *et al.*, 2016*a*; Salama *et al.*, 2019); however, silent lesions outside of an acute relapse are atypical (Cobo-Calvo *et al.*, 2018; Ramanathan *et al.*, 2018). No MRI changes in previously unaffected areas were noted in this MOGAD cohort at follow-up imaging. This once again highlights the importance of brain imaging at the time of the acute attack and of baseline imaging downstream from an acute attack in these conditions.

3.7 Limitations

Limitations in this work include retrospective data collection and small sample sizes. However, statistical models were built according to recommendations made for small clinical studies (Heinze and Dunkler, 2017). Reporting of symptoms such as erectile dysfunction and pain are subjective. Patients with mild attacks and spontaneous recovery would not have been captured in this work. MOGAD myelitis with normal spinal cord imaging has also recently been described but was not considered in this study. Additionally, scans were from different centres and so not all patients were given contrast or had axial views taken. The strength, however, is that this data is more relevant to clinical practice with the observations being useful across centres.

3.8 Conclusion

The clinical implication of this work is a better understanding of the features of myelitis in MOGAD and how these compare to AQP4-NMOSD. It highlights the frequency of short lesions, multiple cord lesions and conus involvement in MOGAD, which, particularly in cases of isolated myelitis, should prompt testing for MOG-Ab. Involvement of the brain and optic nerves either acutely or at relapse also emphasizes that patients with an antibody-negative NMOSD diagnosis should be tested for MOG-Ab. Outcomes were then evaluated

for better risk stratification of patients which suggested that lesion location (brainstem and conus) are important in MOGAD but that age at onset is the most important predictor of outcomes in AQP4-NMOSD. Finally, the differences in these two diseases mean that long-term disability should be defined by different outcomes when considering treatment response.

4. Chapter 4: Non-conventional MRI study methods, cohort and assessments

4.1 Introduction

As described in Chapter 2, an imaging study was designed to investigate the use of non-conventional MRI sequences to further the study of inflammatory spinal cord disease. This chapter outlines the methods for the non-conventional MRI study, the results of which form the content of Chapters 5 to 8.

Sections of the methods presented below are adapted from the publication: *Mariano R, Messina S, Roca-Fernandez A, Leite MI, Kong Y, Palace JA. Quantitative spinal cord MRI in MOG-antibody disease, neuromyelitis optica and multiple sclerosis. Brain. 2020 Nov 18:awaa347. doi: 10.1093/brain/awaa347.*

4.2 Study design

This cross-sectional study was designed to compare structural, quantitative and functional imaging in four participant groups: myelin-oligodendrocyte glycoprotein associated disease (MOGAD), aquaporin-4-positive neuromyelitis optica spectrum disorder (AQP4-NMOSD), relapsing-remitting multiple sclerosis (MS) and healthy volunteers (HV).

4.2.1 Ethics

In adherence to ethical regulations from the United Kingdom National Research Ethics Service, all participants signed specific informed consent for this study (REC reference

number: 17/EE/0246). Additional clinical data was obtained under the Oxford MS and NMOSD Tissue Bank (REC reference number: 16/SC/0224). All enrolled participants had signed consent for their clinical, imaging and laboratory information to be used for research and publication.

4.2.2 Study visit

Each participant underwent a one-hour spinal cord MRI scan together with disability, pain and fatigue scoring during the same study visit.

4.2.3 Power considerations

Sample size considerations included the rarity of the diseases being studied and selecting only those with spinal cord involvement. As outlined in Chapter 1, spinal cord disease occurs in roughly 27% of those with MOGAD (Jurynczyk *et al.*, 2017*b*) and 40% of those with AQP4-NMOSD (Pandit *et al.*, 2015), these further limits availability but it was important for the objectives of this study that only those with cord involvement were included. The study was designed to have the power to detect group differences in the selected metrics based on data from previous studies (Benedetti *et al.*, 2006; Klawiter *et al.*, 2012; Pessôa *et al.*, 2012; Liu *et al.*, 2015; Matthews *et al.*, 2015, Chien *et al.*, 2018*b*) using G*power (Faul *et al.*, 2007) as well as recommendations for imaging studies based on evidence from multiple sclerosis (Altmann *et al.*, 2014; Reich *et al.*, 2015).

4.2.4 Participant recruitment

The NMO clinic Access database, used for the collection of data in Chapter 3, was once again used to screen for adult patients positive for either MOG-Ab or AQP4-Ab and at least one episode of spinal cord involvement during the course of their disease. Testing for the presence of AQP4-Ab and MOG-Ab was performed in the Autoimmune Neurology laboratory in Oxford, using cell-based assays as described in Chapter 1 (Wingerchuk *et al.*, 2014; Waters *et al.*, 2015). All MOG-Ab positive patients were negative for AQP4-Ab; similarly, all AQP4-Ab positive patients were negative for MOG-Ab. As false positives are recognised to occur more commonly with MOG-Ab testing, all results were reviewed by the laboratory team and all clinical data were reviewed by the specialist team in Oxford. No borderline cases were included.

Adult MS patients, recruited as a disease control, were approached at consecutive clinic visits if they were confirmed to be relapsing remitting and to have spinal cord involvement (either symptomatic or asymptomatic). HV were recruited by advertising, as per our ethics regulations. Participants were age and sex matched as closely as possible to the disease groups.

4.2.5 Inclusion criteria

- Confirmed diagnosis of MOGAD or AQP4-NMOSD, with available confirmatory antibody testing, or a diagnosis of relapsing-remitting multiple sclerosis diagnosed by a consultant neurologist (2010 McDonald criteria, no atypical features), or an HV.

- Adult-onset disease.

- Willing and able to give informed consent for participation.

- Fluency in English language in order to complete consent form and MRI safety questionnaire.

- Age 18 years or over at the time of the scan.

- At least one episode of spinal cord involvement in any disease group participant, in MS both symptomatic and asymptomatic lesions were accepted.

- Study visit can be completed at least 6 months after an acute attack, in order to account for the confounding effects of acute inflammation and oedema that would make the results more challenging to interpret.

4.2.6 Exclusion criteria

- Contraindication to MRI scanning, including claustrophobia.

- Unwilling to participate, or unable to fully understand participant information sheet or MRI safety questionnaire.

- Pregnancy.

- A concurrent disease/disorder that, as determined by a specialist neurologist, may confound the data or lead to undue risk to the participant. HV were adequately screened for any previous or current symptoms that may confound the findings.

4.2.7 Statistics

Statistical analysis was performed using SPSS v26.0. ANOVA with a post hoc Tukey or Kruskal-Wallis with a post hoc Dunn test were used to compare group means. Fisher's exact test was used to compare frequencies. A Pearson's correlation was used to correlate the two components of the pain score, described below.

4.2.8 Data protection

This study adhered to the General Data Protection Regulation 2016/679.

4.3 Study cohort demographics and clinical data

Twenty (20) patients with MOGAD, 20 with AQP4-NMOSD, 20 with MS and 20 HV were recruited. The demographics of each cohort are shown in Table 4.1. Where possible key baseline characteristics were matched however there are important differences between these diseases that made complete matching impossible and this was handled by adjusting for differences in the statistical analysis (detailed in each of the statistical analysis paragraphs of each Chapters 5 to 8, respectively). Patients with AQP4-NMOSD were significantly older than the other three groups. AQP4-NMOSD also had a female and non-Caucasian predominance, in keeping with demographics described in the literature (Hor *et al.*, 2020) and the MOGAD group had the shortest disease duration.

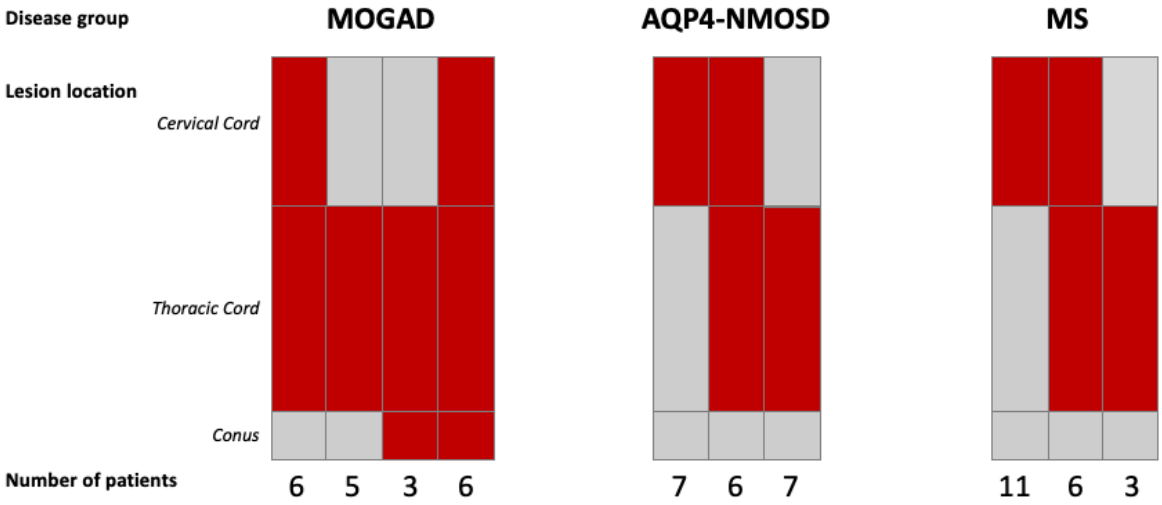
Table 4.1. Demographics and clinical data. *p values shown are based on group comparisons with the group driving the difference highlighted in bold. Adapted from* (Mariano *et al.*, 2020).

Cohort Description	**MOGAD**	**AQP4-NMOSD**	**MS**	**HV**	***p* value**
Total number	20	20	20	20	
Mean age +/- standard deviation	43.4 +/- 10.9	**55.9 +/- 11.7**	45.3 +/- 6.9	44.5 +/- 14.3	**0.003**
Sex ratio M:F	10:10	7:13	11:9	12:8	0.796
Ethnicity White Asian Afro-Caribbean	 20 (100) 0 (0) 0 (0)	 **11** **3** **6**	 20 (100) 0 (0) 0 (0)	 18 (90) 1 (5) 1 (5)	**0.001**
Phenotype (%) Isolated TM TM + ON TM + BS/BR TM + BS/BR + ON	 4 (20) 10 (50) 5 (25) 1 (5)	 10 (50) 4 (20) 3 (20) 3 (10)	 0 (0) 0 (0) 8 (40) 12 (60)		
Median disease duration in months (range)	**40.1 (8.5 – 239.9)**	157.1 (34.4 – 328.6)	147.1 (10.4 – 252.1)		**0.013**
Mean total number of attacks	2	3	3		0.426
Mean number of symptomatic myelitis attacks	1.6	2.4	**0.75**		**<0.001**
Median EDSS (range)	1.5 (0-8)	3 (1-8)	2 (0-6)		0.109
Bladder dysfunction (number requiring catheter)	13 (4)	9 (2)	6 (1)		0.084
Number of patients with neuropathic pain	5	16	9		
Mean total BPI score +/- SD in those with pain	43.0 +/- 29.8	40.1 +/- 15.6	26.2 +/- 20.8		0.346
Mean MFIS score +/- SD	27.4 +/- 18.92	35.9 +/- 20.9	36.05 +/- 14.27	(8.9 +/- 7.2)	0.989
Number of patients with MFIS score ≥38	5	10	8	0	

Patients with MOGAD and AQP4-NMOSD myelitis all had symptomatic spinal cord involvement, and those with MS included both symptomatic and asymptomatic spinal cord

lesions. The distribution of sagittal areas of the cord involved (cervical, thoracic and/or conus) is shown in Figure 4.1 and highlights more conus involvement and lack of isolated cervical cord involvement in MOGAD, and more isolated cervical involvement in MS.

Figure 4.1 Sagittal spinal cord location. *The cumulative sagittal location of lesions throughout the course of the disease in each cohort. Affected areas are shown in red and unaffected areas in grey. Figure adapted from* (Mariano *et al.*, 2020)*.*



4.4 Clinical data and cohort study visit assessments

4.4.1 Clinical data collection

Clinical data, shown in Table 4.1, was collected from the NMO clinic database and patient notes under the appropriate ethics. Clinical MRI scans, or reports where the images were unavailable, were used to document the areas that had been affected during the course of the disease in each participant. In the cervical cord the research images were then compared to this and the participants were classified as having:

- Persistent cervical cord involvement (lesion present on clinical scan and visible on research scan),

- Previous cervical cord involvement (lesion present on clinical scan and no longer visible on research scan), or

- No cervical involvement.

In the thoracic cord only sagittal T2 imaging was acquired in the research protocol, as will be described in more detail below, and so confirmation of persistent or resolved lesions was not possible. Therefore, in the thoracic cord, participants were classified as having:

- Thoracic cord involvement, or

- No thoracic cord involvement.

4.4.1.1 Severity and treatment of the acute attacks

The severity at nadir during acute attacks in the antibody mediated conditions was the same: median (range) 6.0 (3-9) in MOGAD and 6.0 (3-8) in AQP4-NMOSD.

In the antibody-mediated conditions treatment of the acute attack is particularly important (Kleiter *et al.*, 2016). In the AQP4-NMOSD cohort all patients were treated acutely in a range of 1-10 days from the onset of symptoms. A total of 48 myelitis attacks occurred in this cohort. Five (from three patients) were treated with intravenous methylprednisolone, followed by plasma exchange; one was treated with high dose oral prednisolone and the remaining were all treated with intravenous methylprednisolone. In all cases the acute treatment was followed by a tapering dose of oral prednisolone and all of these patients were continued on long-term immunosuppression thereafter. In the MOGAD cohort all patients were treated acutely in a range of 1 to 9 days from the symptom onset. A total of

31 myelitis attacks occurred in this cohort. Twenty-five (25) were treated with intravenous methylprednisolone. Five were treated with high dose oral prednisolone and one was untreated and resolved spontaneously. All those in the MOGAD cohort then received tapering oral prednisolone which continued for a range of six months to one year after their attack. Six of the relapsing MOGAD patients were started on an additional long-term immunosuppressant.

4.4.2 Motor disability

An Expanded Disability Status Scale (EDSS) (Kurtzke, 1983) assessment was conducted on the day of the MRI by a rater with Level C (highest possible) status in EDSS scoring. The detail of this scoring system is described in chapter 3.

The median EDSS scores did not differ significantly between the three groups and are as follows: MOG-Ab 1.5 (0-8), AQP4-Ab 3.0 (1-8) and multiple sclerosis 2 (0-6). However, of note, in patients with MOG-Ab there was a single patient with an EDSS of 8, the remainder of patients all being ≤3.

4.4.3 Bladder dysfunction

Long term bladder dysfunction was assessed as either the presence of current symptoms of bladder dysfunction (at least 6 months after an acute attack), with no other identifiable cause aside from the history of spinal cord disease, or not. Those with bladder dysfunction were then further classified as catheter requiring or not.

Bladder dysfunction occurred predominantly in those with MOGAD (13 with sphincter dysfunction, 4 requiring catheterisation) when compared to AQP4-NMOSD (9 with sphincter dysfunction, 2 requiring catheterisation) and MS (6 with sphincter dysfunction, 1 requiring catheterisation).

4.4.4 Pain scoring

Pain scoring was conducted using the full Brief Pain Inventory (BPI) short form (Cleeland and Ryan, 1994) which consists of 10 questions. Before beginning with the first question participants are asked to score pain related to their spinal cord disease, rather than that of co-existing problems such as musculoskeletal back pain, and also to focus on non-spasm related pain. The scores in the first four questions are combined to indicate pain severity (out of 40). The four components that make up the severity score are separately rated between 0, no pain, to 10, worst pain imaginable. The questions ask about pain on average, current pain, maximal pain in the last 24 hours and minimal pain in the last 24 hours (Cleeland and Ryan, 1994). The seven questions that follow form the functional interference score (out of 70). This incorporates seven questions rated from 0 to 10 to assess the impact of the pain on activity, mood, walking, work, relationships, sleep and enjoyment of life. The maximum total pain score is therefore 110.

More patients with AQP4-NMOSD had pain than those with MOGAD and MS, but the average total pain scores in those with pain did not differ significantly. Pain severity scores correlated with pain interference scores (Pearson's correlation: r = 0.791, p = <0.001).

4.4.5 Fatigue scoring

Fatigue was scored using the Modified Fatigue Impact Scale (MFIS) (Fisk *et al.*, 1994). This questionnaire consists of 21 questions which are rated from 0-4 (0 representing 'never' and 4 representing 'always'). The questions can be further divided into a physical subscale (nine questions), cognitive subscale (ten questions) and psychosocial subscale (two questions). Clinically significant fatigue is thought to be represented by a total score of 38 based on studies that have correlated MFIS scores with other fatigue scales and sought to find comparative values for defining clinical fatigue (Kos *et al.*, 2005; Téllez *et al.*, 2005; Larson, 2013).

Five patients with MOG-Abs, ten patients with AQP4-Abs, eight patients with multiple sclerosis and 0 HV reached the diagnostic score of 38 on the MFIS. The mean MFIS scores in all three disease groups (p = 0.006, <0.001, <0.001 respectively) were significantly higher than in the healthy volunteers (X^2 = 29.13, p = <0.001), but the scores did not differ between the disease groups.

4.5 MRI hardware and imaging modalities

4.5.1 Imaging hardware

All imaging was performed in Oxford's Functional Magnetic Resonance Imaging Centre for the Brain (FMRIB) on a 3-tesla Siemen's MAGNETOM® Prisma MR scanner. The scanner was fitted with a 64-channel head and neck coil and 8-channel spine coil. The head coil was fitted with a mirror mount in order for the participant to look at a fixed cross during the resting state functional MRI acquisition and thereafter they were offered a choice of a

movie or documentary to watch during the scan. Participants were positioned, using cushioning, to minimise cervical lordosis. The laser marker was used to mark the isocentre on the chin. Respiratory bellows and a pulse oximeter were fitted and BIOPAC software was used to record respiratory movements, cardiac cycle and scanner trigger timing.

4.5.2 Imaging sequences

The selected imaging protocols are shown in Table 4.2. The full acquisition details and analysis pipelines are described in the relevant chapters.

Table 4.2. Imaging Protocols

Sequence	**Coverage**	**Details**	**Anatomical marker used to standardise positioning**
3D T1-weighted	Cervical cord	3D T1 MPRAGE. TR: 2.3s. TE: 3.57ms. Flip angle: 9°. PE: A>>P. Resolution: 1x1x1mm^3.	Pons
3D T2-weighted	Cervical cord	3D T2 SPACE. TR: 1.5s. TE: 95ms. GRAPPA acceleration factor 2. PE: H>>F. Resolution: 0.8X0.8X0.8mm^3.	Pons
	Thoracic cord	3D T2 SPACE. TR: 1.5s. TE: 136ms. GRAPPA acceleration factor 2. PE: A>>P. Resolution: 0.8X0.8X0.8mm^3.	Upper border of T1 vertebral body
Axial T2-weighted	Cervical cord	2D T2* MEDIC. TR: 5.6s. TE: 71ms. GRAPPA acceleration factor 2. PE: R>>L. 6 echoes. Resolution: 0.5X0.5X5mm^3.	Anterior atlanto-axial joint
Diffusion tensor	Cervical cord	DTI AP/PA. TR: 6.2s. TE: 72ms. Flip angle: 80°. Resolution: 1×1×4mm^3. b=1000, 32 directions.	Centred at C3/C4
Magnetisation transfer	Cervical cord	MT on/off. TR: 600ms. TE: 8.6ms. Resolution: 0.4x0.4x4mm^3.	Centred at C3/C4
Resting-state functional MRI	Cervical cord	EPI. TR: 1.82. TE: 30ms. Flip angle: 80°. FOV: 128x128mm^2. GRAPPA acceleration factor 2. PE: P>>A. Slices: 20. Resolution: 1.0x1.0x5.0mm^3.	Centred at C3/C4

4.5.3 Rationale for sequence and software selection

The multimodal protocol allows for a robust study of the spinal cord. This includes measurements of atrophy in the cervical and thoracic cord, as well as cervical cord grey matter atrophy and lesion volume. Quantitative measures are used to study the white matter demyelination and integrity in greater detail in the cervical cord. Resting-state functional MRI (RS-fMRI) is acquired as a novel technique to be tested across groups to measure the connectivity in the cervical cord.

Additionally, as described in Chapter 1, the selected techniques (aside from RS-fMRI which is novel) have shown clinical relevance in both MS and NMOSD. The final considerations for sequence selection were the availability of existing sequences and support for piloting, testing and sequence optimisation. These were available for the final selected sequences.

Data were processed with tools from Spinal Cord Toolbox (SCT) v4.0 (De Leener *et al.*, 2017) and FMRIB Software Library (FSL) 6.0 (Jenkinson *et al.*, 2012). A combination of tools across these two platforms were integrated to enable the analysis of each sequence acquired, as is described in Chapters 5 to 8. Training was available for each software package (the FMRIB Graduate Programme was completed at the University of Oxford in 2017; the SCT Workshop was completed at University College London in 2019). Additionally, formal online support, created by the developers, is available for the use of both SCT (https://spinalcordmri.org/) and FSL (https://fsl.fmrib.ox.ac.uk/fsl/fslwiki).

4.6 Limitations

This MRI study has certain general limitations (others specific to the particular analysis or metric acquired will be described in the relevant chapter). First, sample size is a limitation in that subtle differences may not be evident. Second, brain and brainstem findings were not considered in this study. Third, the recognised disease characteristics mean that groups cannot be totally matched, for example, the older age, ethnic differences and higher mean number of myelitis attacks in AQP4-NMOSD. As well as the predominance of cervical cord involvement in MS, as compared to the lower cord involvement in the antibody mediated conditions, particularly in MOGAD where all patients had thoracic cord involvement.

However, groups were fairly matched across many other characteristics and those that were not matched are included in the statistical analyses. Additionally, the homogeneity of a single-centre study where imaging is done on the same scanner (especially because obtaining reliable quantitative spinal cord imaging is challenging), and where consistency and accuracy of diagnosis is maximised (using the same highly specific assays and clinicians and all patients with spinal cord involvement) is an advantage. The findings can then be used to build hypotheses and decide which protocols need to be aligned when taking observations forward into multi-centre studies.

Spinal cord imaging is further limited by the availability of hardware e.g. coils. While the 64-channel head and neck coil offered good quality imaging of the cervical cord, only structural imaging was possible in the thoracic cord, as the spine coil offers only posterior coils. Additionally, both acquisition techniques and analysis pipelines make it challenging to image the cord together with the brainstem or brain. This would be particularly relevant

when linking symptoms, which may be caused by dysfunction at many levels or locations, to MRI findings. In particular, RS-fMRI would benefit from this and new developments in the acquisition of RS-fMRI that capture the brain and brainstem together with the cord will be discussed in Chapter 8.

5. Chapter 5: Structural spinal cord MRI in MOGAD, AQP4-NMOSD and MS

5.1 Introduction and background

Structural MRI of the spinal cord is an important clinical tool for the diagnosis of abnormalities of the spinal cord soft tissue. The features identified on these images are useful for diagnosis and follow-up (Ciccarelli *et al.*, 2019; Moccia *et al.*, 2019). This thesis began by studying the clinical imaging features of spinal cord involvement in myelin oligodendrocyte glycoprotein associated disease (MOGAD), as compared to aquaporin-4-positive neuromyelitis optica spectrum disorder (AQP4-NMOSD) (see Chapter 3). Recent advancements in analysis methods for spinal cord MRI mean that these types of structural images (T1 and T2-weighted anatomical images) can now also be used to segment the different tissue types (white matter, grey matter and lesions) and quantify these by measuring volume or cross-sectional area (CSA) (Rocca *et al.*, 2011; Valsasina *et al.*, 2015; Prados *et al.*, 2016; Gros *et al.*, 2019; Moccia *et al.*, 2019).

As described in Chapter 1, measurements of the cervical cord, thoracic cord and grey matter show clinically relevant differences between neuro-inflammatory conditions and healthy volunteers (HV), with most studies focused on multiple sclerosis (MS) (Moccia *et al.*, 2019). A few previous studies have looked at upper cervical cord CSA in NMOSD, either showing evidence of atrophy (Liu *et al.*, 2015; Schneider *et al.*, 2015, Chien *et al.*, 2018*a*), or no differences between NMOSD and HV (Matthews *et al.*, 2015). Only one considered patients with MOGAD and showed no difference in upper cervical cord CSA compared to

HV (Chien *et al.*, 2018*b*). However, some NMOSD cohorts included antibody-negative patients and the patients did not all have spinal cord involvement. This chapter seeks to address these considerations in the form of a single-centre study where all patients have spinal cord involvement, imaging is done on the same scanner and consistency and accuracy of diagnosis is maximised (using the same highly-specific assays and clinicians).

Although there is clinical overlap between these conditions, as shown in Chapter 1, the underlying pathogenesis for each is unique causing important differences. Most notable is that MS is associated with chronic disease activity and progressive disability outside of relapse, whereas the two antibody diseases (i.e., MOGAD and AQP4-NMOSD) cause a relapsing course with more severe relapses and stability in between relapses (Akaishi *et al.*, 2020). The presence of AQP4-antibody (Ab) is an independent predictor for relapses and so all patients require long-term immunosuppression therapy to prevent relapses (Weinshenker *et al.*, 2006; Jarius *et al.*, 2014; Wingerchuk *et al.*, 2015). In MOGAD relapses occur in 34-46% of patients (Jurynczyk *et al.*, 2017*b*; Cobo-Calvo *et al.*, 2018; Senanayake *et al.*, 2018). Differences between the monophasic and relapsing cohorts of this condition are not yet understood. Understanding what drives the differences between and within these disease groups would offer essential information to our understanding of these conditions as well as to therapeutic development and outcome prediction.

The work presented below is adapted from the publication: *Mariano R, Messina S, Roca-Fernandez A, Leite MI, Kong Y, Palace JA. Quantitative spinal cord MRI in MOG-antibody disease, neuromyelitis optica and multiple sclerosis. Brain. 2020 Nov 18:awaa347. doi: 10.1093/brain/awaa347.*

5.2 Objectives and aims

The objectives and aims of this chapter are as follows:

- To compare three structural measurements (mean cervical cord CSA, mean thoracic cord CSA and mean cervical cord grey matter CSA) across the four study cohorts (MOGAD, AQP4-NMOSD, MS and HV).

- To conduct a sub-group analysis for each disease group to explore differences between affected and unaffected areas of the cord (as defined by lesion location on clinical imaging) and between the monophasic and relapsing patients with MOGAD.

5.3 Hypotheses

Three hypotheses were developed for this chapter, as follows:

- Group-level differences will be found between HV and the AQP4-NMOSD and MS groups.

- The antibody-mediated conditions will show localised damage in areas that were affected during the acute attack.

- The different patterns of involvement in the disease sub-group analyses will provide insight into the underlying mechanisms of the three conditions.

5.4 Methods

5.4.1 Subjects

The 80 participants from the imaging cohort described in Chapter 4 were included in this analysis. Full details of the ethics, recruitment, cohort demographics and clinical assessments are as described in Chapter 4.1 and summarised in Table 4.1.

Patient cohorts were further divided into the following categories (the full methods of which are described in Chapter 4.1):

Cervical cord:

- Persistent (lesion present on clinical scan and visible on research scan),
- Previous (lesion present on clinical scan and no longer visible on research scan), or
- No cervical involvement.

Thoracic cord:

- Thoracic cord involvement, or
- No thoracic cord involvement.

5.4.2 MRI Acquisition

Imaging protocols and acquisition methods are provided in Chapter 4.2. The imaging sequences analysed in this chapter are cervical cord 3D T1-weighted (MPRAGE), cervical and thoracic cord 3D T2-weighted (SPACE) and cervical cord axial T2-weighted. Five axial T2-weighted scans were excluded due to poor quality (one MOGAD, two AQP4-NMOSD and two MS). Seventeen (17) participants (three MOGAD, nine AQP4-NMOSD, four MS and one HV) did not have thoracic 3D T2-weighted imaging acquired.

5.4.3 MRI analysis

Data were processed with tools from Spinal Cord Toolbox (SCT) v4.0 (De Leener *et al.*, 2017) and FMRIB Software Library (FSL) 6.0 (Jenkinson *et al.*, 2012).

Figure 5.1 shows examples of the analysis methodology described below.

5.4.3.1 Cervical cord cross-sectional area

3D T1 images were automatically segmented to generate a cord mask using the DeepSeg (Gros *et al.*, 2019) tool in SCT and manually adjusted, when necessary, using the FSL viewer FSLeyes (McCarthy, 2019) in slices presenting low contrast between cord and cerebrospinal fluid. DeepSeg is a fully automated spinal cord segmentation method based on a deep learning convolutional neural network module trained to effectively segment the spinal cord from MRI images (Gros *et al.*, 2019). T1 images were then labelled per vertebral level and straightened before being registered to a standardised template, the PAM-50 spinal cord template, from SCT using a multi-step registration method based on non-linear

transformations. Quality of registration was visually inspected in the axial and sagittal plane using the quality control mechanism provided by SCT (De Leener *et al.*, 2017). CSA was then computed across the whole cervical cord using the vertebral levels as anatomical markers from C1 to C7. Normalisation was not performed. Previous studies have reported that CSA in the spinal cord may be associated to features such as brain volume or total intracranial volume, but the correlations were low, and no consensus has been reached regarding the best method to normalise cord data (Papinutto *et al.*, 2015) and so studies have published such data without any normalisation performed (Healy *et al.*, 2012; Kearney *et al.*, 2014). Some studies have suggested normalising cervical cord CSA using a brain scaling factor that is inversely proportional to the total intracranial volume (Horsfield *et al.*, 2010; Rocca *et al.*, 2019). However, as not all subjects in this study had available brain imaging this technique was not tested. Finally, it has also been suggested that age and sex may impact these measurements (Papinutto *et al.*, 2015) and so these are taken into consideration in the statistical analysis. HV CSA data is within range of other imaging and cadaveric studies (Frostell *et al*., 2016; Ko *et al.,* 2004). See Figure 5.1 A and B.

5.4.3.2 Cervical cord grey matter

Grey matter segmentation was done using the axial T2* imaging and a derivative of DeepSeg specific to the grey matter, *deepseg_gm* (Perone *et al.*, 2018) across the same number of slices in all participants (approximately C1-C5), two acquisitions were run in order for the axial slices to remain orthogonal to the cord and account for cervical lordosis, the angles of which may impact grey matter quantification. The last four slices were excluded in all participants due to consistently poor quality due to motion artifact. Images

were then registered to the PAM-50 template and grey matter CSA was calculated from the T2*-weighted space using *sct_process_segmentation*. See Figure 5.1 F.

5.4.3.3 Cervical cord lesions

Binary lesion masks were manually generated using both axial MEDIC and sagittal T2-weighted images using FSLeyes (McCarthy, 2019) which were co-registered and then confirmed by a blinded rater. Lesion volume was then calculated from the lesion masks using fslstats (Jenkinson *et al.*, 2012). See Figure 5.1 E, G and H.

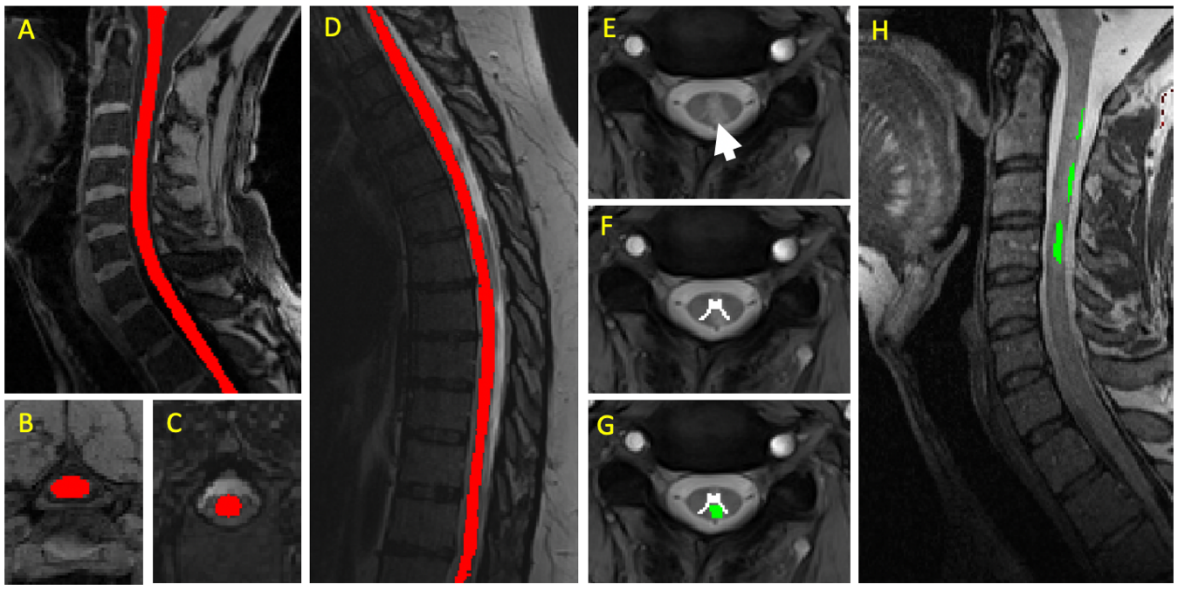
5.4.3.4 Thoracic cord cross-sectional area

Thoracic cord images were analysed to obtain the mean CSA. 3D T2 images were segmented to generate a cord mask using DeepSeg (Gros *et al.*, 2019) and manually adjusted, when necessary, using the FSL viewer FSLeyes (McCarthy, 2019) in slices presenting low contrast between cord and cerebrospinal fluid. A multi-step registration method based on non-linear transformations was used to register each magnetic resonance scan to the PAM-50-T2 spinal cord template (De Leener *et al.*, 2017). Quality of registration was visually inspected using the quality control mechanism provided by SCT. CSA was calculated per vertebral level to encompass the whole thoracic cord but excluding the conus. Therefore, the mean CSA for each participant was taken from T1 to one level above the conus. As described in detail in the cervical cord CSA area analysis (above), these values were not normalized but sex and age were accounted for in the statistical analysis of these measures. See Figure 5.1 C and D.

5.4.4 Statistical analysis

Statistical analysis was performed using SPSS v26.0 and figures created using GraphPad Prism version 6.0c. All comparisons between groups were done using ANCOVA (general linear model in SPSS with age and sex included as continuous and binary variables, respectively) with a post-hoc Bonferroni to correct for multiple comparisons. Comparisons of sub-groups within one cohort were done using a Student's T-test or Mann-Whitney U test when two sub-groups were compared. When more than two sub-groups were compared, an ANCOVA with post-hoc Tukey or Kruskal-Wallis with post-hoc Dunn test were used. The monophasic and relapsing MOGAD cohorts, as well as their comparison to the HV group, were analysed using the general linear model in SPSS with age and sex included to account for the increased proportion of males noted in the monophasic MOGAD group. *p* values were 2-tailed and statistical significance was set at 0.05.

Figure 5.1 Imaging analysis. *Examples of the MRI analysis outputs showing (A) 3DT1 image with a sagittal view of cervical cord segmentation in red, (B) 3DT1 image with an axial view of cervical cord segmentation in red, (C) 3DT2 image with an axial view of thoracic cord segmentation in red, (D) 3DT2 image with a sagittal view of thoracic cord segmentation in red, (E) axial T2-weighted image showing a posterior cord lesion (white arrow) in a patient with MS, (F) axial T2-weighted image with the grey matter segmented in white, (G) axial T2-weighted image with the grey matter segmented in white and lesion segmented in green, and (H) lesion masks shown co-registered with the sagittal T2-weighted image. Figure adapted from* (Mariano *et al.*, 2020).



5.5 Results

The imaging results are shown graphically in Figure 5.2, the between-group comparison, and Figure 5.3, the within-group comparison based on the lesion status sub-groups described in the methods

Figure 5.2 Between-group comparison. *MRI metrics for each participant shown as raw data with lines for mean and standard deviation. * = p value <0.05; ** = p value <0.01; CSA = cross-sectional area. Figure adapted from* (Mariano *et al.*, 2020)

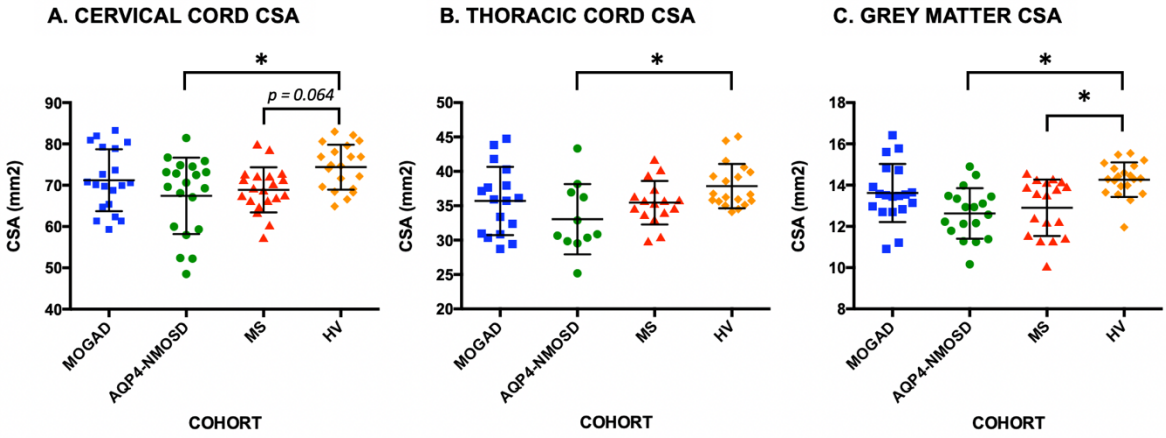
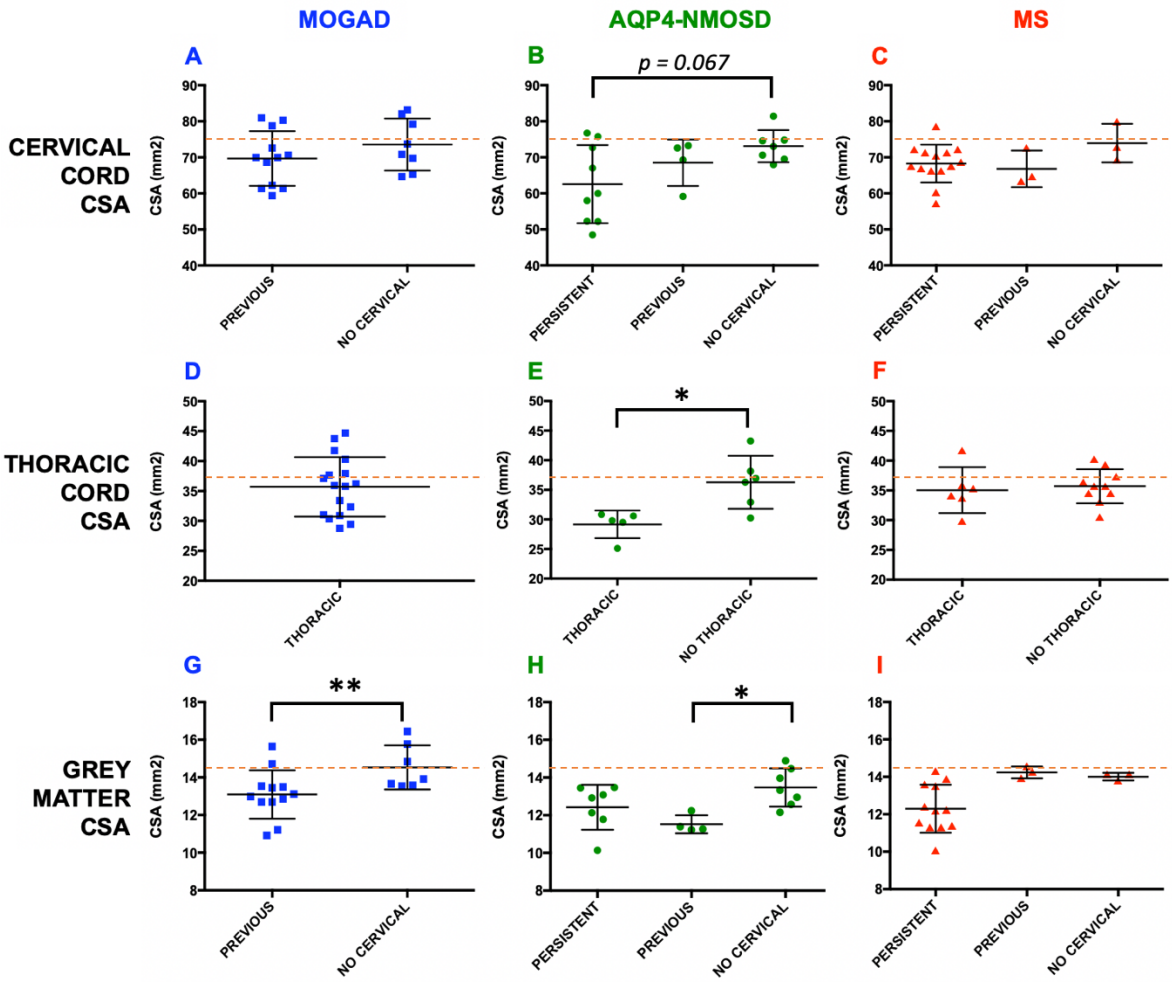


Figure 5.3 Within-group comparison. *MRI metrics for each participant shown as raw data with lines for mean and standard deviation. The orange dotted line represents the healthy volunteer mean for each modality. * = p value <0.05; ** = p value <0.01; CSA = cross-sectional area. Figure adapted from* (Mariano *et al.*, 2020).



5.5.1 Cervical cord lesions

Nine (9) of 13 AQP4-NMOSD and 14 of 17 MS cervical cord lesions were persistent, all 12 cervical cord lesions in MOGAD patients were no longer visible on these follow-up scans.

Mean cervical lesion volume did not differ between AQP4-NMOSD and MS (247.78mm^3 versus 305.56mm^3, p = 0.853); however, the mean number of lesions was significantly different, with a greater number of lesions occurring in patients with multiple sclerosis (1

+/- 0 versus 3 +/- 2, *p* = 0.007), in keeping with the expected single, long lesions in AQP4-Ab disease.

5.5.2 Cervical cord CSA

The cervical cord CSA group comparison is shown in Figure 5.2 A. The ANCOVA results and pairwise comparisons are shown in Table 5.1 and Table 5.2, respectively.

Table 5.1 Cervical cord cross-sectional area ANCOVA

	Type III Sum of Squares	**df**	**Mean Square**	**F**	***p* value**
Corrected model	**1033.096**	**8**	**129.137**	**2.748**	**0.011**
Group	469.585	3	156.528	3.331	0.024
Age	7.574	1	7.574	0.161	0.689
Sex	221.962	1	221.962	4.723	0.033

R^2 = 0.236 (Adjusted R^2 = 0.150)

Table 5.2 Cervical cord cross-sectional area pairwise comparison. *p values shown are adjusted with a Bonferroni correction for multiple comparisons.*

Group	**Comparison Group**	**Mean Difference**	**Std. Error**	***p* value**	**95% Confidence Interval**	
MOGAD	AQP4-NMOSD MS HV	3.328 2.252 -3.528	2.412 2.177 2.191	1.000 1.000 0.670	-3.219 -3.658 -9.474	9.874 8.162 2.417
AQP4-NMOSD	MOGAD MS HV	-3.328 -1.076 **-6.856**	2.412 2.368 **2.445**	1.000 1.000 **0.039**	-9.874 -7.503 **-13.492**	3.219 5.352 **-0.219**
MS	MOGAD AQP4-NMOSD HV	-2.252 1.076 -5.780	2.177 2.368 2.202	1.000 1.000 0.064	-8.162 -5.352 -11.757	3.658 7.503 0.197
HV	MOGAD AQP4-NMOSD MS	3.528 **6.856** 5.780	2.191 **2.445** 2.202	0.670 **0.039** 0.064	-2.417 **0.219** -0.197	9.474 **13.492** 11.757

In patients with MOGAD there was no significant reduction in cervical cord CSA overall compared to HV (Figure 5.2 A) or when comparing those with previous lesions in the cervical cord to those without (Figure 5.3 A).

The patients with AQP4-NMOSD showed a significant reduction in mean cervical cord CSA compared to HV (p = 0.039) (Figure 5.2 A). When examining this further, this appears to be driven by those with cervical cord involvement. The mean cervical cord CSA of those without a history of cervical cord lesions being almost equivalent to HV (73.11mm^2 versus 74.38mm^2, p = 0.815) and a near-significant difference between the 'persistent' and 'thoracic only' groups (p = 0.067) [$F(2,17) = 3.296$, $p = 0.062$] (Figure 5.3 B).

In patients with MS, the cervical cord CSA was lower than HV, although this did not quite reach significance in the group comparison (p = 0.064) (Figure 5.2 A). The relationship with the lesion status was not significant (Figure 5.3 C).

5.5.3 Thoracic cord CSA

The thoracic cord CSA group comparison is shown in Figure 5.2 B. The ANCOVA results and pairwise comparisons are shown in Table 5.3 and Table 5.4, respectively.

Table 5.3 Thoracic cord cross-sectional area ANCOVA

	Type III Sum of Squares	**df**	**Mean Square**	**F**	***p* value**
Corrected model	**187.030**	**5**	**37.406**	**2.197**	**0.067**
Group	141.281	3	47.094	2.766	0.050
Age	3.453	1	3.453	.203	0.654
Sex	15.344	1	15.344	.901	0.346

$R^2 = 0.162$ (Adjusted $R^2 = 0.088$)

Table 5.4 Thoracic cord cross-sectional area pairwise comparison. *p values shown are adjusted with a Bonferroni correction for multiple comparisons.*

Group	Comparison Group	Mean Difference	Std. Error	*p* value	95% Confidence Interval	
MOGAD	AQP4-NMOSD MS HV	2.253 0.156 -2.272	1.676 1.440 1.382	1.000 1.000 0.634	-2.327 -3.781 -6.050	6.833 4.093 1.506
AQP4-NMOSD	MOGAD MS HV	-2.253 -2.097 **-4.525**	1.676 1.692 **1.636**	1.000 1.000 **0.046**	-6.833 -6.722 **-8.997**	2.327 2.528 **-0.053**
MS	MOGAD AQP4-NMOSD HV	-0.156 2.097 -2.428	1.440 1.692 1.400	1.000 1.000 0.530	-4.093 -2.528 -6.255	3.781 6.722 1.399
HV	MOGAD AQP4-NMOSD MS	2.272 **4.525** 2.428	1.382 **1.636** 1.400	0.634 **0.046** 0.530	-1.506 **0.053** -1.399	6.050 **8.997** 6.255

There were no patients with MOGAD that did not have thoracic cord involvement (Figure 5.3 D). They did not differ from HV in the group comparison (Figure 5.2 B); however, it should be noted that there was more variability observed in the MOGAD cohort compared to the HV group and the only patient with MOGAD to reach EDSS >6 had the smallest thoracic CSA in this cohort.

Patients with AQP4-NMOSD had a lower thoracic cord CSA than HV (Figure 5.2 B). This just reached significance (p = 0.046). Again, this appears to be driven by involvement of the thoracic cord, as those that had never been affected by thoracic cord lesions have values comparable to the HV group (36.29mm^2 versus 37.85mm^2, p = 0.367) and a significant difference between the 'thoracic' and 'no thoracic' sub-groups (29.81mm^2 versus 36.59mm^2, p = 0.017) (Figure 5.3 E).

In patients with MS, no significant differences were found in either the group comparison or sub-group analysis (Figure 5.2 B and Figure 5.3 F).

5.5.4 Cervical cord grey matter CSA

The grey matter CSA group comparison is shown in Figure 5.2 C. The ANCOVA results and pairwise comparisons are shown in Table 5.5 and Table 5.6, respectively.

Table 5.5 Cervical cord grey matter cross-sectional area ANCOVA

	Type III Sum of Squares	**df**	**Mean Square**	**F**	***p* value**
Corrected model	**39.939**	**8**	**4.992**	**3.379**	**0.003**
Group	22.186	3	7.395	5.006	0.003
Age	0.419	1	0.419	0.284	0.596
Sex	0.593	1	0.593	1.809	0.529

R^2 = 0.291 (Adjusted R^2 = 0.205)

Table 5.6 Cervical cord grey matter cross-sectional area pairwise comparison. *p values shown are adjusted with a Bonferroni correction for multiple comparisons.*

Group	**Comparison Group**	**Mean Difference**	**Std. Error**	***p* value**	**95% Confidence Interval**	
MOGAD	AQP4-NMOSD MS HV	0.844 0.667 -0.649	0.461 0.402 0.394	0.431 0.609 0.431	-0.410 -0.425 -1.720	2.098 1.759 0.421
AQP4-NMOSD	MOGAD MS HV	-0.844 -0.177 **-1.493**	0.461 0.453 **0.459**	0.431 1.000 **0.011**	-2.098 -1.410 **-2.741**	0.410 1.056 **-0.245**
MS	MOGAD AQP4-NMOSD HV	-0.667 0.177 **-1.316**	0.402 0.453 **0.400**	0.609 1.000 **0.010**	-1.759 -1.056 **-2.404**	0.425 1.410 **-0.228**
HV	MOGAD AQP4-NMOSD MS	0.649 **1.493** **1.316**	0.394 **0.459** **0.400**	0.623 **0.011** **0.010**	-0.421 **0.245** **0.228**	1.720 **2.741** **2.404**

In the group comparison, patients with MOGAD did not have results that differed from the HV cohort (Figure 5.2 C). In the sub-group analysis, shown in Figure 5.3 G, those with affected cords had a significantly reduce grey matter CSA when compared to those with unaffected cervical cords (13.04mm^2 versus 13.92mm^2, p = 0.003). The group with affected cords were then compared to the HV cohort and a significant difference was found (13.04mm^2 versus 14.26mm^2, p = 0.001).

Both patients with AQP4-NMOSD (p = 0.011) and with MS (p = 0.010) showed a significant reduction in grey matter CSA compared to HV in the group comparison (Figure 5.2 C). This effect appears again related to lesion location in AQP4-NMOSD as shown in Figure 5.3 H (p = 0.027) [$x^2(2) = 6.939$, p = 0.023] but not so in MS (Figure 5.3 I).

5.5.5 Cumulative cord involvement

The effect of having both cervical cord and thoracic cord involvement was then considered. In the MOGAD group, no difference was found in the thoracic cord CSA between those with only thoracic cord involvement and those with both thoracic and cervical involvement (37.09mm^2 +/- 4.19 versus 34.47mm^2 +/- 5.51, p = 0.274). As all patients had thoracic cord involvement, the cervical cord CSA comparison is already shown in Figure 5.3 A.

In the AQP4-NMOSD cohort, the mean cervical cord CSA in those with only cervical cord involvement was larger than those with both cervical and thoracic cord involvement, but this did not quite reach significance (69.34mm^2 +/- 4.31 versus 60.16mm^2 +/- 2.81, p = 0.094). Thoracic cord CSA was compared between those with only thoracic cord involvement and those with both cervical and thoracic cord (32.29mm^2 +/- 3.45 versus

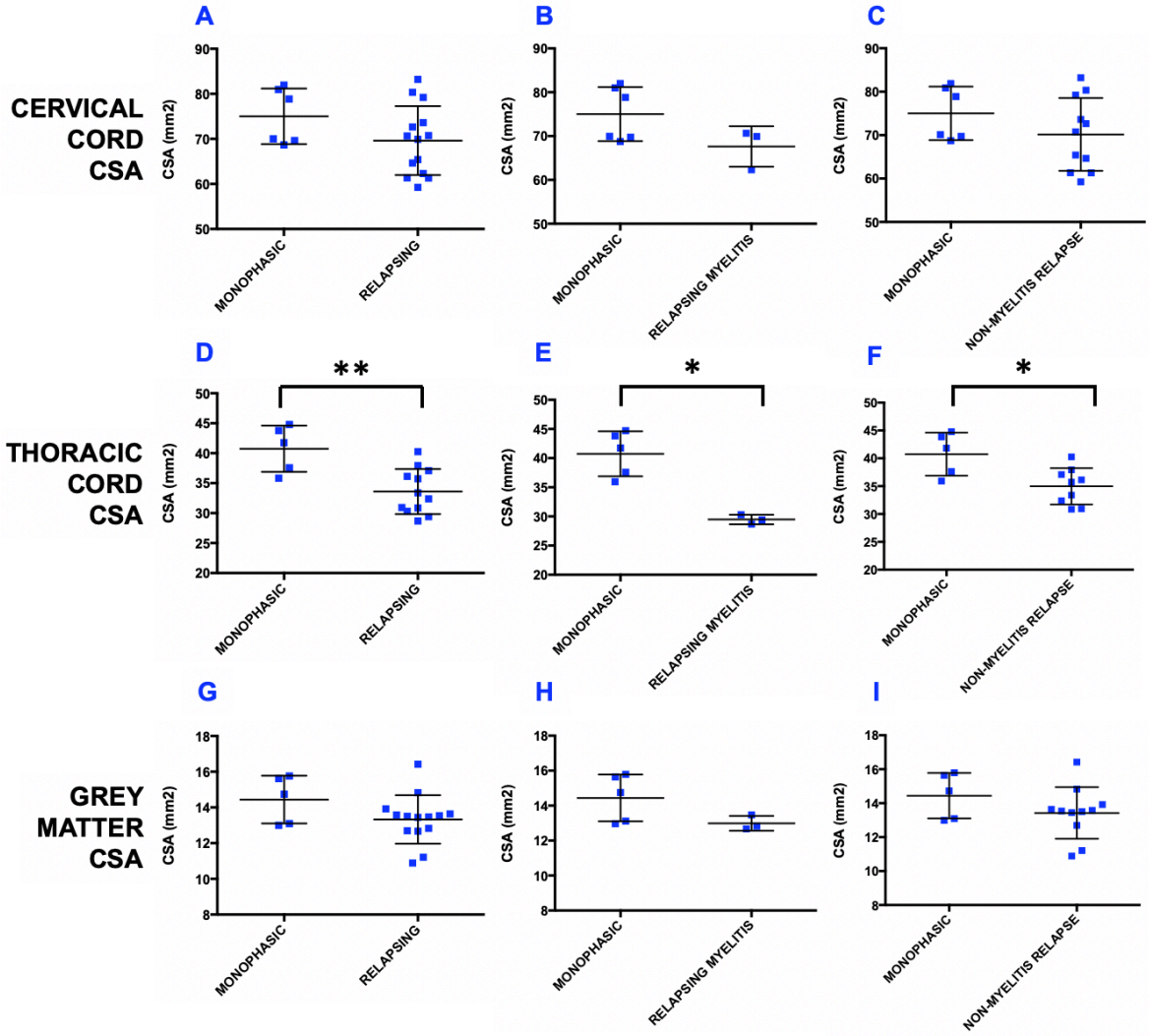
28.42mm^2 +/- 2.91, p = 0.200); again, those with both areas involved had a reduced mean CSA but this was not significant.

In the MS group the same comparisons were made in the cervical cord (67.46mm^2 +/- 1.13 versus 69.00mm^2 +/- 2.97, p = 0.567) and thoracic cord (36.83mm^2 +/- 3.11 versus 35.24mm^2 +/- 4.28, p = 0.599) but no differences were found.

5.5.6 Monophasic versus relapsing disease in MOGAD

In the MOGAD cohort, patients with monophasic disease (mean age = 45.20 +/- 9.58, M:F = 5:1) were compared to those with relapsing disease (mean age = 44.10 +/- 11.76, M:F = 5:9). The results are plotted in Figure 5.4.

Figure 5.4 MOGAD monophasic and relapsing cohort comparison. *MRI metrics for each participant shown as raw data with lines for mean and standard deviation. * = p value <0.05; ** = p value <0.01; CSA = cross-sectional area. Figure adapted from* (Mariano *et al.*, 2020).



Cervical cord CSA (Figure 5.4 A-C), thoracic cord CSA (Figure 5.4 D-F), as well as grey matter CSA (Figure 5.4 G-I) were lower in the 14 relapsing patients and lower values occurred in both those with relapsing myelitis (n = 3) as well as those whose relapses occurred elsewhere (n = 11). This reached significance in the thoracic cord CSA, the location that was affected in all MOGAD patients (33.60mm^2 +/- 3.75 versus 40.75mm^2 +/- 3.86, p = 0.001) and held when comparing the monophasic to relapsing myelitis (40.75mm^2 +/- 3.86 versus 29.48mm^2 +/- 0.81, p = 0.017) as well as those with non-myelitis relapses (40.75mm^2 +/-

3.86 versus 34.96mm^2 +/- 3.27, p = 0.011). Additionally, when comparing thoracic cord CSA of those with relapsing MOG-Ab disease to HV there was a significant difference (33.60mm^2 +/- 3.75 versus 37.86mm^2 +/- 3.22, p = 0.003) but not when comparing monophasic MOGAD to healthy volunteers (40.75mm^2 +/- 3.86 versus 37.86mm^2 +/- 3.22, p = 0.100).

5.6 Discussion

This work contributes to our understanding of spinal cord involvement in MOGAD, by not only comparing this group to HVs but also to AQP4-NMOSD and MS. This allows for a comparison across the cohorts, highlighting both differences and similarities, and builds hypotheses for future studies that seek to determine the underlying pathogenesis of MOGAD. To understand the evolution of spinal cord involvement in these three conditions it is important to consider findings throughout the disease course. Therefore, the results of this research, conducted at least six months after an acute event, are presented in a way that is informed by the earlier presentations.

None of the patients with MOGAD had persistent cord lesions in the cervical cord. This finding is in keeping with the data presented in Chapter 3 where more than 60% of patients had complete resolution of MRI findings at follow-up scanning. This is a clinically relevant finding as these imaging protocols are used in clinical practice in many centres and may be useful diagnostically where a reliable MOG-Ab test is unavailable or gives a low positive and thus less specific result. Those with AQP4-NMOSD had single, predominantly central, long lesions as is typical of this disease (Kim *et al.*, 2015). Patients with MS had multiple short asymmetrical lesions, also in keeping with the literature (Eden *et al.*, 2019). The lesion

volume of persistent lesions in the AQP4-NMOSD and MS cohorts did not differ significantly.

Those with AQP4-NMOSD showed the greatest atrophy, present in all measures: cervical cord, thoracic cord and grey matter. This damage was localised to areas of the cord involved during the acute attack. Those with persistent lesions had the worst metrics while areas of the cord that had never been involved were comparable to healthy volunteers. Lesions in AQP4-NMOSD therefore appeared to cause more localised damage than in MS and MOGAD. This is in keeping with the clinical imaging finding of focal spinal cord atrophy extending over the affected area described in NMOSD (Kim *et al.*, 2015; Wingerchuk *et al.*, 2015). This finding is also supported by a recent publication: in a study of 52 patients with AQP4-NMOSD, Cacciaguerra et al. identified atrophy clusters around at the vertebral levels in which lesions were present using a voxel-wise analysis technique (Cacciaguerra *et al.*, 2020). The involvement of the grey matter is also expected in AQP4-NMOSD, as it typically involves the central cord (Tackley *et al.*, 2014); an abundance of AQP4 antigen can be found in the spinal cord grey matter (Misu *et al.*, 2013) and mouse models of NMOSD have shown damaged astrocytes localised to the grey matter (Oklinski *et al.*, 2016). Finally, in another recent publication, Nakamura et al. showed that thoracic cord atrophy was a feature of AQP4-NMOSD more than in MS but that both conditions showed similar cervical cord atrophy (Nakamura *et al.*, 2020). This growing body of literature, to which the work presented in this chapter contributes, emphasises the value of good quality, single-centre studies in rare diseases that will then complement each other.

In those with MS, grey matter atrophy was noted in the group analysis. Although in MS lesions are not typically central, grey matter damage is well described in pathology, as

described in Chapter 1 (Geurts and Barkhof, 2008, Gilmore *et al.*, 2009*b*) and brain grey matter volume loss is predominant, even in the early stages of MS (Calabrese *et al.*, 2007). Spinal cord grey matter atrophy has also been reported in other studies of relapsing remitting MS, in the absence of white matter atrophy (Schlaeger *et al.*, 2015). The cervical cord CSA reached a near-significant reduction compared to the HV group. This finding is not unexpected as throughout the literature there are mixed findings when comparing patients with relapsing-remitting MS with HV (Rocca *et al.*, 2011, Casserly *et al.*, 2018; Moccia *et al.*, 2019). Consistent findings of significant atrophy are found once patients reach the secondary progressive phase or are diagnosed as primary progressive in the first instance (Tsagkas *et al.*, 2018). However, as outlined in Chapters 1 and 4, a relapsing-remitting cohort was specifically recruited for this study as an appropriate disease control for the antibody-mediated conditions which are known to be relapsing and not thought to have a progressive phase. No clear differences were found between those with lesions and those without in the MS sub-group analysis. This suggests abnormalities in the normal appearing spinal cord. This is an expected finding due to the background neurodegeneration and the findings of quantitative abnormalities in normal appearing brain tissue in MS (Moll *et al.*, 2011). However, it must be taken into consideration that as subclinical lesion activity is typical in MS, and frequent enough MRI scans cannot be performed, normal appearing tissue on MRI could include previous 'MRI resolved' lesions. Additionally, the cervical cord is the most commonly affected area of the spinal cord in MS (Eden *et al.*, 2019) and so the number of patients without documented cervical cord involvement was very small.

In MOGAD no overall group differences were found. The lack of difference compared to the HV cohort in the group analysis is consistent with the good clinical recovery noted in MOGAD (see Chapter 3). However, this may also indicate that the damage is less severe in MOGAD and so the effect size is smaller, which would require future studies with a larger number of participants.

Central cord involvement is well reported in those with MOGAD (see Chapters 1 and 3) and, as noted in chapter 3, a recent study described the 'H' sign seen on acute axial T2 imaging in MOGAD where involvement of the cord appears to be limited to the grey matter and was thought by the authors to represent grey matter demyelination (Dubey *et al.*, 2019) as oligodendrocytes containing MOG are found in the grey matter of the spinal cord (Kang *et al.*, 2013). Grey matter involvement in MOGAD disease is proving to be increasingly important with a cortical phenotype now recognised (Ogawa *et al.*, 2017), documented grey matter involvement in ADEM-like disease (Hacohen *et al.*, 2017) and reports of acute flaccid myelitis associated with MOG-Ab (Wang *et al.*, 2018; Dubey *et al.*, 2019). This finding of grey matter atrophy in previously affected cord areas in MOGAD further supports that grey matter involvement is an important aspect of this condition and, at the time of publication of this work, was the first quantitative evidence of long-term damage of grey matter in this condition. Recently, another study has described grey matter atrophy in the deep grey matter structures of the brain in MOGAD compared to healthy controls (Messina *et al.*, 2020; Zhuo *et al.*, 2020). In Chapter 3, the clinical outcomes of myelitis in MOGAD were assessed and the association between conus lesions and the requirement for long-term catheterisation was described. However, as was highlighted, conus involvement does not fully explain the spectrum of sphincter dysfunction in MOGAD,

which may also involve supraconal structures (Li *et al.*, 2020). Given the importance of the grey matter in micturition pathways and sphincter control mechanisms (Fowler *et al.*, 2008), this sphincter dysfunction may be due to grey matter damage in the lower cord and improvements in thoracic cord imaging techniques would assist in studying this. It is also of interest that, as described above, grey matter atrophy is a feature of MS which, like MOGAD, is considered to be a primary demyelinating condition and where spinal cord demyelination may be extensive and exceed white matter demyelination (Gilmore *et al.*, 2009*b*, *a*; Schlaeger *et al.*, 2015).

The effect of relapses in the MOGAD was then considered. It has been established that the presence of AQP4-Ab is predictive of relapsing disease and so it is recommended that all patients be treated with immunosuppressive treatment to prevent relapses (Weinshenker *et al.*, 2006; Jarius *et al.*, 2014; Wingerchuk *et al.*, 2015). However, as mentioned previously, in MOGAD, relapse rates of 34-46% (Jurynczyk *et al.*, 2017*b*; Cobo-Calvo *et al.*, 2018; Senanayake *et al.*, 2018) have been reported and so many patients may remain monophasic in their disease course; this has important treatment implications. In this cohort, the relapsing and monophasic patients with MOGAD were compared and in the thoracic cord (which was affected in all patients); relapsing patients had a significantly lower CSA, even if these were non-myelitis relapses, for example, ON. It has been argued that, if followed-up for long enough, all patients with MOGAD disease may eventually have a relapse and it is a continuum. However, our findings suggest that relapsing MOGAD may be a phenotype distinct from monophasic disease. This may also explain why studies that have largely described MOGAD patients with relapsing disease argue against it being a milder disease than AQP4-NMOSD (Jarius *et al.*, 2016*a*) and this emphasises the

importance of studying an incident cohort in any new disease condition, to avoid the bias of only studying patients that are diagnosed at relapse. This also opens an interesting avenue for further research into predictors of relapse in MOGAD to assess if the degree of atrophy in the affected area (in the cord, brain or optic nerves) after recovery may be predictive of those that will relapse in future.

Finally, a longitudinal study combining brain, spinal cord and optical coherence tomography findings to assess the above hypotheses across the central nervous system would be very valuable.

5.7 Limitations

The general limitations of this study are discussed in Chapter 4. In addition, the lack of detailed thoracic imaging means that the thoracic cord lesions and grey matter could not be studied, which may be especially relevant in the study of MOGAD.

5.8 Conclusion

Quantification of tissue loss in neuroinflammatory conditions, downstream of an acute attack, provides valuable information about disease pathophysiology and prognosis. Both patients with MOGAD and AQP4-NMOSD show localised atrophy. In MOGAD this appears to more significantly involve the grey matter. In AQP4-NMOSD this was found in all metrics, as the damage is more severe. In MOGAD differences were found between monophasic and relapsing patients, suggesting the relapsing MOGAD may represent a more severe phenotype of the disease.

6. Chapter 6: Quantitative spinal cord MRI in MOGAD, AQP4-NMOSD and MS

6.1 Introduction and background

Advanced cord imaging techniques are currently largely limited to research studies. They are used to investigate microstructural abnormalities which reflect tissue damage. In this chapter diffusion tensor imaging (DTI), for the study of neuroaxonal integrity, and magnetisation transfer ratio (MTR), for the study of myelin content, are acquired and analysed across the four participant groups.

DTI provides a number of popular quantitative indices that are used as surrogate measures of microstructural abnormalities. Two of these measures were selected: fractional anisotropy (FA) and mean diffusivity (MD). FA is a value between zero and one that measures the degree of diffusion asymmetry in a voxel and is used to evaluate directionality of tracts (Mori, 2007; Cohen-Adad and Wheeler-Kingshott, 2014). MD is a measure of the average diffusion within a voxel (Mori, 2007; Cohen-Adad and Wheeler-Kingshott, 2014). Neuroinflammatory lesions reveal an increase in diffusion and loss of anisotropy (Inglese and Bester, 2010), with an expected decrease in FA and increase in MD. FA and MD in the spinal cord have been measured in a number of different studies, particularly in multiple sclerosis (MS) (Agosta *et al.*, 2005; Hesseltine *et al.*, 2006; Ciccarelli *et al.*, 2007; Valsasina *et al.*, 2007; Martin *et al.*, 2015), with a few studies having shown differences in these metrics in patients with neuromyelitis optica spectrum disorder (NMOSD) as compared to healthy volunteers (HV) (Qian *et al.*, 2011; Pessôa *et al.*, 2012;

Rivero *et al.*, 2014). This technique has not previously been used to study the spinal cord of patients with myelin oligodendrocyte glycoprotein associated disease (MOGAD).

MTR quantifies the magnetisation between freely mobile protons and those bound to macromolecules, such as myelin, providing an indirect estimate of myelin content (Cohen-Adad and Wheeler-Kingshott, 2014). A reduction in MTR in the spinal cord of patients with MS has been reported (Oh *et al.*, 2013*a*; Alcaide-Leon *et al.*, 2018; Combès *et al.*, 2019) and post-mortem MRI of the brain and spinal cord has been used to show that MTR is affected by myelin content in MS, evidencing its usefulness as a surrogate marker of demyelination and degeneration (Mottershead *et al.*, 2003; Schmierer *et al.*, 2018). A reduction in MTR has also been noted in previous study of patients with NMOSD (Filippi *et al.*, 1999). All three conditions studied in this chapter are considered to be demyelinating diseases (either primary or secondary) and so this is a relevant measure for comparison. MTR has also not previously been used to study the spinal cord in MOGAD.

Both DTI and MTR have limitations. DTI lacks specificity for demyelination and axonal loss as it is influenced by several different physical parameters such as myelination, axonal density, axonal diameter, and orientation of fibre bundles (Beaulieu, 2002; Sen and Basser, 2005). MTR not only depends on the size of the macromolecular pool but also on the exchange rate between bound and mobile proton pools, which may reduce its specificity for myelin imaging (McCreary *et al.*, 2009). It has, therefore, been suggested that studies combining DTI and MTR provides a more robust and specific assessment of pathology as the use of two sets of markers sensitive to white matter pathology based on different biophysical properties increase the reliability of the study results (Smith *et al.*, 2010; Cohen-Adad *et al.*, 2011). Therefore, together with the structural imaging described in

Chapter 5, both DTI and MTR were acquired and compared across the four cohorts. The same group and sub-group comparisons, as in Chapter 5, will be shown using these quantitative metrics.

The work presented below is adapted from the publication: *Mariano R, Messina S, Roca-Fernandez A, Leite MI, Kong Y, Palace JA. Quantitative spinal cord MRI in MOG-antibody disease, neuromyelitis optica and multiple sclerosis. Brain. 2020 Nov 18:awaa347. doi: 10.1093/brain/awaa347.*

6.2 Objective and aims

The objectives and aims of this chapter are as follows:

- To compare three quantitative measurements (mean cervical cord FA, mean cervical cord MD and mean cervical cord MTR) across the four study cohorts (MOGAD, AQP4-NMOSD, MS and HV).

- To conduct a sub-group analysis for each disease group to explore differences between affected and unaffected areas of the cord (as defined by lesion location on clinical imaging) and between the monophasic and relapsing patients with MOGAD.

6.3 Hypotheses

Three hypotheses were developed for this chapter, as follows:

- Group-level differences will be found between HV and the AQP4-NMOSD and MS groups.

- The antibody-mediated conditions will show localised damage in areas that were affected during the acute attack.

- The different patterns of involvement in the disease sub-group analyses will provide insight into the underlying mechanisms of the three conditions.

6.4 Methods

6.4.1 Subjects

The 80 participants from the imaging cohort described in Chapter 4 were included in this analysis. Full details of the ethics, recruitment, cohort demographics and clinical assessments are as described in Chapter 4.1 and summarised in Table 4.1.

Patient cohorts were further divided into the following categories (the full methods of which are described in Chapter 4.1):

Cervical cord:

- Persistent (lesion present on clinical scan and visible on research scan),

- Previous (lesion present on clinical scan and no longer visible on research scan), or

- No cervical involvement.

No quantitative imaging was acquired in the thoracic cord.

6.4.2 MRI acquisition

Imaging protocols and acquisition methods are provided in Chapter 4.2. The imaging sequences analysed in this chapter are cervical cord diffusion tensor imaging and magnetisation transfer ration. Seven participants did not have diffusion imaging acquired (two MOGAD, three AQP4-NMOSD and two MS). Four did not have magnetisation transfer imaging (one MOGAD, one MS and one HV).

6.4.3 MRI analysis

Data were processed with tools from Spinal Cord Toolbox (SCT) v4.0 (De Leener *et al.*, 2017) and FMRIB Software Library (FSL) 6.0 (Jenkinson *et al.*, 2012).

Figure 6.1 shows examples of the analysis methodology described below.

6.4.3.1 Cervical Cord DTI

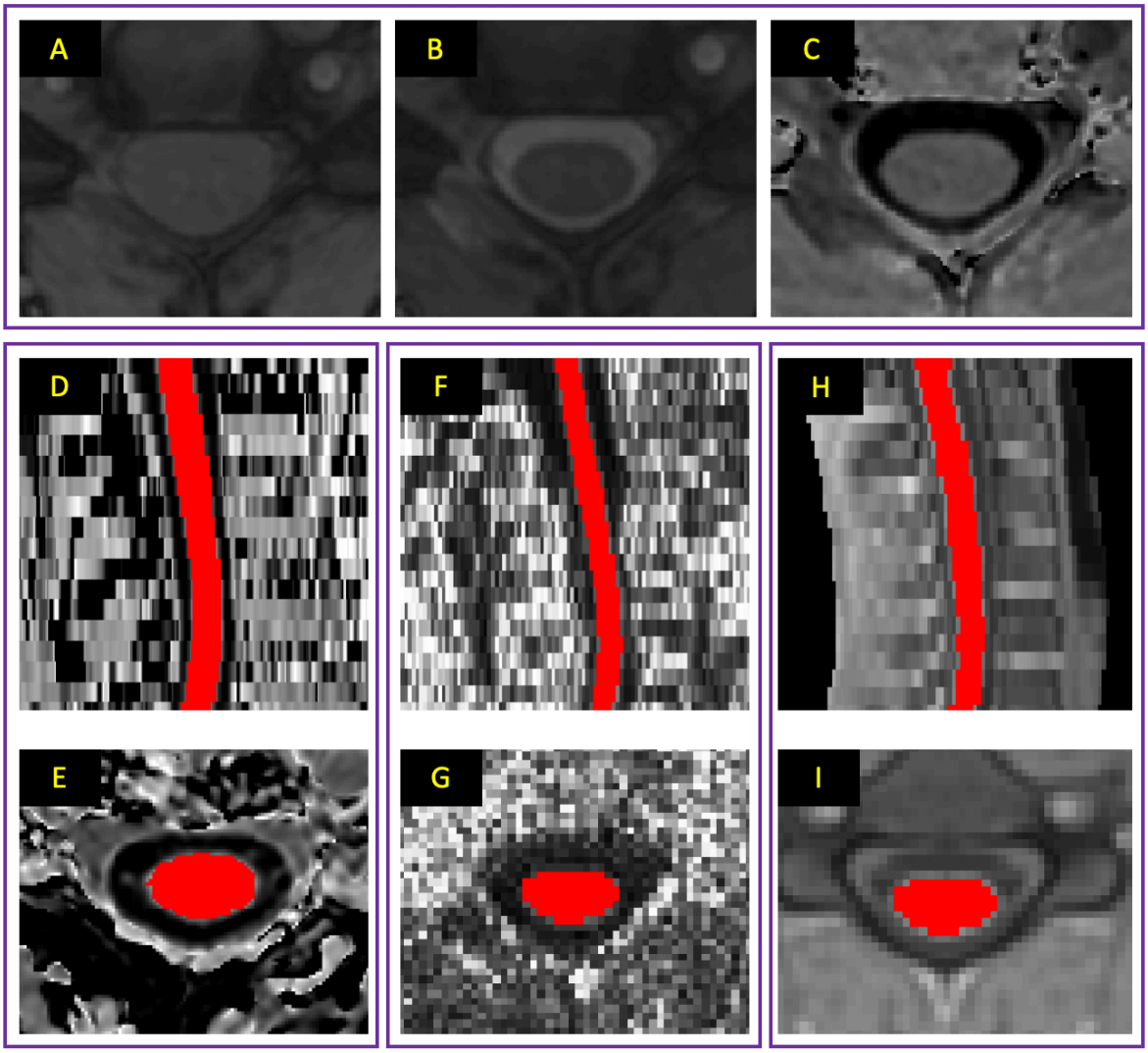
Diffusion data was acquired across the same number of slices in all participants (approximately C1-C6) in two phase encoding directions: AP (anterior-posterior) and PA (posterior-anterior) and merged. FSL tools topup (Smith *et al.*, 2004; Andersson and Sotiropoulos, 2016) and eddy (Andersson and Sotiropoulos, 2016) were used for distortion and eddy current correction. Dtifit (Jenkinson *et al.*, 2012) was then used to generate fractional anisotropy (FA) and mean diffusivity (MD) maps. The cord was segmented within the native DTI space and this mask was applied to each quantitative map. A multi-step registration method based on non-linear transformations was used to register the FA/MD

image to the PAM-50 spinal cord template via the previously registered anatomical references with SCT tool register_multimodal (De Leener *et al.*, 2017). The template was then warped into FA/MD image and the metrics were then extracted per slice using sct_extract_metric (De Leener *et al.*, 2017). Lesion masks were co-registered, and the metrics then extracted in both the lesional and non-lesional areas for comparison.

6.4.3.2 Cervical Cord MTR

MT-weighted imaging was acquired across the same number of slices in all participants (approximately C2-C5). The MT-on image was registered to MT-off image and MTR map was computed using SCT (MTR = (MToff-MTon)/MToff*100%). The MTR image was registered to the PAM-50 spinal cord template using the SCT tool register_multimodal (De Leener *et al.*, 2017). The template was then warped into the native metric space and metrics were then extracted per slice using sct_extract_metric. Lesion masks were co-registered, and the metric then extracted in both the lesional and non-lesional areas for comparison.

Figure 6.1 Imaging analysis. *Examples of the MRI analysis outputs showing (A) MT-off image, (B) MT-on image, which are used together to create the (C) MTR image, (D) segmented cord shown in red in the MTR sagittal plane and (E) axial plane, (F) FA map with segmented cord in red shown in the sagittal plane and (G) axial plane, the PAM-50 template warped into the native metric space in (H) the sagittal plane and (I) axial plane, with the cord segmented and shown in red.*



6.4.4 Statistical analysis

Statistical analysis was performed using SPSS v26.0 and figures created using GraphPad Prism version 6.0c. All comparisons between groups were done using ANCOVA (general linear model in SPSS with age and sex included as continuous and binary variables, respectively) with a post-hoc Bonferroni to correct for multiple comparisons. Comparisons

of sub-groups within one cohort were done using a Student's T-test or Mann-Whitney U test when two sub-groups were compared. When more than two sub-groups were compared, an ANOVA with post-hoc Tukey or Kruskal-Wallis with post-hoc Dunn test were used. The monophasic and relapsing MOGAD cohorts, as well as their comparison to the HV group, were analysed using the general linear model in SPSS with age and sex were included to account for the increased proportion of males noted in the monophasic MOGAD group. *p* values were 2-tailed and statistical significance was set at 0.05.

6.5 Results

The imaging results are shown graphically in Figure 6.2, the between-group comparison, and Figure 6.3, the within-group comparison, based on the lesion status sub-groups described above.

Figure 6.2 Between-group comparison. *MRI metrics for each participant shown as raw data with lines for mean and standard deviation. * = p value <0.05; ** = p value <0.01; FA = fractional anisotropy; MD = mean diffusivity; MTR = magnetisation transfer ratio. Figure adapted from* (Mariano *et al.*, 2020).

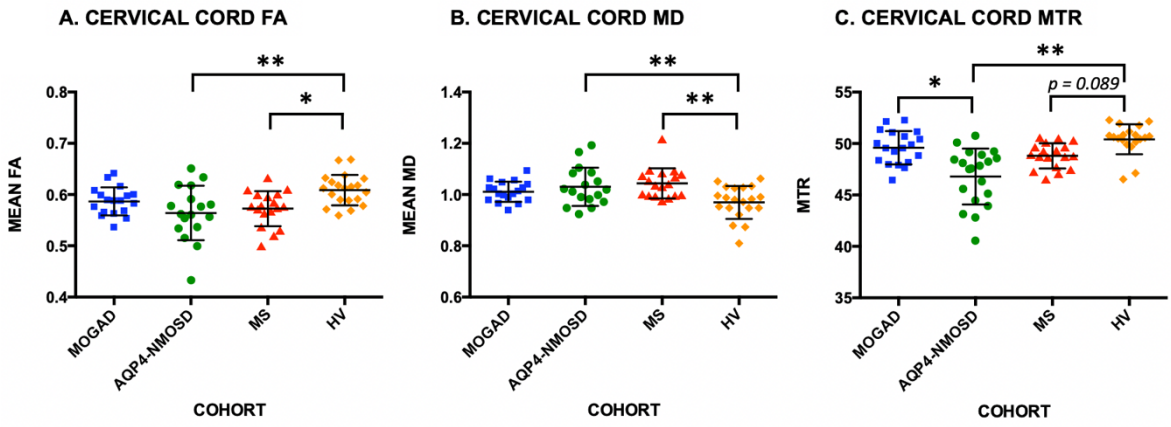
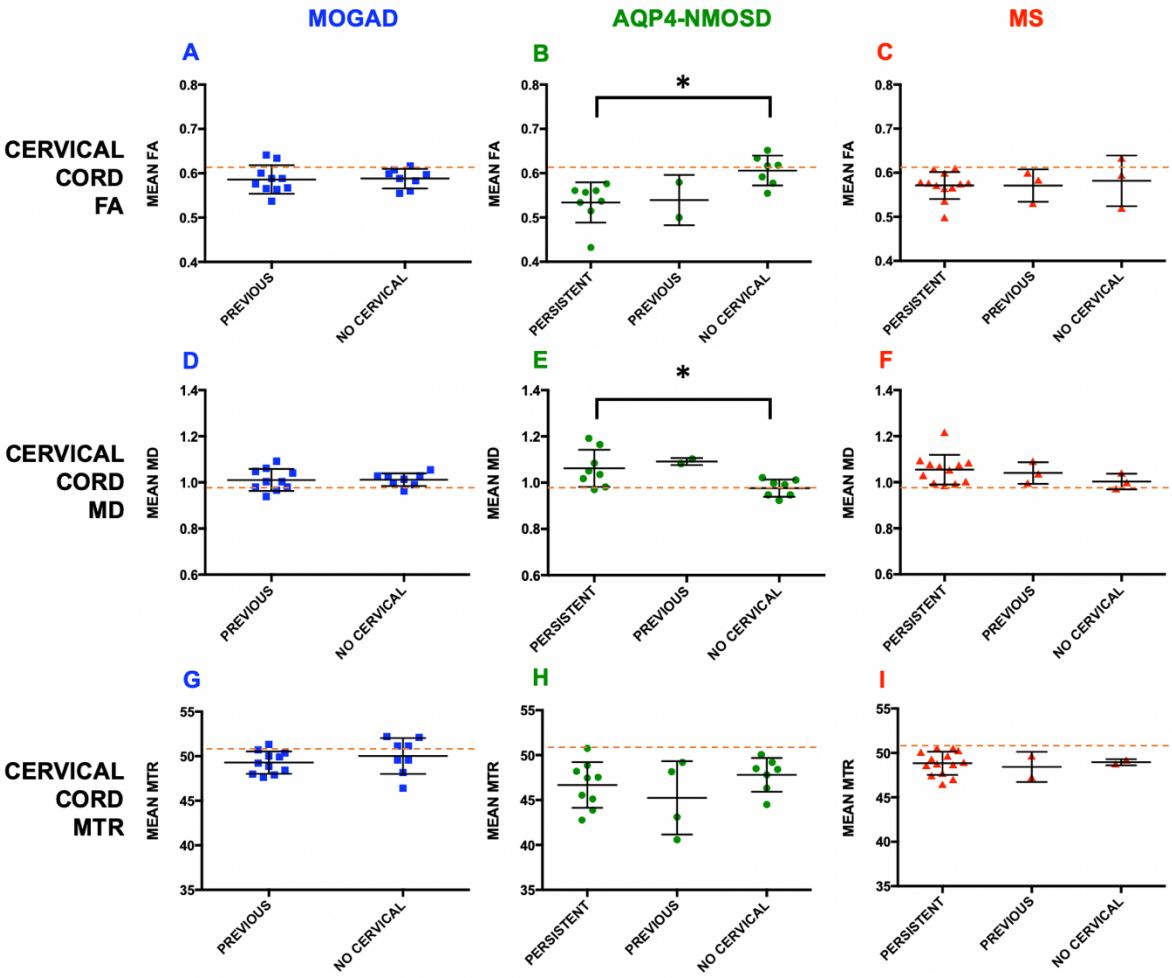


Figure 6.3 Within-group comparison. *MRI metrics for each participant shown as raw data with lines for mean and standard deviation. The orange dotted line represents the healthy volunteer mean for each modality. * = p value <0.05; ** = p value <0.01; FA = fractional anisotropy; MD = mean diffusivity; MTR = magnetisation transfer ratio. Figure adapted from* (Mariano *et al.*, 2020)*.*



6.5.1 Cervical cord DTI

The FA and MD results, shown graphically in Figure 6.2 A and B, are detailed in Tables 6.1 to 6.4.

In this group comparison there was no significant difference between the MOGAD cohort and HV in either FA or MD (Figure 6.2 A and B). There were also no differences found between the affected and never-affected cervical cords (Figure 5.3 A and C).

Both AQP4-NMOSD and MS patients had FA (decreased) and MD (increased) results significantly different from the HV group. In the AQP4-NMOSD group the same pattern existed as noted in the structural results in Chapter 5 where the difference appeared to be driven by those with affected cervical cords (Figure 5.3 B and D). In the AQP4-NMOSD FA sub-group analysis a difference was found between 'persistent' and 'no cervical' (p = 0.016) [$x^2(2) = 8.089$, $p = 0.006$]. Similarly, in the AQP4-NMOSD MD sub-group analysis a difference found between 'persistent' and 'no cervical' (p = 0.049) [$x^2(2) = 7.003$, $p = 0.015$]. This pattern was not present in the MS group (Figure 5.3 C and F).

Table 6.1 Cervical cord fractional anisotropy ANCOVA

	Type III Sum of Squares	**df**	**Mean Square**	**F**	***p* value**
Corrected model	**0.034**	**8**	**0.004**	**3.313**	**0.003**
Group	0.020	3	0.007	5.265	0.003
Age	0.001	1	0.001	0.730	0.396
Sex	0.008	1	0.008	6.302	0.015

$R^2 = 0.293$ (Adjusted $R^2 = 0.204$)

Table 6.2 Cervical cord fractional anisotropy pairwise comparison. *p values shown are adjusted with a Bonferroni correction for multiple comparisons.*

Group	**Comparison Group**	**Mean Difference**	**Std. Error**	***p* value**	**95% Confidence Interval**	
MOGAD	AQP4-NMOSD MS HV	0.022 0.013 -0.025	0.014 0.012 0.012	0.654 1.000 0.203	-0.015 -0.020 -0.058	0.059 0.045 0.007
AQP4-NMOSD	MOGAD MS **HV**	-0.022 -0.010 **-0.048**	0.014 0.014 **0.014**	0.654 1.000 **0.005**	-0.059 -0.046 **-0.085**	0.015 0.027 **-0.011**
MS	MOGAD AQP4-NMOSD **HV**	-0.013 0.010 **-0.038**	0.012 0.014 **0.012**	1.000 1.000 **0.012**	-0.045 -0.027 **-0.070**	0.020 0.046 **-0.006**
HV	MOGAD **AQP4-NMOSD** **MS**	0.025 **0.048** **0.038**	0.012 **0.014** **0.012**	0.203 **0.005** **0.012**	-0.007 **0.011** **0.006**	0.058 **0.085** **0.070**

Table 6.3 Cervical cord mean diffusivity ANCOVA

	Type III Sum of Squares	**df**	**Mean Square**	**F**	***p* value**
Corrected model	**0.101**	**8**	**0.013**	**3.827**	**0.001**
Group	0.065	3	0.022	6.541	0.001
Age	0.016	1	0.016	4.895	0.031
Sex	0.028	1	0.028	8.461	0.005

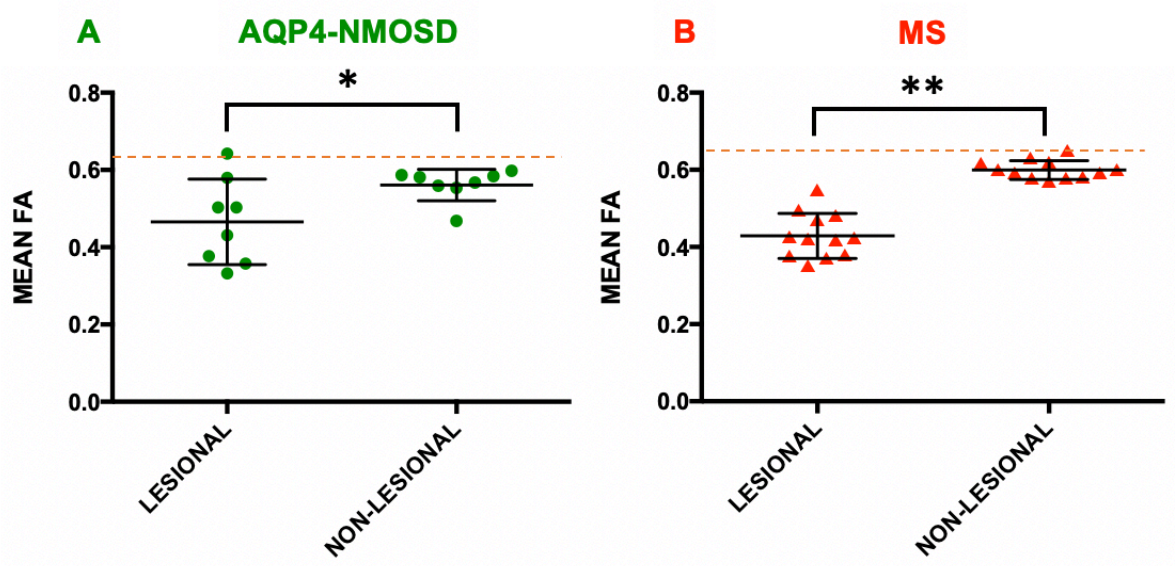
R^2 = 0.324 (Adjusted R^2 = 0.239)

Table 6.4 Cervical cord mean diffusivity pairwise comparison. *p values shown are adjusted with a Bonferroni correction for multiple comparisons.*

Group	**Comparison Group**	**Mean Difference**	**Std. Error**	***p* value**	**95% Confidence Interval**	
MOGAD	AQP4-NMOSD MS HV	-0.029 -0.032 0.045	0.022 0.019 0.019	1.000 0.637 0.115	-0.088 -0.084 -0.006	0.031 0.021 0.097
AQP4-NMOSD	MOGAD MS **HV**	0.029 -0.003 **0.074**	0.022 0.022 **0.022**	1.000 1.000 **0.007**	-0.031 -0.062 **0.015**	0.088 0.056 **0.134**
MS	MOGAD AQP4-NMOSD **HV**	0.032 0.003 **0.077**	0.019 0.022 **0.019**	0.637 1.000 **0.001**	-0.021 -0.056 **0.025**	0.084 0.062 **0.129**
HV	MOGAD **AQP4-NMOSD** **MS**	-0.045 **-0.074** **-0.077**	0.019 **0.022** **0.019**	0.115 **0.007** **0.001**	-0.097 **-0.134** **-0.129**	0.006 **-0.015** **-0.025**

Cervical lesional FA was significantly reduced compared to the normal-appearing spinal cord in both AQP4-NMOSD (0.46±0.10 versus 0.56±0.04, *p* = 0.037) and MS (0.43 ± 0.06 versus 0.59 ± 0.02, *p* = 0.001). However, as shown in Figure 6.4 A and B, both the lesional and non-lesional tissue FA values fall below the healthy control mean. The mean lesional FA did not differ between groups (0.46 versus 0.43, *p* = 0.539).

Figure 6.4 Lesional Fractional Anisotropy. *MRI metrics for lesions in each participant with (A) AQP4-NMOSD and (B) MS shown as raw data with lines for mean and standard deviation. No patients with MOGAD had residual lesions. The orange dotted line represents the healthy volunteer mean. * = p value <0.05; ** = p value <0.01; FA = fractional anisotropy. Figure adapted from* (Mariano *et al.*, 2020).



6.5.2 Cervical cord MTR

Patients with MOGAD did not differ from HV in the group comparison but were significantly different from those with AQP4-NMOSD, who had lower MTR values than MOGAD (Figure 6.2 C). No differences were noted between the affected and never-affected cervical cords in the MOGAD group (Figure 6.3 G).

Patients with AQP4-NMOSD had significantly lower MTR values than both MOGAD (as described above) and HV (Figure 6.2 C). However, in this measure no differences were noted in the AQP4-NMOSD sub-group analysis (Figure 6.3 H), where all sub-groups had values below the HV mean.

Patients with MS had lower MTR values than those with HV but this did not quite reach significance (p = 0.089) and no differences were noted in the sub-group analysis (Figure 6.3I).

Table 6.5 Cervical cord magnetisation transfer ratio ANCOVA

	Type III Sum of Squares	**df**	**Mean Square**	**F**	***p* value**
Corrected model	**183.719**	**8**	**22.965**	**7.350**	**0.000**
Group	61.654	3	20.551	6.577	0.001
Age	38.262	1	38.262	12.245	0.001
Sex	*4.479*	*1*	*4.479*	*1.433*	*0.235*

R^2 = 0.467 (Adjusted R^2 = 0.404)

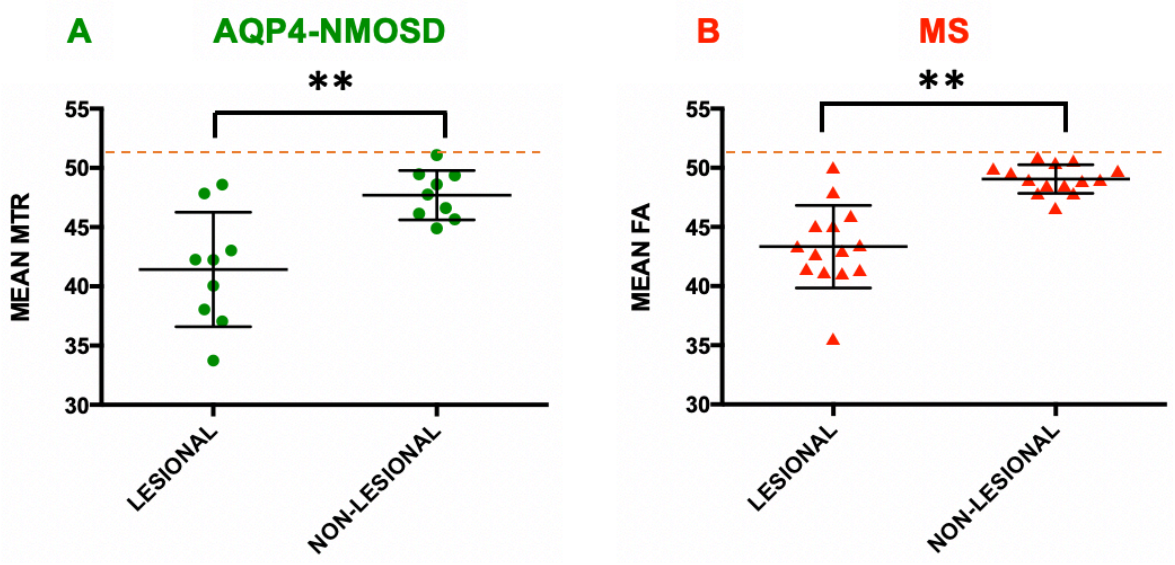
Table 6.6 Cervical cord magnetisation transfer ratio pairwise comparison. *p values shown are adjusted with a Bonferroni correction for multiple comparisons.*

Group	**Comparison Group**	**Mean Difference**	**Std. Error**	***p* value**	**95% Confidence Interval**	
MOGAD	**AQP4-NMOSD**	**2.032**	**0.631**	**0.012**	**0.318**	**3.746**
	MS	0.769	0.584	1.000	-0.818	2.357
	HV	-0.703	0.578	1.000	-2.274	0.869
AQP4-NMOSD	**MOGAD**	**-2.032**	**0.631**	**0.012**	**-3.746**	**-0.318**
	MS	-1.263	0.633	0.301	-2.984	0.458
	HV	**-2.735**	**0.643**	**0.000**	**-4.484**	**-0.986**
MS	MOGAD	-0.769	0.584	1.000	-2.357	0.818
	AQP4-NMOSD	1.263	0.633	0.301	-0.458	2.984
	HV	-1.472	0.588	0.089	-3.072	0.127
HV	MOGAD	0.703	0.578	1.000	-0.869	2.274
	AQP4-NMOSD	**2.735**	**0.643**	**0.000**	**0.986**	**4.484**
	MS	1.472	0.588	0.089	-0.127	3.072

Cervical lesional MTR was significantly reduced compared to the normal-appearing spinal cord in both AQP4-NMOSD (41.43 ± 2.08 versus 47.70 ± 4.85, *p* = 0.003) and MS (43.10 ± 1.03 versus 49.40 ± 3.82, P40.001) and the mean lesional values did not differ significantly

between groups (41.43 ± 2.08 versus 43.10 ± 1.03, *p* = 0.269). Again, as shown in Figure 6.5 A and B, both the lesional and non-lesional tissue MTR values fall below the HV mean.

Figure 6.5 Lesional Magnetisation Transfer Ratio. *MRI metrics for each participant with (A) AQP4-NMOSD and (B) MS shown as raw data with lines for mean and standard deviation. No patients with MOGAD had residual lesions. The orange dotted line represents the healthy volunteer mean. * = p value <0.05; ** = p value <0.01; MTR = magnetisation transfer ratio. Figure adapted from* (Mariano *et al.*, 2020).



6.5.3 Cumulative cord involvement

The effect of having both cervical cord and thoracic cord involvement was then considered in the AQP4-NMOSD and MS cohorts. All patients with MOGAD had thoracic cord involvement and so this analysis could not be conducted on this group.

In the AQP4-NMOSD cohort those with cervical cord involvement only were compared to those with both cervical cord and thoracic cord involvement across the three metrics: FA (0.55 +/- 0.03 versus 0.51 +/- 0.06, *p* = 0.171), MD (1.03 +/- 0.05 versus 1.12 +/- 0.07, *p* = 0.070) and MTR (46.30 +/- 3.08 versus 46.19 +/- 3.16, *p* = 0.798).

In the MS cohort the same comparisons were made using FA (0.58 +/- 0.03 versus 0.56 +/- 0.02, p = 0.157), MD (1.05 +/- 0.07 versus 1.05 +/- 0.05, p = 0.675) and MTR (48.96 +/- 1.44 versus 48.49 +/- 1.09, p = 0.351).

6.5.4 Monophasic versus relapsing MOGAD

In the MOGAD cohort, patients with monophasic disease (mean age = 45.20 +/- 9.58, M:F = 5:1) were compared to those with relapsing disease (mean age = 44.10 +/- 11.76, M:F = 5:9). No differences were found in FA (0.59 +/- 0.03 versus 0.59 +/- 0.02, p = 0.779), MD (1.00 +/- 0.03 versus 1.01 +/- 0.04, p = 0.238), or MTR (48.80 +/- 1.79 versus 49.96 +/- 1.46, p = 0.200).

6.6 Discussion

The work in this chapter evidences the value of multimodal MRI as it provides additional useful information for the study of disease. Building on the between-group and within-group comparisons in Chapter 5, a consistent pattern emerges across the different imaging modalities. AQP4-NMOSD continues to show the most severe damage, localised to areas affected during acute attack. MS shows abnormalities compared to HV but no clear pattern with regard to lesion location. MOGAD shows no difference to HV in quantitative imaging measures after recovery from myelitis and also shows a significantly higher MTR than the AQP4-NMOSD group. Despite the different sequences and analysis pipelines, these consistent results, when all measures are considered together, make the overall study findings more compelling.

In MOGAD no group differences were noted compared to HV, in keeping with the results of Chapter 5. However, in addition to the lack of difference between the MOGAD and HV groups there were also no differences found between the affected and never-affected cord in this analysis. Finally, this group also had a significantly higher MTR than in AQP4-NMOSD. As the quantitative measures studied in this chapter are thought to better represent myelination and axonal integrity, these findings together may suggest that the white matter is either less affected, recovers better in the course of MOGAD, or a combination thereof.

First, as mentioned previously, subtle changes or milder pathology may be missed in group comparisons (with conservative statistics used to correct for multiple comparisons) and limited sample sizes. A larger cohort of MOGAD patients, or multi-centre study, would be needed in order to confirm this finding. Secondly, the lesser involvement of the cervical cord in this condition may also mean that the more affected cord area (thoracic and conus) is not imaged. Finally, MOGAD patients had fewer myelitis relapses than those with AQP4-NMOSD.

However, as these imaging findings are in keeping with the good clinical recovery and resolution of clinical imaging findings in MOGAD (described in Chapter 3), some interesting hypotheses can still be drawn from this work regarding the question of the lesser severity of white matter involvement or better recovery thereof. If the acute presentation of myelitis in MOGAD is considered, the severity at nadir is generally found to be similar to that of AQP4-NMOSD (Jurynczyk *et al.*, 2017*b*; Dubey *et al.*, 2019; Mariano *et al.*, 2019). However, as described in Chapter 3, it has been shown that gadolinium enhancement is less frequent in acute imaging of MOGAD myelitis when compared to AQP4-NMOSD and

MS and that less cord swelling was noted in MOGAD as compared to AQP4-NMOSD (Dubey *et al.*, 2019), which may suggest a lesser degree of inflammation in the acute setting. The same study also found cases of acute MOGAD myelitis which, on axial views of T2 images showed signal hyperintensity limited to the grey matter, which may support the hypothesis that the white matter is less affected acutely (Dubey *et al.*, 2019) and this is also consistent with the only significant finding in MOGAD in this MRI study being that of grey matter atrophy in the previously affected cervical cord (Chapter 5). Recently, cases of MOGAD patients with symptoms of myelitis and no lesions noted on clinical imaging have been reported (Pérez *et al.*, 2019; Sechi *et al.*, 2020). Although considerations must be made regarding the timing and quality of the MRI scan, another hypothesis may be that, in those cases, inflammation is restricted to the grey matter and does not result in adequate inflammatory change to create the T2 signal hyperintensity that would be identified as a lesion on MRI.

On the other hand, acute brain lesions in MOGAD are characterised by inflammatory demyelination (Höftberger *et al.*, 2020). This finding may be more in favour of better recovery as opposed to less severe acute disease. One hypothesis suggested by Hoftberger et al. regarding recovery in MOGAD is that as MOG is expressed on mature oligodendrocytes, but not on oligodendrocyte progenitor cells, rapid recruitment of new oligodendrocytes occurs in the lesions and is associated with rapid and complete remyelination (Brunner *et al.*, 1989; Seifert *et al.*, 2007; Höftberger *et al.*, 2020). This may also, in part, explain the observation of resolution of lesions on follow-up imaging in MOGAD.

Pathology studies in AQP4-NMOSD show lesions to be extensive and destructive (Lucchinetti *et al.*, 2014), which explains the differences noted between AQP4-NMOSD and HV, as well as compared to MOGAD in the MTR analysis. MTR represents demyelination but also axonal loss and cellular tissue changes (Cohen-Adad and Wheeler-Kingshott, 2014) and so may better represent the overall more destructive underlying disease processes in AQP4-NMOSD. Those with AQP4-NMOSD also have more cervical cord involvement than MOGAD and are also more likely to have relapsing myelitis (Mariano *et al.*, 2019), which may explain this further.

In MS the findings were similar to those described in Chapter 5, with group differences noted but no differences in the sub-group analysis. Again, the frequent involvement of the cervical cord in MS (Eden *et al.*, 2019) together with subclinical activity (Siva, 2013) need to be considered when interpreting the sub-group results.

The final consideration is whether or not, in addition to providing useful information about the conditions, the structural and quantitative metrics have any association with clinical outcomes. This is addressed in Chapter 7.

6.7 Limitations

The general limitations of the MRI are described in Chapter 4.1. In addition, this chapter is limited by only measuring quantitative MRI metrics in the cervical cord. Although theoretically feasible in the thoraco-lumbar cord (Ugorji *et al.*, 2015), these MRI methods need further optimisation related to limited ability to surround the area of interest with coils, as can be done around the neck; respiratory induced fluctuations; chest movement, which creates local fluctuations in the B0 field creating phase errors in EPI-based diffusion

images (Van de Moortele *et al.*, 2002; van Gelderen *et al.*, 2007); and the curvature of the thoraco-lumbar cord which renders it more difficult to image planes perpendicular to the cord.

6.8 Conclusion

Quantitative MRI provides valuable information about spinal cord involvement in inflammatory demyelinating conditions. The findings in this chapter, together with those described in Chapter 5, show consistent patterns across the different group comparisons, regardless of MRI metric. This establishes a more robust understanding of these conditions. Myelitis with AQP4-NMOSD shows the most severe, localised damage. In MS, metrics show significant change in comparison to HV; however, the relationship with lesion location is not as pronounced. Finally, in MOGAD, metrics are comparable with HV, except for the finding of localised grey matter atrophy in previously affected cords (Chapter 5). The combination of grey matter atrophy with the relative lack of abnormalities found in white matter metrics is an interesting finding that can be used to build hypotheses for future research.

7. Chapter 7: The clinical relevance of structural and quantitative MRI metrics

7.1 Introduction and background

After describing the structural and quantitative metrics of this spinal cord MRI study in the three conditions of interest (Chapters 5 and 6), the clinical relevance of these metrics is considered in Chapter 7, including an assessment of the ability to discriminate between the three conditions using a combination of the metrics.

The MRI metrics described in Chapters 5 and 6 are thought to be specific to underlying biological processes but not to specific disease types pathology (Kearney *et al.*, 2015; Marcello Moccia *et al.*, 2019). Similar relationships between these metrics and clinical outcomes have been described in multiple sclerosis (MS) and neuromyelitis optica spectrum disorder (NMOSD) (summary shown in Chapter 1, Table 1.6), showing that these measures may be useful as quantitative measures of disability, independent of disease type. In MS, measurements of cervical cord cross-sectional area (CSA), diffusion metrics and magnetisation transfer ratio (MTR) have shown clinical relevance in terms of disability, prognosis and progression (Filippi *et al.*, 1999; Wozniak and Lim, 2006; Klawiter *et al.*, 2011, Oh *et al.*, 2013*a*; Cohen-Adad and Wheeler-Kingshott, 2014; Martin *et al.*, 2015; Rocca *et al.*, 2019). In particular, cervical cord CSA has been shown to be a highly relevant outcome (Casserly *et al.*, 2018) and as having potential as a primary outcome in clinical trials for progressive MS (Cawley *et al.*, 2018; Prados and Barkhof, 2018). In NMOSD, a few small studies have shown relationships between cervical cord CSA, thoracic cord CSA and cervical

cord fractional anisotropy (FA) and disability (Qian *et al.*, 2011, Pessôa *et al.*, 2012; Rivero *et al.*, 2014, Chien *et al.*, 2018*b*), and one study showed that FA measured within the specific white matter tracts of the spinal cord associated with clinical outcomes specific to that tract, for example, FA within the corticospinal tract and measures of motor disability (Naismith *et al.*, 2013). A single study has looked at cervical cord atrophy in MOGAD, together with AQP4-NMOSD, and showed an association between atrophy and disability, independent of disease type (Chien *et al.*, 2018*b*). It would, therefore, appear that measures of atrophy or demyelination (MOGAD and MS being primary demyelinating diseases and in AQP4-NMOSD astrocyte damage leading to secondary demyelination) would be associated with disability, regardless of the specific cause. Therefore, the first hypothesis underlying the analysis in this chapter is that the extent of the damage in the cord that is driving the disability and not the disease type.

The second part of this chapter seeks to establish if lesion location, residual lesion volume, atrophy measures and quantitative metrics, downstream from an acute attack, may be useful to discriminate these conditions when assessed in combination. A combination of brain MRI features have been shown to be useful when a discriminatory model is applied (Jurynczyk *et al.*, 2017*a*). The same methodology (a principal component analysis followed by an orthogonal partial least squares analysis) was applied to the spinal cord data collected and the value of combining all the metrics into one model in order to discriminate these conditions was assessed.

The work presented below is adapted from the publication: *Mariano R, Messina S, Roca-Fernandez A, Leite MI, Kong Y, Palace JA. Quantitative spinal cord MRI in MOG-antibody*

disease, neuromyelitis optica and multiple sclerosis. Brain. 2020 Nov 18:awaa347. doi: 10.1093/brain/awaa347.

7.2 Objectives and aims

The objectives and aims of this chapter are as follows:

- To study the relationship between the MRI metrics and clinical outcomes measured and establish which may be the most relevant across the three disease groups.

- To explore the value of tract-based fractional anisotropy in the corticospinal and spinothalamic tracts and their association to disability and pain, respectively.

- To assess if combining the spinal cord MRI features together with the quantitative metrics may allow for discrimination between the conditions.

7.3 Hypotheses

Three hypotheses were developed for this chapter, as follows:

- MRI metrics, in particular atrophy and diffusion tensor imaging metrics, will show an association with disability, independent of disease type.

- A tract-based analysis of fractional anisotropy will show an association between disability and corticospinal tract measures, and pain scores and spinothalamic tract measures.

- A combination of clinical MRI features together with quantitative metrics will enable the discrimination of the three conditions.

7.4 Methods

7.4.1 Subjects and clinical assessments

The 80 participants from the imaging cohort described in Chapter 4 were included in this analysis. Full details of the cohort demographics and clinical assessments are described in Chapter 4.1 and summarised in Table 4.1.

The clinical outcome measured are:

- Expanded disability status score (EDSS),
- Presence of sphincter dysfunction and catheter requirements (binary variables),
- Brief pain inventory (BPI) score, and
- Modified fatigue impact scale (MFIS) score.

7.4.2 MRI: acquisition and analysis

The MRI metrics, described in Chapters 5 and 6, that are used in this chapter are:

- Cervical cord CSA,
- Cervical cord grey matter CSA,

- Cervical cord FA,
- Cervical cord MD, and
- Cervical cord MTR.

The thoracic cord measurements were not used in the regression models below as many participants, especially in the AQP4-NMOSD group, were missing this measure. They were, however, added to the discriminatory analysis as the software used for that analysis is able to account for missing data.

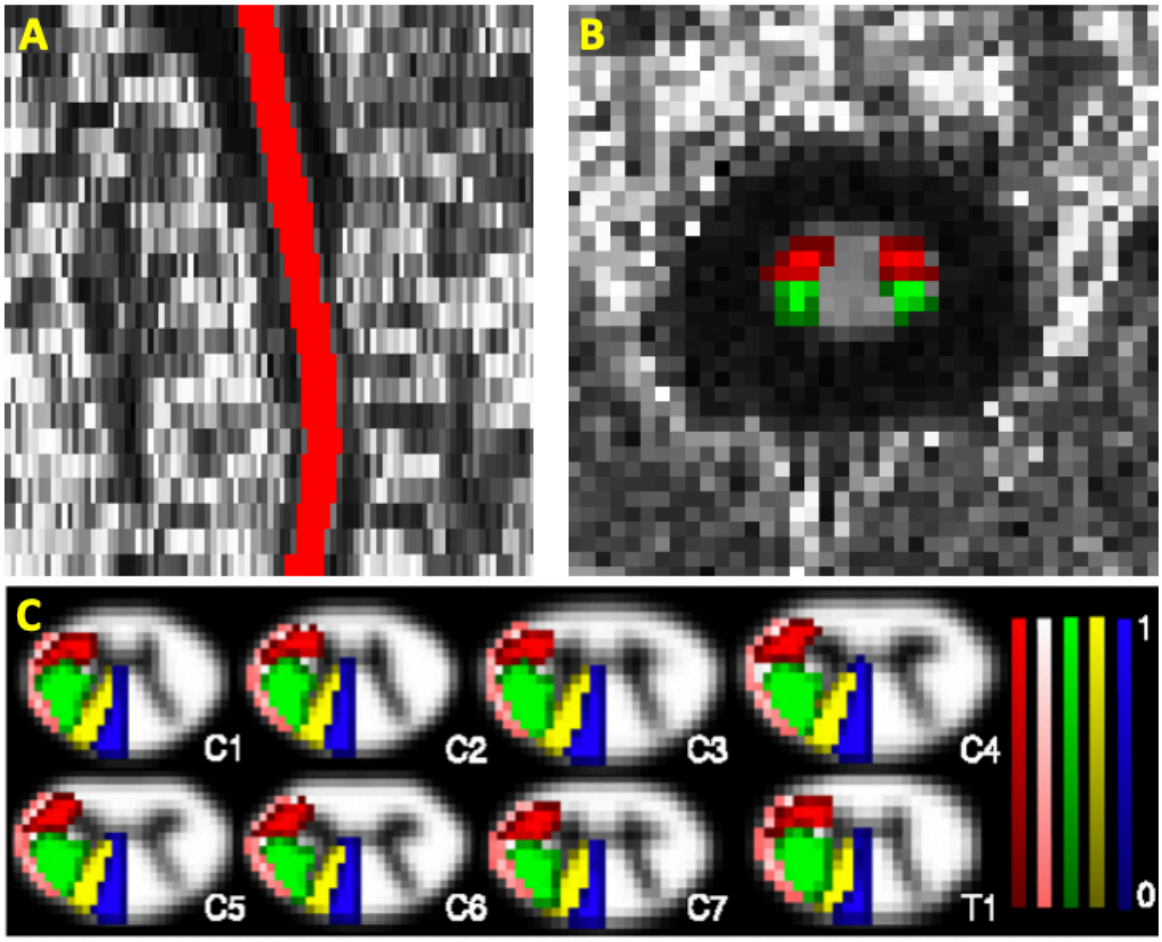
In addition to the above MRI metrics, two further measures were acquired for this chapter, using the diffusion data. Data were processed with tools from Spinal Cord Toolbox (SCT) v4.0 (De Leener *et al.*, 2017) and FMRIB Software Library (FSL) 6.0 (Jenkinson *et al.*, 2012).

A tract-based analysis was done, and FA was extracted from probabilistic white matter masks of the lateral corticospinal and lateral spinothalamic tracts using the PAM-50 atlas. FA was selected specifically for the tract-based analysis (as opposed to MD or MTR) as it has been shown to have the most potential as a marker of disability (Martin *et al.*, 2015). The white matter atlas used was created to overcome the biases associated with manual delineation and partial volume effect (Lévy *et al.*, 2015). Figure 7.1 shows an example of this analysis. Therefore, these two additional MRI metrics are tested in models below based on *a priori* hypotheses regarding their location and the associated symptoms, namely:

- Mean cervical cord spinothalamic tract FA (STT FA) to be tested in the pain model, and

- Mean cervical cord corticospinal tract FA (CST FA) to be tested in the disability model.

Figure 7.1 Imaging analysis. *Examples of additional MRI analysis outputs showing (A) the spinal cord segmented in native FA space, (B) the lateral spinothalamic (red) and lateral corticospinal (green) tracts warped into native FA space, and (C) the white matter atlas in the PAM-50 space as shown in the paper by Levy et al. describing the methodology of the white matter atlas. In this image the following tracts can be seen: left lateral spinothalamic (red), spinocerebellar (pink), left lateral corticospinal tract (green), cuneatus (yellow) and fasciculus gracilis (blue)* (Lévy *et al.*, 2015). *(A) and (B) adapted from* (Mariano *et al.*, 2020)



7.4.3 Statistics

7.4.3.1 Clinical outcome models

Statistical analysis was performed using SPSS v26.0 and figures created using GraphPad Prism version 6.0c. Regression models were used to study the relationship between the MRI metrics and clinical outcomes listed above. The three disease groups were combined, but disease type was included as a nominal variable in the multiple regression models. Where the disease group showed significance, the model was then run with each disease as a binary variable to investigate which condition was driving the outcome.

The first step in the analysis process was MRI variable selection. This was done for each clinical outcome using a stepwise regression with the clinical outcome as the dependent variable and the MRI metrics as the independent variables, as has been recommended for small clinical studies with multiple variables (Heinze and Dunkler, 2017). Then, multiple regression models were built with the selected MRI variable, the disease type and clinically relevant covariates (age, sex, and disease duration) as independent variables. The dependent variables for each model were the clinical outcomes: EDSS score, BPI score and MFIS score. The dependent variables were not transformed, and all models were checked using standardised residual plots to ensure that residuals were approximately normally distributed. Logistic regression models were used to assess sphincter dysfunction, catheter requirement and the final fatigue model where patients were classified as either fatigued or not based on the established cut-off of ≥38. *p* values were 2-tailed and statistical significance was set at 0.05.

7.4.3.2 Discriminatory model

Descriptive (sagittal lesion location), structural (cervical cord, thoracic cord, grey matter measurements and lesion volume) and quantitative (cervical cord FA, MD and MTR) were included in the discriminatory analysis. First, a principal component analysis was run using SIMCA v14.0.0.1359 (MKS Data Analytics Solutions, Sweden) to assess for spontaneous, unsupervised clustering. Thereafter, a predictive regression analysis was run and an orthogonal partial least square analysis (OPLSDA) model with seven cross-validation rounds and 200 iterations, comparing the three conditions in pairs (MOGAD vs AQP4-NMOSD, MOGAD vs MS, and AQP4-NMOSD vs MS). Each model was assessed for total variation in X (R2X), the total variation in Y (R2Y) and the accuracy of the prediction (q2). An R2Y of 100% suggests the model can explain all variation between groups. A higher R2Y and q2 mean a better separation. A q2 of 0.4 is generally accepted as the threshold for significance (Waterman *et al*., 2010). The predictors were then classified by level of importance using the variable importance for the projection (VIP) measure. Variables with a VIP ≥1.5 are considered the best classifiers.

7.5 Results

7.5.1 Disability

A stepwise regression with EDSS as the dependent variable and all the MRI metrics as independent variables produced a single significant model with cervical cord CSA as the dependent variable (Table 7.1 and 7.2).

Table 7.1 Stepwise regression model: disability model 1. *Dependent variable = EDSS.*

	Standardised Beta Co-efficient	**Std. Error**	***p value***
Cervical cord CSA	-0.372	0.035	0.010

Adjusted R^2 = 0.12, p value = 0.010

Table 7.2 Stepwise regression for disability model 1: excluded variables. *Dependent variable = EDSS.*

	Standardised Beta Co-efficient	**t**	***p value***	**Partial Correlation**	**Collinearity Tolerance**
Cervical cord MTR	0.065	0.440	0.662	0.066	0.892
Cervical cord MD	-0.010	-0.059	0.953	-0.009	0.729
Cervical cord grey matter CSA	0.085	0.479	0.634	0.072	0.622
Cervical cord FA	-0.210	-1.504	0.140	-0.221	0.954

The stepwise regression was then repeated with CST FA replacing the mean cervical cord FA, to assess if the tract-specific measure would be more relevant, but the same model was produced with cervical cord CSA as the only significant independent variable (Tables 7.3 and 7.4).

Table 7.3 Stepwise regression model: disability model 2. *Dependent variable = EDSS. Mean cervical cord fractional anisotropy replaced with corticospinal tract fractional anisotropy.*

	Standardised Beta Co-efficient	**Std. Error**	***p value***
Cervical cord CSA	-0.372	0.035	0.010

Adjusted R^2 = 0.12, p value = 0.010

Table 7.4 Stepwise regression for disability model 2: excluded variables. *Dependent variable = EDSS. Mean cervical cord fractional anisotropy (FA) replaced with corticospinal tract (CST FA).*

	Standardised Beta Co-efficient	**t**	***p value***	**Partial Correlation**	**Collinearity Tolerance**
Cervical cord MTR	0.065	0.440	0.662	0.066	0.892
Cervical cord MD	-0.010	-0.059	0.953	-0.009	0.729
Cervical cord grey matter CSA	0.085	0.479	0.634	0.072	0.622
CST FA	-0.191	-1.352	0.183	-0.200	0.945

A multiple regression model was then built with EDSS as the dependent variable and including cervical cord CSA together with the clinically relevant covariates listed in the methods. Cervical cord CSA remained significant (Table 7.5).

Table 7.5 Multiple regression model for disability. *Dependent variable = EDSS.*

	Standardised Beta Co-efficient	**Std. Error**	***p value***	**Tolerance**	**VIF**
Disease group	-0.034	0.291	0.796	-0.076	-0.259
Age	0.086	0.020	0.509	0.013	0.665
Sex	-0.133	0.468	0.309	-0.482	-1.028
Disease duration	0.120	0.003	0.395	0.003	0.858
Cervical cord CSA	**-0.272**	**0.031**	**0.045**	**-0.065**	**-2.057**

Adjusted R^2 = 0.20; p = 0.052

7.5.2 Sphincter dysfunction

Logistic regression models with either the presence or absence of sphincter dysfunction and those with the presence or absence of catheter requirement showed no association with any of the MRI variables.

7.5.3 Pain

The first stepwise regression with total BPI score as the dependent variable and mean FA included in the MRI metrics showed no significant associations. When mean FA was replaced with STT FA, a single significant model was produced between the total BPI pain score and STT FA (Table 7.6 and 7.7).

Table 7.6 Stepwise regression model: pain. *Dependent variable = total BPI Score.*

	Standardised Beta Co-efficient	**Std. Error**	***p value***
STT	-0.438	57.01	0.001

Adjusted R^2 = 0.18, p value = 0.001

Table 7.4 Stepwise regression for pain: excluded variables. *Dependent variable = total BPI score.*

	Standardised Beta Co-efficient	**t**	***p value***	**Partial Correlation**	**Collinearity Tolerance**
Cervical cord MTR	-0.156	-1.207	0.662	-0.172	0.975
Cervical cord FA	0.116	0.568	0.953	0.082	0.402
Cervical cord MD	-0.223	-1.425	0.634	-0.201	0.659
Cervical cord CSA	-0.010	-0.074	0.183	-0.011	0.955

To investigate this further a univariate test between STT FA and each separate component of the BPI score was used to show that both components (severity and interference) were associated with STT FA (Table 7.8).

Table 7.8 Univariate regression for the two components of the pain score.

	Standardised Beta Co-efficient	**Std. Error**	***p value***	**R^2**
Dependent variable: BPI Severity Score				
STT FA	-0.345	21.743	0.011	0.10
Dependent variable: BPI Interference Score				
STT FA	-0.492	37.212	<0.001	0.23

A multiple regression model was then built with total BPI score as the dependent variable, STT FA and the same clinically relevant variables listed in the methods and used in the EDSS model. STT FA remained significant and, in addition, AQP4-NMOSD was independently predictive of a higher pain score (Table 7.9).

Table 7.9 Multiple regression model for pain. *Dependent variable = total BPI score.*

	Beta	**Std. Error**	***p value***	**Tolerance**	**VIF**
Disease group (AQP4-NMOSD)	**0.362**	**6.411**	**0.011**	**0.712**	**1.405**
Age	0.048	0.272	0.731	0.690	1.449
Sex	-0.128	5.997	0.350	0.824	1.213
Disease duration	-0.165	0.035	0.196	0.854	1.171
STT FA	**-0.414**	**55.866**	**0.001**	**0.899**	**1.112**

Adjusted R^2 = 0.30, p value = <0.001

Finally, to further validate the relevance of the STT FA and pain, the same regression model was created using CST FA instead of STT FA. The model was not significant (p = 0.117), and CST FA did not show a significant relationship with total BPI score (B = -0.221, SE = 64.155, *p* = 0.127).

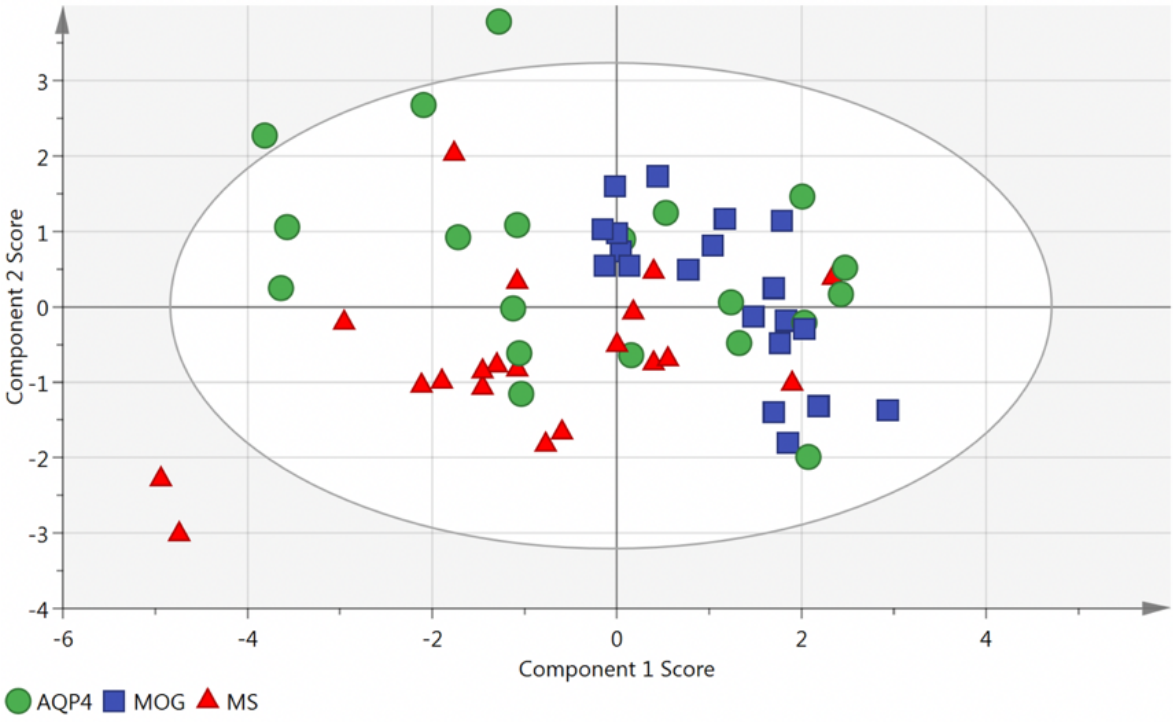
7.5.4 Fatigue

Neither regression models with fatigue score as a continuous variable or logistic regression models separating patients based on the cut-off score of ≥38 showed any association with the MRI variables.

7.5.5 Discriminatory model

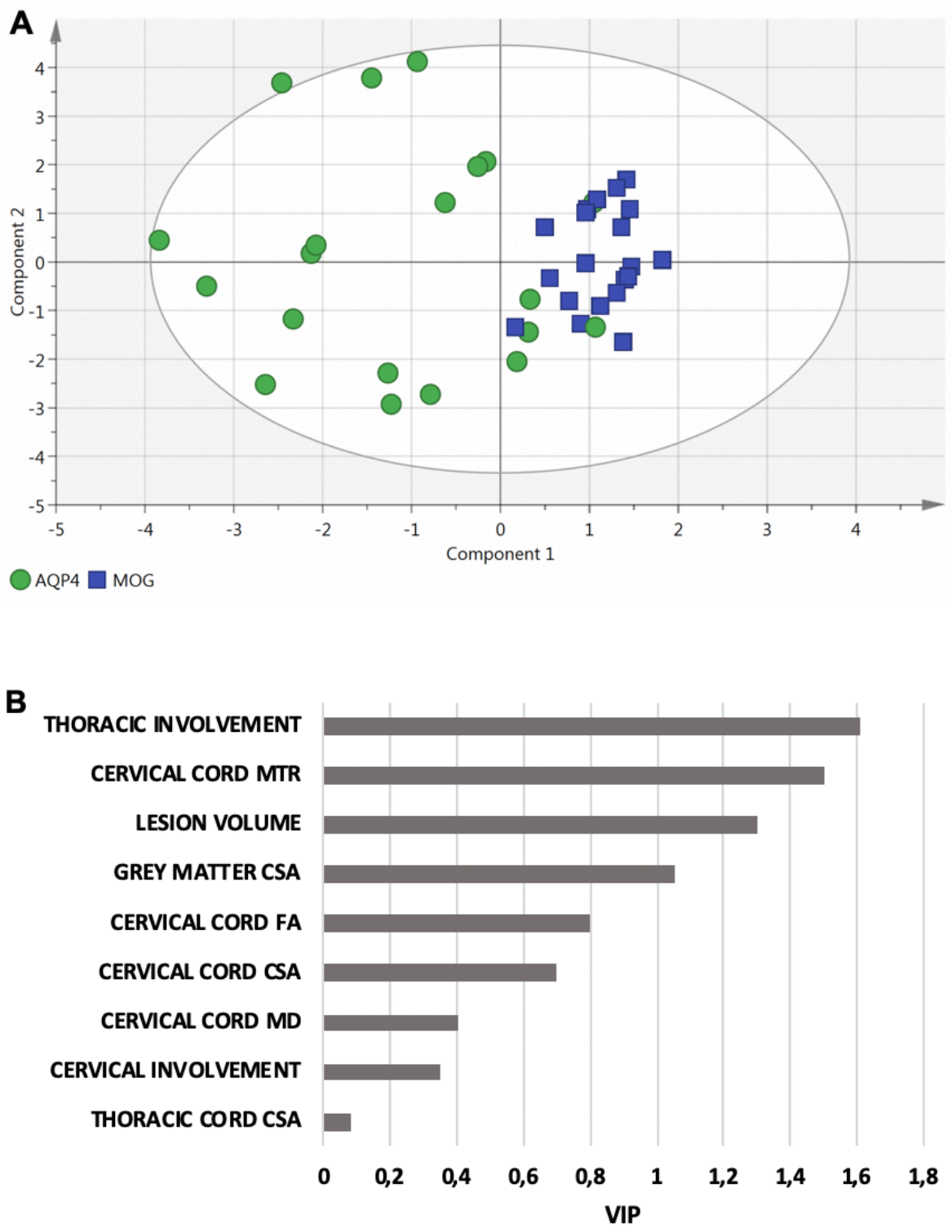
After inputting the MRI variables into a principal component analysis, patients with MOGAD tended to spontaneously separate (Figure 7.2).

Figure 7.2 Principal component analysis. *Image showing the trend of spontaneous clustering in the MOGAD group. Figure adapted from* (Mariano *et al.*, 2020).



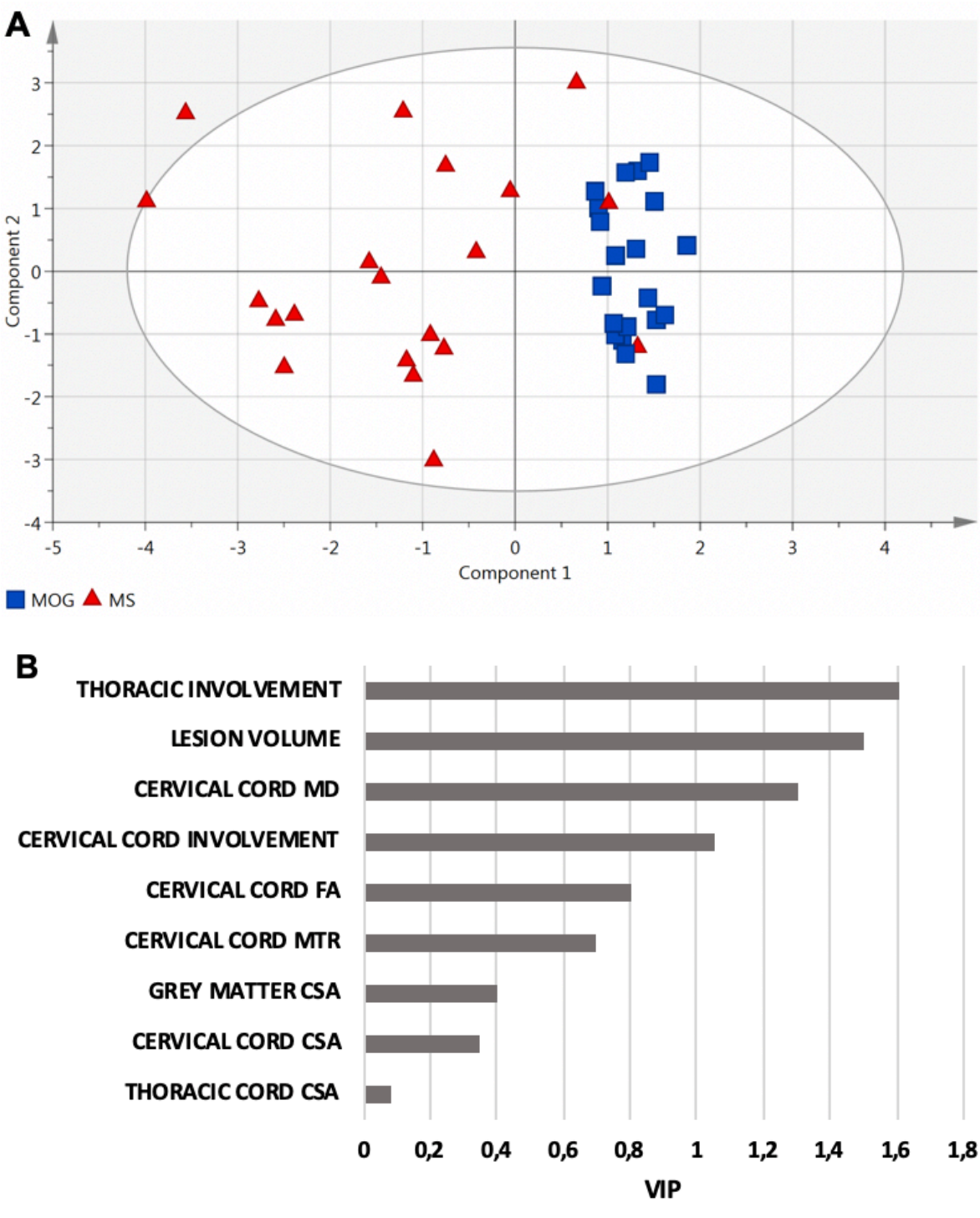
Each pair was then tested separately using the OPLS-DA model. A moderately predictive model was created to distinguish MOGAD from AQP4-NMOSD (q2 = 0.49, R2Y 58%), as shown in Figure 7.3 A. The most important predictors (VIP ≥ 1.5) are shown in Figure 7.3 B.

Figure 7.3 Discriminatory analysis. *Orthogonal partial least squares analysis showing (A) a moderately predictive model for MOGAD and AQP4-NMOSD, and (B) the discriminators ranked by VIP score. Figure adapted from* (Mariano *et al.*, 2020).



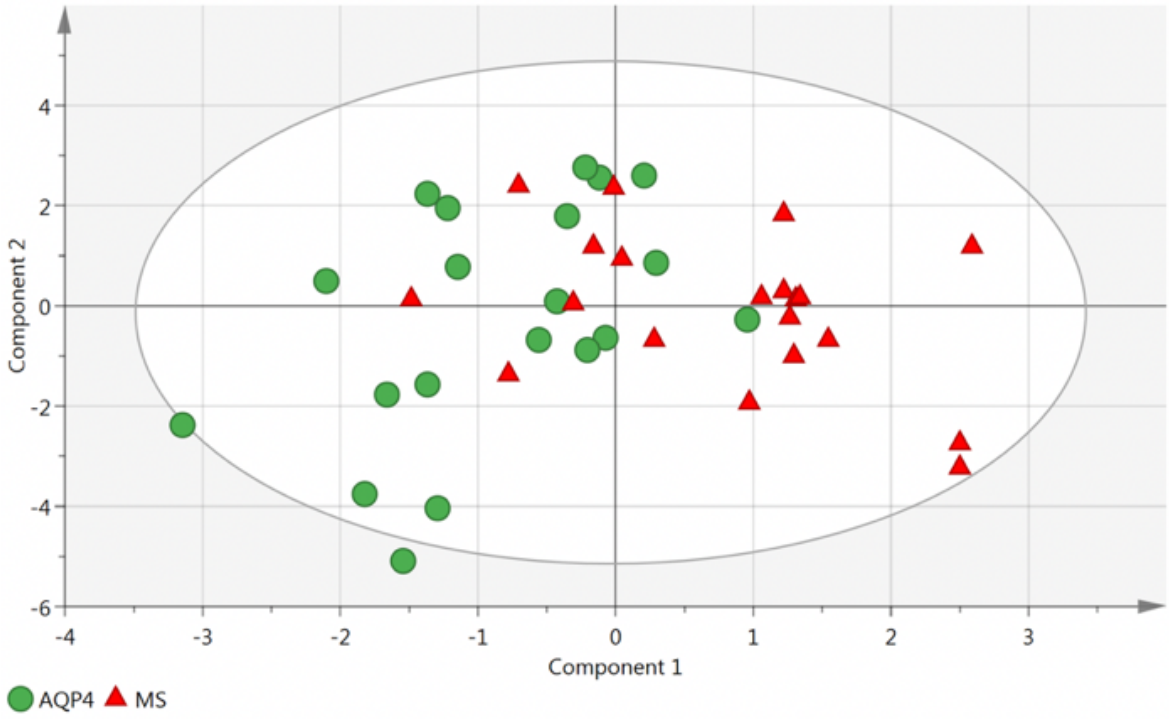
A moderately predictive model was also created to distinguish MOGAD from MS (q2 = 0.51, R2Y 62%), as shown in Figure 7.4 A. The most important predictors (VIP ≥ 1.5) were thoracic cord lesions and lesion volume, and are shown in Figure 7.4 B.

Figure 7.4 Discriminatory analysis. *Orthogonal partial least squares analysis showing (A) a moderately predictive model for MOGAD and MS, and (B) the discriminators ranked by VIP score. Figure adapted from* (Mariano *et al.*, 2020).



Finally, AQP4-NMOSD and MS could not be adequately discriminated (q2 = 0.14, R2Y 42%), as shown in Figure 7.5.

Figure 7.5 Discriminatory analysis. *Orthogonal partial least squares analysis showing a poorly predictive model for AQP4-NMOSD and MS. Figure adapted from* (Mariano *et al.*, 2020).



7.6 Discussion

In this chapter, the MRI metrics described in Chapter 5 and 6 and clinical outcomes described in Chapter 4 were brought together to assess for potential predictors of disability, pain and fatigue and to determine if a combination of the MRI features studied would allow for better discrimination of the disease conditions. This work highlights potential areas of interest and builds hypotheses for further research. Results from small samples across three groups should be interpreted in light of the limitations which is discussed below, together with the results.

The findings in this chapter suggest that cervical cord atrophy is a relevant MRI metric associated with disability in neuroinflammatory spinal cord disease. It has already been suggested as an outcome measure for clinical trials in primary progressive MS (Cawley *et al.*, 2018) and has also been shown to be clinically useful in other conditions, such as HTLV-1-associated neurological disease (Azodi *et al.*, 2017). It proved to be the only imaging metric that was significant in the stepwise regression for disability across the three diseases. Although the overall regression model for disability only accounted for 20% of the disability outcome, this is not an uncommon finding, as shown in other studies that look to find MRI markers of disability (Tsagkas *et al.*, 2018; Song *et al.*, 2020). Correlations of disability with imaging outcomes is complex because disability scoring is imperfect and imaging markers need to capture total pathology (volume loss and damage in remaining tissue) and account for the eloquence of different areas affected (although spinal cord is likely to be eloquent). It would appear, within this work and from the other published studies described, that atrophy in the spinal cord may be the most feasible measurement to acquire from a practical perspective, as well as the most relevant. While the recovery of remaining tissue may be different depending on the underlying condition, as shown in Chapter 6 (no differences were found in the quantitative measures of tissue integrity in MOGAD between affected and never-affected cord), atrophy may be a more universal measure of irreversible damage. Studies have largely focused on brain imaging markers as spinal cord imaging is notoriously difficult, particularly to standardise across centres to allow for larger cohorts. Future work should identify feasible methods for validating and incorporating the measurement of spinal cord atrophy into clinical trials together with brain imaging markers.

The analysis of MRI findings and how they associated with pain scores also showed interesting results. Naismith et al. previously reported an association between posterior column FA and finger vibratory thresholds in MS and NMOSD, as well as between diffusion metrics in the corticospinal tract and other measures of disability such as the 9-hole peg test and 25-foot timed walk (Naismith *et al.*, 2013). This work adds to these findings by investigating if the same tract-specific relationships are present with pain. While average cervical cord FA did not associate with pain scores, a relationship was found when specifically measuring FA within the lateral spinothalamic tracts. Basing the analysis on biologically plausible areas of interest allows for more meaningful results to be found. Further analysis also showed that, while the regression model used total BPI score results, the STT FA associated with both the severity and interference measures when assessed separately. And finally, the regression model was not significant when STT FA was replaced with CST FA, further indicating the potential specificity of these measures and usefulness of isolating specific tracts.

Additionally, it is interesting to note that having AQP4-NMOSD was an independent predictor of pain. In Chapter 3 it was shown that patients with AQP4-NMOSD were more likely to have pain at the time of their acute myelitis presentation. Furthermore, studies assessing the impact of neuropathic pain in neuroinflammatory conditions have shown that patients with AQP4-NMOSD tend to have more severe neuropathic pain than patients with MS (Kong *et al.*, 2016, Tackley *et al.*, 2016*b*, Asseyer *et al.*, 2020*a*). Less research has been done in the types and nature of pain in MOGAD. From recent studies it seems that more typical findings are that of acute retro-bulbar pain or headache associated with episodes of optic neuritis (Asseyer *et al.*, 2020*b*); although neuropathic pain can occur, it

may be less frequent than in NMOSD (Asseyer *et al.*, 2020*a*). An interesting observation is that in both AQP4-NMOSD and MS, thoracic cord lesions have been associated with more neuropathic pain (Okuda *et al.*, 2014, Tackley *et al.*, 2016*b*). However, the MOGAD cohort described in this study, in which all patients had thoracic cord lesions during the course of their disease, had the lowest number of patients who reported pain. Therefore, it is likely a combination of location, specific damage to particular tracts and possibly additional factors related specifically to astrocyte damage that leads to overall more pain in AQP4-NMOSD.

No spinal cord metric used in this study was able to capture sphincter dysfunction, particularly prominent in those with MOGAD. However, it may be that these imaging metrics do not capture this clinical outcome as they are measured only in the cervical cord. As discussed in Chapter 5, the grey matter in the lower cervical cord may be the most appropriate location to measure the damage leading to this outcome.

The final clinical outcome studied was fatigue: there was no measure within the spinal cord that was able to explain fatigue and it is possible that fatigue is mainly driven by brain pathology, although this may depend on the type of fatigue (Bisecco *et al.*, 2018). It is a symptom that was experienced in all three conditions. Fatigue is a complex symptom with pathways that are still unclear (Braley and Chervin, 2010). It may be that studies of functionality, such as resting state functional MRI, which has shown some promise in brain imaging studies of fatigue (Bisecco *et al.*, 2018; Jaeger *et al.*, 2019), are more useful in better understanding this symptom. This is explored further in Chapter 8.

Finally, discriminatory models were tested. These models show a moderate ability to differentiate MOGAD disease cords from those with AQP4-NMOSD or MS but not AQP4-NMOSD from MS. As mentioned previously, in the brain it has been shown that clinical features of acute brain scans were able to differentiate the antibody mediated conditions from MS but not from each other (Matthews *et al.*, 2013, Jurynczyk *et al.*, 2017*a*; Juryńczyk *et al.*, 2017). In this analysis lesion location, together with quantitative MRI metrics at follow-up are considered. It is interesting that MOGAD could be moderately discriminated from both AQP4-NMOSD and MS. While the predictive strength may not be adequate for individual patient diagnostic precision, these findings further support the evidence that MOGAD is a distinct entity, which may be related to its milder phenotype with good recovery and the frequency of lesions in the thoracic cord. In this cross-sectional comparison, AQP4-NMOSD and MS could not be accurately differentiated. This is likely a result of the degree of cord damage that occurs in both conditions and as acute findings such as lesion length or axial location were not included. A prospective longitudinal study would be necessary to further explore this as one would expect worsening of all metrics in MS independent of relapse. Future work would need to include larger cohorts to provide validation cohorts, which due to the number of patients in this study were not possible to create.

7.7 Limitations

These models were created with a limited number of patients across three disease groups, making the patient cohort more heterogenous, which means they should be interpreted with caution. However, previous studies in NMOSD have been conducted on as few as ten patients, as it is a rare disease (Qian *et al.*, 2011). With an increased number of clinical trials

taking place to test new drugs in NMOSD, it provides a good opportunity for standardised spinal cord MRI sequences to be established and used across different sites in order to begin to validate these findings. Measuring spinal cord atrophy as a secondary outcome may be a feasible first step.

Another consideration to make is that patients with MOGAD had the least disability and their quantitative measures did not differ from healthy volunteers in the group analysis. Patients with AQP4-NMOSD showed a pattern of localised cord damage. Therefore, future work is needed to study the interactions of these MRI metrics in each disease cohort, taking into consideration the disease type, areas of the cord involved and the number of cord relapses. More sophisticated statistical models can be applied to larger cohorts of participants that would assist in elucidating these relationships in a more robust way.

Finally, advancements in MRI will also enable additional measures to be obtained in the thoracic cord which would be exceptionally valuable in MOGAD.

7.8 Conclusion

Multimodal MRI provides valuable information about spinal cord involvement in neuroinflammatory conditions. Spinal cord MRI metrics have clinical significance in their association with disability and pain. Tract-based measurements of quantitative metrics may provide more relevant information when studying specific symptoms.

8. Chapter 8: Functional MRI in the spinal cord of MOGAD, AQP4-NMOSD and MS

8.1 Introduction and background

This chapter explores the use of the novel technique of resting-state function MRI (RS-fMRI) in the spinal cord in neuroinflammatory conditions. First, contributing to our current knowledge by describing the results in the healthy volunteer cohort and then comparing these results to the three disease cohorts being studied.

As described in Chapter 1, RS-fMRI studies in the spinal cord of healthy individuals have reported identifiable ventral and dorsal networks thought to represent motor and sensory processing (Barry *et al.*, 2014, 2016; Kong *et al.*, 2014; Liu *et al.*, 2016; San Emeterio Nateras *et al.*, 2016, Eippert *et al.*, 2017*b*). A single study has used RS-fMRI to assess the spinal cord in multiple sclerosis (MS) compared to controls (Conrad *et al.*, 2018). This study, done at 7T, showed that networks were overall intact but that lesions in MS were associated with focal abnormalities in connectivity (both increased and decreased connectivity noted). This technique has not been used to study the spinal cord in either myelin-oligodendrocyte glycoprotein associated disease (MOGAD) or aquaporin-4-positive neuromyelitis optica spectrum disorder (AQP4-NMOSD).

The approach taken in this chapter is based on the above studies. The spinal cord central grey matter can be divided into ventral (motor) and dorsal (sensory) horns, where either ascending or descending white matter tracts will synapse (Cohen-Adad and Wheeler-Kingshott, 2014). At rest, the connectivity is expected to be strongest between the ventral

horns and dorsal horns, respectively (Barry *et al.*, 2014, 2016; Kong *et al.*, 2014, Eippert *et al.*, 2017*b*). This distinct bilateral connectivity between ventral and dorsal horns maybe affected either by underlying disease processes or lesions within the cord (Conrad *et al.*, 2018; Powers *et al.*, 2018) and will be studied here across the four groups.

RS-fMRI was selected as part of the imaging protocol in this study for a number of reasons. First, as opposed to task-based fMRI, resting-state does not require the performance of specific tasks, which is useful when dealing with cohorts of patients with differing levels of disability. This makes it a potentially useful tool in clinical populations. Secondly, functional connectivity may exist between areas that are not structurally connected (Honey *et al.*, 2009) and so studying functional connectivity may offer additional insight into pathological states. In MS the clinic-radiological paradox has been described (Barkhof, 2002) where the association between the extent of clinical imaging findings and clinical outcomes has been inconsistent and overall, generally poor. Various confounders have been discussed and it has been recommended that in clinical studies we should not rely on a single MRI measure as combining different types provides us with multidimensional information. The added value of quantifying atrophy and white matter integrity has already been shown in Chapters 5 and 6. However, our understanding of the impact on function, and the compensatory mechanisms that may arise, as well as associations with clinical outcomes remain weak. Symptoms such as fatigue have not been fully explained and so the addition of RS-fMRI may also be useful when studying such a symptom, as has been shown in a study of RS-fMRI of the spinal cord in fibromyalgia where increased ventral but decreased dorsal connectivity associated with increased levels of fatigue (Martucci *et al.*, 2019). The addition of RS-fMRI may assist us in bridging the gaps that exist. Finally, the addition of RS-

fMRI to the sequences already described in previous chapters means that functional connectivity measures can be studied alongside structural measures, providing a unique opportunity to study the relationship between the two.

As described in Chapter 1, spinal cord imaging is challenging due to susceptibility and pulsation artifacts, low signal-to-noise ratio, a smaller cross-sectional area, motion artifacts related to cerebrospinal fluid flow and with each cardiac and respiratory cycle (Cohen-Adad and Wheeler-Kingshott, 2014; Stroman *et al.*, 2015). These challenges are even more pronounced in the acquisition of RS-fMRI, where susceptibility distortions and the effect of physiological noise are more pronounced than in the brain (Eippert *et al.*, 2017*a*). The methods outlined below will explain the measures taken to account for these challenges. Additionally, the sequence used was to enable the scan to be done on a 3 Tesla scanner, as has been established as a feasible option (Kong *et al.*, 2014, Eippert *et al.*, 2017*b*), with an acquisition time of approximately ten minutes, making it a more feasible option in the clinical setting than scans done over longer periods of time and on 7 Tesla scanners.

8.2 Objectives and aims

- To contribute to the current growing field of RS-fMRI in the spinal cord by studying and describing this technique in a cohort of healthy volunteers, also assessing for differences based on age and sex.

- To investigate differences in cervical cord connectivity between MOGAD, AQP4-NMOSD, MS and healthy volunteers.

- To study associations that may exist between structural and quantitative metrics in the spinal cord of healthy volunteers and disease cohorts.

- To investigate the effect of cord lesions on connectivity.

- To determine whether cord connectivity measures have clinical applicability as they relate to disability, pain and fatigue.

8.3 Hypotheses

- Identifiable dorsal and ventral networks will exist in healthy volunteers.

- There will be differences between the connectivity strength between healthy volunteers and the disease groups, due to underlying structural damage.

- Relationships will be found between connectivity strength and the presence of lesions.

- Dorsal connectivity will associate with pain scores and ventral connectivity will associate with disability.

8.4 Methods

8.4.1 Subjects

A total of 76 participants from the imaging cohort were included in this analysis, as shown in Table 8.1 below. One participant was excluded as physiological noise-modelling (PNM) measures were not acquired at the time of the scan. Three participants did not have RS-

fMRI scans acquired due to time constraints, where sequences needed to be repeated due to scan quality and preference was given to structural images. PNM measures were recorded alongside scanning.

Cohort and clinical assessments described in Chapter 4.1 Imaging protocols and acquisition methods are provided in Chapter 4.2.

Table 8.1 Demographics of the RS-fMRI cohort

	MOGAD	AQP4-NMOSD	MS	HV
Number	20	17	19	20
Mean age +/- SD	43.4 +/- 10.9	57.81 +/- 11.20	43.87 +/- 6.93	44.5 +/- 14.3
Sex F:M	10:10	12:5	11:8	12:8
Ethnicity (%) Caucasian Afro-Caribbean Asian	 20 (100) 0 (0) 0 (0)	 10 (59) 5 (29) 2 (12)	 19 (100) 0 (0) 0 (0)	 18 (90) 1 (5) 1 (5)
Phenotype (%) Isolated TM TM + ON TM + BS/BR TM + BS/BR + ON	 4 (20) 10 (50) 5 (25) 1 (5)	 9 (53) 3 (18) 3 (18) 2 (11)	 0 (0) 0 (0) 8 (42) 11 (58)	-
Median disease duration in months (range)	40.1 (8.5 – 239.9)	137.1 (22.6 – 289.8)	142.1 (10.4 – 252.1)	-
Mean total number of attacks	2	3	3	-
Mean number of symptomatic myelitis attacks	1.1	2.2	0.74	-
Median EDSS (range)	1.5 (0-8)	3 (1-8)	2 (0-6)	-
Sphincter dysfunction (number requiring catheter)	13 (4)	8 (2)	5 (1)	-
Mean BPI +/- SD	2.04 +/- 4.16	6.25 +/- 4.04	2.32 +/- 3.5	0
Mean MFIS +/- SD	27.4 +/- 18.92	35.9 +/- 21.9	36.9 +/- 14.1	8.9 +/- 7.2

8.4.2 Assessment of lesions

Only current lesions present on the research scans were considered for this analysis. The presence or absence of a lesion at each vertebral level (C1-C6) was represented as a binary variable (0 = no lesion; 1 = lesion present).

No patients with MOGAD had lesions present. Nine patients with AQP4-NMOSD and fourteen with MS had persistent lesions.

8.4.3 MRI pre-processing

Data were processed with tools from Spinal Cord Toolbox (SCT) v4.0 (De Leener *et al.*, 2017) and FMRIB Software Library (FSL) 6.0 (Jenkinson *et al.*, 2012).

First, slice timing correction was done using FSL slicetimer and slice-wise motion correction was performed using FSL flirt (Jenkinson *et al.*, 2012). Slice-wise motion correction is used as spinal cord displacement varies according to the cardiac and respiratory cycle (Stroman *et al.*, 2014) . Spatial smoothing (2x2x8mm^3 full width at half maximum Gaussian kernel) was performed using the SCT tool sct_maths.

Next FEAT (FMRIB's Expert Analysis Tool) was used (Woolrich *et al.*, 2001) to carry out physiological noise regression and high pass filtering (using a cut off of 100s). Physio data was processed using popp and pnm_evs (part of Physiological noise modelling (PNM) tool in FSL). The model included cardiac, respiratory and interaction effects leading to a total of 32 regressors, as described previously (Eippert *et al.*, 2017*a*). X and Y motion regressors were extracted using MATLAB R2019_a. A CSF mask was generated manually for each

subject using FSLeyes to extract average time courses from CSF. FSL Feat was then used to regress out motion (X and Y), physiological regressors and CSF. High pass temporal filtering (100s) was applied. The final output generated a 4D file that was used for further analysis.

Anatomical data used in this analysis was segmented and registered to the PAM-50 template, as previously described. Spinal cord segmentation in the native fMRI space was done using SCT DeepSeg (Gros *et al.*, 2019). Co-registration of the fMRI data to the anatomical data and template was done using the SCT tool sct_register_multimodal.

8.4.4 MRI analysis

A seed-based functional connectivity analysis was conducted across the grey matter horns at each level of the cervical cord acquired for each individual (C1-C6). The grey matter probabilistic mask from PAM-50 was warped into the functional space. Using the grey matter mask, binary grey matter horn masks (one for each ventral and dorsal horn) were then generated manually for each vertebral level, as shown in Figure 8.1. All horn masks were at least two voxels apart. These were checked alongside the anatomical images to ensure registration was accurate and each vertebral level was correctly labelled. Time courses were extracted from each horn mask using FSL fslmeants. These were merged uniformly for each participant. This text file was then loaded into MATLAB R2019_a to create a 24x24 correlation matrix (4 horns at 6 levels per participant). Pearson correlation coefficients were computed for each pair of horns. Only full correlations were used to simplify interpretation of the results. These coefficients were then converted into z-scores using a Fisher transformation ($z = \tanh^{-1}(r)(dof - 3)^{1/2}$). The z-scores were then extracted using predesigned coordinates for each horn pair of interest.

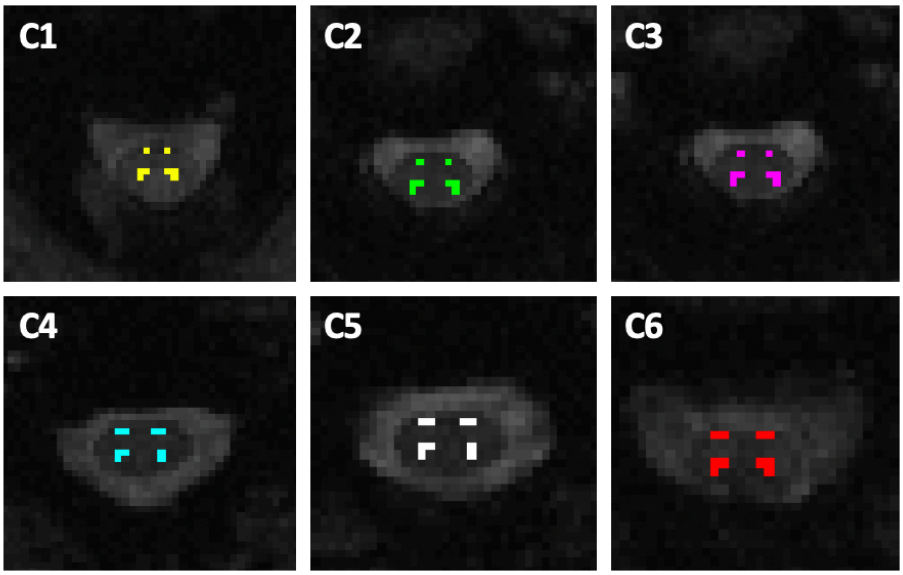
The horn pairs are labelled as follows:

- V-V = ventral-ventral
- D-D = dorsal-dorsal
- LV-LD = left ventral-left dorsal
- LV-RD = left ventral-right dorsal
- RV-RD = right ventral – right dorsal
- RV-LD = right ventral – left dorsal

Four individual z-scores were excluded as they exceeded the maximum z-score value (the participant data was reviewed in each case but no error was found in the pre-processing or analysis pipeline and so it was assumed that this may have been due to acquisition artefact). Due to the differing size of participants, two participants did not have data acquired at C1 and five participants did not have data acquired at C6 as these were not captured with the FOV centred at C3/C4 as described in the scan acquisition protocol.

The temporal signal-to-noise ratio (tSNR) was extracted from each vertebral level and included as a regressor in statistical models to account for connectivity confounders such as image intensity changes, signal dropout and noise.

Figure 8.1 Grey matter horn masks in the functional space across C1-C6 in a single participant.



8.4.5 Statistical analysis

Z-scores were extracted for each horn pair for every participant across the six cervical segmental levels. Linear mixed-effects models were used in order to compare horn pairs within each group in order to test which pairs had the strongest connectivity, with the subject included as a random factor. Linear mixed-effects models were then used to compare the groups, with the subject was included as a random factor. The assumptions for the model were checked by plotting residuals. Pairwise comparisons were done on the estimated marginal means and corrected for multiple comparisons using a Bonferroni correction. Regression models to assess the relationship between connectivity and cross-sectional area were, once again, built using a linear mixed-effects model, with the subject included as a random factor. Univariate regression models were used to explore the relationships between the average dorsal and ventral Z-score values and the quantitative

cord measures and the average dorsal and ventral Z-scores with clinical measures. tSNR was included as a covariate in all models to account for acquisition-related changes in connectivity. Significance was two-tailed and set at 0.05.

8.5 Results

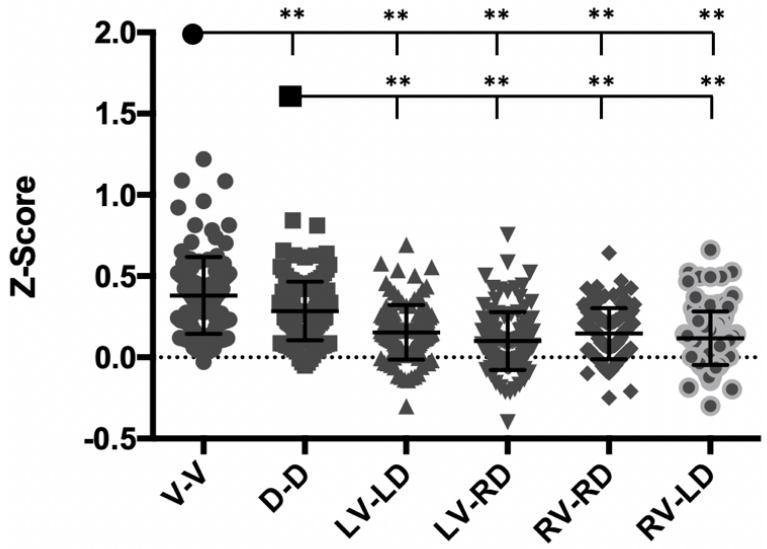
8.5.1 Healthy volunteer cohort analysis

As resting state functional MRI of the spinal cord is a novel technique in the spinal cord, the healthy volunteer group was analysed and described in the first instance.

8.5.1.1 Connectivity pairs

Connectivity data across the six cervical levels acquired are plotted as six pairs and are shown in Figure 8.3. Ventral-ventral connectivity was the highest of all pairings, followed by dorsal-dorsal. These were both significantly higher than all the remaining pairings and the ventral also higher than the dorsal. The remaining pairs four pairs were not significantly different from each other.

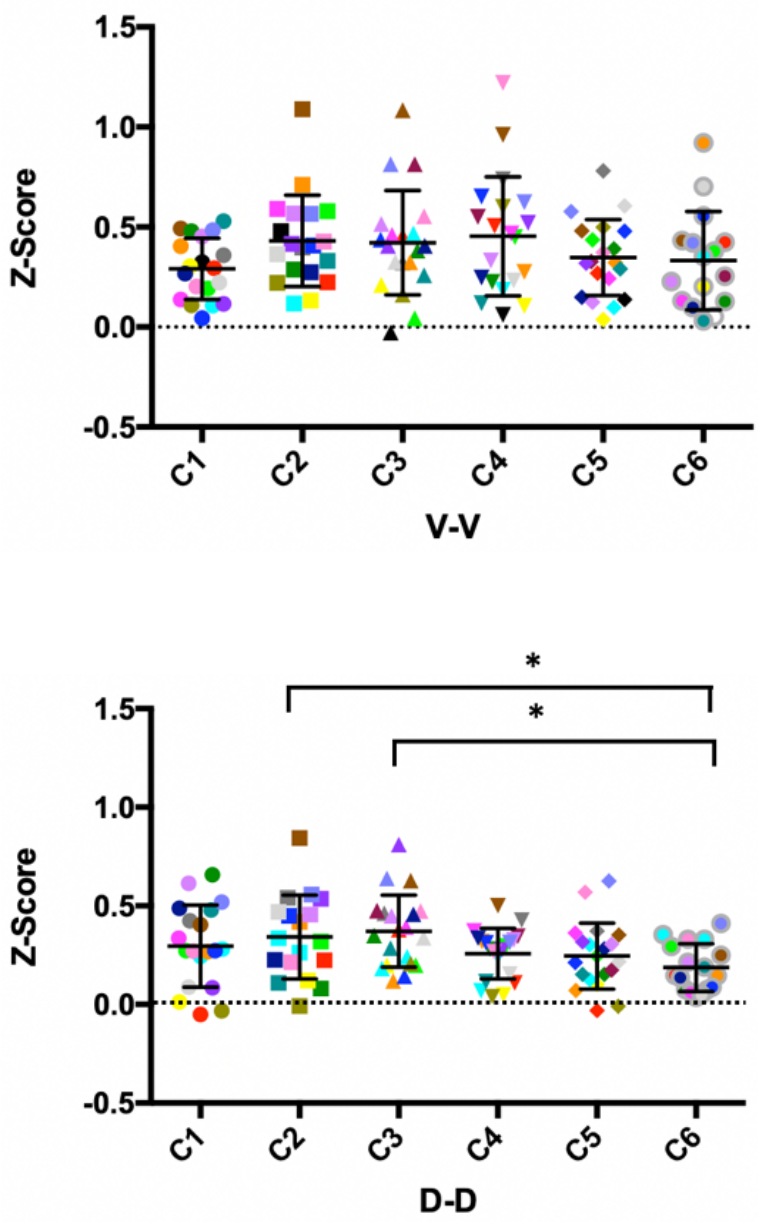
Figure 8.2 Healthy volunteer connectivity by horn pair. *Connectivity data for each horn pair in the healthy volunteer cohort. Raw data shown with significance based on a linear mixed-effects model which included the subject as a random factor, tSNR as a covariate and with a Bonferroni correction for multiple comparisons. Bars represent mean and standard deviation. * = p value <0.05; ** = p value <0.01.V = ventral; D = dorsal; LV = left ventral; LD = left dorsal; RV = right ventral; RD = right dorsal.*



8.5.1.2 Cervical vertebral levels

Ventral-ventral and dorsal-dorsal connectivity across vertebral levels is plotted in Figure 8.4. There were no significant differences across levels in the ventral-ventral connectivity. In the dorsal-dorsal connectivity analysis, C2 and C3 showed a significantly higher correlation than C6.

Figure 8.3 Healthy volunteer connectivity by cervical level. *Ventral (V) and dorsal (D) connectivity pairs shown across the cervical levels (C1-C6) in the healthy volunteer cohort. Raw data shown with significance based on a linear mixed-effects model which included the subject as a random factor, tSNR as a covariate and with a Bonferroni correction for multiple comparisons. Bars represent mean and standard deviation. Each colour represents an individual participant. * = p value <0.05; ** = p value <0.01.*

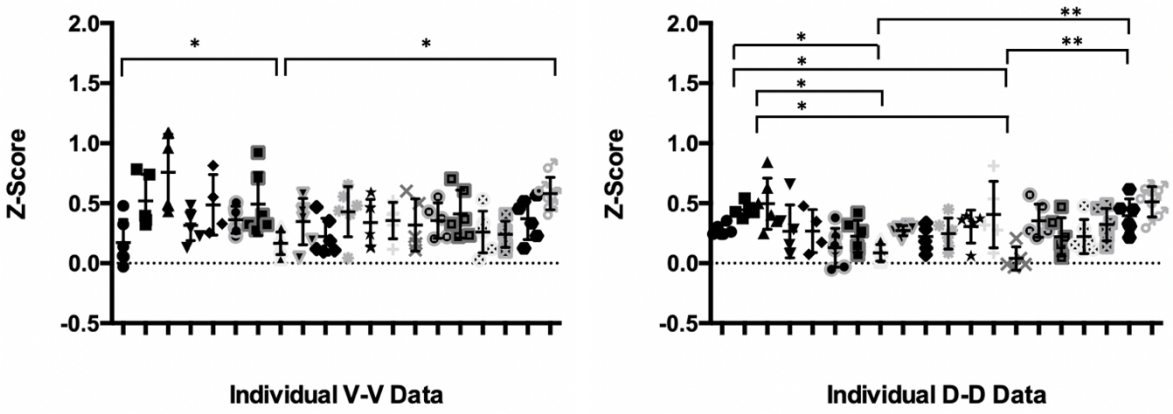


8.5.1.3 Individual subjects

Individual subject data across the six cervical levels for each healthy volunteer are plotted in Figure 8.5. Subject level differences were noted, particularly in the D-D connectivity. This

supported the use of linear effect modelling for further analyses and the inclusion of the subject a random factor.

Figure 8.4 Individual healthy volunteer data*. Ventral (V) and dorsal (D) connectivity across the six cervical levels. Raw data is shown. Significance based on a Kruskal-Wallis comparison with a post-hoc Dunn test for multiple comparisons. Bars represent mean and standard deviation. * = p value <0.05; ** = p value <0.01. Each shape represents an individual participant.*



8.5.1.4 Age and sex

No relationship was noted between V-V or D-D scores and the age of the healthy volunteer participants as shown in Table 8.2 and Table 8.3, respectively. The mean connectivity scores did not differ between male and female participants (Figure 8.6).

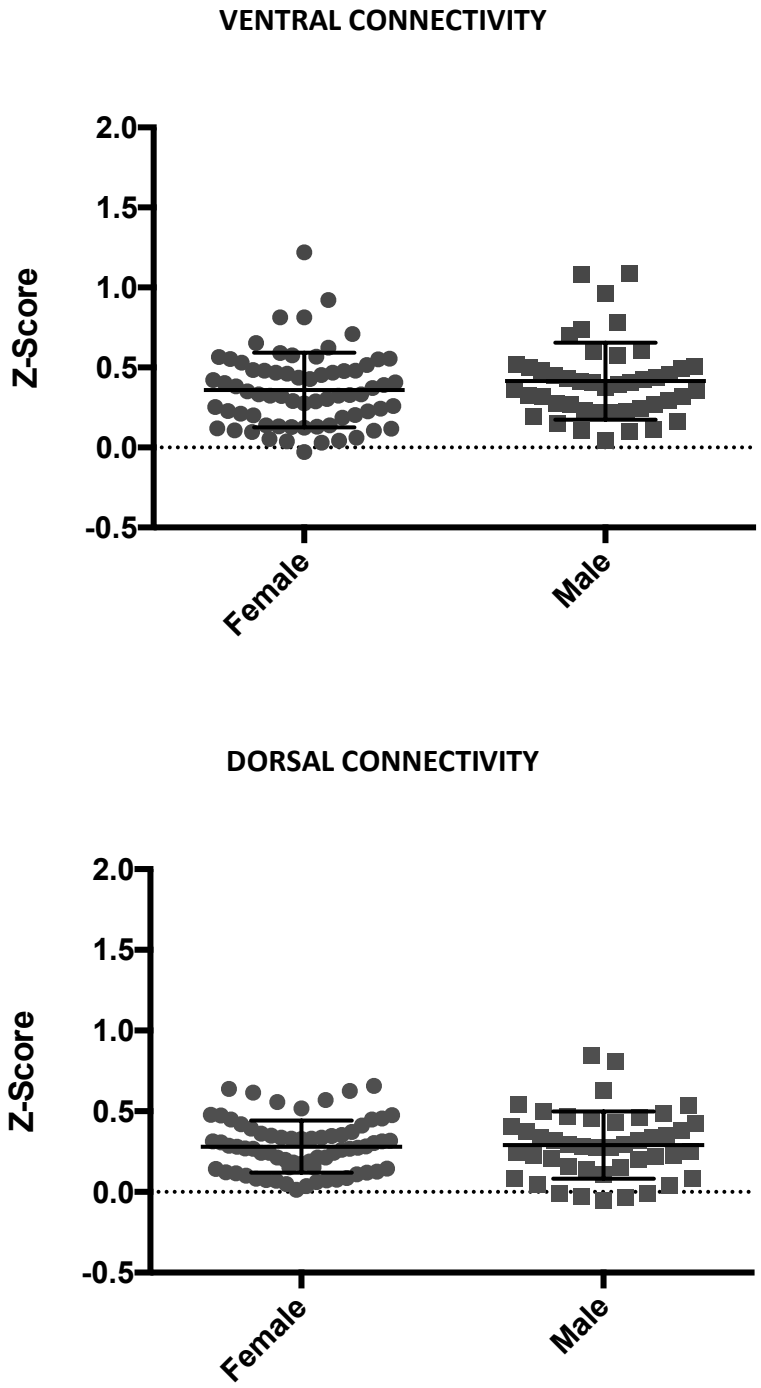
Table 8.2 *Univariate linear regression with V-V Z-score as the dependent variable and age as the independent variable.*

	Beta	**Std. Error**	***p* value**
Age	0.111	0.002	0.256

Table 8.3 *Univariate linear regression with D-D Z-score as the dependent variable and age as the independent variable.*

	Beta	**Std. Error**	***p* value**
Age	0.109	0.001	0.248

Figure 8.5 Healthy volunteer connectivity based on sex. *Ventral (V) and dorsal (D) Z-scores in male and female healthy volunteers. Bars represent mean and standard deviation.*



8.5.1.5 Cross-sectional area

Figure 8.7 shows the cross-sectional area measurements for the healthy volunteer group across cervical levels C1-C6. These measurements were included in a linear mixed-effects regression model with the connectivity Z-scores, with the subject included as a random factor and tSNR as a covariate. Ventral-ventral connectivity was increased with an increased cross-sectional area (B = 0.007, SE = 0.32, *p* value = 0.046), see Table 8.4. Dorsal-dorsal connectivity also showed an increase with increased cross-sectional area but this did not reach significance (B = 0.002, SE = 0.003, *p* value = 0.32), see Table 8.5.

Figure 8.6 Healthy volunteer cord area across cervical levels. *Cross-sectional area across cervical levels C1-C6 in the healthy volunteer cohort. Each colour represents an individual participant.*

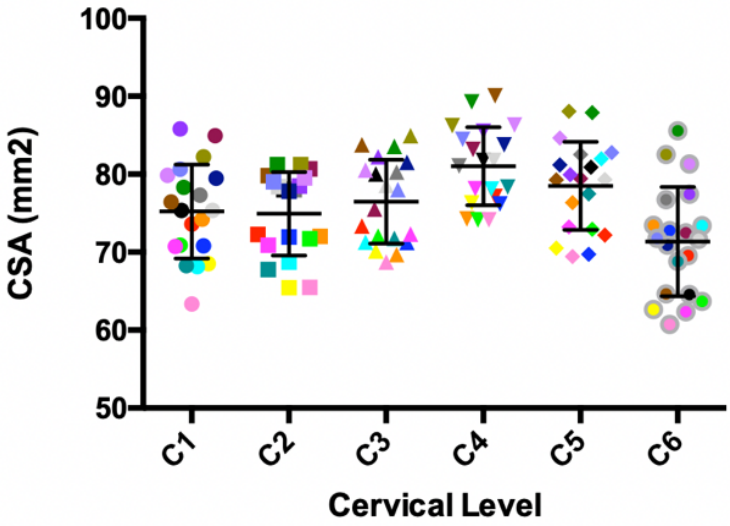


Table 8.4 *Ventral connectivity linear mixed-effects model, with subject included as a random factor. V-V Z-score as the dependent variable, with cross-sectional area (CSA) and tSNR included as independent variables.*

	Beta	**Std. Error**	***p* value**
CSA	0.007	0.003	**0.0463**
tSNR	-0.002	0.005	0.6559

Table 8.5 *Dorsal connectivity linear mixed-effects model, with subject included as a random factor. D-D Z-score as the dependent variable, with cross-sectional area (CSA) and tSNR included as independent variables.*

	Beta	**Std. Error**	***p* value**
CSA	0.002	0.003	0.3249
tSNR	0.005	0.004	0.2162

8.5.1.6 Exploratory analysis of quantitative MRI metrics in the healthy volunteers

Univariate relationships between quantitative MRI metrics acquired at the time of the scanning (as described in Chapters 6 and 7) and average connectivity measures were analysed. No significant associations were found, as shown in Table 8.6 and 8.7.

Table 8.6 *Ventral connectivity univariate linear regression models.*

	Beta	**Std. Error**	***p* value**
GM	0.142	0.053	0.820
MTR	0.131	0.024	0.594
MD	-0.058	0.544	0.807
FA	-0.274	1.137	0.243

Table 8.7 *Dorsal connectivity univariate linear regression models.*

	Beta	**Std. Error**	***p* value**
GM	-0.322	0.456	0.153
MTR	-0.130	0.018	0.595
MD	-0.111	0.439	0.643
FA	-0.054	0.955	0.820

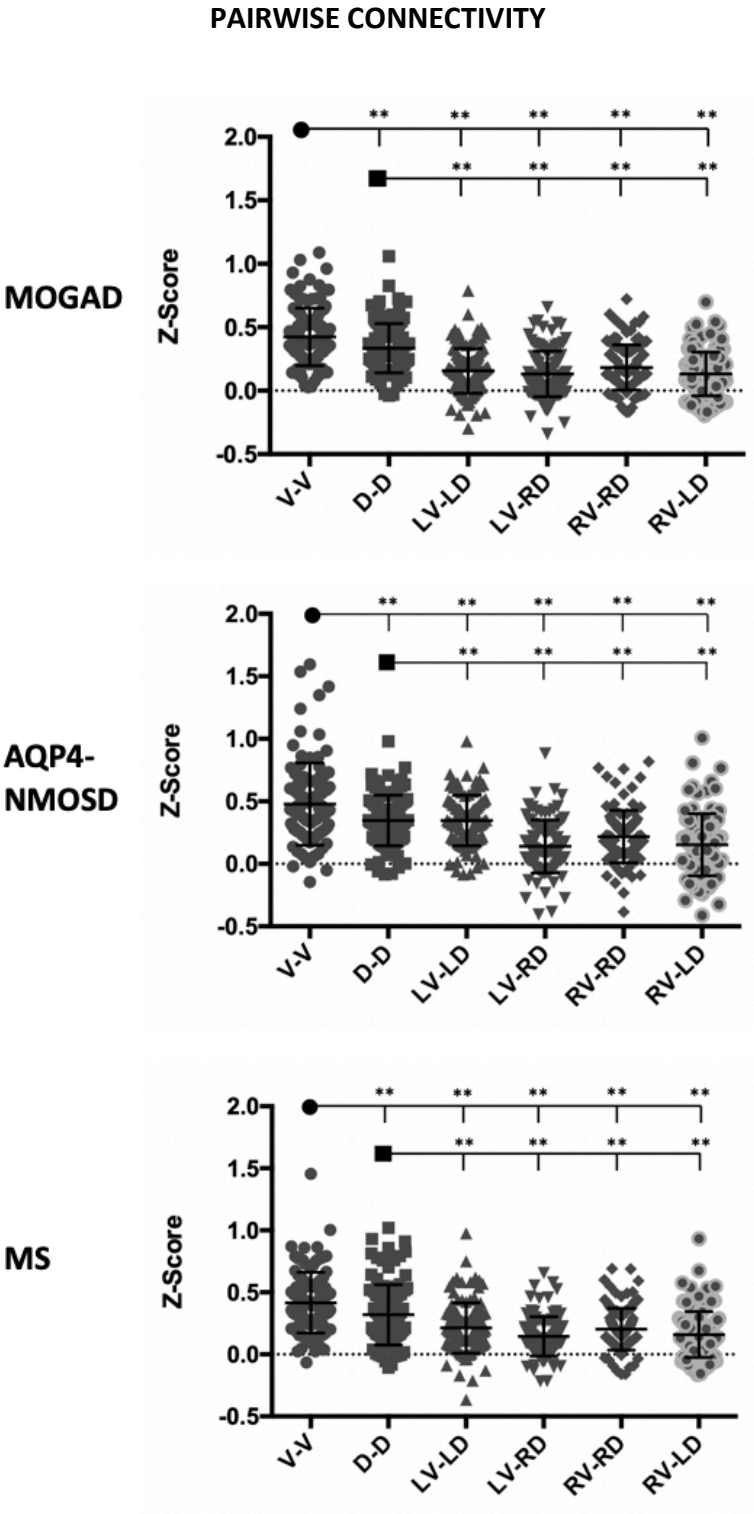
8.5.2 MOGAD, AQP4-NMOSD and MS cohort analysis

Each disease group was then analysed individually in the same way the healthy volunteers were above, before a four-group comparison was done.

8.5.2.1 Connectivity pairs

The same pattern of connectivity (highest in V-V, followed by D-D), as seen in the healthy volunteers, was maintained across all three disease cohorts, shown in Figure 8.8. but with more variation and some individual patients with higher connectivity noted in AQP4-NMOSD.

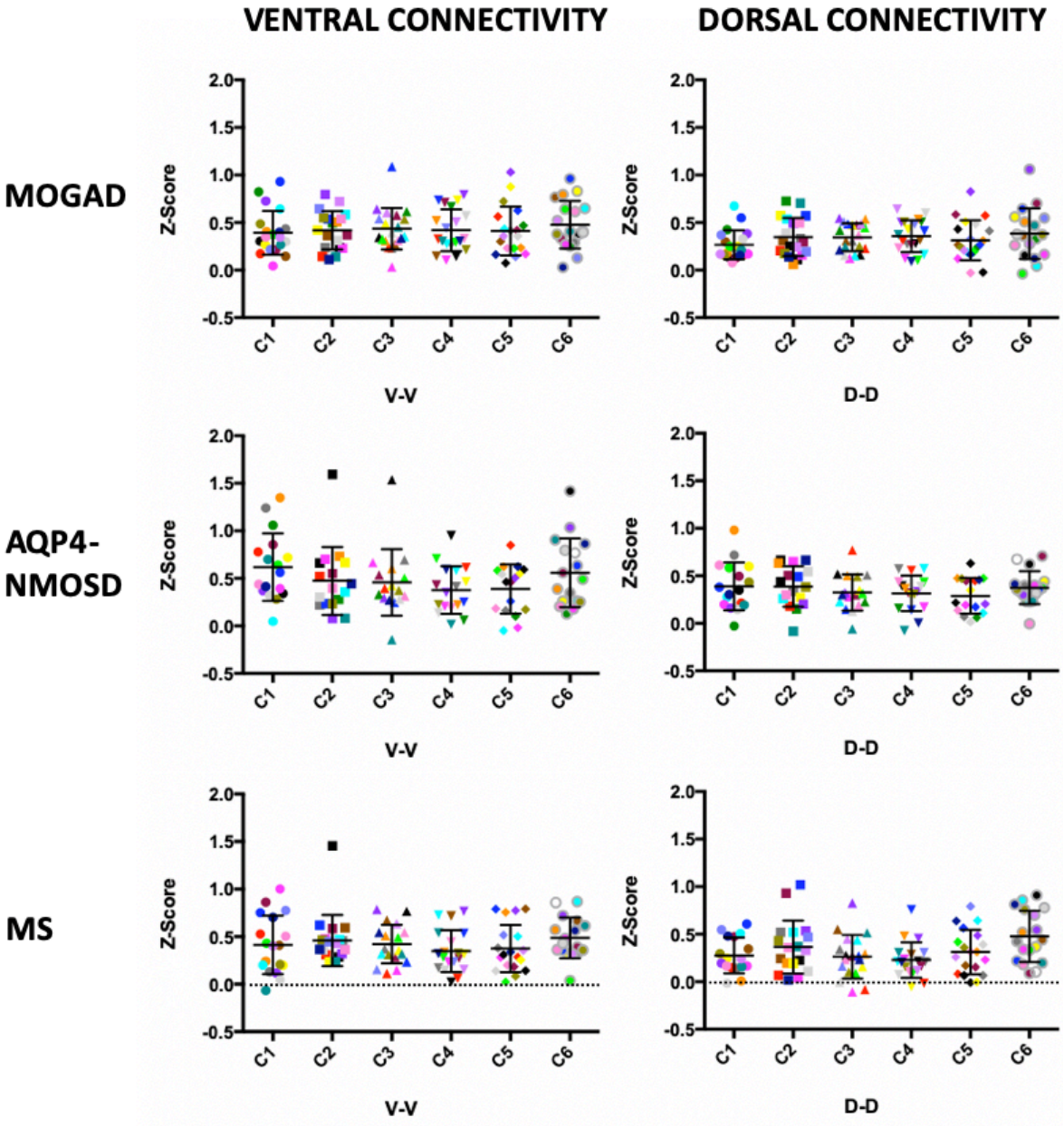
Figure 8.7 Connectivity data for each horn pair in MOGAD, AQP4-NMOSD and MS*. Raw data shown with significance based on a linear mixed-effects model which included the subject as a random factor, tSNR as a covariate and with a Bonferroni correction for multiple comparisons. Bars represent mean and standard deviation. * = p value <0.05; ** = p value <0.01; V = ventral; D = dorsal; LV = left ventral; LD = left dorsal; RV = right ventral; RD = right dorsal.*



8.5.2.2 Cervical vertebral levels

No significant differences were found within each group across cervical vertebral levels in the ventral-ventral or dorsal-dorsal connectivity (Figure 8.9).

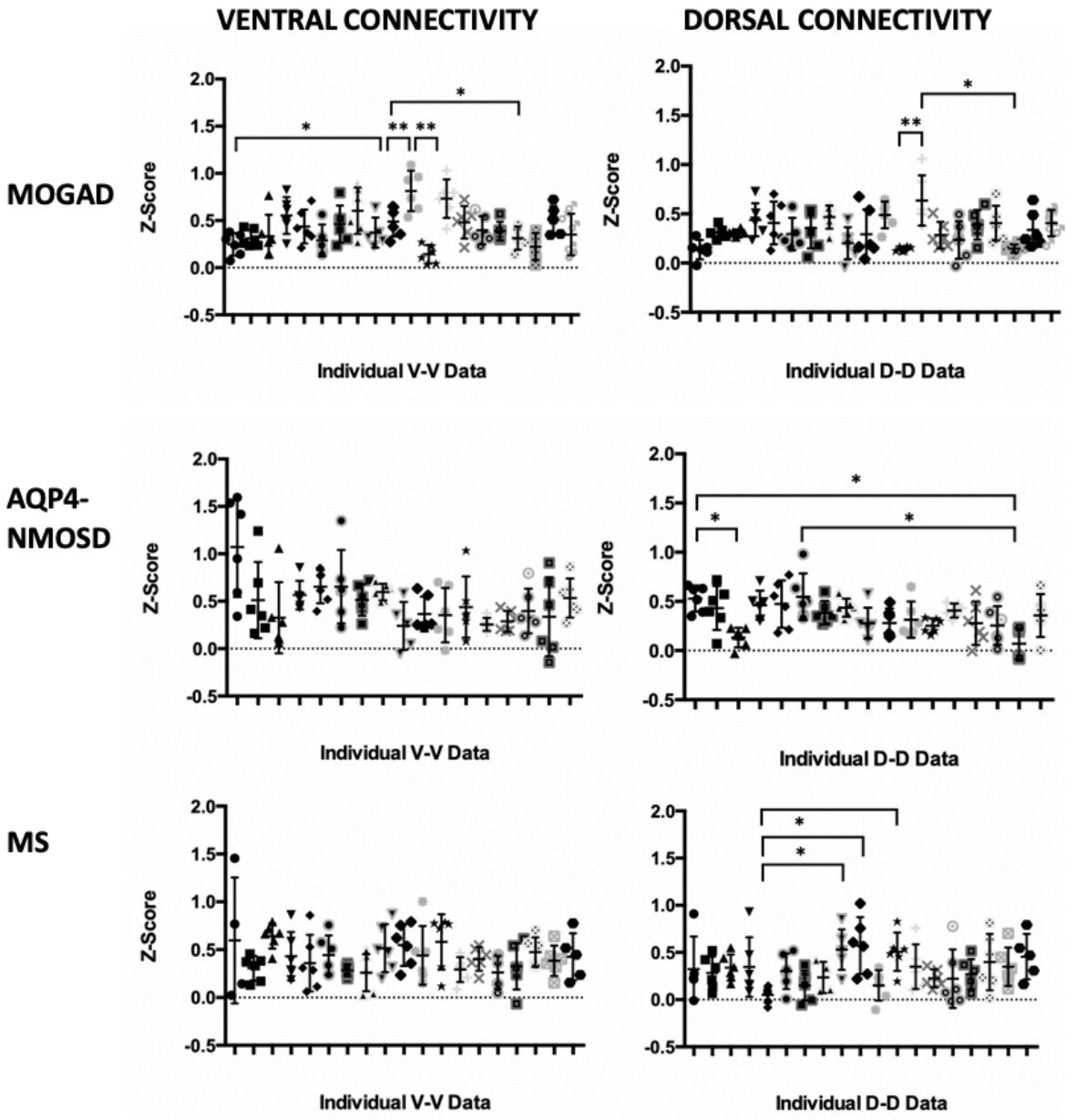
***Figure 8.8 Ventral (V) and dorsal (D) connectivity pairs shown across the cervical levels (C1-C6) in MOGAD, AQP4-NMOSD and MS**. Raw data shown with significance based on a linear mixed-effects model which included the subject as a random factor, tSNR as a covariate and with a Bonferroni correction for multiple comparisons. Bars represent mean and standard deviation. * = p value <0.05; ** = p value <0.01. Each colour represents an individual participant within each cohort.*



8.5.2.3 Individual subjects

Individual subject data across the six cervical levels for each of the three cohorts are plotted in Figure 8.10. Subject level differences were noted, as shown. As in the healthy volunteers, there was more variability in D-D connectivity between subjects.

Figure 8.9 Individual subject ventral (V) and dorsal (D) connectivity in MOGAD, AQP4-NMOSD and MS. *Raw data is shown. Significance based on a Kruskal-Wallis comparison with a post-hoc Dunn test for multiple comparisons. Bars represent mean and standard deviation. * = p value <0.05; ** = p value <0.01. Each shape represents an individual participant.*



8.5.2.4 Cross-sectional area

The relationship between cross-sectional area and connectivity in the disease cohorts differed from that of the healthy controls. Ventral connectivity showed an inverse relationship with cross-sectional area in the antibody-mediated conditions. This also held for dorsal connectivity in the AQP4-NMOSD cohort. In the MS group no significant relationship was found. The MOGAD cohort results are shown in Table 8.8, the AQP4-NMOSD in Table 8.9 and MS in Table 8.10.

Table 8.8 *MOGAD linear mixed-effects model, with subject included as a random factor. V-V and D-D Z-scores as the dependent variable, with cross-sectional area (CSA) and tSNR included as independent variables.*

	Beta	**Std. Error**	***p value***
Ventral Connectivity			
CSA	-0.008	0.003	**0.007**
tSNR	-0.011	0.006	0.077
Dorsal Connectivity			
CSA	-0.002	0.003	0.299
tSNR	-0.004	0.005	0.408

Table 8.9 *AQP4-NMOSD linear mixed-effects model, with subject included as a random factor. V-V and D-D Z-scores as the dependent variable, with cross-sectional area (CSA) and tSNR included as independent variables.*

	Beta	**Std. Error**	***p value***
Ventral Connectivity			
CSA	-0.012	0.004	**0.003**
tSNR	0.004	0.009	0.627
Dorsal Connectivity			
CSA	-0.005	0.002	**0.046**
tSNR	0.007	0.005	0.202

Table 8.10 *MS linear mixed-effects model, with subject included as a random factor. V-V and D-D Z-scores as the dependent variable, with cross-sectional area (CSA) and tSNR included as independent variables.*

	Beta	**Std. Error**	***p value***
Ventral Connectivity			
CSA	-0.004	0.004	0.264
tSNR	-0.002	0.005	0.777
Dorsal Connectivity			
CSA	-0.005	0.005	0.269
tSNR	0.007	0.007	0.341

8.5.2.5 Exploratory analysis of quantitative MRI metrics

No significant relationships were found with any of the quantitative metrics in and average connectivity scores across the disease cohorts. The MOGAD cohort results are shown in Table 8.11, the AQP4-NMOSD in Table 8.12 and MS in Table 8.13.

Table 8.11. *MOGAD univariate linear regression models.*

	Beta	**Std. Error**	***p value***
Ventral Connectivity			
GM	-0.303	0.029	0.207
MTR	0.040	0.024	0.872
MD	0.402	0.943	0.098
FA	0.054	1.466	0.831
Dorsal Connectivity			
GM	-0.081	0.023	0.743
MTR	-0.123	0.016	0.615
MD	0.379	0.670	0.120
FA	-0.083	1.029	0.743

Table 8.12. *AQP4-NMOSD univariate linear regression models.*

	Beta	**Std. Error**	***p value***
Ventral Connectivity			
GM	0.062	0.044	0.820
MTR	-0.155	0.018	0.552
MD	-0.424	0.694	0.101
FA	0.333	0.961	0.208
Dorsal Connectivity			
GM	0.230	0.028	0.392
MTR	-0.324	0.011	0.204
MD	-0.253	0.457	0.344
FA	0.321	0.612	0.225

Table 8.13. *MS univariate linear regression models.*

	Beta	**Std. Error**	***p value***
Ventral Connectivity			
GM	-0.152	0.020	0.561
MTR	-0.208	0.023	0.424
MD	-0.070	0.487	0.782
FA	0.139	0.830	0.584
Dorsal Connectivity			
GM	0.014	0.024	0.956
MTR	0.036	0.030	0.892
MD	-0.192	0.546	0.445
FA	0.086	0.953	0.735

8.5.3 Four-group comparison of MOGAD, AQP4-NMOSD, MS and HV

The average ventral and dorsal connectivity scores did not differ between the groups (ventral model: $X^2(3) = 2.241$, $p = 0.524$; dorsal model: $X^2(3) = 4.536$, $p = 0.209$).

As the effect size of the functional connectivity measures appear to be small and localised, a linear mixed-effects model was built to compare the ventral and dorsal connectivity at each cervical level across groups, with the subject as a random factor and tSNR included as a covariate. A pairwise comparison was then done on the estimated marginal means, with a Bonferroni correction for multiple comparisons. The following significant differences were found:

Ventral connectivity:

C1: ventral connectivity was higher in AQP4-NMOSD than in healthy volunteers (Table 8.14).

Table 8.14 Pairwise comparison of ventral connectivity at C1.

Interaction	Beta	Std. Error	*p* value
AQP4-NMOSD - HV	**0.2787**	**0.0949**	**0.0270**
AQP4-NMOSD - MOGAD	0.1722	0.0953	0.4504
AQP4-NMOSD - MS	0.1587	0.0952	0.5999
HV - MOG	-0.1065	0.0854	1.0000
HV - MS	-0.1200	0.0876	1.0000
MOG - MS	-0.0135	0.0867	1.0000

C6: ventral connectivity was higher in AQP4-NMOSD than in healthy volunteers (Table 8.15)

Table 8.15 Pairwise comparison of ventral connectivity at C6

Interaction	Beta	Std. Error	*p* value
AQP4-NMOSD - HV	**0.3169**	**0.1022**	**0.0172**
AQP4-NMOSD - MOGAD	0.1762	0.0994	0.4857
AQP4-NMOSD - MS	0.1557	0.0996	0.7380
HV - MOG	-0.1407	0.0904	0.7490
HV - MS	-0.1612	0.0929	0.5251
MOG - MS	-0.0205	0.0891	1.0000

Dorsal connectivity:

C6: dorsal connectivity was higher in MS than in healthy volunteers (Table 8.16).

Table 8.16 Pairwise comparison of dorsal connectivity at C6

Interaction	Beta	Std. Error	*p* value
AQP4-NMOSD - HV	0.19740	0.0803	0.100
AQP4-NMOSD - MOGAD	0.00251	0.0809	1.000
AQP4-NMOSD - MS	-0.06636	0.0803	1.000
HV - MOG	-0.19489	0.0730	0.060
HV - MS	**-0.26376**	**0.0739**	**0.004**
MOG - MS	-0.06887	0.0730	1.0000

8.5.4 Effect of lesions

To further investigate the differences in the ventral connectivity in AQP4-NMOSD and dorsal connectivity in MS, a binary variable representing whether or not a lesion was

currently present at that cervical level was added (lesion = 1; no lesion = 0). No significant effects were seen in the MS cohort. In the AQP4-NMOSD cohort, cross-sectional area retained its inverse relationship with connectivity (smaller cord area, higher connectivity) and lesions appeared to lead to a reduction in connectivity at the level in which they were present, as shown in Table 8.17 and Table 8.18.

Table 8.17 *AQP4-NMOSD ventral connectivity linear mixed-effects model, with subject included as a random factor. V-V Z-score as the dependent variable, with cross-sectional area (CSA), tSNR and the presence of a lesion included as independent variables.*

	Beta	**Std. Error**	***p value***
CSA	-0.013	0.004	**0.001**
tSNR	-0.002	0.005	0.685
LESION	-0.188	0.074	**0.013**

Table 8.18 *AQP4-NMOSD dorsal connectivity linear mixed-effects model, with subject included as a random factor. D-D Z-score as the dependent variable, with cross-sectional area (CSA), tSNR and the presence of a lesion included as independent variables.*

	Beta	**Std. Error**	***p value***
CSA	-0.005	0.005	0.266
tSNR	0.006	0.007	0.411
LESION	-0.027	0.064	0.666

8.5.5 Clinical outcomes

An exploratory univariate analysis was conducted looking at the measures in the disease groups to assess for relationships between these measures and the clinical scores: pain, disability and fatigue.

No significant relationships were found when including all patients together or in the MOGAD and MS groups when analysed individually.

In the AQP4-NMOSD cohort significant univariate relationships existed between the average D-D Z-score (as the independent variable) and total BPI score for pain (B = -0.615, R^2 = 0.38, p = 0.009). The relationship with average V-V Z-score was not significant. A significant relationship was also found between the average D-D Z-score and fatigue (B = -0.501, R^2 = 0.25, p = 0.041). The relationship with average V-V Z-score was not significant. No significant relationship existed with disability score.

8.6 Discussion

This chapter describes results across four cohorts using a novel imaging technique for studying the spinal cord in vivo. This began with an analysis of the healthy volunteer cohort. The higher correlation of the ventral and dorsal networks is in keeping with the underlying physiology and previous studies (Kong *et al.*, 2014; Barry *et al.*, 2016, Eippert *et al.*, 2017*b*), confirming that distinct and robust functional networks exist in the spinal cord without a particular task. There were no age or sex differences noted in this cohort of healthy volunteers. Differences in connectivity were noted between individual subjects and very minimally across cord levels. In particular, dorsal connectivity is more variable across both cervical cord levels and subjects, with very little difference in ventral connectivity overall in the healthy volunteer cohort. One hypothesis may be that the ventral horn is more uniform anatomically, with fewer laminae and a more focused physiological output. This differs from the dorsal horns to which spatially and molecularly distinct sensory afferents convey information (Hochman, 2007).

The relationship between these connectivity measures and quantitative MRI metrics were then analysed in the healthy volunteer cohort. An increased cross-sectional area was associated with a higher V-V correlation. This relationship did not reach significance in the D-D connectivity. Although this research is exploratory, this is an interesting point to consider as cord size may affect connectivity measures either due to an intrinsic reason or due to an acquisition-related phenomenon and so may need to be accounted for in work of this nature, which has not yet been described in previous studies. There were no associations between connectivity Z-scores and diffusion or MTR metrics.

The three disease cohorts were then analysed and compared. Only a single paper exists in the literature that has studied this technique at 7T in cohort of MS patients (Conrad *et al.*, 2018). Conrad et al. showed small, localised connectivity differences where lesions were present (both increased or decreased connectivity was observed) but no overall differences were found between the MS cohort and the control group.

The aim of the work presented in this chapter was to test this methodology in different disease groups and at 3 Tesla, a more widely available field strength, and in a clinically feasible acquisition time (approximately 10min).

All three disease groups showed the same pattern of connectivity across the six pairs. Ventral connectivity remained the strongest, followed by dorsal connectivity. The same predominance of individual subject variability in the dorsal connectivity values, but not the ventral, was found.

Interestingly the relationship between ventral connectivity and cross-sectional area in the antibody-mediated conditions was the inverse of that in the healthy volunteers. This relationship was also present between cross-sectional area and dorsal connectivity in the AQP4-NMOSD cohort. This was not noted in the MS group, where no significant associations were found. This may be due to the overall more severe cord atrophy in AQP4-NMOSD. The damage in the antibody-mediated conditions is also localised, as shown in Chapter 6 and 7, and they both have a more predictable central lesion location (Tackley *et al.*, 2014; Dubey *et al.*, 2019). This may lead to a more well-defined relationship between the cord damage and the connectivity measures, with the location of the damage and atrophy having a more pronounced effect on ventral connectivity, specifically.

The finding of increased connectivity in the disease cohorts was also supported by the group comparison. AQP4-NMOSD showed increased ventral connectivity at C1 and C6, while the MS group showed increased dorsal connectivity at C6 compared to healthy volunteers.

Different hypotheses exist for the finding of increased connectivity in disease models, as this finding has been reported in both task-based (Agosta *et al.*, 2008) and resting-state studies of the spinal cord in MS (Conrad *et al.*, 2018). One hypothesis is that this reflects a compensatory mechanism within local grey matter in response to lesions or axonal loss (Kearney *et al.*, 2015). Supporting this theory, Agosta et al. showed bilateral recruitment of grey matter regions in response to stimulation in patients with more white matter damage (Agosta *et al.*, 2008). The suggestion of a compensatory mechanism leading to increased connectivity has also been found in the brain of MS patients, where a study by Zhou et al. showed increased functional connectivity in areas of the brain which were more

structurally disconnected due to damage (Zhou *et al.*, 2014). Another hypothesis is that the increased connectivity is due to a disruption of inhibitory interneurons, either by destruction or dysfunction of their role. This reduction in number and size of interneurons has been described in pathology studies in MS (Gilmore *et al.*, 2009*a*). Further work would need to be done in order to better understand the local changes and their effect in the spinal cord.

The effect of current cord lesions was then explored. This effect was not significant in either the ventral or dorsal connectivity in the MS group. In AQP4-NMOSD the presence of a lesion was significantly associated with a reduction in ventral connectivity at that level. This may reflect that atrophy leads to a compensatory increase in connectivity but that lesional tissue may represent a disruption of local architecture and therefore a decrease in connectivity. This finding of a reduction of connectivity due to lesions has been shown in MS in both the brain (Tahedl *et al.*, 2018) and spinal cord (Conrad *et al.*, 2018). It has also been shown by Chen et al. in squirrel monkeys, where after the introduction of a unilateral dorsal lesion, connectivity was reduced within the slice of the lesion (Chen *et al.*, 2015). In the study by Conrad et al., lesions had a variable effect of either increasing or decreasing connectivity between the horn pairs depending on their location. Once again, the more consistent central location of lesions in AQP4-NMOSD may mean that the effect of these lesions is greater at the group level. Cord lesions in MS preferentially occupy the lateral and posterior cord (Geraldes *et al.*, 2018), which may explain the group level difference noted in dorsal connectivity as opposed to ventral connectivity.

Finally, an exploratory analysis was conducted between clinical outcomes and the connectivity measures based on *a priori* hypotheses. Significant associations were found

between dorsal connectivity and both pain and fatigue scores in the AQP4-NMOSD group. This may be a result of this group having a more uniform involvement of the cord, as described above and so a more consistent involvement of specific cord areas. Interestingly in MS, studies in the brain have shown that fatigue is associated with functional reorganisation of non-motor networks (Bisecco *et al.*, 2018) which is in keeping with the relationship being only with dorsal, and not ventral connectivity, in the cord. These relationships were not significant when considering all patient across the cohorts, or in the other disease groups individually. These are provisional findings that will need to be explored further in future work, in studies designed to specifically study these symptoms in the appropriate paradigms and should include findings in the brain. Both are complex symptoms that are unlikely to be explained by a single connectivity score but it does suggest interesting avenues for future research.

The work in this chapter suggests that different underlying mechanisms may lead to differing effects on the connectivity measures. Direct comparison of disease cohorts to a healthy volunteer group may therefore not be the most useful method of analysis, as pathology may increase or decrease values and so finding distinct differences between disease cohorts and controls may not be a relevant outcome. Additionally, other factors may contribute: this group of patients were recruited outside of an acute relapse and it has been shown in animal models that there is recovery of functional connectivity measures after an induced injury from 7-24 weeks later in the spinal cord (Chen *et al.*, 2015) and also recovery noted with a few months of a lesion in the brain in multiple sclerosis (Droby *et al.*, 2016). This may be particularly relevant in the antibody-mediated conditions where silent lesions are atypical and so functional connectivity may have

recovered. The course of the disease in each individual participant was also heterogenous, when considering a combination of the number of cord attacks, their disease duration and the specific cervical cord level and location of the lesion.

Overall, functional connectivity appears to be a dynamic measure. This may also fluctuate over time. One study suggested that in MS this trajectory begins with a compensatory increase in connectivity and a decrease later on in the disease (Rocca *et al.*, 2012). This would necessitate a longitudinal study to capture changes not found in this cross-sectional analysis or a larger cross-sectional cohort.

Spinal cord RS-fMRI may therefore be more useful in studying individual participants during acute attacks and then at specific time intervals thereafter to better elucidate the relationship between the different temporal changes in the cord and the connectivity measures. It may be that connectivity measures are more useful at the individual level as opposed to group level analyses in disease models. Once validated, this could be a useful tool to differentiate, for example, a true relapse from a pseudo-relapse in an individual, where traditional imaging techniques can be inconclusive (Kessler *et al.*, 2016). This will require further study but also advances in the acquisition and analysis of spinal cord resting state data.

Recently, a new method has been described that is able to recover fine-grained components of spontaneous spinal cord activity in an unprecedented level of detail in both the grey and white matter (Kinany *et al.*, 2020). And another publication describes the acquisition of simultaneous cord and brain resting state data (Vahdat *et al.*, 2020). In a short amount of time rapid growth has taken place in this field of study. This work in this

chapter, which begins to unpack the effect of disease on functional connectivity measures will assist in the creation of hypothesis driven research in future resting state studies.

These developments will also enable future studies to address some of the limitations through their ability to analyse the different tissue types and include the brain in the same acquisition. Grey matter segmentation techniques are also evolving, and this will further improve findings in disease cohorts where the underlying architecture is distorted. Additionally, larger sample sizes and understanding the effect of medications on functional connectivity would also be imperative. Studies in the brain have shown that drugs used to treat neurological conditions do have an effect on connectivity measures and patterns (Xiao *et al.*, 2019); this includes drugs commonly used to treat neuropathic pain e.g., carbamazepine. The impact of these on spinal cord connectivity is not yet known but needs to be investigated. Finally, the ability to study RS-fMRI in the thoracic cord would be a major advance.

8.7 Limitations

The limitations relevant to this MRI study more generally are discussed in chapter 4. However, additional specific limitations exist. First, during acquisition the use of ZOOM IT for reduced field of view could not be applied due to safety concerns. A recent change in the safety profile means this can be used more widely and future studies may benefit from better quality imaging with this added tool (Wheeler-Kingshott *et al.*, 2002). The rating of lesions as a binary variable is a coarse measurement and more a more specific analysis based on specific tracts affected by lesions and looking at the difference in the effects of white matter and grey matter lesions may provide more detailed information. The regions

of interest were created by dividing the four grey matter horns, but connectivity could be assessed in smaller subnetworks or a spatial independent component analysis may be applied (Kong *et al.*, 2014). Brain lesions in relevant tracts may lead to connectivity differences in the cord. The simultaneous acquisition of brain and cord functionality may better elucidate this relationship in future (Vahdat *et al.*, 2020).

8.8 Conclusion

Distinct and robust functional networks exist in the spinal cord without a particular task. The connectivity patterns between the grey matter horns in the spinal cord are physiologically plausible. Damage in the spinal cord may lead to either a compensatory increase or a decrease in connectivity. An association exists in the antibody-mediated conditions between cord cross-sectional area and ventral connectivity, with a more atrophic cord having a higher ventral connectivity. Whereas the presence of a lesion at the level of the cord in AQP4-NMOSD was associated with a decrease in ventral connectivity at that level. Overall, group-level differences were found within the cervical cord levels with increased ventral connectivity in AQP4-NMOSD at C1 and C6; and increased dorsal connectivity in MS at C6, compared to healthy controls. Connectivity changes appear to be localised and the different mechanisms underlying a disease pathology may have different effects on connectivity measures. Further work is needed to better understand these relationships and whether or not they may be more valuable at the individual level. This would require not only a larger sample size but should be designed in consideration of the above findings.

9. Chapter 9: Discussion

9.1 Introduction

The research reported in this thesis enhances our knowledge of spinal cord involvement in myelin oligodendrocyte glycoprotein associated disease (MOGAD). In particular, studying this condition alongside aquaporin-4-positive neuromyelitis optica spectrum disorder (AQP4-NMOSD) and multiple sclerosis (MS) provided the opportunity to not only study this new disease but also to compare it to its most likely differentials, which expands the clinical application of the work. The use of non-conventional spinal cord imaging modalities evidences their value in our study of diseases that impact the spinal cord, both for their clinical relevance and ability to provide *in-vivo* surrogate markers for tissue damage that may indicate underlying pathophysiology.

9.2 Summary of key findings

The key findings are presented in response to the overall research objectives. Table 9.1 provides a summary.

9.2.1 Overall research objectives (as described in Chapter 2)

- To study the clinical course and radiological findings of myelitis in patients with MOGAD and compare them to patients with AQP4-NMOSD.

- To study the features of myelitis in MOGAD using structural and quantitative MRI measures, and compare them to patients with AQP4-NMOSD, MS and healthy

volunteers (HVs), in order to better understand the underlying disease mechanisms.

- To investigate differences in resting-state functional connectivity in patients with MOGAD, AQP4-NMOSD and MS, and compare them to HVs.

- To determine the clinical applicability of the structural, quantitative and functional MRI measures as they relate to disability, relapse-risk, pain and fatigue.

9.2.2 Key findings

9.2.2.1 Clinical presentation of myelitis in MOGAD

- The acute clinical presentation of MOGAD and AQP4-NMOSD myelitis are largely similar but sphincter dysfunction is more prominent in MOGAD and pain is more prominent in AQP4-NMOSD, both acutely and at long-term follow-up.

- Concomitant involvement of the brain and optic nerves, either acutely or at relapse, is more common in MOGAD than AQP4-NMOSD. Patients with AQP4-NMOSD are more likely to have relapsing myelitis and can often have isolated cord involvement throughout the course of their disease.

9.2.2.2 Acute MRI findings

- Short cord lesions, multiple cord lesions and conus involvement are more common in MOGAD than AQP4-NMOSD.

9.2.2.3 Long-term outcomes and follow-up imaging

- Despite similar disability at nadir, patients with MOGAD recover mobility better than those with AQP4-NMOSD.

- Patients with MOGAD are often left with severe sphincter dysfunction, despite good recovery of motor dysfunction.

- The need for long-term catheterisation in MOGAD is commonly associated with the presence of a conus lesion during the acute attack.

- The presence of a brainstem lesion at the time of the myelitis indicates poorer recovery in patients with MOGAD, while age is the most important factor in AQP4-NMOSD (older patients were less likely to recover well).

- Although younger patients with AQP4-NMOSD show better recovery from attacks of myelitis, they are more likely to relapse. In patients with MOGAD no specific clinical predictors of relapse were found.

- Patients with MOGAD are more likely to have resolution of MRI findings on follow-up scans.

9.2.2.4 Structural and quantitative MRI findings

- Multi-modal MRI provides us with valuable information about spinal cord involvement in neuroinflammatory conditions.

- In patients with MOGAD, the quantitative metrics studied are comparable with HVs in the group analysis. However, in areas previously affected by lesions grey matter atrophy was noted compared to both unaffected areas of the cord in MOGAD and grey matter CSA in HVs.

- Patients with relapsing MOGAD have more thoracic atrophy than those with monophasic disease, even when relapses do not affect the spinal cord.

- Myelitis with AQP4-NMOSD shows the most severe, localised damage in areas involved in the acute episode with a consistent pattern observed across different metrics (cross-sectional area (CSA) of the cervical cord, thoracic cord and grey matter, as well as magnetisation transfer ratio (MTR) and diffusion tensor imaging (DTI) metrics).

- In patients with MS, metrics show significant differences compared to HVs but the relationship with lesion location is not as pronounced.

- A discriminatory analysis of these metrics could moderately discriminate MOGAD from both AQP4-NMOSD and MS.

- Cervical cord CSA associated weakly with disability outcomes and spinothalamic tract fractional anisotropy (FA) associated moderately with pain scores.

9.2.2.5 Resting-state functional MRI

- Distinct and robust functional networks exist in the spinal cord without a particular task and these network patterns appear to be preserved in all three disease cohorts.

- In the HV cohort, no relationships were found between cord connectivity measures and demographic features, but a positive correlation was found between cervical cord CSA and ventral connectivity.

- Damage in the spinal cord may lead to either a compensatory increase or a decrease in connectivity.

- Contrary to the findings in the HV group, an association was found in the antibody-mediated conditions between cord CSA and ventral connectivity, with a more atrophic cord having a higher ventral connectivity.

- The presence of a lesion at the level of the cord in AQP4-NMOSD was associated with a decrease in ventral connectivity at that level.

- Overall, group-level differences were found within the cervical cord levels with increased ventral connectivity in AQP4-NMOSD at C1 and C6; and increased dorsal connectivity in MS at C6, compared to HVs.

- Connectivity changes appear to be localised and the different mechanisms underlying a disease pathology may have different effects on connectivity measures.

Table 9.1 Summary of key research findings. *Typical features in each disease.*

	MOGAD	AQP4-NMOSD	MS
Clinical findings			
Onset presentation	Severe Often with sphincter involvement	Severe Often present with pain	Mild to severe
Acute Cord MRI			
Long lesion	++	+++	-
Short lesion	++	+	+++
Multiple lesions	++	-	+++
Sagittal location	Thoracic/conus	Cervical/thoracic	Cervical
Axial location	Central	Central	Lateral/dorsal
Associated Lesions on Brain MRI	++	+	+++
Asymptomatic lesions	May occur in brain or brainstem during acute attack. Extremely rare outside of relapse.	May occur in brain or brainstem during acute attack. Extremely rare outside of relapse.	Classically occur throughout the central nervous system and accumulate over time.
Clinical course	May be relapsing and, if so, typically involves optic nerves.	Relapsing condition. A relapsing myelitis phenotype is most common.	Relapsing condition with involvement of sites throughout the central nervous system.
Predictors of relapse	No clear predictors but cord atrophy appears more severe in relapsing disease and needs to be investigated further.	Define as a relapsing conditioning but younger age group may indicate a higher risk of relapse.	Defined as a relapsing condition.
Disability	Good recovery but prominent sphincter dysfunction.	Poorer recovery with prominent pain symptoms.	Accumulation of disability due to chronic neurodegeneration.
Predictors of disability	Brainstem lesion during acute attack. Cervical cord cross-sectional area.	Older age at time of attack. Cervical cord cross-sectional area.	Cervical cord cross-sectional area.

	MOGAD	AQP4-NMOSD	MS
Research MRI findings in the affected cord			
Cervical cord atrophy	←→	++	+
Thoracic cord atrophy	←→	++	←→
Grey matter atrophy	+	++	++
Fractional anisotropy	←→	↓↓	↓↓
Mean diffusivity	←→	↑↑	↑↑
Magnetisation transfer ratio	←→	↓↓↓	↓
Resting state	←→	↑ ventral connectivity ↑ ventral connectivity with ↑ atrophy and ↓ with lesions	↑ dorsal connectivity

9.3 Interpretation and application of findings and suggestions for future work

9.3.1 A focus on MOGAD

The study of MOGAD is a rapidly evolving field. This work has contributed to the understanding of spinal cord involvement in this condition and, together with other studies, assists in piecing together the knowledge needed to provide appropriate clinical management.

The conclusions of this work need to be considered in light of the limitations, such as sample size in the non-conventional imaging study and demographic differences that, although accounted for in all statistical analyses, cannot be matched entirely. However, each aspect was designed as a component of a high-quality, single-centre study with consistent and accurate diagnoses across participants. Participants were selected only if they had a history of spinal cord involvement, unlike many other studies which include heterogenous phenotypes.

As outlined in Chapter 1, when studying a new disease, such as MOGAD, in addition to clinical trials and treatment protocols, there are other important concepts that also need to be addressed:

- The establishment of criteria for early and accurate diagnosis, i.e., what should prompt testing for MOG-antibody.

- A better understanding of the underlying disease mechanisms and pathogenesis.

- Predictors of outcomes, such as relapse-risk and disability.

Answering these questions fully is outside the scope of this study, but, as spinal cord involvement is a hallmark feature, the findings in this thesis may be useful in building hypotheses for future work and could assist in deciding on protocols that should be included when taking observations forward into larger multi-centre studies. This work is particularly valuable as it is the first time quantitative imaging techniques have been applied to the spinal cord in MOGAD. These findings would need to be combined with brain MRI, optical coherence tomography, neurophysiological assessments, pathology studies and new biomarkers, such as neurofilament light chain, glial fibrillary acidic protein and myelin basic protein in order for a full and complete study of MOGAD and the development of a full set of specific diagnostic criteria.

Some of the important observations from this study of the spinal cord, in relation to the points above, are as follows:

9.3.1.1 The establishment of criteria for early and accurate diagnosis (i.e., what should prompt testing for MOG-antibody)

Patients with MOGAD may fulfil the criteria for antibody negative NMOSD, as described in Chapter 1. The clinical study in Chapter 3 supports the testing for MOG-antibodies in patients with myelitis that present with an antibody-negative NMOSD phenotype but emphasises the need for unique diagnostic criteria for MOGAD due to the number of differences described.

Importantly, the presence of multiple cord lesions, short cord lesions, predominance of thoracic cord lesions and involvement of the conus are important findings that make MOGAD more likely. Additionally, optic neuritis or acute demyelinating encephalomyelitis (ADEM)-like brain lesions together with evidence of spinal cord disease are also important presentations in which to consider testing for MOG-Ab. These findings are also in keeping with two other recent studies of myelitis in MOGAD (Dubey *et al.*, 2019; Ciron *et al.*, 2020). While large multi-centre studies have specific advantages, multiple studies involving smaller numbers but showing the same results may still provide good evidence when combined. This may be particularly relevant in rare diseases.

An additional observation from the clinical MRI scans is that the term “short cord lesion” has become somewhat synonymous with MS. However, in the case of MS these are classically <1 vertebral body, asymmetrical lesions that involve the lateral and posterior cord (Geraldes *et al.*, 2018, Ciccarelli *et al.*, 2019). Nomenclature is important and it is essential that we avoid misunderstandings. Therefore, it may be prudent to find an alternative term to describe these lesions in MOGAD, which are often less than three vertebral segments but longer than one and are more commonly central.

Finally, the disease course and long-term outcomes may also be an important consideration. This would include findings such as a clinical picture of residual sphincter dysfunction with good recovery of mobility and the resolution of lesions on clinical MRI at follow-up. A single follow-up scan at recovery may be useful to document lesion resolution. However, of note, it has been shown that multiple follow-up MRIs outside of relapse, as may be done in MS, is likely less useful in MOGAD due to the lack of residual lesions (or T2-hyperintensity) and that the development of new, silent lesions is less common in MOGAD or less likely to be captured (Fadda *et al.,* 2021).

9.3.1.2 A better understanding of the underlying disease mechanisms and pathogenesis.

Although small effects may be missed with smaller sample sizes, this work suggests that the better clinical recovery seen in patients with MOGAD is mirrored by quantitative MRI values that were comparable to HVs, whereas clear abnormalities were seen in both AQP4-NMOSD and MS. Although MOGAD is considered to be a primary demyelinating condition, MRI markers of white matter damage that are thought to better represent myelination and axonal integrity (diffusion metrics and MTR) were not found to be statistically different to HVs in the group analysis. This may either represent that white matter is less affected or that the type of damage recovers better in the course of MOGAD, as was discussed in detail in Chapter 6.

What may be more interesting is the finding of grey matter atrophy in affected cords. As detailed in Chapter 5, grey matter involvement is being increasingly described in MOGAD (Hacohen *et al.*, 2017, Ogawa *et al.*, 2017; Dubey *et al.*, 2019). This is the first documentation of long-term damage in the grey matter and was recently supported by

findings in brain in a study by Zhuo. et al which found that patients with MOGAD had grey matter atrophy in the frontal and temporal lobe as well as in the deep grey matter compared to HVs (Zhuo *et al.*, 2020). This finding in the grey matter also provides us with additional insight into the prominence of sphincter dysfunction in MOGAD. As conus involvement does not fully explain the extent and frequency of long-term sphincter dysfunction in this condition, involvement of the grey matter lower in the cord supports the hypothesis that this may be due to supraconal grey matter disruption affecting the important micturition and sphincter control mechanisms (Li *et al.*, 2020).

Pathological studies comparing the grey matter involvement in both MOGAD and MS, which are both considered primary demyelinating conditions but have significant grey matter involvement, would be valuable.

9.3.1.3 Predictors of outcomes such as relapse-risk and disability

There are currently no clear predictors for relapse-risk and disability in MOGAD. This work sought to assess for potential factors that may be of interest for future studies in relation to spinal cord disease. This is specifically important in MOGAD as not all patients relapse and so this would affect long-term treatment decision making more than in AQP4-NMOSD and MS, where treatment protocols are well-established. As disability in MOGAD is relapse-related, predictors of disability from the acute attack would be more relevant to guiding acute treatment and predictors of relapse would assist in deciding on whether ongoing immunosuppression may be necessary.

Disability

In the clinical study, lesions in the brainstem and conus at the time of the acute attack associated with poorer long-term overall disability and the need for long-term catheterisation, respectively. These findings may prompt clinicians to advocate for more extensive acute treatment in patients with residual symptoms.

Relapse-risk

The finding in Chapter 5 indicates that relapsing MOGAD may be a more severe phenotype (relapsing patients had significantly more thoracic cord atrophy than monophasic patients, whether the relapses occurred in the cord or elsewhere). This provides an interesting hypothesis for future work that could indicate that spinal cord atrophy after an acute attack may increase the risk of future relapse and indicate earlier immunosuppressive treatment. Additionally, it would need to be assessed as to whether these patterns exist in other areas of the central nervous system, for example, brain atrophy measures, optic nerve atrophy or changes in the retinal nerve fibre layers as measured by optical coherence tomography.

9.3.2 A focus on spinal cord MRI

In addition to studying a new disease, this thesis seeks to highlight the importance of spinal cord imaging in neuroinflammatory conditions, both acutely and at follow-up. It also evidences the use of non-conventional MRI techniques in the spinal cord.

9.3.2.1 Clinical MRI

MRI is an essential tool in the clinical setting. The work in this thesis, particularly in Chapter 3, emphasises the need for standardised protocols to be implemented for the assessment of neuroinflammatory conditions in clinical settings.

Often in suspected MS only the cervical cord is imaged (Ciccarelli *et al.*, 2019). The increased frequency of conus involvement in MOGAD, which may be missed if not specifically imaged, means that in cases of suspected inflammatory myelitis dedicated cervical and thoracic imaging should be done, together with axial imaging at the level of any suspected lesion as axial location is important for differentiating MS lesions from the antibody-mediated conditions. This may be particularly important in cases of MOGAD presenting with short cord lesions.

Additionally, follow-up imaging is an important part of the management of neuroinflammatory conditions in the cord. While availability of resources in different settings should be taken into consideration, the findings in this thesis motivate for follow-up MRI scans of the spinal cord outside of a relapse as they may provide vital information that assists with both diagnosis and prognosis, such as the resolution of MRI lesions in MOGAD.

9.3.2.2 Non-conventional MRI

As described in Chapter 1, spinal cord imaging faces many different challenges in terms of acquisition and analysis. However, it is a valuable tool for specific studies of the spinal cord

or to complement studies of the brain. The ability to study the central nervous system as a whole is invaluable to the study of neurological conditions.

The usefulness of quantitative imaging methods to study the spinal cord is evidenced in this thesis and in particular shows the translational application of techniques that can be used to answer a clinical question. MRI provides us with the opportunity to study conditions *in-vivo* and the use of multimodal MRI may assist us in overcoming the clinico-radiological paradox that so often exists (Barkhof, 2002) by showing an association with clinical outcomes.

There is potential for these methods to become more widely used and to enter clinical practice. However, a range of different imaging modalities were used in this thesis and these can be stratified based on feasibility and clinical application. Measures such as DTI, MTR and functional measures are difficult to obtain and analyse and so require the support of a dedicated research centre. However, good quality structural imaging at 3 Tesla is more widely available, even in clinical centres. The use of software such as Spinal Cord Toolbox (De Leener *et al.*, 2017) and tools such as DeepSeg (Gros *et al.*, 2019), on clinical images, to segment the cord and enable measurement of cross-sectional area using an automated deep learning algorithm have the potential to make these measurements standard practice in the near-future. A large multi-centre study that seeks to establish normal ranges for CSA in the cervical and thoracic cord, accounting for confounders such as age, sex and height, would assist in the advancement of such techniques.

The creation of an international collaborative effort, led by Dr Julien Cohen-Adad, which seeks to standardise imaging acquisition across scanners (Alley *et al.*, 2018) and provide

support to researchers working in the field of spinal cord imaging [https://spinalcordmri.org/] is an important step in spinal cord imaging become a more widely used research tool.

This is an exciting field and if the standardisation of spinal cord protocols and analysis methods across centres can be achieved, spinal cord imaging will prove to be an important tool for the study of disease and measuring outcomes for clinical trials.

10. Bibliography

Agosta F, Benedetti B, Rocca MA, Valsasina P, Rovaris M, Comi G, et al. Quantification of cervical cord pathology in primary progressive MS using diffusion tensor MRI. Neurology 2005; 64: 631 LP – 635.

Agosta F, Valsasina P, Caputo D, Stroman PW, Filippi M. Tactile-associated recruitment of the cervical cord is altered in patients with multiple sclerosis. NeuroImage (Orlando, Fla) 2008; 39: 1542–1548.

Akaishi T, Takahashi T, Misu T, Abe M, Tadashi I, Juichi F, et al. Progressive patterns of neurological disability in multiple sclerosis and neuromyelitis optica spectrum disorders. Sci Rep 2020; 10: 1–7.

Alcaide-Leon P, Cybulsky K, Sankar S, Casserly C, Leung G, Hohol M, et al. Quantitative spinal cord MRI in radiologically isolated syndrome. Neurol Neuroimmunol NeuroInflammation 2018; 5: 1–10.

Alley S, Gilbert G, Wheeler-Kingshott CAMG, Samson RS, Grussu F, Martin A, et al. Consensus acquisition protocol for quantitative {MRI} of the cervical spinal cord at 3T. Proc Jt Annu Meet ISMRM-ESMRMB, Paris, Fr 2018: 799.

Alonso A, Hernan M. Temporal trends in the incidence of multiple sclerosis. Neurology 2008; 71: 129–135.

Altmann D., Button T, Schmierer K, Hunter K, Tozer D., Wheeler-Kingshott C., et al. Sample

sizes for lesion magnetisation transfer ratio outcomes in remyelination trials for multiple sclerosis. Mult Scler Relat Disord 2014; 3: 237–243.

Andersson JLR, Sotiropoulos SN. An integrated approach to correction for off-resonance effects and subject movement in diffusion MR imaging. Neuroimage 2016; 125: 1063–1078.

Asgari N, Skejoe HPB, Lillevang ST, Steenstrup T, Stenager E, Kyvik KO. Modifications of longitudinally extensive transverse myelitis and brainstem lesions in the course of neuromyelitis optica (NMO): A population-based, descriptive study. BMC Neurol 2013; 13: 1.

Asnafi S, Morris PP, Sechi E, Pittock SJ, Weinshenker BG, Palace J, et al. The frequency of longitudinally extensive transverse myelitis in MS: A population-based study. Mult Scler Relat Disord 2020; 37: 101487.

Asseyer S, Cooper G, Paul F. Pain in NMOSD and MOGAD: A Systematic Literature Review of Pathophysiology, Symptoms, and Current Treatment Strategies. Front Neurol 2020; 11

Asseyer S, Hamblin J, Messina S, Mariano R, Siebert N, Everett R, et al. Prodromal headache in MOG-antibody positive optic neuritis. Mult Scler Relat Disord 2020; 40: 101965.

Azodi S, Nair G, Enose-Akahata Y, Charlip E, Vellucci A, Cortese I, et al. Imaging spinal cord atrophy in progressive myelopathies: HTLV-I-associated neurological disease (HAM/TSP) and multiple sclerosis. Ann Neurol 2017; 82: 719–728.

Bannerman PG, Hahn A, Ramirez S, Morley M, Bnnemann C, Yu S, et al. Motor neuron

pathology in experimental autoimmune encephalomyelitis: studies in THY1-YFP transgenic mice. Brain 2005; 128: 1877–1886.

Barkhof F. The clinico-radiological paradox in multiple sclerosis revisited. Curr Opin Neurol 2002; 15: 239–245.

Barnett M, Prineas J, Buckland M, Parratt J, Pollard J. Massive astrocyte destruction in neuromyelitis optica despite natalizumab therapy. Mult Scler 2011; 18: 108–112.

Barry RL, Conrad BN, Smith SA, Gore JC. A practical protocol for measurements of spinal cord functional connectivity. Sci Rep 2018; 8: 1–10.

Barry RL, Rogers BP, Conrad BN, Smith SA, Gore JC. Reproducibility of resting state spinal cord networks in healthy volunteers at 7 Tesla. Neuroimage 2016; 133: 31–40.

Barry RL, Smith SA, Dula AN, Gore JC. Resting state functional connectivity in the human spinal cord. Elife 2014; 2014: 1–15.

Baumann M, Sahin K, Lechner C, Hennes EM, Schanda K, Mader S, et al. Clinical and neuroradiological differences of paediatric acute disseminating encephalomyelitis with and without antibodies to the myelin oligodendrocyte glycoprotein. J Neurol Neurosurg Psychiatry 2015; 86: 265–272.

Beaulieu C. The basis of anisotropic water diffusion in the nervous system – a technical review. NMR Biomed 2002; 15: 435–455.

Benedetti B, Valsasina P, Judica E, Martinelli V, Ghezzi A, Capra R, et al. Grading cervical

cord damage in neuromyelitis optica and MS by diffusion tensor MRI. Neurology 2006; 67: 161.

Bergers E, Bot JCJ, Van Der Valk P, Castelijns JA, Lycklama A Nijeholt GJ, Kamphorst W, et al. Diffuse signal abnormalities in the spinal cord in multiple sclerosis: Direct postmortem in situ magnetic resonance imaging correlated with in vitro high-resolution magnetic resonance imaging and histopathology. Ann Neurol 2002; 51: 652–656.

Bijsterbosch J, Smith SM, Beckmann CF. Introduction to resting state fMRI functional connectivity. Oxford; 2017

Bisecco A, Nardo F Di, Docimo R, Caiazzo G, d'Ambrosio A, Bonavita S, et al. Fatigue in multiple sclerosis: The contribution of resting-state functional connectivity reorganization. Mult Scler J 2018; 24: 1696–1705.

Bot JCJ, Barkhof F, Polman CH, Lycklama À Nijeholt GJ, De Groot V, Bergers E, et al. Spinal cord abnormalities in recently diagnosed MS patients: Added value of spinal MRI examination. Neurology 2004; 62: 226–233.

Braley TJ, Chervin RD. Fatigue in multiple sclerosis: mechanisms, evaluation, and treatment. Sleep 2010; 33: 1061.

Brändle SM, Obermeier B, Senel M, Bruder J, Mentele R, Khademi M, et al. Distinct oligoclonal band antibodies in multiple sclerosis recognize ubiquitous self-proteins. Proc Natl Acad Sci U S A 2016; 113: 7864.

Brunner C, Lassmann H, Waehneldt T V., Matthieu J, Linington C. Differential

Ultrastructural Localization of Myelin Basic Protein, Myelin/Oligodendroglial Glycoprotein, and 2',3'-Cyclic Nucleotide 3'-Phosphodiesterase in the CNS of Adult Rats. J Neurochem 1989; 52: 296–304.

Cacciaguerra L, Valsasina P, Mesaros S, Martinelli V, Drulovic J, Filippi M, et al. Spinal Cord Atrophy in Neuromyelitis Optica Spectrum Disorders Is Spatially Related to Cord Lesions and Disability. Radiology 2020; 297: 154.

Calabrese M, Atzori M, Bernardi V, Morra A, Romualdi C, Rinaldi L, et al. Cortical atrophy is relevant in multiple sclerosis at clinical onset. J Neurol 2007; 254: 1212–1220.

Casserly C, Seyman EE, Alcaide-Leon P, Guenette M, Lyons C, Sankar S, et al. Spinal Cord Atrophy in Multiple Sclerosis: A Systematic Review and Meta-Analysis. J Neuroimaging 2018; 28: 556–586.

Cassinotto C, Deramond H, Olindo S, Aveillan M, Smadja D, Cabre P. MRI of the spinal cord in neuromyelitis optica and recurrent longitudinal extensive myelitis. J Neuroradiol 2009; 36: 199–205.

Cawley N, Tur C, Prados F, Plantone D, Kearney H, Abdel-Aziz K, et al. Spinal cord atrophy as a primary outcome measure in phase II trials of progressive multiple sclerosis. Mult Scler J 2018; 24: 932–941.

Charil A, Caputo D, Cavarretta R, Sormani MP, Ferrante P, Filippi M. Cervical cord magnetization transfer ratio and clinical changes over 18 months in patients with relapsing-remitting multiple sclerosis: a preliminary study. Mult Scler 2006; 12: 662–665.

Chen LM, Mishra A, Yang P-F, Wang F, Gore JC. Injury alters intrinsic functional connectivity within the primate spinal cord. Proc Natl Acad Sci 2015; 112: 5991–5996.

Chien C, Brandt AU, Schmidt F, Bellmann-Strobl J, Ruprecht K, Paul F, et al. MRI-based methods for spinal cord atrophy evaluation: A comparison of cervical cord cross-sectional area, cervical cord volume, and full spinal cord volume in patients with aquaporin-4 antibody seropositive neuromyelitis optica spectrum disorders. Am J Neuroradiol 2018; 39: 1362–1368.

Chien C, Scheel M, Schmitz-Hübsch T, Borisow N, Ruprecht K, Bellmann-Strobl J, et al. Spinal cord lesions and atrophy in NMOSD with AQP4-IgG and MOG-IgG associated autoimmunity. Mult Scler J 2018: 135245851881559.

Ciccarelli O, Cohen JA, Reingold SC, Weinshenker BG, Amato MP, Banwell B, et al. Spinal cord involvement in multiple sclerosis and neuromyelitis optica spectrum disorders. Lancet Neurol 2019; 18: 185–197.

Ciccarelli O, Thomas D, De Vita E, Wheeler-Kingshott C, Kachramanoglou C, Kapoor R, et al. Low Myo-inositol indicating astrocytic damage in a case series of neuromyelitis optica. Ann Neurol 2013; 74: 301–305.

Ciccarelli O, Wheeler-Kingshott CA, McLean MA, Cercignani M, Wimpey K, Miller DH, et al. Spinal cord spectroscopy and diffusion-based tractography to assess acute disability in multiple sclerosis. Brain 2007; 130: 2220–2231.

Ciron J, Cobo-Calvo A, Audoin B, Bourre B, Brassat D, Cohen M, et al. Frequency and

characteristics of short versus longitudinally extensive myelitis in adults with MOG antibodies: A retrospective multicentric study. Mult Scler 2020; 26: 936–944.

Cleeland CS, Ryan KM. Pain assessment: Global use of the Brief Pain Inventory. Ann Acad Med Singapore 1994; 23: 129–138.

Cobo-Calvo A, Ruiz A, Maillart E, Audoin B, Zephir H, Bourre B, et al. Clinical spectrum and prognostic value of CNS MOG autoimmunity in adults: The MOGADOR study. Neurology 2018; 90: e1858–e1869.

Cobo-calvo A, Sepúlveda M, Rollot F, Armangué T, Ruiz A, Maillart E, et al. Evaluation of treatment response in adults with relapsing MOG-Ab-associated disease. 2019; 1: 1–12.

Cohen-Adad J, El Mendili MM, Lehéricy S, Pradat PF, Blancho S, Rossignol S, et al. Demyelination and degeneration in the injured human spinal cord detected with diffusion and magnetization transfer MRI. Neuroimage 2011; 55: 1024–1033.

Cohen-Adad J, Wheeler-Kingshott CAM. Quantitative MRI of the spinal cord. San Diego, CA; 2014

Cohen JA, Reingold SC, Polman CH, Wolinsky JS. Disability outcome measures in multiple sclerosis clinical trials: current status and future prospects. Lancet Neurol 2012; 11: 467–476.

Collongues N, Marignier R, Zéphir H, Blanc F, Vukusic S, Outteryck O, et al. High-risk syndrome for neuromyelitis optica: a descriptive and comparative study. Mult Scler 2011; 17: 720–724.

Combes AJE, Matthews L, Lee JS, Li DKB, Carruthers R, Traboulsee AL, et al. Cervical cord myelin water imaging shows degenerative changes over one year in multiple sclerosis but not neuromyelitis optica spectrum disorder. NeuroImage Clin 2017; 16: 17–22.

Combès B, Kerbrat A, Ferré JC, Callot V, Maranzano J, Badji A, et al. Focal and diffuse cervical spinal cord damage in patients with early relapsing–remitting MS: A multicentre magnetisation transfer ratio study. Mult Scler 2019; 25: 1113–1123.

Compston A, Coles A. Multiple sclerosis. Lancet (British Ed 2008; 359: 1221–1231.

Confavreux C, Compston DA, Hommes OR, Mcdonald WI, Thompson AJ. EDMUS, a European database for multiple sclerosis. J Neurol Neurosurg Psychiatry 1992; 55: 671.

Conrad BN, Barry RL, Rogers BP, Maki S, Mishra A, Thukral S, et al. Multiple sclerosis lesions affect intrinsic functional connectivity of the spinal cord. Brain 2018; 141: 1650–1664.

Constantinescu CS, Farooqi N, O'Brien K, Gran B. Experimental autoimmune encephalomyelitis (EAE) as a model for multiple sclerosis (MS). Br J Pharmacol 2011; 164: 1079–1106.

Cree B, Bennett J, Kim HJ, Weinshenker B, Pittock S, Wingerchuk B, et al. and on behalf of the N-Momentum Study Investigators. Inebilizumab for the Treatment of Neuromyelitis Optica Spectrum Disorder (N-MOmentum): A Double-blind, Randomised Placebo-controlled Phase 2/3 Trial. The Lancet (British Edition) 2019; 1352-363.

Devic E. Myélite aiguë dorso-lombaire avec névrite optique. In: Autopsie. 1894. p. 434–439

Droby A, Yuen K, Muthuraman M, Reitz S-C, Fleischer V, Klein J, et al. Changes in brain functional connectivity patterns are driven by an individual lesion in MS: a resting-state fMRI study. Brain Imaging Behav 2016; 10: 1117–1126.

Dubey D, Pittock SJ, Krecke KN, Flanagan EP. Association of extension of cervical cord lesion and area postrema syndrome with neuromyelitis optica spectrum disorder. JAMA Neurol 2017; 74: 359–361.

Dubey D, Pittock SJ, Krecke KN, Morris PP, Sechi E, Zalewski NL, et al. Clinical, Radiologic, and Prognostic Features of Myelitis Associated with Myelin Oligodendrocyte Glycoprotein Autoantibody. JAMA Neurol 2019; 76: 301–309.

Eden D, Gros C, Badji A, Dupont SM, De Leener B, Maranzano J, et al. Spatial distribution of multiple sclerosis lesions in the cervical spinal cord. Brain 2019; 142: 633–646.

Eippert F, Kong Y, Jenkinson M, Tracey I, Brooks J. Denoising spinal cord fMRI data: Approaches to acquisition and analysis. Neuroimage 2017; 154: 255–266.

Eippert F, Kong Y, Winkler AM, Andersson JL, Finsterbusch J, Büchel C, et al. Investigating resting-state functional connectivity in the cervical spinal cord at 3T. NeuroImage (Orlando, Fla) 2017; 147: 589–601.

Evangelou N, DeLuca G, Owens T, Esiri M. Pathological study of spinal cord atrophy in multiple sclerosis suggests limited role of local lesions. BRAIN 2005; 128: 29–34.

Fadda G, Banwell B, Waters P, Marrie RA, Yeh EA, O'Mahony J, et al. and on behalf of the Canadian Pediatric Demyelinating Disease Network. Silent New Brain MRI Lesions in Children with MOG-Antibody Associated Disease. Ann Neurol 2021; 89(2):408-413.

Faul F, Erdfelder E, Lang A-G, Buchner A. G*Power 3: a flexible statistical power analysis program for the social, behavioral, and biomedical sciences. Behav Res Methods 2007; 39: 175.

Filippi M, Preziosa P, Banwell BL, Barkhof F, Ciccarelli O, De Stefano N, et al. Assessment of lesions on magnetic resonance imaging in multiple sclerosis: practical guidelines. Brain 2019; 142: 1858–1875.

Filippi M, Rocca MA, Moiola L, Martinelli V, Ghezzi A, Capra R, et al. MRI and magnetization transfer imaging changes in the brain and cervical cord of patients with Devic's neuromyelitis optica. Neurology 1999; 53: 1705–1705.

Fisk J, Pontefract A, Ritvo P, Archibald C, Murray T. The impact of fatigue on patients with multiple sclerosis. J Neurol Sci 1994; 21: 9–14.

Flanagan EP, Weinshenker BG, Krecke KN, Lennon VA, Lucchinetti CF, Mckeon A, et al. Short Myelitis Lesions in Aquaporin-4-IgG–Positive Neuromyelitis Optica Spectrum Disorders. JAMA Neurol 2015; 72: 81–87.

Flanagan EP, Weinshenker BG, Krecke KN, Pittock SJ. Asymptomatic myelitis in neuromyelitis optica and autoimmune aquaporin-4 channelopathy. Neurol Clin Pract 2015; 5: 175–177.

Fowler C, Griffiths D, De Groat W. The neural control of micturition. Nat Rev Neurosci 2008; 9: 453.

Frostell A, Hakim R, Thelin EP, Mattson P, Svensson M. 2016. A Review of the Segmental Diameter of the Healthy Human Spinal Cord. Front. Neurol. 7.

Fujihara K, Misu T, Nakashima I, Takahashi T, Bradl M, Lassmann H, et al. Neuromyelitis optica should be classified as an astrocytopathic disease rather than a demyelinating disease. Clin Exp Neuroimmunol 2012; 3: 58–73.

Fumincelli L, Mazzo A, Martins JCA, Henriques FMD, Orlandin L. Quality of life of patients using intermittent urinary catheterization. Rev Lat Am Enfermagem 2017; 25

van Gelderen P, de Zwart JA, Starewicz P, Hinks RS, Duyn JH. Real-time shimming to compensate for respiration-induced B0 fluctuations. Magn Reson Med 2007; 57: 362.

Geraldes R, Ciccarelli O, Barkhof F, De Stefano N, Enzinger C, Filippi M, et al. The current role of MRI in differentiating multiple sclerosis from its imaging mimics. Nat Rev Neurol 2018; 14: 199–213.

Geurts JJ, Barkhof F. Grey matter pathology in multiple sclerosis. Lancet Neurol 2008; 7: 841–851.

Gilmore CP, Deluca GC, Bö L, Owens T, Lowe J, Esiri MM, et al. Spinal cord neuronal pathology in multiple sclerosis. Brain Pathol 2009; 19: 642–649.

Gilmore CP, Geurts JJG, Evangelou N, Bot JCJ, van Schijndel RA, Pouwels PJW, et al. Spinal

cord grey matter lesions in multiple sclerosis detected by post-mortem high field MR imaging. Mult Scler 2009; 15: 180–188.

Gold R, Linington C, Lassmann H. Understanding pathogenesis and therapy of multiple sclerosis via animal models: 70 years of merits and culprits in experimental autoimmune encephalomyelitis research. Brain 2006; 129: 1953–1971.

Granella F, Tsantes E, Siena E, Borgonovo G, Curti E. Spinal cord lesions are frequently asymptomatic in relapsing remitting multiple sclerosis. A retrospective MRI survey. Eur J Neurol 2017; 24: 311–311.

Gros C, De Leener B, Badji A, Maranzano J, Eden D, Dupont SM, et al. Automatic segmentation of the spinal cord and intramedullary multiple sclerosis lesions with convolutional neural networks. Neuroimage 2019; 184: 901–915.

Hacohen Y, Hemingway C, Ciccarelli O, Mankad K, Barkhof F, Vincent A, et al. Diagnostic algorithm for relapsing acquired demyelinating syndromes in children. Neurology 2017; 89: 269–278.

Hamid SHM, Whittam D, Mutch K, Linaker S, Solomon T, Das K, et al. What proportion of AQP4-IgG-negative NMO spectrum disorder patients are MOG-IgG positive? A cross sectional study of 132 patients. J Neurol 2017; 264: 2088.

Hamid SHM, Whittam D, Saviour M, Alorainy A, Mutch K, Linaker S, et al. Seizures and encephalitis in myelin oligodendrocyte glycoprotein IgG disease vs aquaporin 4 IgG disease. JAMA Neurol 2018; 75: 65–71.

Hayashida S, Masaki K, Yonekawa T, Suzuki SO, Hiwatashi A, Matsushita T, et al. Early and extensive spinal white matter involvement in neuromyelitis optica. Brain Pathol 2017; 27: 249–265.

Healy BC, Arora A, Hayden DL, Ceccarelli A, Tauhid SS, Neema M, et al. Approaches to Normalization of Spinal Cord Volume: Application to Multiple Sclerosis. J Neuroimaging 2012; 22: e12–e19.

Heinze G, Dunkler D. Five myths about variable selection. Transpl Int 2017; 30: 6–10.

Hesseltine SM, Law M, Babb J, Rad M, Lopez S, Ge Y, et al. Diffusion Tensor Imaging in Multiple Sclerosis: Assessment of Regional Differences in the Axial Plane within Normal-Appearing Cervical Spinal Cord. Am J Neuroradiol 2006; 27: 1189 LP – 1193.

Hochman S. Spinal cord. Curr Biol 2007; 17: R950–R955.

Höftberger R, Guo Y, Flanagan EP, Lopez-Chiriboga AS, Endmayr V, Hochmeister S, et al. The pathology of central nervous system inflammatory demyelinating disease accompanying myelin oligodendrocyte glycoprotein autoantibody. Acta Neuropathol 2020; 139: 875–892.

Höftberger R, Sepulveda M, Armangue T, Blanco Y, Rostásy K, Cobo Calvo A, et al. Antibodies to MOG and AQP4 in adults with neuromyelitis optica and suspected limited forms of the disease. Mult Scler 2015; 21: 866–874.

Honey CJ, Sporns O, Cammoun L, Gigandet X, Thiran JP, Meuli R, et al. Predicting human resting-state functional connectivity from structural connectivity. Proc Natl Acad Sci U S A

2009; 106: 2035–2040.

Hor JY, Asgari N, Nakashima I, Broadley SA, Leite MI, Kissani N, et al. Epidemiology of Neuromyelitis Optica Spectrum Disorder and Its Prevalence and Incidence Worldwide. Front Neurol 2020; 11: 501.

Horsfield MA, Sala S, Neema M, Absinta M, Bakshi A, Sormani MP, et al. Rapid semi-automatic segmentation of the spinal cord from magnetic resonance images: Application in multiple sclerosis. NeuroImage (Orlando, Fla) 2010; 50: 446–455.

Hyun J-W, Kim S-H, Jeong IH, Lee SH, Kim HJ. Bright spotty lesions on the spinal cord: an additional MRI indicator of neuromyelitis optica spectrum disorder? J Neurol Neurosurg Psychiatry 2015; 86: 1280.

Inglese M, Bester M. Diffusion imaging in multiple sclerosis: research and clinical implications. NMR Biomed 2010; 23: 865–872.

Jaeger S, Paul F, Scheel M, Brandt A, Heine J, Pach D, et al. Multiple sclerosis–related fatigue: Altered resting-state functional connectivity of the ventral striatum and dorsolateral prefrontal cortex. Mult Scler J 2019; 25: 554–564.

Jarius S, Jacobi C, De Seze J, Zephir H, Paul F, Franciotta D, et al. Frequency and syndrome specificity of antibodies to aquaporin-4 in neurological patients with rheumatic disorders. Mult Scler J 2011; 17: 1067–1073.

Jarius S, Kleiter I, Ruprecht K, Asgari N, Pitarokoili K, Borisow N, et al. MOG-IgG in NMO and related disorders: a multicenter study of 50 patients. Part 3: Brainstem involvement -

frequency, presentation and outcome. J Neuroinflammation 2016; 13: 281.

Jarius S, Paul F, Aktas O, Asgari N, Dale RC, de Seze J, et al. MOG encephalomyelitis: international recommendations on diagnosis and antibody testing. Nervenarzt 2018: 1–10.

Jarius S, Ruprecht K, Kleiter I, Borisow N, Asgari N, Pitarokoili K, et al. MOG-IgG in NMO and related disorders: a multicenter study of 50 patients. Part 2: Epidemiology, clinical presentation, radiological and laboratory features, treatment responses, and long-term outcome. J Neuroinflammation 2016; 13: 280.

Jarius S, Wildemann B. AQP4 antibodies in neuromyelitis optica: Diagnostic and pathogenetic relevance. Nat Rev Neurol 2010; 6: 383–392.

Jarius S, Wildemann B. The history of neuromyelitis optica. J Neuroinflammation 2013; 10: 8.

Jarius S, Wildemann B, Paul F. Neuromyelitis optica: Clinical features, immunopathogenesis and treatment. Clin Exp Immunol 2014; 176: 149–164.

Jarius S, Lechner C, Wendel E, Baumann M, Breu M, Schimmel M, et al. Cerebrospinal fluid findings in patients with myelin oligodendrocyte glycoprotein (MOG) antibodies. Part 2: Results from 108 lumbar punctures in 80 pediatric patients. J Neuroinflammation 2020; 17: 1–28.

Jenkinson M, Beckmann CF, Behrens TE., Woolrich MW, Smith SM. FSL. Neuroimage 2012; 62: 782–790.

Johns TG, Bernard CCA. The Structure and Function of Myelin Oligodendrocyte Glycoprotein. J Neurochem 1999; 72: 1–9.

Jurynczyk M, Geraldes R, Probert F, Woodhall MR, Waters P, Tackley G, et al. Distinct brain imaging characteristics of autoantibody-mediated CNS conditions and multiple sclerosis. Brain 2017; 140: 617–627.

Juryńczyk M, Jacob A, Fujihara K, Palace J. Myelin oligodendrocyte glycoprotein (MOG) antibody-associated disease: Practical considerations. Pract Neurol 2019; 19: 187–195.

Jurynczyk M, Messina S, Woodhall MR, Raza N, Everett R, Roca-Fernandez A, et al. Clinical presentation and prognosis in MOG-antibody disease: A UK study. Brain 2017; 140: 3128–3138.

Juryńczyk M, Tackley G, Kong Y, Geraldes R, Matthews L, Woodhall M, et al. Brain lesion distribution criteria distinguish MS from AQP4-antibody NMOSD and MOG-antibody disease. J Neurol Neurosurg Psychiatry 2017; 88: 132–136.

Kanamori Y, Nakashima I, Takai Y, Nishiyama S, Kuroda H, Takahashi T, et al. Pain in neuromyelitis optica and its effect on quality of life: a cross-sectional study. Neurology 2011; 77: 652.

Kang SH, Li Y, Fukaya M, Lorenzini I, Cleveland DW, Ostrow LW, et al. Degeneration and impaired regeneration of gray matter oligodendrocytes in amyotrophic lateral sclerosis. Nat Neurosci 2013; 16: 571.

Karni A, Bakimer-Kleiner R, Abramsky O, Ben-Nun A. Elevated Levels of Antibody to Myelin

Oligodendrocyte Glycoprotein Is Not Specific for Patients With Multiple Sclerosis. Arch Neurol 1999; 56: 311–315.

Kearney H, Miller DH, Ciccarelli O. Spinal cord MRI in multiple sclerosis—diagnostic, prognostic and clinical value. Nat Rev Neurol 2015; 11: 327–338.

Kearney H, Yiannakas MC, Abdel-Aziz K, Wheeler-Kingshott CAM, Altmann DR, Ciccarelli O, et al. Improved MRI quantification of spinal cord atrophy in multiple sclerosis. J Magn Reson Imaging 2014; 39: 617–623.

Kessler RA, Mealy MA, Levy M. Early indicators of relapses vs pseudorelapses in neuromyelitis optica spectrum disorder. Neurol Neuroimmunol neuroinflammation 2016; 3: e269.

Kim HJ, Paul F, Lana-Peixoto MA, Tenembaum S, Asgari N, Palace J, et al. MRI characteristics of neuromyelitis optica spectrum disorder: An international update. Neurology 2015; 84: 1165–1173.

Kimbrough DJ, Fujihara K, Jacob A, Lana-Peixoto MA, Isabel Leite M, Levy M, et al. Treatment of neuromyelitis optica: Review and recommendations. Mult Scler Relat Disord 2012; 1: 180–187.

Kinany N, Pirondini E, Micera S, Van De Ville D. Dynamic Functional Connectivity of Resting-State Spinal Cord fMRI Reveals Fine-Grained Intrinsic Architecture. Neuron (Cambridge, Mass) 2020; 108: 424-435.e4.

Kitley J, Leite MI, Küker W, Quaghebeur G, George J, Waters P, et al. Longitudinally

extensive transverse myelitis with and without aquaporin 4 antibodies. JAMA Neurol 2013; 70: 1375–1381.

Kitley J, Leite MI, Nakashima I, Waters P, McNeillis B, Brown R, et al. Prognostic factors and disease course in aquaporin-4 antibody-positive patients with neuromyelitis optica spectrum disorder from the United Kingdom and Japan. Brain 2012; 135: 1834–1849.

Kitley J, Waters P, Woodhall M, Leite M, Murchison A, George J, et al. Neuromyelitis optica spectrum disorders with aquaporin-4 and myelin-oligodendrocyte glycoprotein antibodies: a comparative study. JAMA Neurol 2014; 71: 276–283.

Kitley J, Woodhall M, Waters P, Leite MI, Devenney E, Craig J, et al. Myelin-oligodendrocyte glycoprotein antibodies in adults with a neuromyelitis optica phenotype. Neurology 2012; 79: 1273–1277.

Klawiter EC, Schmidt RE, Trinkaus K, Liang HF, Budde MD, Naismith RT, et al. Radial diffusivity predicts demyelination in ex vivo multiple sclerosis spinal cords. Neuroimage 2011; 55: 1454–1460.

Klawiter EC, Xu J, Naismith RT, Benzinger TL, Shimony JS, Lancia S, et al. Increased radial diffusivity in spinal cord lesions in neuromyelitis optica compared with multiple sclerosis. Mult Scler J 2012; 18: 1259–1268.

Kleiter I, Gahlen A, Borisow N, Fischer K, Wernecke KD, Wegner B, et al. Neuromyelitis optica: Evaluation of 871 attacks and 1,153 treatment courses. Ann Neurol 2016; 79: 206–216.

Ko H-Y, Park JH, Shin, YB, Baek SY, 2004. Gross quantitative measurements of spinal cord segments in human. Spinal Cord 42, 35-40.

Kong Y, Eippert F, Beckmann CF, Andersson J, Finsterbusch J, Büchel C, et al. Intrinsically organized resting state networks in the human spinal cord. Proc Natl Acad Sci 2014; 111: 18067–18072.

Kong Y, Okoruwa H, Revis J, Tackley G, Leite MI, Lee M, et al. Pain in patients with transverse myelitis and its relationship to aquaporin 4 antibody status. J Neurol Sci 2016; 368: 84–88.

Kos D, Kerckhofs E, Carrea I, Verza R, Ramos M, Jansa J. Evaluation of the Modified Fatigue Impact Scale in four different European countries. Mult Scler 2005; 11: 76–80.

Kuhlmann T, Lassmann H, Bruck W. Diagnosis of inflammatory demyelination in biopsy specimens: a practical approach. Acta Neuropathol 2008; 115: 275.

Kurtzke JF. Rating neurologic impairment in multiple sclerosis: An expanded disability status scale (EDSS). Neurology 1983; 33: 1444–1452.

Larson RD. Psychometric properties of the modified fatigue impact scale. Int J MS Care 2013; 15: 15.

De Leener B, Lévy S, Dupont SM, Fonov VS, Stikov N, Louis Collins D, et al. SCT: Spinal Cord Toolbox, an open-source software for processing spinal cord MRI data. Neuroimage 2017; 145: 24–43.

Lemus H, Warrington A, Rodriguez M. Multiple Sclerosis: Mechanisms of Disease and Strategies for Myelin and Axonal Repair. Neurol Clin 2018; 36: 1–11.

Lennon VA, Kryzer TJ, Pittock SJ, Verkman AS, Hinson SR. IgG marker of optic-spinal multiple sclerosis binds to the aquaporin-4 water channel. J Exp Med 2005; 202: 473.

Lennon VA, Wingerchuk DM, Kryzer TJ, Pittock SJ, Lucchinetti CF, Fujihara K, et al. A serum autoantibody marker of neuromyelitis optica: distinction from multiple sclerosis. Lancet (British Ed 2004; 364: 2106–2112.

Leocani L, Rovaris M, Boneschi FM, Medaglini S, Rossi P, Martinelli V, et al. Multimodal evoked potentials to assess the evolution of multiple sclerosis: a longitudinal study. J Neurol Neurosurg Psychiatry 2006; 77: 1030.

Lévy S, Benhamou M, Naaman C, Rainville P, Callot V, Cohen-Adad J. White matter atlas of the human spinal cord with estimation of partial volume effect. Neuroimage 2015; 119: 262–271.

Li V, Malladi P, Simeoni S, Pakzad M, Everett R, Satukijchai C, et al. A clinico-neurophysiological study of urogenital dysfunction in MOG-antibody transverse myelitis. Neurology 2020; 95: e2924.

Lindert R-B, Haase CG, Brehm U, Linington C, Wekerle H, Hohlfeld R. Multiple sclerosis: B- and T-cell responses to the extracellular domain of the myelin oligodendrocyte glycoprotein. Brain 1999; 122: 2089–2100.

Liu X, Zhou F, Li X, Qian W, Cui J, Zhou IY, et al. Organization of the intrinsic functional

network in the cervical spinal cord: A resting state functional MRI study. Neuroscience 2016; 336: 30–38.

Liu Y, Wang J, Daams M, Weiler F, Hahn HK, Duan Y, et al. Differential patterns of spinal cord and brain atrophy in NMO and MS. Neurology 2015; 84: 1465 LP – 1472.

Lucchinetti C, Bruck W, Parisi J, Scheithauer B, Rodriguez M, Lassmann H. Heterogeneity of multiple sclerosis lesions: Implications for the pathogenesis of demyelination. Ann Neurol 2000; 47: 707–717.

Lucchinetti CF, Guo Y, Popescu BFG, Fujihara K, Itoyama Y, Misu T. The pathology of an autoimmune astrocytopathy: Lessons learned from neuromyelitis optica. Brain Pathol 2014; 24: 83–97.

Mader S, Gredler V, Schanda K, Rostasy K, Dujmovic I, Pfaller K, et al. Complement activating antibodies to myelin oligodendrocyte glycoprotein in neuromyelitis optica and related disorders. J Neuroinflammation 2011; 8: 184.

Mariano R, Flanagan EP, Weinshenker BG, Palace J. A practical approach to the diagnosis of spinal cord lesions. Pract Neurol 2018; 18: 187–200.

Mariano R, Messina S, Kumar K, Kuker W, Leite MI, Palace J. Comparison of Clinical Outcomes of Transverse Myelitis Among Adults With Myelin Oligodendrocyte Glycoprotein Antibody vs Aquaporin-4 Antibody Disease. JAMA Netw open 2019; 2: e1912732.

Mariano R, Messina S, Roca-Fernandez A, Leite MI, Kong Y, Palace JA. Quantitative spinal cord MRI in MOG-antibody disease, neuromyelitis optica and multiple sclerosis. Brain

2020: 1–15.

Martin AR, Aleksanderek I, Cohen-Adad J, Tarmohamed Z, Tetreault L, Smith N, et al. Translating state-of-the-art spinal cord MRI techniques to clinical use: A systematic review of clinical studies utilizing DTI, MT, MWF, MRS, and fMRI. NeuroImage Clin 2015; 10: 192–238.

Martucci KT, Weber KA, Mackey SC. Altered Cervical Spinal Cord Resting-State Activity in Fibromyalgia. Arthritis Rheumatol 2019; 71: 441–450.

Masuda H, Mori M, Uzawa A, Uchida T, Ohtani R, Kuwabara S. Difference in fatigue and pain between neuromyelitis optica spectrum disorder and multiple sclerosis. PLoS One 2020; 15: e0224419.

Matthews L, Kolind S, Brazier A, Leite MI, Brooks J, Traboulsee A, et al. Imaging surrogates of disease activity in neuromyelitis optica allow distinction from multiple sclerosis. PLoS One 2015; 10: 1–19.

Matthews L, Marasco R, Jenkinson M, Küker W, Luppe S, Leite MI, et al. Distinction of seropositive NMO spectrum disorder and MS brain lesion distribution. Neurology 2013; 80: 1330.

McCarthy P. FSLeyes [Internet]. 2019[cited 2019 Oct 23] Available from: https://doi.org/10.5281/zenodo.3403671#.XbAuog_Uj0t

McCreary CR, Bjarnason TA, Skihar V, Mitchell JR, Yong VW, Dunn JF. Multiexponential T2 and magnetization transfer MRI of demyelination and remyelination in murine spinal cord.

Neuroimage 2009; 45: 1173–1182.

Messina S, Mariano R, Roca-Fernandez A, Cavey A, Jurynczyk M, Leite MI, et al. Contrasting the brain imaging features of MOG-Antibody disease, with AQP4-Antibody NMOSD and Multiple Sclerosis. medRxiv 2020: 2020.09.22.20198978.

Min J, Kim B, Lee K. Development of extensive brain lesions following fingolimod (FTY720) treatment in a patient with neuromyelitis optica spectrum disorder. Mult Scler J 2011; 18: 113–115.

Misu T, Fujihara K, Kakita A, Konno H, Nakamura M, Watanabe S, et al. Loss of aquaporin 4 in lesions of neuromyelitis optica: distinction from multiple sclerosis. Brain 2007; 130: 1224–1234.

Misu T, Höftberger R, Fujihara K, Wimmer I, Takai Y, Nishiyama S, et al. Presence of six different lesion types suggests diverse mechanisms of tissue injury in neuromyelitis optica. Acta Neuropathol 2013; 125: 815–827.

Moccia M, Ruggieri S, Ianniello A, Toosy A, Pozzilli C, Ciccarelli O. Advances in spinal cord imaging in multiple sclerosis. Ther Adv Neurol Disord 2019; 12: 1–19.

de Mol C, Wong Y, van Pelt E, Wokke B, Siepman T, Neuteboom R, et al. The clinical spectrum and incidence of anti-MOG-associated acquired demyelinating syndromes in children and adults. Mult Scler 2020; 26: 806–814.

Moll NM, Rietsch AM, Thomas S, Ransohoff AJ, Lee JC, Fox R, et al. Multiple sclerosis normal-appearing white matter: Pathology-imaging correlations. Ann Neurol 2011; 70:

764–773.

Van de Moortele P-F, Pfeuffer J, Glover GH, Ugurbil K, Hu X. Respiration-induced B0 fluctuations and their spatial distribution in the human brain at 7 Tesla. Magn Reson Med 2002; 47: 888.

Mori S. Introduction to diffusion tensor imaging. Amsterdam ; London: Elsevier; 2007

Mottershead J, Schmierer K, Clemence M, Thornton J, Scaravilli F, Barker G, et al. High field MRI correlates of myelin content and axonal density in multiple sclerosis. J Neurol 2003; 250: 1293–1301.

Muccilli A, Seyman E, Oh J. Spinal Cord MRI in Multiple Sclerosis. Neurol Clin 2018; 36: 35–57.

Murray TJ. Multiple sclerosis [electronic resource] : the history of a disease. New York: Demos Medical Pub.; 2005

Naismith RT, Xu J, Klawiter EC, Lancia S, Tutlam NT, Wagner JM, et al. Spinal cord tract diffusion tensor imaging reveals disability substrate in demyelinating disease. Neurology 2013; 80: 2201.

Nakamura Y, Liu Z, Fukumoto S, Shinoda K, Sakoda A, Matsushita T, et al. Spinal cord involvement by atrophy and associations with disability are different between multiple sclerosis and neuromyelitis optica spectrum disorder. Eur J Neurol 2020; 27: 92–99.

O'Connell K, Hamilton-Shield A, Woodhall M, Messina S, Mariano R, Waters P, et al.

Prevalence and incidence of neuromyelitis optica spectrum disorder, aquaporin-4 antibody-positive NMOSD and MOG antibody-positive disease in Oxfordshire, UK. J Neurol Neurosurg Psychiatry 2020; 91: 1126–1128.

O'Connor KC, Mclaughlin KA, De Jager PL, Chitnis T, Bettelli E, Xu C, et al. Self-antigen tetramers discriminate between myelin autoantibodies to native or denatured protein. Nat Med 2007; 13: 211.

Ogawa S, Lee TM, Kay AR, Tank DW. Brain magnetic resonance imaging with contrast dependent on blood oxygenation. Proc Natl Acad Sci U S A 1990; 87: 9868.

Ogawa R, Nakashima I, Takahashi T, Kaneko K, Akaishi T, Takai Y, et al. MOG antibody-positive, benign, unilateral, cerebral cortical encephalitis with epilepsy. Neurol Neuroimmunol NeuroInflammation 2017; 4: 1–10.

Oh J, Saidha S, Chen M, Smith SA, Prince J, Jones C, et al. Spinal cord quantitative MRI discriminates between disability levels in multiple sclerosis. Neurology 2013; 80: 540–547.

Oh J, Zackowski K, Chen M, Newsome S, Saidha S, Smith SA, et al. Multiparametric MRI correlates of sensorimotor function in the spinal cord in multiple sclerosis. Mult Scler 2013; 19: 427–435.

Ohnari K, Okada K, Takahashi T, Mafune K, Adachi H. Evoked potentials are useful for diagnosis of neuromyelitis optica spectrum disorder. J Neurol Sci 2016; 364: 97–101.

Oklinski MK, Skowronski MT, Skowronska A, Rützler M, Nørgaard K, Nieland JD, et al. Aquaporins in the spinal cord. Int J Mol Sci 2016; 17: 1–18.

Okuda DT, Melmed K, Matsuwaki T, Blomqvist A, Craig ADB. Central neuropathic pain in MS is due to distinct thoracic spinal cord lesions. Ann Clin Transl Neurol 2014; 1: 554–561.

Palace J. Making the diagnosis of multiple sclerosis. J Neurol Neurosurg Psychiatry 2001; 71: II3–II8.

Palace J, Leite MI, Nairne A, Vincent A. Interferon Beta Treatment in Neuromyelitis Optica: Increase in Relapses and Aquaporin 4 Antibody Titers. Arch Neurol 2010; 67: 1016–1017.

Palace J, Lin DY, Zeng D, Majed M, Elsone L, Hamid S, et al. Outcome prediction models in AQP4-IgG positive neuromyelitis optica spectrum disorders. Brain 2019; 142: 1310–1323.

Palace J, Wingerchuk B, Fujihara K, Berthele A, Oreja-Guevara C, Kim HJ, et al. and On Behalf of the Prevent Study Group. Benefits of Eculizumab in AQP4 Neuromyelitis Optica Spectrum Disorder: Subgroup Analyses of the Randomized Controlled Phase 3 PREVENT Trial. Multiple Sclerosis and Related Disorders 2021; 102641.

Pandit L, Asgari N, Apiwattanakul M, Palace J, Paul F, Leite M, et al. Demographic and clinical features of neuromyelitis optica: A review. Mult Scler J 2015; 21: 845–853.

Panicker JN, Fowler CJ, Kessler TM. Lower urinary tract dysfunction in the neurological patient: clinical assessment and management. Lancet Neurol 2015; 14: 720–732.

Papinutto N, Schlaeger R, Panara V, Zhu AH, Caverzasi E, Stern WA, et al. Age, Gender and Normalization Covariates for Spinal Cord Gray Matter and Total Cross-Sectional Areas at Cervical and Thoracic Levels: A 2D Phase Sensitive Inversion Recovery Imaging Study. PLoS One 2015; 10: e0118576.

Papp V, Illes Z, Magyari M, Koch-Henriksen N, Kant M, Pfleger CC, et al. Nationwide prevalence and incidence study of neuromyelitis optica spectrum disorder in Denmark. Neurology 2018; 91: e2265.

Dos Passos GR, Elsone L, Luppe S, Kitley J, Messina S, Rodríguez Cruz PM, et al. Seasonal distribution of attacks in aquaporin-4 antibody disease and myelin-oligodendrocyte antibody disease. J Neurol Sci 2020; 415: 116881.

Dos Passos GR, Oliveira LM, da Costa BK, Apostolos-Pereira SL, Callegaro D, Fujihara K, et al. MOG-IgG-associated optic neuritis, encephalitis, and myelitis: Lessons learned from neuromyelitis optica spectrum disorder. Front Neurol 2018; 9: 1–10.

Patzold U, Pocklington PR. Course of multiple sclerosis. First results of a prospective study carried out of 102 MS patients from 1976-1980. Acta Neurol Scand 1982; 65: 248.

Pérez CA, Garcia-Tarodo S, Troxell R. MRI-Negative Myelitis Associated With Myelin Oligodendrocyte Glycoprotein Antibody Spectrum Demyelinating Disease. Child Neurol open 2019; 6: 2329048X19830475.

Perone C, Calabrese E, Cohen-Adad J. Spinal cord gray matter segmentation using deep dilated convolutions. Sci Rep 2018; 8: 1–13.

Pessôa FMC, Lopes FCR, Costa JVA, Leon SVA, Domingues RC, Gasparetto EL. The cervical spinal cord in neuromyelitis optica patients: A comparative study with multiple sclerosis using diffusion tensor imaging. Eur J Radiol 2012; 81: 2697–2701.

Popescu BFG, Guo Y, Jentoft ME, Parisi JE, Lennon VA, Pittock SJ, et al. Diagnostic utility of

aquaporin-4 in the analysis of active demyelinating lesions. Neurology 2015; 84: 148–158.

Powers JM, Ioachim G, Stroman PW. Ten key insights into the use of spinal cord fmri. Brain Sci 2018; 8

Prados F, Barkhof F. Spinal cord atrophy rates: Ready for prime time in multiple sclerosis clinical trials? Neurology 2018; 91: 157–158.

Prados F, Cardoso MJ, Yiannakas MC, Hoy LR, Tebaldi E, Kearney H, et al. Fully automated grey and white matter spinal cord segmentation. Sci Rep 2016; 6: 1–10.

Pu S, Long Y, Yang N, He Y, Shan F, Fan Y, et al. Syndrome of inappropriate antidiuretic hormone secretion in patients with aquaporin-4 antibody. J Neurol 2015; 262: 101–107.

Qian W, Chan Q, Mak H, Zhang Z, Anthony MP, Yau KKW, et al. Quantitative assessment of the cervical spinal cord damage in neuromyelitis optica using diffusion tensor imaging at 3 Tesla. J Magn Reson Imaging 2011; 33: 1312–1320.

Ramagopalan S, Sadovnick A. Epidemiology of multiple sclerosis. Neurol Clin 2011; 29: 207–217.

Ramanathan S, Dale RC, Brilot F. Anti-MOG antibody: The history, clinical phenotype, and pathogenicity of a serum biomarker for demyelination. Autoimmun Rev 2016; 15: 307–324.

Ramanathan S, Mohammad S, Tantsis E, Nguyen TK, Merheb V, Fung VSC, et al. Clinical course, therapeutic responses and outcomes in relapsing MOG antibody-associated

demyelination. J Neurol Neurosurg Psychiatry 2018; 89: 127–137.

Reich DS, White R, Cortese IC, Vuolo L, Shea CD, Collins TL, et al. Sample-size calculations for short-term proof-of-concept studies of tissue protection and repair in multiple sclerosis lesions via conventional clinical imaging. Mult Scler J 2015; 21: 1693–1704.

Reindl M, Linington C, Brehm U, Egg R, Dilitz E, Deisenhammer F, et al. Antibodies against the myelin oligodendrocyte glycoprotein and the myelin basic protein in multiple sclerosis and other neurological diseases: a comparative study. Brain 1999; 122: 2047–2056.

Reindl M, Di Pauli F, Rostásy K, Berger T. The spectrum of MOG autoantibody-associated demyelinating diseases. Nat Rev Neurol 2013; 9: 455–461.

Rivero RLM, Oliveira EML, Bichuetti DB, Gabbai AA, Nogueira RG, Abdala N. Diffusion tensor imaging of the cervical spinal cord of patients with Neuromyelitis Optica. Magn Reson Imaging 2014; 32: 457–463.

Rocca M, Absinta M, Valsasina P, Copetti M, Caputo D, Comi G, et al. Abnormal cervical cord function contributes to fatigue in multiple sclerosis. Mult Scler 2012; 18: 1552–1559.

Rocca MA, Horsfield MA, Sala S, Copetti M, Valsasina P, Mesaros S, et al. A multicenter assessment of cervical cord atrophy among MS clinical phenotypes. Neurology 2011; 76: 2096.

Rocca MA, Valsasina P, Meani A, Gobbi C, Zecca C, Rovira À, et al. Clinically relevant cranio-caudal patterns of cervical cord atrophy evolution in MS. Neurology 2019; 93: e1852–e1866.

Rodríguez Cruz PM, Matthews L, Boggild M, Cavey A, Constantinescu CS, Evangelou N, et al. Time- and region-specific season of birth effects in multiple sclerosis in the United Kingdom. JAMA Neurol 2016

Rovaris M, Gallo A, Riva R, Ghezzi A, Bozzali M, Benedetti B, et al. An MT MRI study of the cervical cord in clinically isolated syndromes suggestive of MS. Neurology 2004; 63: 584.

Rovira A, De Stefano N. MRI monitoring of spinal cord changes in patients with multiple sclerosis. Curr Opin Neurol 2016; 29: 445–452.

Salama S, Khan M, Pardo S, Izbudak I, Levy M. MOG antibody–associated encephalomyelitis/encephalitis. Mult Scler J 2019; 25: 1427–1433.

San Emeterio Nateras O, Yu F, Muir ER, Bazan C, Franklin CG, Li W, et al. Intrinsic Resting-State Functional Connectivity in the Human Spinal Cord at 3.0 T. Radiology 2016; 279: 262.

Sato DK, Callegaro D, Lana-Peixoto MA, Waters PJ, Jorge FM de H, Takahashi T, et al. Distinction between MOG antibody-positive and AQP4 antibody-positive NMO spectrum disorders. Neurology 2014; 82: 474 LP – 481.

Schlaeger R, Papinutto N, Panara V, Bevan C, Lobach I V., Bucci M, et al. Spinal cord gray matter atrophy correlates with multiple sclerosis disability. Ann Neurol 2014; 76: 568–580.

Schlaeger R, Papinutto N, Zhu AH, Lobach I V., Bevan CJ, Bucci M, et al. Association between thoracic spinal cord gray matter atrophy and disability in multiple sclerosis. JAMA Neurol 2015; 72: 897–904.

Schlaeger R, Schindler C, Grize L, Dellas S, Radue EW, Kappos L, et al. Combined visual and motor evoked potentials predict multiple sclerosis disability after 20 years. Mult Scler 2014; 20: 1348–1354.

Schmierer K, McDowell A, Petrova N, Carassiti D, Thomas DL, Miquel ME. Quantifying multiple sclerosis pathology in post mortem spinal cord using MRI. Neuroimage 2018; 182: 251–258.

Schneider R, Bellenberg B, Kleiter I, Gold R, Köster O, Weiler F, et al. Cervical cord and ventricle affection in neuromyelitis optica. Acta Neurol Scand 2015; 135: 324–331.

Sechi E, Krecke KN, Pittock SJ, Dubey D, Lopez-Chiriboga AS, Kunchok A, et al. Frequency and characteristics of MRI-negative myelitis associated with MOG autoantibodies. Mult Scler 2020; 27: 303.

Seifert T, Bauer J, Weissert R, Fazekas F, Storch M. Notch1 and its ligand Jagged1 are present in remyelination in a T-cell- and antibody-mediated model of inflammatory demyelination. Acta Neuropathol 2007; 113: 195–203.

Sen PN, Basser PJ. A Model for Diffusion in White Matter in the Brain. Biophys J 2005; 89: 2927–2938.

Senanayake B, Jitprapaikulsan J, Aravinthan M, Wijesekera JC, Ranawaka UK, Riffsy MT, et al. Seroprevalence and clinical phenotype of MOG-IgG-associated disorders in Sri Lanka. J Neurol Neurosurg Psychiatry 2018; 90: 1381.

Sepúlveda M, Aldea M, Escudero D, Llufriu S, Arrambide G, Otero-Romero S, et al.

Epidemiology of NMOSD in Catalonia: Influence of the new 2015 criteria in incidence and prevalence estimates. Mult Scler 2018; 24: 1843–1851.

Siva A. Asymptomatic MS. Clin Neurol Neurosurg 2013; 115: S1–S5.

Slavin A., Johns T., Orian J., Bernard CC. Regulation of Myelin Oligodendrocyte Glycoprotein in Different Species throughout Development. Dev Neurosci 1997; 19: 69–78.

Smith SA, Jones CK, Gifford A, Belegu V, Chodkowski B, Farrell JAD, et al. Reproducibility of tract-specific magnetization transfer and diffusion tensor imaging in the cervical spinal cord at 3 tesla. NMR Biomed 2010; 23: 207–217.

Smith SM, Jenkinson M, Woolrich MW, Beckmann CF, Behrens TE., Johansen-Berg H, et al. Advances in functional and structural MR image analysis and implementation as FSL. Neuroimage 2004; 23: S208–S219.

Song X, Li D, Qiu Z, Su S, Wu Y, Wang J, et al. Correlation between EDSS scores and cervical spinal cord atrophy at 3T MRI in multiple sclerosis: A systematic review and meta-analysis. Mult Scler Relat Disord 2020; 37: 101426.

Stroman PW, Bacon M, Schwab JM, Bosma R, Cadotte D, Carlstedt T, et al. The current state-of-the-art of spinal cord imaging: Methods. Neuroimage 2015; 84: 1070–1081.

Stroman PW, Wheeler-Kingshott C, Bacon M, Schwab JM, Bosma R, Brooks J, et al. The current state-of-the-art of spinal cord imaging: Methods. Neuroimage 2014; 84: 1070–1081.

Suchdev K, Razmjou S, Venkatachalam P, Khan OA, Mohamed W, Ibrahim MS. Late onset neuromyelitis optica mimicking an acute stroke in an elderly patient. J Neuroimmunol 2017; 309: 1–3.

Tackley G, Kuker W, Palace J. Magnetic resonance imaging in neuromyelitis optica. Mult Scler 2014: 1153–1164.

Tackley G, O'Brien F, Rocha J, Woodhall M, Waters P, Chandratre S, et al. Neuromyelitis optica relapses: Race and rate, immunosuppression and impairment. Mult Scler Relat Disord 2016; 7: 21–25.

Tackley G, Vecchio D, Hamid S, Jurynczyk M, Kong Y, Gore R, et al. Chronic neuropathic pain severity is determined by lesion level in aquaporin 4-antibody-positive myelitis. J Neurol Neurosurg Psychiatry 2016

Tahara M, Oeda T, Okada K, Kiriyama T, Ochi K, Maruyama H, Fukaura H, Nomura K, Shimizu Y, Mori M, Nakashima I, Misu T, Umemura A, Yamamoto K, Sawada, H. Safety and efficacy of rituximab in neuromyelitis optica spectrum disorders (RIN-1 study): A multicentre, randomised, double-blind, placebo-controlled trial. Lancet Neurology 2020; 19(4), 298-306.

Tahedl M, Levine S, Greenlee M, Weissert R, Schwarzbach J. Functional Connectivity in Multiple Sclerosis: Recent Findings and Future Directions. Front Neurol 2018; 9: 828.

Téllez N, Río J, Tintoré M, Nos C, Galán I, Montalban X. Does the Modified Fatigue Impact Scale offer a more comprehensive assessment of fatigue in MS? Mult Scler 2005; 11: 198–202.

Thompson AJ, Banwell BL, Barkhof F, Carroll WM, Coetzee T, Comi G, et al. Diagnosis of multiple sclerosis: 2017 revisions of the McDonald criteria. Lancet Neurol 2018; 17: 162–173.

Traboulsee A, Greenberg B, Bennett J, Szczechowski L, Fox E, Shkrobot S, et al. Safety and efficacy of satralizumab monotherapy in neuromyelitis optica spectrum disorder: A randomised, double-blind, multicentre, placebo-controlled phase 3 trial. Lancet Neurology 2020; 19(5), 402-412.

Tsagkas C, Magon S, Gaetano L, Pezold S, Naegelin Y, Amann M, et al. Spinal cord volume loss. Neurology 2018; 91: e349–e358.

Tsao WC, Lyu RK, Ro LS, Lao MF, Chen CM, Wu YR, et al. Clinical correlations of motor and somatosensory evoked potentials in neuromyelitis optica. PLoS One 2014; 9: 1–13.

Ugorji CO, Samson RS, Liechti MD, Panicker JN, Miller DH, Wheeler-Kingshott CAM, et al. Grey and White Matter Magnetisation Transfer Ratio Measurements in the Lumbosacral Enlargement: A Pilot In Vivo Study at 3T. PLoS One 2015; 10: e0134495.

Vahdat S, Khatibi A, Lungu O, Finsterbusch J, Büchel C, Cohen-Adad J, et al. Resting-state brain and spinal cord networks in humans are functionally integrated. PLoS Biol 2020; 18: e3000789.

Valsasina P, Aboulwafa M, Preziosa P, Messina R, Falini A, Comi G, et al. Cervical Cord T1-weighted Hypointense Lesions at MR Imaging in Multiple Sclerosis: Relationship to Cord Atrophy and Disability. Radiology 2018; 288: 234.

Valsasina P, Agosta F, Absinta M, Sala S, Caputo D, Filippi M. Cervical cord functional MRI changes in relapse-onset MS patients. J Neurol Neurosurg Psychiatry 2010; 81: 405.

Valsasina P, Agosta F, Benedetti B, Caputo D, Perini M, Salvi F, et al. Diffusion anisotropy of the cervical cord is strictly associated with disability in amyotrophic lateral sclerosis. J Neurol Neurosurg Psychiatry 2007; 78: 480–484.

Valsasina P, Rocca M, Horsfield M, Copetti M, Filippi M. A longitudinal MRI study of cervical cord atrophy in multiple sclerosis. J Neurol 2015; 262: 1622–1628.

Viegas S, Weir A, Esiri M, Kuker W, Waters P, Leite MI, et al. Symptomatic, radiological and pathological involvement of the hypothalamus in neuromyelitis optica. J Neurol Neurosurg Psychiatry 2009; 80: 679.

Vukusic S, Confavreux C. Prognostic factors for progression of disability in the secondary progressive phase of multiple sclerosis. J Neurol Sci 2003; 206: 135–137.

Wallin MT, Culpepper WJ, Nichols E, Bhutta ZA, Gebrehiwot TT, Hay SI, et al. Global, regional, and national burden of multiple sclerosis 1990–2016: a systematic analysis for the Global Burden of Disease Study 2016. Lancet Neurol 2019; 18: 269–285.

Wang C, Narayan R, Greenberg B. Anti-Myelin Oligodendrocyte Glycoprotein Antibody Associated With Gray Matter Predominant Transverse Myelitis Mimicking Acute Flaccid Myelitis: A Presentation of Two Cases. Pediatr Neurol 2018; 86: 42–45.

Waterman CL, Currie RA, Cottrell LA, Dow J, Wright J, Waterfield CJ, et al. An integrated functional genomic study of acute phenobarbital exposure in the rat. BMC Genomics 2010; 11: 9.

Waters P, Jarius S, Littleton E, Leite M, Jacob S, Gray B, et al. Aquaporin-4 antibodies in neuromyelitis optica and longitudinally extensive transverse myelitis. Arch Neurol 2008; 65: 913–919.

Waters P, Woodhall M, O'Connor KC, Reindl M, Lang B, Sato DK, et al. MOG cell-based assay detects non-MS patients with inflammatory neurologic disease. Neurol Neuroimmunol NeuroInflammation 2015; 2: e89.

Wei P, Li J, Gao F, Ye D, Zhong Q, Liu S. Resting state networks in human cervical spinal cord observed with fMRI. Eur J Appl Physiol 2010; 108: 265–271.

Weier K, Mazraeh J, Naegelin Y, Thoeni A, Hirsch JG, Fabbro T, et al. Biplanar MRI for the assessment of the spinal cord in multiple sclerosis. Mult Scler 2012; 18: 1560–1569.

Weinshenker BG, Wingerchuk DM, Vukusic S, Linbo L, Pittock SJ, Lucchinetti CF, et al. Neuromyelitis optica IgG predicts relapse after longitudinally extensive transverse myelitis. Ann Neurol 2006; 59: 566–569.

Wheeler-Kingshott C, Stroman P, Schwab J, Bacon M, Bosma R, Brooks J, et al. The current state-of-the-art of spinal cord imaging: applications. Neuroimage 2014; 84: 1082–1093.

Wheeler-Kingshott CA., Hickman SJ, Parker GJ., Ciccarelli O, Symms MR, Miller DH, et al. Investigating Cervical Spinal Cord Structure Using Axial Diffusion Tensor Imaging.

NeuroImage (Orlando, Fla) 2002; 16: 93–102.

Wingerchuk DM, Pittock SJ, Lucchinetti CF, Lennon VA, Weinshenker BG. A secondary progressive clinical course is uncommon in neuromyelitis optica. Neurology 2007; 68: 603.

Wingerchuk DM, Pittock SJ, Waters PJ, Weinshenker BG, Bennett JL, Jarius S. Evaluation of aquaporin-4 antibody assays. Clin Exp Neuroimmunol 2014; 5: 290–303.

Wingerchuk DM, Tan CT, Mao Z, Qiu W, Hu X, Weinshenker BG. International consensus diagnostic criteria for neuromyelitis optica spectrum disordersAuthor Response. Neurology 2015; 86: 491–492.

Woolrich M, Ripley B, Brady M, Smith S. Temporal autocorrelation in univariate linear modeling of FMRI data. Neuroimage 2001; 14: 1370–1386.

Wozniak JR, Lim KO. Advances in white matter imaging: A review of in vivo magnetic resonance methodologies and their applicability to the study of development and aging. Neurosci Biobehav Rev 2006; 30: 762–774.

Xiao F, Koepp MJ, Zhou D. Pharmaco-fMRI: A Tool to Predict the Response to Antiepileptic Drugs in Epilepsy. Front Neurol 2019; 10: 1203.

Yetkin FZ, Haughton VM, Papke RA, Fischer ME, Rao SM. Multiple sclerosis: specificity of MR for diagnosis. Radiology 1991; 178: 447.

Yoshizawa T, Nose T, Moore GJ, Sillerud LO. Functional Magnetic Resonance Imaging of Motor Activation in the Human Cervical Spinal Cord. NeuroImage (Orlando, Fla) 1996; 4:

174–182.

Zalewski NL, Morris PP, Weinshenker BG, Lucchinetti CF, Guo Y, Pittock SJ, et al. Ring-enhancing spinal cord lesions in neuromyelitis optica spectrum disorders. J Neurol Neurosurg Psychiatry 2017; 88: 218–225.

Zhou F, Zhuang Y, Gong H, Wang B, Wang X, Chen Q, et al. Altered Inter-Subregion Connectivity of the Default Mode Network in Relapsing Remitting Multiple Sclerosis: A Functional and Structural Connectivity Study. PLoS One 2014; 9: e101198.

Zhou J, Lu X, Zhang Y, Ji T, Jin Y, Xu M, et al. Follow-up study on Chinese children with relapsing MOG-IgG-associated central nervous system demyelination. Mult Scler Relat Disord 2019; 28: 4–10.

Zhuo Z, Duan Y, Tian D, Wang X, Gao C, Ding J, et al. Brain structural and functional alterations in MOG antibody disease. Mult Scler 2020: 1352458520964415.